CALIFORNIA
ENERGY COMMISSION

Energy Research and Development Division

FINAL PROJECT REPORT

Enabling Anaerobic Digestion Deployment to Convert Municipal Solid Waste to Energy

Gavin Newsom, Governor
March 2020 | CEC-500-2020-011

PREPARED BY:

Primary Authors:

Thomas W. Kirchstetter, PI
Corinne D. Scown, Co-PI
Andy Satchwell
Ling Jin
Sarah J. Smith
Chelsea V. Preble
Jahon Amirebrahimi
Michael D. Sohn
Nancy J. Brown
Sarah Nordahl
Jay Devkota
Yijun He
Tin Ho
Randy L. Maddalena
Nicholas W. Tang
Wei Zhou
Sharon S. Chen
Toshifumi Hotchi

Lawrence Berkeley National Laboratory
1 Cyclotron Road
Berkeley, CA 94720
Phone: 510-486-4000 | Fax: 510-486-6996
http://www.lbl.gov

Contract Number: EPC-14-044

PREPARED FOR:
California Energy Commission

Prab Sethi
Project Manager

Jonah Steinbuck, Ph.D.
Office Manager
ENERGY GENERATION RESEARCH OFFICE

Laurie ten Hope
Deputy Director
ENERGY RESEARCH AND DEVELOPMENT DIVISION

Drew Bohan
Executive Director

ACKNOWLEDGEMENTS

The authors are grateful to many people for supporting this research and especially thank Greg Ryan, Osvaldo Cordero, John Pena, Spencer Morgan, James Moore, and Amelin Norzamini of the Zero Waste Energy Development Company for their partnership in conducting this work, including access to their facility and their facility data. Similarly, the authors thank John Doyle, Fred Ochoa, and Beto Ochoa of Z-Best for allowing the authors to make measurements at their composting facility. The authors also thank Ekpa Akpan, Abigail Shull, and Stephanie Molloy of the City of San Jose. Bay Area Air Quality Management District staff was very helpful, providing the researchers with key sampling equipment and discussing results. The authors especially thank Phil Martien, Sally Newman, and Abhinav Guha. Also appreciated are the time and insights of the technical advisory committee members Phil Martien, Bill Monson, Julia Levin, Todd Pray, Donald Lucas, Jack Brouwer, and John Hake. Several students contributed to this project, including Brandon Yee, Yannick Johnson, Marie-Anne Hatte, Caroline Loffredo, Isabelle Kavanagh, and Kelly Archer. Finally, the authors thank Woody Delp for data logging assistance.

PREFACE

The California Energy Commission's (CEC) Energy Research and Development Division supports energy research and development programs to spur innovation in energy efficiency, renewable energy and advanced clean generation, energy-related environmental protection, energy transmission and distribution, and transportation.

In 2012, the Electric Program Investment Charge (EPIC) was established by the California Public Utilities Commission to fund public investments in research to create and advance new energy solution, foster regional innovation and bring ideas from the lab to the marketplace. The CEC and the state's three largest investor-owned utilities—Pacific Gas and Electric Company, San Diego Gas and Electric Company and Southern California Edison Company—were selected to administer the EPIC funds and advance novel technologies, tools, and strategies that provide benefits to their electric ratepayers.

The CEC is committed to ensuring public participation in its research and development programs, which promote greater reliability, lower costs, and increase safety for the California electric ratepayer and include:

- Providing societal benefits.
- Reducing greenhouse gas emissions in the electricity sector at the lowest possible cost.
- Supporting California's loading order to meet energy needs first with energy efficiency and demand response, next with renewable energy (distributed generation and utility scale), and finally with clean conventional electricity supply.
- Supporting low-emission vehicles and transportation.
- Providing economic development.
- Using ratepayer funds efficiently.

Enabling Anaerobic Digestion Deployment to Convert Municipal Solid Waste to Energy is the final report for the Enabling Anaerobic Digestion Deployment for Municipal Solid Waste-to-Energy project (Contract Number EPC-14-044) conducted by Lawrence Berkeley National Laboratory. The information from this project contributes to the Energy Research and Development Division's EPIC Program.

For more information about the Energy Research and Development Division, please visit the Energy Commission's research website (www.energy.ca.gov/research/) or contact the Energy Commission at 916-327-1551.

ABSTRACT

Municipal solid waste is used to produce energy at power plants and landfills, termed "waste-to-energy." Waste products used at these plants include organic materials like as plant or animal waste, paper, cardboard, food waste, grass clippings, leaves, and wood. One method of converting organic materials to energy is anaerobic digestion of organic municipal solid waste, which produces methane-rich biogas for energy production. Waste-to-energy plants support California's renewable energy goals and reduce landfilling and associated methane emissions. Only about 15 percent of California's organic municipal solid waste is diverted for energy production, however, and this fraction is decreasing because of economic, regulatory, and policy barriers. A multidisciplinary research team at Lawrence Berkeley National Laboratory worked with the Zero Waste Energy Development Company and the City of San Jose to help overcome key barriers to enable sustainable scale-up of waste processing and energy production. During the project, the company more than doubled its waste intake to 90,000 tons per year. The team developed methods and quantified emission rates of greenhouse gases, ammonia, hydrogen sulfide, volatile organic compounds, and oxides of nitrogen from Zero Waste's on- and offsite activities. The project team produced an odor transport framework and regional impact model, along with environmental life-cycle and economic analysis models, to assess net environmental, societal, and financial impacts. The team evaluated life-cycle emissions for current Zero Waste operations and alternative scenarios. Outdoor composting is the largest source of Zero Waste's odor and greenhouse gas emissions. The plant achieves substantial emissions reductions relative to landfilling but could improve if biogas was used to fuel heavy-duty trucks. The team identified three factors to improve the business case for larger-scale plants: (i) long-term feedstock and digestate management contracts, as well as net electricity compensation prior to plant construction; (ii) investment in waste recovery to support cleaner feedstocks; and (iii) financial mechanisms to overcome large, lumpy (intermittent rather than regular) capital expenditures.

Keywords: Anaerobic digestion, municipal solid waste, biogas, waste-to-energy, scale-up, composting, life-cycle assessment, BioMAT, greenhouse gas emissions, odor transport, waste processing, landfill methane avoidance, SB 1383, short-lived climate pollutants, air pollution, bioenergy

Please use the following citation for this report:

Kirchstetter, Thomas W., C. D. Scown, A. Satchwell, L. Jin, S. J. Smith, C. Preble, J. Amirebrahimi, M. Sohn, N. Brown, J. Devkota, Y. He, T. Ho, R. Maddalena, S. Nordahl, N. Tang, and W. Zhou. 2020. *Enabling Anaerobic Digestion Deployment to Convert Municipal Solid Waste to Energy*. California Energy Commission. Publication Number: CEC-500-2020-011.

TABLE OF CONTENTS

LIST OF FIGURES

Page

LIST OF TABLES

Page

EXECUTIVE SUMMARY

Introduction

About 15 percent of California's organic waste or biomass is presently diverted from the waste stream to produce energy. Production of energy from waste biomass aligns with California's clean energy policies, diverts waste from landfills, reduces landfill methane and fossil carbon dioxide (CO_2) emissions, reduces fossil fuel reliance, and improves grid reliability and resiliency. Energy from anaerobic digestion (a process in which microorganisms break biodegradable material down in the absence of oxygen) of organic municipal solid waste diverted from landfills can help diversify the mix of resources in the state's electric generation portfolio. It can also help municipal governments achieve sustainability goals. The potential for electricity generated from municipal solid waste is approximately 5 percent of California's energy supply, and those facilities would be eligible under the Renewable Portfolio Standard.

The fraction of biomass used to produce energy is decreasing because of challenges that affect the business case for waste-to-energy facilities. Challenges include air pollution permitting, air quality concerns such as odor and negative effects on the public, high capital costs, long waits for utility interconnection, uncertainties associated with compensation for power output and coproducts (waste heat, gas, fertilizer, and compost), and unproven greenhouse gas reduction benefits.

Project Purpose

This research project developed a new analytical method that commercial biogas/bioenergy stakeholders can use to scale up operations and overcome through demonstration and evaluation at key process points. The Lawrence Berkeley National Laboratory research team for this project, composed of research scientists and experts in waste management, bioenergy production, and public policy, studied the dry anaerobic digestion and composting activities of the Zero Waste Energy Development Company (ZWEDC) in San Jose (Santa Clara County). During this project, ZWEDC, scaled up its operations from processing 40,000 tons per year in its initial development phase to now processing nearly 90,000 tons per year of organic municipal solid waste. Because the challenges and opportunities ZWEDC faced are similar to those faced by other companies, the analysis in this project can apply broadly to making other waste projects and processes more economically attractive and environmentally beneficial.

The goals of this research project were to:

- Characterize and quantify greenhouse gas (GHG), air pollutant, and odor-causing emissions; determine odor dispersion patterns, source-receptor relationship (the effect of placing an emissions source in one region on the air quality of a receptor in a different region), and governing conditions; and recommend feasible odor-control strategies.

- Determine net changes in life-cycle (direct and indirect) emissions of CO_2, methane, and nitrous oxide.
- Identify economic and policy factors affecting the ability of ZWEDC to export power.
- Provide recommendations to enable production and use of renewable electricity.
- Develop strategies for overcoming technical hurdles to plant scale-up such as digester technology choice, biogas quality, combined heat and power system operation, waste heat use, and air quality.
- Determine onsite demand and opportunities for export of coproducts, including biogas, waste heat, fertilizer, and compost.

Project Process

The research team worked with ZWEDC and the City of San Jose and included guidance from a technical advisory committee. The team obtained and analyzed ZWEDC's data records for municipal solid waste intake and compost production, biogas and electricity production, and expenses and income from 2015 to 2018. Researchers reviewed the scientific literature for estimates of pollutant emissions from anaerobic digestion and composting. Researchers also developed measurement methods and quantified emissions rates of GHGs, odorous and toxic compounds, and other air pollutants. With this foundation, the team developed economic, odor transport, and environmental life-cycle assessment models. Finally, researchers assessed policy and economic barriers. As part of this project, ZWEDC established a schedule for scale-up of waste intake and onsite electricity generation.

Air Pollutant Emissions Characterization

The research team's measurements focused on GHGs (CO_2, methane, nitrous oxide); ammonia; hydrogen sulfide; nitrogen oxides (NO_x); black carbon particulate matter; and volatile organic compounds. The team measured pollutant emissions from the following key sources:

- Composting windrows: After terminating onsite composting activity because of odor complaints, ZWEDC trucked digested municipal solid waste (digestate) to Z-Best, an organic composting company in Gilroy, California. The digestate is put into commercial composting bags 100 meters long, 6 meters wide, and 3 meters tall. The filled bags, referred to as windrows, are aerated using blowers that cycle on and off over 14 weeks. The research team designed a sampling procedure for measuring the variability in GHG and odorous compound emissions among multiple windrows during the 14-week composting cycle.
- Enclosed flare: ZWEDC uses an enclosed incineration process (enclosed flare) to convert methane to carbon dioxide when the methane cannot be burned onsite for electricity generation. The flaring occurs regularly at the end of each anaerobic digestion cycle when the methane content of the biogas is too lean

(with a low fuel-to-air ratio) to burn in the combined heat and power units. Researchers measured biogas composition and flare exhaust composition during many weeks of ZWEDC's operation between 2016 and 2019 and identified a relationship between NO_x emissions and the amount of ammonia contained in flared biogas.

- Combined heat and power units: ZWEDC employs two combined heat and power units rated for 800 kilowatts and equipped with a selective catalytic reduction system to control NO_x emissions.
- Biofilters: To remove pollutants from the exhaust air system of its plant, ZWEDC operates four biofilters downstream as well as acid scrubbers. The biofilters and acid scrubbers continuously process air coming from the waste-receiving hall, ultra-lean biogas with less than 3 percent methane from the digester start-up and shutdown phases, and effluent from composting tunnels that aerate material prior to its being trucked to Z-Best for composting. The project team measured emissions at a single spot on top of one biofilter for one week and developed a way to make similar time-integrated measurements at different spots at all four biofilters during a day.
- Biogas bladder vent: ZWEDC stores biogas from anaerobic digestion of organic municipal solid waste in two bladders before it is used for combined heat and power production, flared, or vented to the atmosphere. Accumulation in the storage bladders depends on rates of biogas production and consumption via one of these three pathways. Gas consumption at the combined heat and power units can be low for a variety of reasons, including unit maintenance. To avoid overpressurizing and rupturing the bladder, biogas must either be flared or vented directly to the atmosphere. At the ZWEDC facility, a water column connected to the bladder prevents venting of biogas to the atmosphere until the pressure of the stored biogas exceeds the setpoint, after which the flare is activated to consume biogas. At times, the biogas consumption rate of the flare is not sufficient to prevent the release of biogas to the atmosphere through the valve. The project team developed a method to verify the frequency and duration of biogas venting and estimate the volume of biogas released to the atmosphere.

Odor Transport Modeling

The research team reviewed and analyzed past odor complaints made to ZWEDC in relation to local air circulation patterns and onsite operations to identify odor sources and data requirements for subsequent dispersion modeling. The team then combined literature research and field measurements to characterize five odor-generating sources (continuous or intermittent) at ZWEDC with respect to the rates of odor emissions, the characteristics of the source, and the frequency of emissions. The team collected and processed meteorological (both at surface and upper atmosphere) and terrain data for use in the U.S. Environmental Protection Agency's AERMOD plume model that links odor

sources to offsite impacts at downwind locations. The researchers analyzed the simulated odor concentrations to determine effects on local communities around the ZWEDC plant.

The project team developed an innovative odor impact assessment framework by determining separation distances required to avoid odor annoyance and evaluating dependencies on odor impact criteria. Researchers used separation distance to identify measurement results that would: (1) determine time and location characteristics of odor dispersion; (2) identify influential sources, times, and operating conditions; (3) determine odor impacts in relation to varying project waste-processing capacity; and (4) develop mitigation priorities and strategies.

Life-Cycle Assessment

The team constructed an inventory model to quantify the net GHG, volatile organic compounds, NO_x, sulfur dioxide, carbon monoxide, ammonia, and particulate matter 2.5 emissions. The model included data on mass and energy flows among key sectors and activities that play a direct or indirect role in organic waste management and energy production. The model relies on freely available data and packages so it is transparent and easy to set up and run on any personal computer. Valuable data included measured values taken onsite at ZWEDC and Z-Best and when possible researchers used those values rather than general literature data. To judge the relative importance of GHG and air pollutant emissions across a common measurement, the team used a $42 per tonne (metric ton) CO_2-equivalent cost for GHG emissions and two different models to generate results for monetized human health damages.

The team constructed multiple scenarios for this project. These scenarios reflect: (1) the base case (landfilling of all organics except yard waste, which is composted), (2) current ZWEDC operations; (3) ZWEDC operations with landfilling of digestate; (4) ZWEDC operations with direct land application of digestate in place of composting; (5) ZWEDC operations with biogas cleanup and compression for use in retrofitted or new trucks previously running on diesel; and (6) ZWEDC operations with biogas cleanup and compression for pipeline injection to replace fossil natural gas.

Policy and Economic Barrier Assessment

The research team identified regulatory and policy barriers that affected the ZWEDC facility (as well as anaerobic digester facilities more broadly) in three major process stages: (1) waste sorting, delivery, and processing; (2) anaerobic digester/biogas management and utilization; and (3) outputs and residuals processing. The team used operational and financial data from the ZWEDC facility where appropriate, and concluded with implications for policymakers and regulators who seek to broaden the use of solid waste biomass technologies and align with public policy goals.

The team compiled financial records and operational data to create a model to express costs and revenues of the plant operating under different waste intake levels from

current capacity up to three times capacity. The researchers also examined different operating scenarios including composting onsite versus offsite and different levels of waste stream contamination. For an incoming waste stream, researchers used operating data to estimate the digester capacity required, the biogas and electricity produced, and tonnages of residuals, recyclable materials, digestate, and compost generated. This data was then paired with financial data and known cost parameters, such as per-ton trucking costs, to estimate the average annual costs and revenues over plant lifetime. The team also calculated net present value, internal rate of return, and average per-ton costs and profit metrics. Finally, the project team analyzed the parameters deemed most important to facility economic success: capital costs, electricity sales price, and tipping fees.

Project Results

Air Pollutant Emissions Characterization

The research team determined emissions factors as follows:

- Fuel-based emission factors (grams of pollutant emitted per kilogram of methane burned) based on a carbon balance method for combustion sources.
- Time-based emission factors (grams of pollutant emitted per hour) based on volumetric flow rate for non-combustion sources.
- Municipal solid waste mass-based emission factors (grams of pollutant emitted per kilogram of municipal solid waste digested).

Air quality agencies can use these emission rates to help develop emission inventories, and the rates serve as inputs to the odor modeling and lifecycle analysis in this research project.

CO_2 emissions per kg of municipal solid waste digested were much higher from the composting windrows than from the other sources measured. Researchers also determined that on a 20-year global warming potential time horizon, biogas flaring and combined heat and power production respectively accounted for 5 percent and 10 percent of total CO_2-equivalent emissions per kg of municipal solid waste digested. The global warming potential for these activities was mostly from CO_2 emissions from the near-complete conversion of methane in the biogas to carbon dioxide during combustion. Twenty percent of the CO_2-equivalent emissions were from the biofilters, mostly from methane. The 14-week composting cycle was responsible for 65 percent of the total CO_2-equivalent emissions per kg of municipal solid waste digested. Methane comprised 63 percent of those emissions from composting, with CO_2 emissions making up most of the remaining fraction. Significant methane emissions over the full 14-week composting cycle indicates that some anaerobic activity persists despite aeration.

A strong relationship between biogas ammonia content and flare NO_x emissions was measured, which can help inform the permitting or abatement of other facilities. The ammonia concentration in the flared biogas increased from about 20 parts per million

(ppm) to more than 1,000 ppm over the course of the lean biogas flaring event. As the fuel-ammonia increased, emitted NO_x concentrations also increased. The dominant NO_x formation pathway was determined to be fuel NO_x (conversion of biogas ammonia to NO_x) rather than thermal NO_x (conversion of molecular nitrogen in the air to NO_x). Results suggest that 50 percent of fuel-ammonia is emitted as NO_x.

A total of 12 distinct biogas venting events were measured over a period of several months. Biogas venting had been occurring below the setpoint of the pressure relief valve and thus unknowingly. After evidence of unknown venting was confirmed, the water column height of the valve was better maintained and venting emissions below the setpoint of the pressure relief valve ceased.

Odor Transport Modeling

The research revealed that odor character and intensity vary greatly by source. Compost windrows dominated the odor emissions, followed by biofilter exhausts and biogas venting. Biogas venting is an intermittent source with unknown emission frequency until this study and the above-described emissions measurements. Leakage from delivery trucks and the receiving hall is a minor contributor.

Dispersion modeling revealed time-dependent areas of impact for odor. Odor transport is consistently in the southeast-ward direction with affected areas largely within ,2000 meters of non-residence areas. Greater impacts were found during hours with low atmospheric mixing (early morning/evening and late afternoon) and in fall and winter seasons.

The research team found that offsite odor impacts depended on the source and largely driven by compost emissions if onsite operation was present. Composting emissions were the most challenging to tackle. Separation distances of more than 3,000 meters are required (based on 2 percent exceedance probability of 5 odor units per cubic meter exposure) for the onsite composting operation. Biofilters and other sources under the current operation conditions do not generally impose significant odor impacts on communities located 2,000 meters or more downwind. These emissions will not limit the facility scaleup to 1.5–2 times of current capacity.

Impact of biogas venting depends on operational conditions (contamination levels and venting frequency) and can affect local communities during hours with low atmospheric mixing. The project team used these findings to recommend best practices that include scheduling high-odor generating processes during high-mixing hours (middle of the day) or outside of human active hours before 7 am or after 9 pm. Also, the project team recommends maintaining the water column of the pressure release valve for biogas venting during the early morning and the end of the day to reduce the probability of venting during those higher impact times.

The analysis also revealed policy relevant findings. Separation distances required for siting a facility depend on the impact criteria (allowable exceedance frequency and

threshold concentration) which are determined by policy makers. More research and air pollution monitoring data are needed for developing odor impact criteria to ensure appropriate protection of the exposed population. This study identified a strong log-linear relationship between separation distances and total odor emission rates. Such a relationship is instrumental for future facility planning and siting. Further investigation with data from other facilities is needed to validate whether this the relationship holds generally true.

Life-Cycle Assessment

The results indicate that, on the basis of 100-year global warming potential, emissions from decomposition of organics in landfills dominate even in well-managed landfills in California with gas capture systems. Landfilling organic waste is the most GHG-intensive option on a per-tonne basis, with a GHG footprint of 800 kilograms CO_2-equivalent (kg CO_2-eq.) per tonne of organic waste. In anaerobic digester scenarios where some or all digestate must be landfilled, GHG emissions are net positive but still dramatically lower (54-87 kg CO_2-eq.per tonne of organic waste). Composting results in the lowest GHG footprint, totaling -76 kg CO_2-eq per tonne of organic waste. A large GHG sequestration credit and a more limited fertilizer offset credit are both based on expected benefits from land application of the compost. The scenario that combines dry anaerogic digestion, electricity generation, and composting digestate (ZWEDC current operations) results in a net GHG footprint of -12 kg CO_2-eq per tonne of organic waste. If biogas is upgraded to renewable natural gas and used to offset diesel fuel use in a fleet of new or retrofitted trucks, the net GHG footprint is reduced to -56 kg CO_2-eq per tonne of organic waste. Upgrading biogas to renewable natural gas and injecting it into the pipeline for use in place of fossil natural gas results in reduced GHG mitigation (-22 kg CO_2-eq per tonne of organic waste) relative to the scenario in which renewable natural gas offsets diesel use.

The monetized damage results indicate that the social cost of landfilling wet organic waste is approximately $40-50 per tonne (this does not include private costs associated with operating the landfill). Because GHG-related damages make up the largest fraction of the overall monetized damages for landfilling, this value will change depending on the assumed social cost of carbon. For other scenarios, both integrated assessment models indicated that ammonia emissions are the dominant contributor to social costs in every case where some or all organic material is composted. This is because ammonia emissions per tonne of organic waste processed are at least two orders of magnitude greater than any other non-GHG pollutant in each scenario that includes composting. Both models indicated that the composting scenario resulted in the greatest social costs, exceeding that of landfilling, if damages from ammonia are included. The scenarios in which waste is sent for dry anaerobic digestion and digestate is landfilled or land-applied have much lower social costs. Future measurements of NH_3 emissions from landfills and on land where digestate has been applied will be essential to developing a more comprehensive understanding of these social costs.

Policy Barrier Assessment

In response to recent legislation mandating waste diversion, California will face a steep increase in accessible organic waste supply within a decade. Assembly Bill 1826 (Chesbro, Chapter 727, Statutes of 2014) and Senate Bill 1383 (Lara, Chapter 395, Statutes of 2016) mandate a high degree of organic waste diversion and processing for commercial and public sectors. These regulatory mandates will require increased organic waste diversion and with a lack of processing infrastructure, there will be a need for expanded and new anaerobic digestion facilities.

The challenges in the waste management sector in California are multifaceted and involve several state agencies. The project team offers several considerations for policymakers and regulators across California state agencies — CalRecycle, the California Air Resources Board, the California Public Utilities Commission, and the California Energy Commission — to address the challenges and develop policy solutions more likely to achieve the desired environmental and economic outcomes:

- State mandates specifying organics separation may improve feedstock quality for solid waste biomass facilities. Additionally, major investments in waste infrastructure may be required to optimize the collection and processing of organic waste, which otherwise is considered a low-value contaminant relative to other recyclable residential collection streams.
- More research and measurement efforts are needed to characterize the odor sources associated with anaerobic digester facilities and air permitting agencies could work with first adopters of anaerobic digestion to better understand emissions prior to enforcing monetary penalties.
- State utility regulators can address interconnection barriers and establish rules that do not unduly burden anaerobic digester facility generating systems. Additionally, anaerobic digester facility planners should consider the additional time and cost implications of interconnection standards, as well as the details of the standards when making decisions about facility design and project budgets.
- Price levels and rules for the biomass tariff program, BioMAT, and other similar biomass feed-in tariff programs, should consider the environmental benefits of solid waste biomass technologies, particularly benefits of diverting waste from landfills. Tariff program deadlines should also align with timing of state policies for bioenergy, such as SB 1122 (Rubio, Chapter 612, Statutes of 2012), and methane reductions (SB 1383), among other state environmental policies.

Implementation in Scale Up of Waste Intake and Power Production and Economic Assessment

The goals for scaling up ZWEDC were established both on a tons of waste intake basis and on the basis of on-site electricity generation. As part of the project, the following schedule for scale-up was established:

- End of year 1: waste intake to 50,000 tons (45,359 tonnes) organic waste per year
- End of year 2: waste intake to 70,000 tons (63,503 tonnes) organic waste per year and 1 MW generation
- End of year 3: waste intake to 90,000 tons (81,647 tonnes) organic waste per year and 1.6 MW generation (Phase 1)
- Double total capacity; install additional 90,000 tons (81,647 tonnes) per year of anaerobic digestion capacity and corresponding composting capacity, possibly increasing net combined heat and power capacity to 4 MW (Phase 2)

ZWEDC achieved its Phase 1 goal of 90,000 tons per year of organic waste intake and 1.6 MW of nameplate combined heat and power capacity through the end of 2015, though the combined heat and power capacity was installed prior to the start of our project in 2014. ZWEDC has successfully operated at Phase 1 capacity, despite high residual content and unforeseen operational challenges. Yet, ZWEDC has postponed further scale-up and noted several financial factors in its decision to remain at Phase I capacity, including lack of consistent feedstock at increased scale to justify the high capital and construction costs.

The researchers developed an economic model of the ZWEDC anaerobic digester facility to understand how economic and policy barriers have affected plant profitability and the likelihood of successful scale-up. Further, the project team used the model to understand the potential financial situation under various plant sizes and operating scenarios, as well as scenarios that may make a future scale-up more desirable.

Project findings identified several key concerns for short-term anaerobic digester facility financial viability, including:

- Digestate and residual management are large costs that can be highly variable, limiting the facility's ability to manage its overall costs.
- Improved biogas yields would increase electricity sales and profit, but would also require operational improvements.
- Three factors to improve the business case and motivation for larger scale facilities:
    - Establish long-term feedstock and digestate management contracts, as well as net electricity compensation prior to facility construction;
    - Invest in waste recovery to support cleaner feedstocks; and
    - Consider supportive financial mechanisms to overcome large, lumpy capital expenditures.

Benefits to California

This research is important to ratepayers because the results can inform efforts to increase the diversion of organic waste from the waste stream to use in distributed

electricity generation, waste heat use, and compost production, all of which will result in greater electricity reliability and lower costs. The benefits to investor-owned utility ratepayers stem from three considerations. First, using organic waste instead of fossil fuel can help insulate ratepayers from fluctuations and long-term increases in fossil fuel prices. Second, using waste heat reduces costs and increases safety by improving the overall efficiency of the waste-to-energy facilities, thus avoiding additional fossil fuel demand and environmental impacts. Third, distributed electricity generation can help reduce transmission and distribution costs and improve grid reliability.

CHAPTER 1: Introduction

Motivation

Production of energy from waste biomass aligns with California's clean energy policies, diverts waste from landfills, reduces landfill methane and fossil carbon dioxide (CO_2) emissions, reduces fossil fuel reliance, and improves grid reliability and resiliency. Energy from waste can help diversify the mix of resources in the state's electric generation portfolio. It can also help municipal governments achieve sustainability goals.

Presently, only about 15 percent of California's organic waste is diverted for energy production, and this fraction is decreasing due to challenges that may result in an unsuitable business case for waste-to-energy facilities including regulatory and permitting challenges, air quality concerns, high capital costs, long waiting periods for interconnection, and uncertainties associated with compensation for power output and co-products.

Background

This project focuses on the dry anaerobic digestion (AD)[1] and composting facility built and operated by Zero Waste Energy Development Company (ZWEDC) in San José, California. Although its initial scale allows it to process only a fraction of San José's organic municipal solid waste (MSW), it is currently the largest dry anaerobic digestion facility in the United States. Operations began in late 2013 and the facility was processing 40,000 tons per year in its initial development phase, yielding approximately 400 cubic meters per hour of biogas with a methane content of 50–55 percent. During this project, ZWEDC scaled up operations and now processes approximately 90,000 tons (approximately 82,000 tonnes) per year of organic municipal solid waste.

The project was specifically focused on the sustainable scale-up and wider deployment of AD technology in California. Barriers to scale-up of operations with the current capacity and potential future capacity expansion include: (1) odor problems and associated public adversity, (2) policy and economic barriers to maximizing net energy export, and (3) incomplete life-cycle cost and environmental evaluations to support decision-making for export of co-products, which include waste heat, gas, fertilizer, and compost. The multidisciplinary team composed of research scientists and experts in

[1] Anaerobic digestion is a collection of processes by which microorganisms break down biodegradable material in the absence of oxygen, converting organic material into roughly equal amounts of carbon dioxide and methane.

waste management, bioenergy production, and public policy conducted this research project with the following goals:

- Characterize and quantify key odor-causing emissions and governing conditions, determine odor dispersion patterns and source-receptor relationships, and recommend feasible odor control strategies
- Determine net changes in life-cycle (direct and indirect) GHG emissions (carbon dioxide [$CO_{2]}$, methane [CH_4], and nitrous oxide [N_2O])
- Identify economic and policy factors affecting ZWEDC's ability to export power
- Provide recommendations that will enable production and utilization of additional electricity
- Develop strategies for overcoming technical hurdles to facility scale-up, including those associated with digester technology choice, biogas quality, combined heat and power (CHP) system operation, waste heat utilization, and air quality
- Determine on-site demand and opportunities for export of co-products, including biogas, waste heat, fertilizer, and compost

The purpose of the project is to provide a new and compelling analytical framework that commercial biogas/bioenergy stakeholders can use to scale up operations and overcome deployment challenges through demonstration and evaluation. Since there are common barriers and enhancement opportunities for other facilities, this analysis has broad applicability for making other facilities and their processes more economically attractive and environmentally benign.

Report Structure

Chapter 2 provides a facility overview. Chapter 3 describes air emissions measurement, modeling, and approaches for minimizing odor. Chapter 4 assess the life-cycle cost, energy, and greenhouse gas impacts. Chapter 5 describes policy and economic barriers. Chapter 6 describes ZWEDC scale-up and financial modeling of facility economics at increasing scale. Chapter 7 concludes the analytical work with project impacts and conclusions. Technical detail about analytical assumptions, methodologies, and datasets are included in the technical appendices.

CHAPTER 2:
Facility Overview

Facility Background and Timeline

Site

The dry anaerobic digestion facility built and operated by Zero Waste Energy Development Company (ZWEDC), referred to throughout the text as ZWEDC or the ZWEDC facility, was constructed on an approximately 40-acre plot of land owned by the City of San Jose. It is located on Los Esteros Road, in an industrial area near the southern tip of the San Francisco Bay. Nearby facilities include a wastewater treatment plant, materials processing facility, and recycling facility. The land was previously the site of the Nine Par landfill until 1969, and required redevelopment to be suitable for construction of the new anaerobic digestion (AD) facility. For example, to avoid damage resulting from uneven settling, the entire facility is built on a floating base made of multiple "rafts" that disperse the weight of each digester and the receiving and operations area (Goldstein 2018). The site originally included an area for composting of solid digestate, as shown in Figure 1, although odor complaints ultimately resulted in the relocation of all composting operations to an offsite facility. This will be discussed in more detail later in the report.

Figure 1: Aerial View of ZWEDC Facility

Source: Lawrence Berkeley National Laboratory

Selected Anaerobic Digestion Technology

Anaerobic digestion (AD) has been used to produce flammable gas (biogas) for hundreds of years after humans discovered the phenomenon in natural environments such as wetlands. In anaerobic digestion, microbes grow in a limited-oxygen environment (often underwater) to ultimately produce methane, along with carbon dioxide and other trace gases. This is achieved in a multi-step process including: (1) hydrolysis, the breakdown of complex biopolymers to monomers and oligomers more easily metabolized by downstream microbes, (2) acidogenesis, the production of short-chain volatile organic acids, (3) acetogenesis, the production of acetate and hydrogen, and (4) methanogenesis, the production of methane and carbon dioxide. Unlike modern biotechnology, which often relies on a single strain in very controlled conditions, AD is not precisely controlled and the microbial community is often established by inoculating new systems with material from other operational facilities. The microbial community may evolve based on the mixture of feedstock available and operating conditions.

The ZWEDC site relies on the Kompoferm anaerobic digestion technology, which is part of the SMARTFERM suite of technologies offered by the German company Eggersmann. The thermophilic inoculate was obtained from the East Bay Municipal Utility District (EBMUD) wastewater treatment facility. Dry AD is distinct from wet AD in that dry digesters operate at significantly higher solids loading (20 to >40 percent) compared to wet digesters (<10 to 20 percent). The waste is typically loaded into dry digesters in the form of piles rather than slurries pumped into liquid-filled tanks at wet AD facilities. This strategy has both advantages and disadvantages relative to wet AD. For example, wet AD facilities such as those found at wastewater treatment plants require much less inorganic contamination and even small items such as cutlery can cause problems in piping and pumps. Rotating drum screens can help achieve size reduction and filter inorganic contamination, but this equipment comes at an energy and economic cost.

For dry AD facilities, even large inorganic contaminants can enter the digesters, but these contaminants limit biogas yields per tonne of material and may contribute to serious problems, such as increased contaminants in the biogas, digester upset, or low-quality compost generated from the digestate. Dry AD's ability to handle inorganic contaminants makes it a suitable fit for mixed organic waste collection systems with varying degrees of contamination.

Facility Operations Overview

The ZWEDC facility was designed to accept approximately 81,650 tonnes (90,000 tons) of waste annually. Figure 2 shows a simplified overview of the facility's operations. After pre-processing, an extruder is used to remove excess water from contaminants. Contaminants are separated and sent to the Newby Island landfill and organics are loaded into the digesters.

The anaerobic digestion itself is a batch process lasting 21 days. There are 16 digester bays, separated into two "banks" of 8 digesters, that can be independently loaded and

operated (Figure 3 shows a digester bay after the 21-day process has been completed). Each bank of 8 digesters has its own 425,000 gallon (1,609,000 liter) percolate tank. Biogas is generated in the digesters and the percolate tanks. The biogas is sent to storage bladders on the roof of the facility (see Figure 1) that store gas at atmospheric pressure.

Most of the biogas is fed to an on-site combined heat and power (CHP) facility comprised of two 800 kW lean-combustion engines, for a combined capacity of 1.6 MW, a portion of which is exported to the grid. Waste heat is recovered and used to heat the digesters to 52–55°C (125–131°F), which is the temperature range required for the thermophilic AD process. Biogas is flared in two specific cases: (1) when methane concentrations are between 2 percent and 20 percent, and (2) when rich gas (methane content > 20 percent) supply exceeds bladder storage capacity. The latter case is most common if one of the generators is not operational. In the former case, operators use rich gas to supplement lean gas as needed to maintain the appropriate air-to-fuel ratio in the flare.

Residual solids from the digesters, referred to as digestate, are sent to four in-vessel composting (IVC) tunnels. The residence time in these tunnels is 4–5 days, and the goal of this batch process is to allow for ammonia and odorous emissions to be captured and treated in the on-site biofilter before the material is ultimately composted for a longer period in outdoor windrows. Originally, the post-IVC organics were composted on-site in windrows that were regularly turned and aerated. However, due to odor complaints, the material is now trucked to Gilroy, CA, where it is bagged and composted for 16 weeks at the Z-Best facility. The finished compost is sold by Z-Best for applications such as landscaping and agriculture.

Figure 2: Simplified ZWEDC Operations Overview

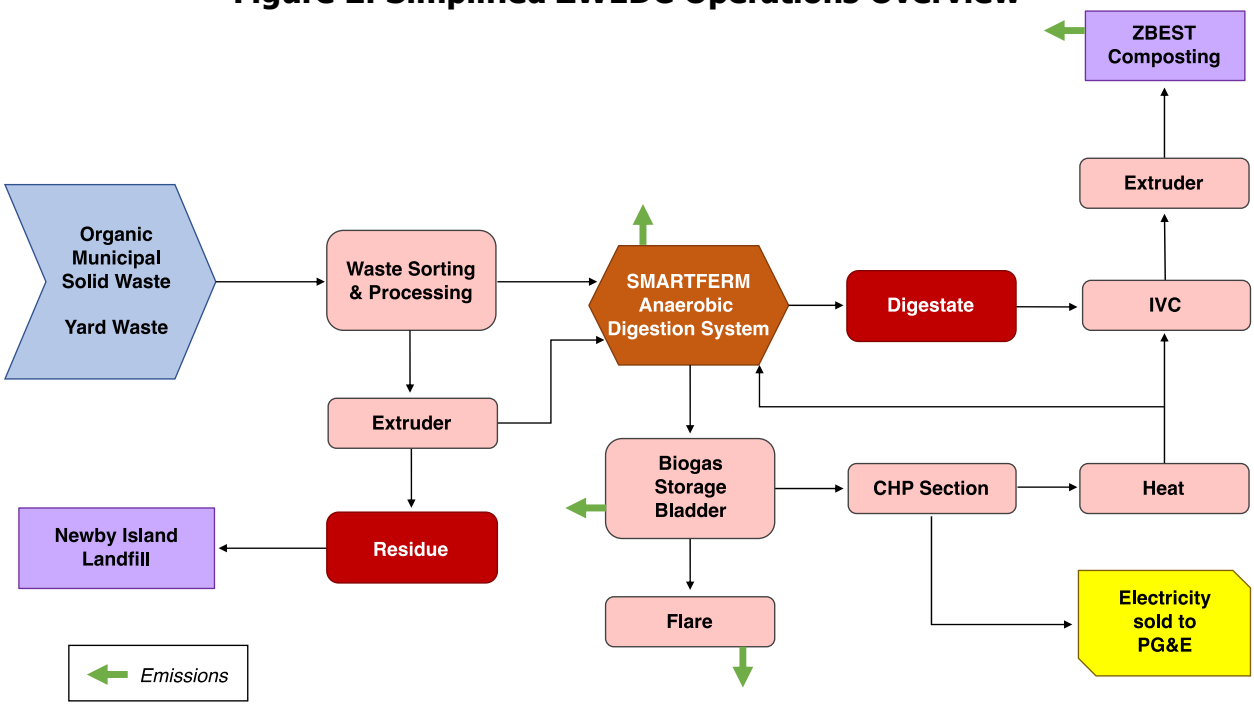

Source: Lawrence Berkeley National Laboratory

Figure 3: One Anaerobic Digester Bay at ZWEDC After 21-Day Process Completed

Source: Lawrence Berkeley National Laboratory

Waste Inbound and Outbound Material Overview

ZWEDC receives and processes both mixed municipal solid waste, and source separated organics material (yard waste and manure). The majority of the facility overall inbound material originates from businesses in the city of San Jose. The facility also receives additional inbound material from the cities of Palo Alto (mixed MSW and source separated yard waste), Los Altos (source separated manure); from the Sunnyvale

Materials Recovery and Transfer (SMaRT) Station (a material recycling facility that processes municipal solid waste from the cities of Sunnyvale, Mountain View, and Palo Alto, and serves an estimated population of 280,000); and various private grocery stores and retailers within the county of Santa Clara. Inorganic contaminants screened from the inbound material is sent to disposal either at the Newby Island landfill (~ 9km from the facility), or the Marina Sanitary Landfill (~111 km from the facility). All organic material, except incompatible yard waste, received at the facility are fed to the dry anaerobic digester for biogas production. Yardwaste, as well as the post-digested biomaterial ("digestate") is transported about 73 km to Z-Best, a large-scale composting facility in Gilroy.

Figure 4: Example of Inbound Organic Stream 4 (OS4) Waste at ZWEDC

Source: Lawrence Berkeley National Laboratory

Commercial Organics

As discussed above the majority of the mixed commercial waste received at ZWEDC (~5,100 tonnes per month) originates from businesses in San Jose. Commercial solid waste from the city of San Jose that is delivered to ZWEDC is categorized into organic streams (OS) depending on allowable amount of inorganic contamination by weight per load - OS1 (no more than 5% contamination), OS2 (more than 5% and no more than 10% contamination), OS3 (more than 10% and no more than 20% contamination), OS4 (more than 20% and no more than 30% contamination). Additional amounts of mixed municipal waste are delivered to the facility from the city of Palo Alto (~1,100 tonnes per month) and the SMaRT station (~800 tonnes per month).

Yard Waste

Yard waste received at the ZWEDC facility originates from the City of Palo Alto. On average, Palo Alto delivers an average of 1,040 tonnes of yard waste to the facility per month, although only the fraction with sufficiently small particle sizes (material referred to as "fines") is loaded into the digesters, while more bulky material is routed directly to

Z-Best. Generally, this waste is low in residuals and negative externalities are minimal; odor impact is either pleasant or neutral. Based on expected delay rates for herbaceous components such as grass and leaves (discussed in more detail later), these components likely do break down and contribute to biogas yields.

Manure

Manure delivered to ZWEDC facility originates from Los Altos Hills, and includes manure from horse, cow, rabbit, chicken farms. These manures contain less than 5 percent residuals, resembling OS1 waste type, but make up a very small fraction of overall waste intake at ZWEDC.

Biogas Yields and Facility Energy Balance

During the period of January, 2016 to July, 2018 and based on actual facility data, ZWEDC fed approximately 8,279 tonnes of waste to the 16 dry anaerobic digesters monthly, on average. This waste excluded inorganic waste sent to landfill, yard waste (except fines, which are retained for use in the digesters), and recyclables. Thus, supplied waste generated an average of 373,302 cubic meters biogas per month yielding an average of 45 cubic meters (~1600 cubic feet) of biogas per tonne of waste fed into the digester (Figure 5). This is half of the 90 cubic meters per tonne estimated for the Kompoferm system, although that estimate likely does not account for significant inorganic contamination in the waste intake. Out of this produced biogas, 116,760 cubic meters were fed to one of the CHP generators (CHP1) and 126,445 cubic meters were fed to the other CHP generator (CHP2) per month. The remaining biogas was sent to the flare for rich and lean burns with an average of 93,981 and 51,211 cubic meters per month of biogas respectively. On average, about 39 percent of biogas produced at the facility was flared (Figure 6). Along with the biogas, the digester also yields digestate as the byproduct. Approximately 6,875 tonnes per month of solid digestate left the facility, out of which, about 4,041 tonnes was sent to Z-Best for further composting.

Figure 5: Cubic Feet Biogas Yield per Tonne of Waste in Digesters

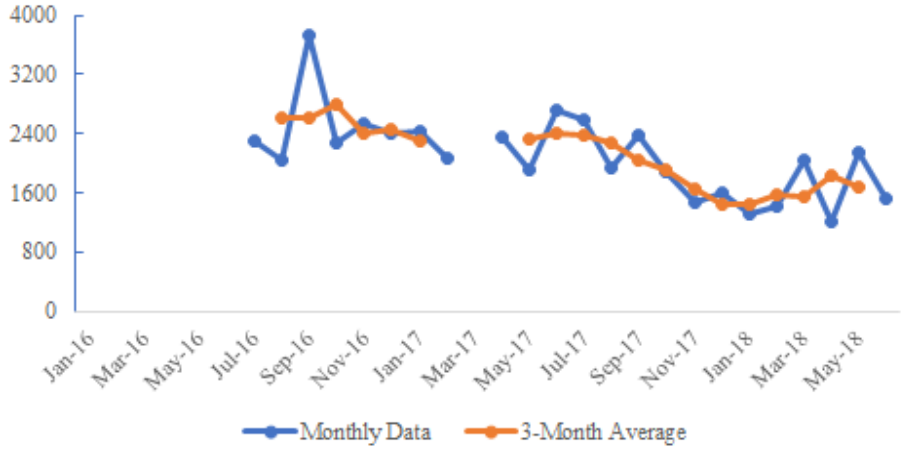

Source: Lawrence Berkeley National Laboratory

Between January, 2016 and July, 2018, the ZWEDC facility consumed 113,180 kWh per month of electricity, on average, to operate waste sorting machinery, anaerobic digesters, lighting, pumping, and other facility end-uses. The plant produced 533,576 kWh electricity every month from the two CHP units (CHP1 and CHP2). This is approximately a 5:1 ratio for energy produced to energy consumed. Net electricity of 420,396 kWh per month, on average, was sold to Pacific Gas & Electric (PG&E) through the BioMAT program. Further, with 5,447 tonnes of waste fed into the digester every month, the energy production per month was 99 kWh per tonne of waste inside the digester (Figure 6). Maximum energy was generated during the month of May, 2016 and January, 2018 had the least energy generation (Figure 6) due to lower than average waste intake.

Figure 6: Electricity Produced per Tonne of Waste in Digesters

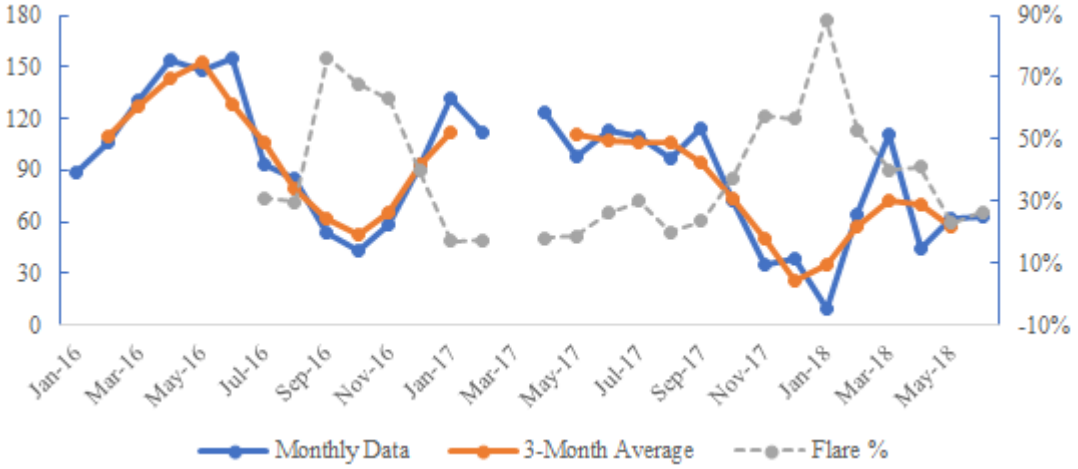

Source: Lawrence Berkeley National Laboratory

Inbound and Outbound Waste Logistics

The majority of the MSW accepted at ZWEDC originates in the City of San Jose and three locations in Santa Clara County: the City of Palo Alto, the Sunnyvale SMaRT Station, and Los Altos. Most of San Jose's MSW food waste as well as Palo Alto's residential green waste is sent to ZWEDC. Various companies and organizations within Santa Clara County, including grocery stores, company offices, and private retailers, also send organic solid waste to ZWEDC via direct-haul. A breakdown of inbound waste by source is shown in Figure 7.

Figure 7: Tonnes of Inbound Waste at ZWEDC Facility from Various Sources

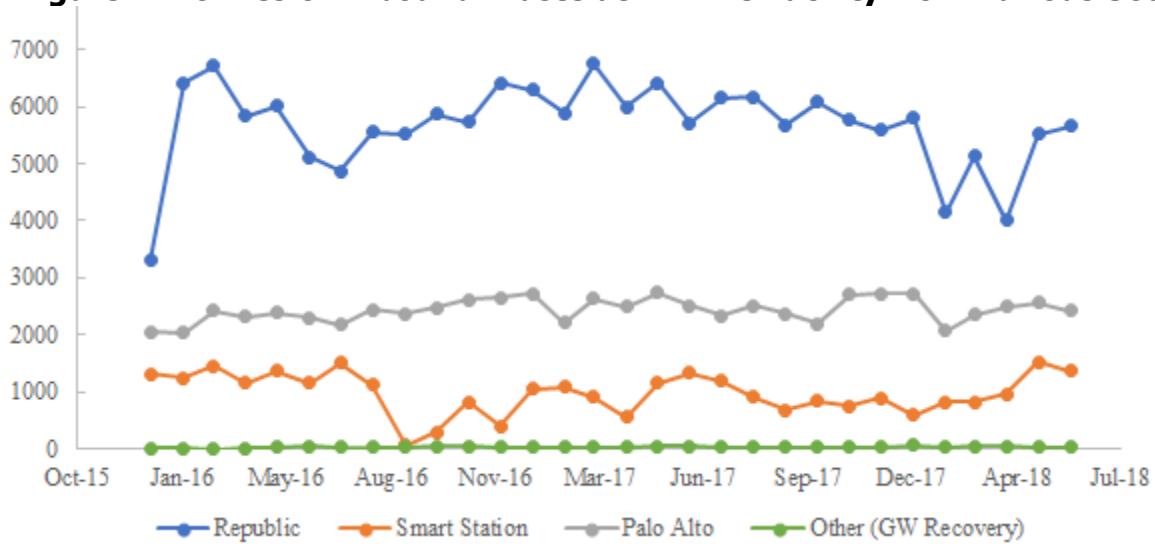

Source: Lawrence Berkeley National Laboratory

Residuals and Recyclables

Inorganics and trash sent to Newby and Marina landfills along with the recyclables are characterized as residuals. Between December, 2015 and June, 2018, the ZWEDC facility delivered an average of 2,030 tons of residuals (consisting of 1,800 tons of trash) to Newby Landfill, 203 tons of trash to Marina landfill, and 13 tons of recyclables sent to a nearby facility (Figure 8).

Figure 8: Tonnes of Outbound Waste from ZWEDC Facility

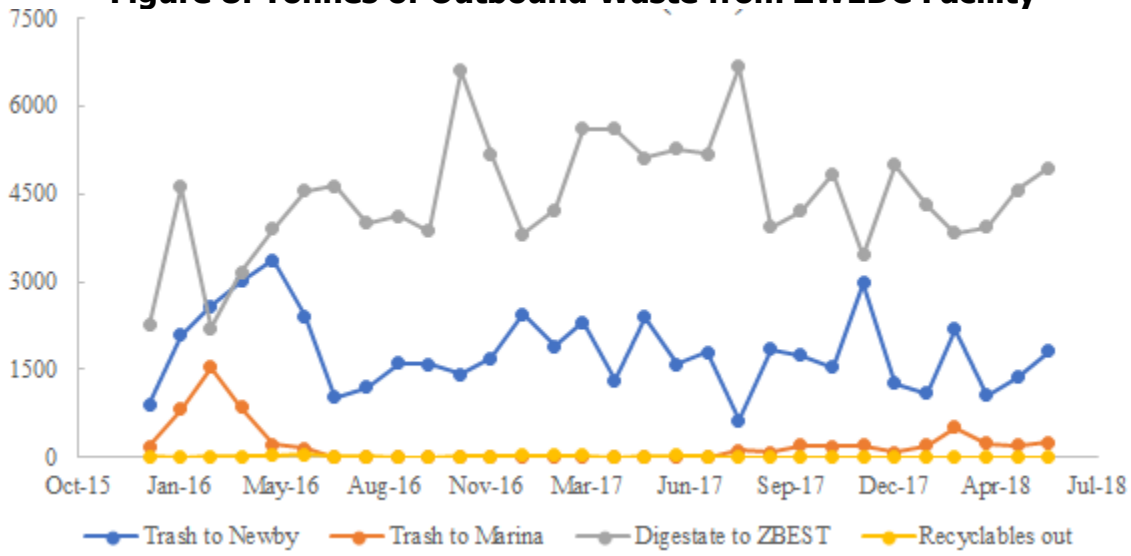

Source: Lawrence Berkeley National Laboratory

Digestate

On average between December, 2015 and June, 2018, 4,450 tons of digestate was sent to Z-Best facility for further composting every month (Figure 8) out of the 6,004 tons of waste that went into the anaerobic digesters. Our measurements show a steady mass reduction of 25 percent between the waste fed into digesters and the digestate ready for shipment to Z-Best. This digestate is bagged in plastic sheeting and kept separate from other organics coming into Z-Best, where it undergoes a 14-week composting process before being sold for landscaping and agricultural uses.

CHAPTER 3:
Air Emissions Measurement, Modeling, and Odor Mitigation

Anaerobic digestion (AD) of municipal solid waste (MSW) and composting of the subsequent digestate material can result in the emission of greenhouse gases (GHGs), toxic air pollutants that may pose human health concerns, and odorous compounds that may be a public nuisance. Additionally, secondary byproducts from reactive compounds may increase atmospheric concentrations of criteria air pollutants, namely ozone and particulate matter.

This chapter describes the measurement and quantification of emissions of these compounds throughout the AD and composting process and dispersion modeling of odorous pollutants. The project team measured emissions from the AD process and operations in situ at the ZWEDC facility and emissions from composting in situ at the Z-Best facility. This work sought to: (1) characterize the sources of emitted air pollutants and quantify the rates of those emissions; (2) suggest possible protocols for taking measurements that are reproducible by others; (3) evaluate the atmospheric transport of odors; and (4) develop a tool to evaluate the potential for adverse impacts on downwind receptors. Goals 1 and 2 support the odor modeling of Goals 3 and 4, serve as inputs for the life-cycle analyses to evaluate the environmental benefits of AD/composting of MSW compared to landfilling that are described in Chapter 4, and advance the state of scientific practice in measuring and quantifying pollutant emissions at waste-to-energy facilities. Outcomes of this research include new information about the relationship between fuel nitrogen content and oxides of nitrogen pollution from the combustion of biogas in enclosed flares, and estimates of the efficacy of emission controls used at the ZWEDC facility. Goals 3 and 4 support the policy and societal implications of siting such waste-to-energy facilities in urban areas.

This chapter is presented in two parts. In Part 1, the direct measurement of emissions at ZWEDC and Z-Best are discussed. In Part 2, the modeling of atmospheric transport of odorous compounds is outlined.

Part 1: Measurement of Air Emissions

Air Pollutants Measured and Their Sources

Table 1 summarizes the pollutant species, their significance, and the sources included in this study. These measurements focused on: GHGs carbon dioxide (CO_2), methane (CH_4), nitrous oxide (N_2O); toxic and odorous ammonia (NH_3), hydrogen sulfide (H_2S), and volatile organic compounds (VOCs); nitrogen oxides (NO_x = NO + NO_2), which are

precursors to atmospheric formation of particulate matter and ozone; and black carbon (BC), a short-lived climate pollutant (SLCP) and product of incomplete combustion.

Table 1: Measured Air Pollutants, Their Significance, and Sampled Sources

Pollutant	Significance	En-closed Flare	CHP	Outdoor Com-posting	Bio-filter	Bladder Vent	Indoor Receiving Hall
CO_2	GHG	●	●	●	●	●	
CH_4	GHG	●	●	●	●	●	
N_2O	GHG	●	●	●	●		
NH_3	Odorous, toxic, PM precursor	●	●	●	●		
H_2S	Odorous, toxic	●	●	●	●		
VOCs	Odorous, PM and O3 precursor			●	●		●
NO_x	Toxic, PM and O3 precursor	●	●				
BC	SLCP	●					

All sampled sources are at ZWEDC in San José, California, except the outdoor composting, which takes place at Z-Best Products in Gilroy, California.

Source: Lawrence Berkeley National Laboratory

As described in Chapter 2, the ZWEDC facility features a negatively pressurized receiving hall that includes waste sorting, sixteen dry anaerobic digesters, and four in-vessel composting (IVC) tunnels. ZWEDC operates four biofilters that are paired in series with acid scrubbers, which together serve as odor and VOC control for the facility's exhaust air system before emission to the atmosphere.

Biogas produced by the AD process is stored in two bladders before it is either (i) combusted for electricity and heat production in two combined heat and power (CHP) units, (ii) flared, or (iii) vented to the atmosphere. The first pathway that produces energy is preferred but if the biogas consumption rate is lower than the production rate, then the bladder biogas pressure rises. To avoid over-pressurizing and rupturing storage bladders, the biogas must either be flared or vented directly to the atmosphere. Flaring is preferred over venting because flaring converts CH_4 to CO_2 and the iron

sponge upstream of the flare removes H_2S. Thus, flaring reduces the emission of a potent GHG and a toxic compound from the facility compared to atmospheric venting. Solid digestate material that remains after the AD process is aerated in the IVC tunnels prior to being trucked to the Z-Best facility for composting.

Consumption of biogas at the CHP units and flare, composting of the post-AD digestate material, processing the facility's air at the biofilters, and venting from the storage bladder are the main emissions sources of air pollutants from this waste-to-energy process. Figure 9 shows the relative amount of biogas consumed at the flare and CHP units. Flaring can include "rich burns" in which rich biogas (>25 percent CH_4) from the storage bladder is intentionally burned to prevent over-pressurization and venting, as described above. There are also regular "lean burns" that occur during the end of each anaerobic digestion cycle when the methane content of the biogas is too lean for combustion in the CHP units (<25 percent CH_4). In this context, lean and rich burns refer to the methane content of the biogas, rather than combustion conditions in the flare.

Figure 9: Biogas Consumption at Flare and CHPs

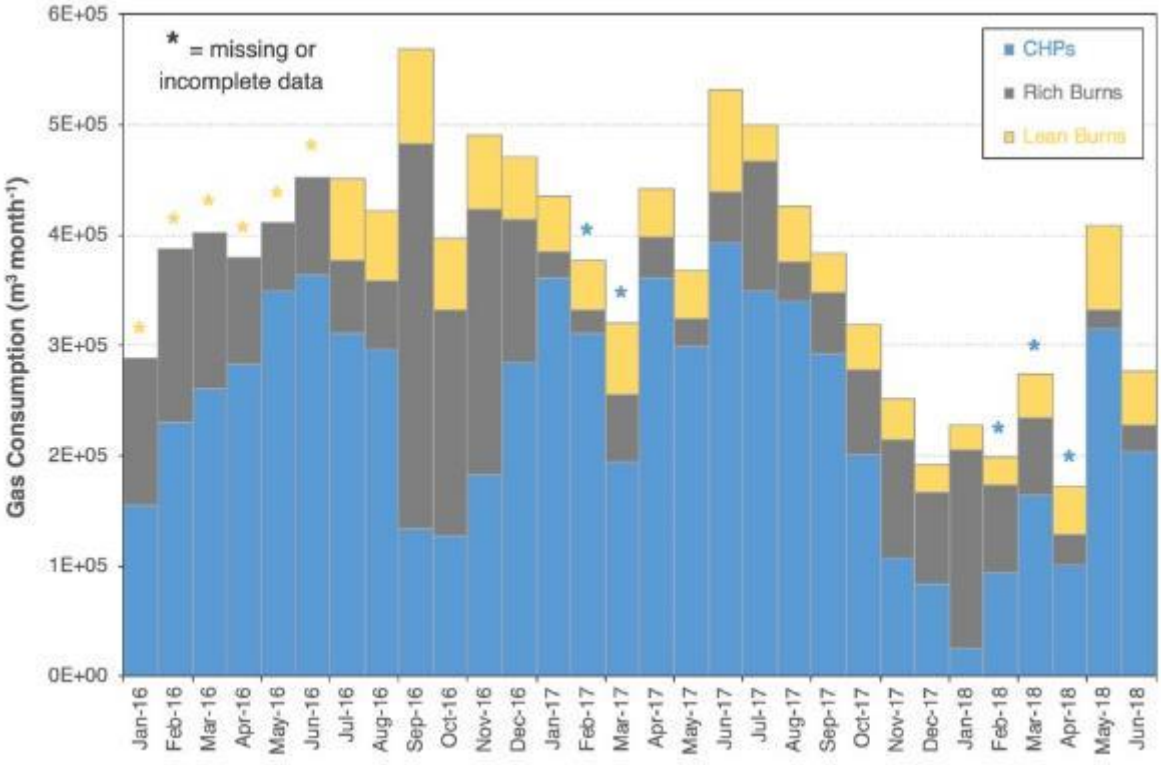

Monthly biogas consumption at the two CHP units and at the flare during both rich and lean biogas burns. Those months with missing or incomplete data due to system communication issues are noted with an asterisk, such that total gas consumption was likely higher than reported during those months.

Source: Lawrence Berkeley National Laboratory

Instrumentation and Emission Factor Calculations

Measurements of pollutant concentrations were made with a suite of fast-responding, high-grade instruments, which are summarized in Table A-1. Measured concentrations were then converted to fuel-based emission factors or time-based emission rates. For the sources of biogas combustion (CHP units and flare), a carbon balance method was used to calculate fuel-based emission factors for each pollutant species, measured in grams of pollutant emitted per kilogram of methane combusted (g per kg, or g kg^{-1}). For the emission sources driven by aerated flow (composting, biofilters, and venting), time-based emission factors were calculated as the product of measured pollutant concentrations and flow rate, and are reported as grams of pollutant emitted per hour (g per hour, or g h^{-1}). Additionally, we calculated emission factors for each species to relate the emitted pollutant mass to the amount of MSW handled and the volume of biogas produced at ZWEDC. For equations and further details on emission factor calculations, please see Appendix A.

Emissions from Enclosed Flare

Flare Operation

ZWEDC employs an enclosed ZTOF® biogas flare system manufactured by John Zink Company (Tulsa, Oklahoma) to convert methane to carbon dioxide when methane cannot be combusted onsite for electricity generation. The flare stack is approximately 2 meters (m) in diameter and 9 m in height. It is designed to operate at temperatures between 760 ºC and 980 ºC to achieve at least a 98 percent destruction efficiency of non-methane hydrocarbons. Flare temperature is measured by thermocouples installed at 5.1 m, 6.7 m, and 8.2 m above ground level. The flare is designed to operate at flow rates up to 1100 m^3 per hour for lean biogas and up to 700 m^3 per hour for rich biogas.

Methane is regularly combusted in the flare at the end of each anaerobic digestion cycle when the methane content of the biogas is too lean for combustion in the CHP units. This lean biogas results from the purging of the digestion chambers at the end of each anaerobic cycle, when ambient air is introduced to the digester so that it can be safely opened and emptied of digestate material. Lean biogas is sent to the flare when the methane content in the digester is <25 percent and continues until the increasingly diluted methane content is less than 3 percent. At this point, the remaining ultra-lean gas (<3 percent CH_4) is sent to the biofilters.

Figure 10 shows an example of flare operations during a typical lean biogas burn. During these lean burn events, the flare is first ignited with rich biogas. The rich biogas is then mixed with the increasingly lean biogas to maintain a blend with about 20 percent CH_4 and combusted at an approximately constant temperature of around 800 to 900 ºC. The flow of lean gas is constant over time, but as the methane content of that lean fuel decreeses from about 25 percent to 3 percent, the flow of rich gas increases to compensate.

In addition to the typical lean biogas burns described above, the ZWEDC facility sometimes uses the flare to burn rich biogas. Such irregular flare use occurs when the accumulation of biogas in the storage bladders exceeds consumption by the CHP units. When the volume of biogas in either of the two storage bladders approaches maximum capacity and bladder pressure exceeds 7 mbar, stored biogas is automatically sent to the flare to prevent unwanted venting of biogas. Such flaring of rich biogas generally occurs when one or both of the CHP units are not operational. If unwanted venting of rich biogas occurred, it would release raw, untreated biogas with typical concentrations of 50 to 55 percent CH_4 and >1000 ppm H_2S directly to the atmosphere.

Figure 10 also shows an example of flare operations during a typical rich biogas burn. During these events, only rich gas is combusted. The flow of rich biogas to the flare and the flare temperature are both relatively constant.

As noted above, the reference to lean and rich burns refer to the methane content of the biogas and does not describe the combustion in the flare. During rich biogas flaring events, the air and biogas are not premixed. During lean biogas flaring events, the air and biogas are somewhat premixed as a result of digester purging, as discussed above. Excess air is drawn into the flare via louvers at the base of the exhaust stack so that the combustion is overall fuel-lean to ensure complete oxidation of the flared biogas. Biogas fuel is not pre-mixed with this excess air prior to combustion.

Figure 10: Typical Lean and Rich Biogas Flaring Events

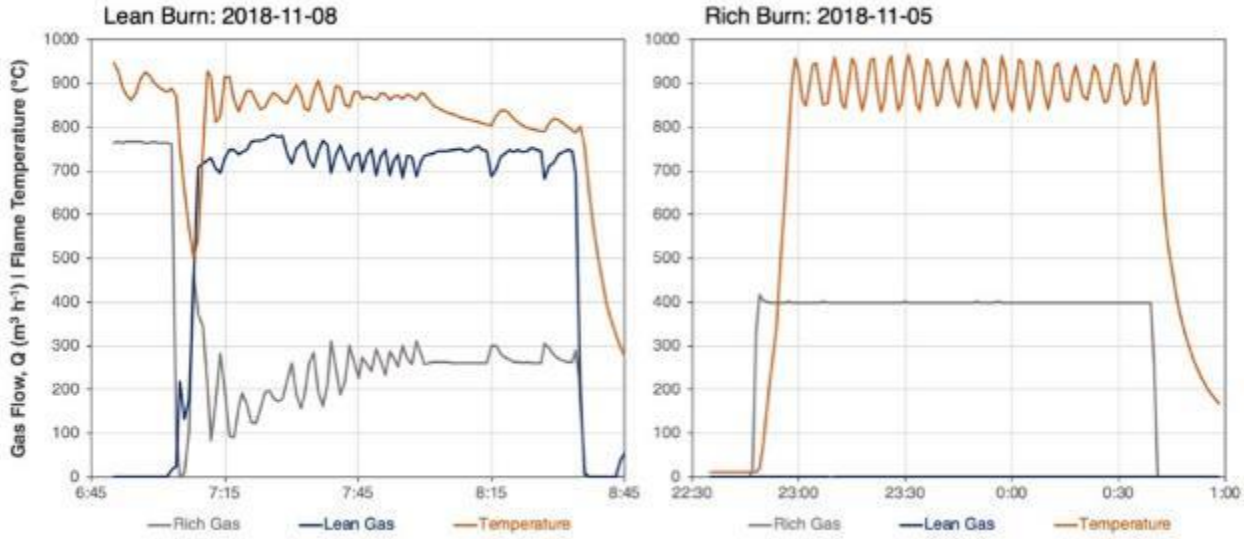

Volumetric flow rates of rich and lean biogas delivered to the flare and reported flare temperature during a typical lean biogas (left) and rich biogas (right) flaring event.

Source: Lawrence Berkeley National Laboratory

NO_x Formation Pathways

NO_x emissions are a common concern from industrial flares. There are two main NO_x formation pathways during lean combustion. In one process, NO_x can be generated

thermally during combustion at flame temperatures above 1600 °C (Flagan and Seinfeld 1988). At these temperatures, molecular nitrogen (N_2) in air can be cleaved to form NO—a formation pathway known as thermal NO_x. NO_x can also be formed from nitrogen-bound species contained in the fuel that are oxidized during combustion—a process known as fuel NO_x (Flagan and Seinfeld 1988). The presence of ammonia and other organic nitrogen compounds in the biogas produced at ZWEDC are likely an important source of such fuel NO_x formation. These nitrogen species in the biogas originate from the nitrogen content of the MSW feedstock, in particular from food waste (Riber et al. 2009; Jokela and Rintala 2003). Because the ZWEDC flare operates at temperatures well below the thermal NO_x threshold of 1600 °C, it is likely that fuel NO_x is the dominant formation pathway for emitted nitrogen oxides.

Current NO_x emission standards for industrial flares are set according to emission estimates from the Environmental Protection Agency (AP-42) that are based upon a 1973 flare emissions study (McDaniel 1983; EPA 1995). These guidelines may underestimate NO_x generation from a biogas flare, however, because the historical industrial flares that serve as the basis for emission estimates contained little to no nitrogen compounds. In contrast, biogas contains significant amounts of ammonia. As a result, the importance of fuel NO_x as a component of nitrogen oxide emissions from the ZWEDC flare and others like it are likely underrepresented. A major focus of the following measurements was to better estimate NO_x emissions, and the relationship between emitted NO_x and the ammonia content of the biogas fuel.

Sampling Flared Biogas and Exhaust

The flared biogas and corresponding exhaust were directly measured multiple times in 2016, 2017, and 2018 to quantify and characterize NO_x emissions from the ZWEDC flare. Ammonia is a major reduced nitrogen species in the biogas and likely the most important source of fuel NO_x. The sampling setup used during the 2016 and 2017 measurements was automated to selectively capture lean biogas flaring events, as this regular flaring was assumed to dominate flare activity. Subsequent analysis of facility operations indicated that rich biogas flaring events occurred more frequently than previously assumed, and visual observations of sooty flaring events indicated black carbon emissions could be significant during these rich biogas burns. In response, the sampling protocol for the 2018 measurement events was modified. These measurements mirrored the previous sampling design and were made continuously for one week to capture both lean and rich biogas burns and a broader set of pollutant species.

A schematic of the sampling setup used in 2018 is shown in Figure 11 and refers to the instrumentation outlined in Table A-1. The automated system used in 2016 and 2017 was similar and is shown in Figure A-1 and Figure A-2 of the Appendix.

Concentrations of NH_3, CH_4, and CO_2 in the flared biogas were measured concurrently with concentrations of CO_2, NO_x, N_2O, CO, O_2, and BC in the flare's exhaust. To prevent condensation losses of NH_3 in the sampling line and to bring the measured

concentrations down to the operational ranges of the instruments, the sampled biogas was diluted with compressed nitrogen from a cylinder by a factor of 6.8 at the sampling port. The sample line was also heated to reduce potential line losses of NH_3. The flare effluent was simultaneously sampled from a port at the top of the exhaust stack, which split to a gas sampling line of Teflon tubing and particle sampling line of conductive tubing. Both of these lines extended down to a condensate trap, featuring three 50 milliliter (mL) glass impingers submerged in an ice water bath. The particle line flowed through two glass impingers that were connected in series and the gas line was connected separately to the third impinger. The outlet of the gas line was diluted with ambient air by a factor of 6.3 to bring concentrations into the operational range of the analyzers. All analyzers were housed for a five-day period in 2018 in a mobile sampling platform that was positioned at the base of the enclosed flare, as shown in Figure 12. Over this period, the system captured four lean burns and thirteen rich burns, as one of the CHP units was not operational. Between 2016 and 2017, the system sampled 25 lean burn events.

Figure 11: Schematic of Flare Sampling System

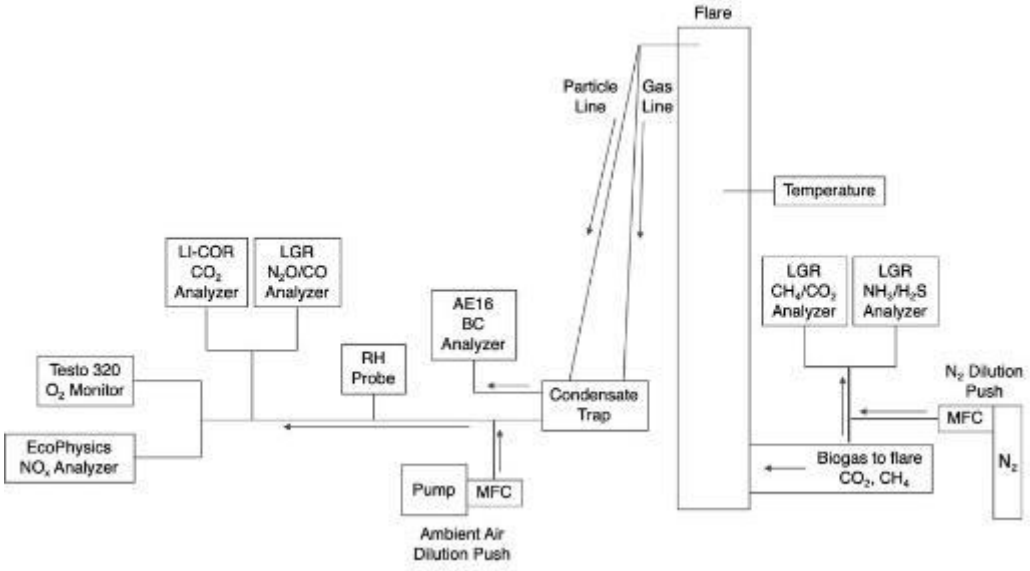

Real-time analyzers continuously sampled from the pipe where biogas is delivered to the flare and from top of the flare stack. The biogas sampling line was heated and immediately diluted, the exhaust sampling lines ran through a condensate trap line, and the exhaust gas line was subsequently diluted. A modified setup was used in 2016 and 2017, as shown in the Appendix.

Source: Lawrence Berkeley National Laboratory

Figure 12: Continuous Sampling Setup at Flare

The mobile sampling platform for continuously monitoring emissions at the flare in 2018. The particle and gas lines extended down from the top of the exhaust stack to the condensate trap and analyzers housed in the mobile platform (left). The line for sampling flared biogas was diluted and heated (right). Biogas is delivered in the green pipe to the right and excess air is drawn in through the louvers at the base of the flare; the fuel and biogas is not pre-mixed before combustion.

Source: Lawrence Berkeley National Laboratory

Relationship Between Biogas Ammonia and Emitted NO_x

NH_3 concentrations increase as the biogas becomes leaner over a digester shutdown. Figure 13 plots the concentration of ammonia measured in the flared biogas and the corresponding emitted NO_x concentration over a typical lean and rich burn. The NH_3 concentration in the flared biogas increases from about 20 ppm to more than 1000 ppm over the course of the lean burn. As the fuel NH_3 increases, emitted NO_x concentrations also increase. During the rich burn, on the other hand, both the fuel NH_3 and emitted NO_x concentrations remain nearly constant around 20 ppm over the course of the flaring event. This difference in fuel NH_3 may be related to changes in pH, as the digestion system shifts during a shutdown from an acidic anaerobic state to an increasingly more alkaline aerobic condition that promotes volatilization of ammonia (Kirchmann and Witter 1989).

Figure 13: Biogas NH_3 Concentration and Corresponding Emitted NO_x Concentration

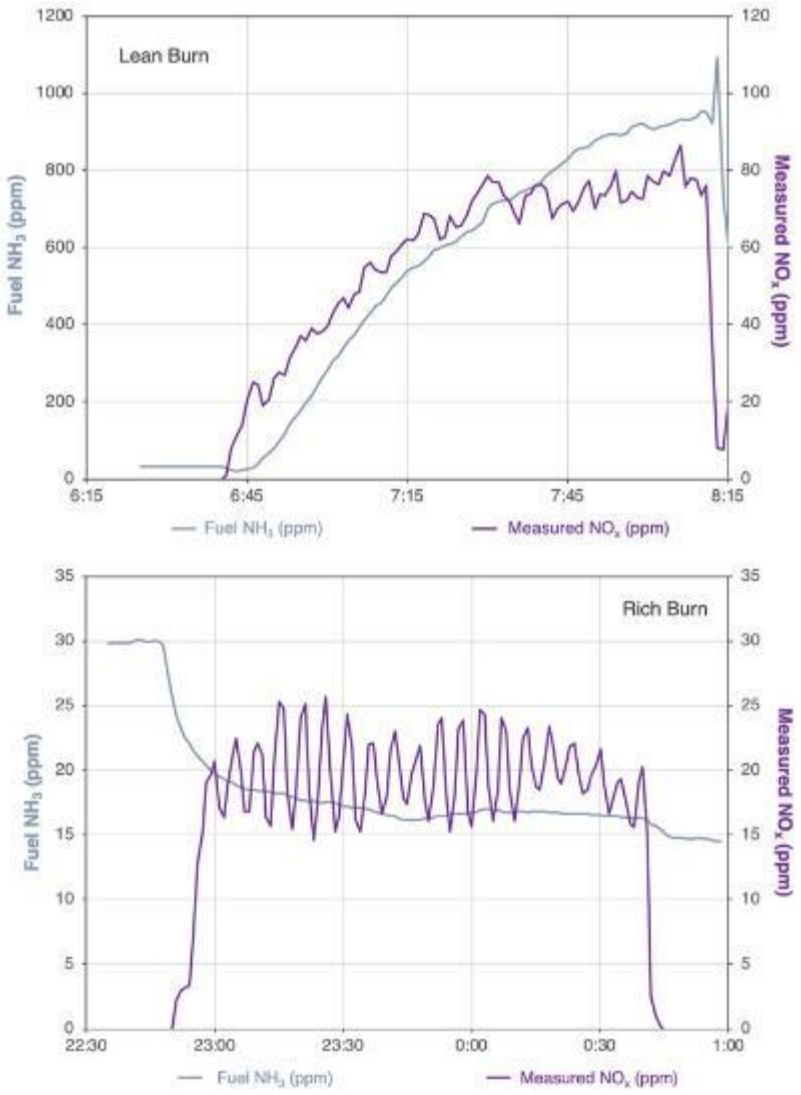

Minute-average concentrations of NH_3 measured in the flared biogas and corresponding emitted NO_x concentration over a typical lean (top) and rich (bottom) biogas flaring event.

Source: Lawrence Berkeley National Laboratory

Figure 14 shows minute-average flare exhaust NO_x emission factors versus the corresponding NH_3 concentration measured in the flared biogas during lean and rich burns sampled in 2018. The NO_x emission rate increases with increasing NH_3 concentration in the flared biogas. When NH_3 concentration exceeds approximately 200 ppm, the fuel NO_x formation pathway dominates. These elevated ammonia concentrations and NO_x emissions are typical of lean biogas flaring events. When the biogas ammonia concentration is below about 200 ppm—typical of rich biogas—the thermal NO_x formation pathway is significant. As a result, reducing the ammonia

content of the flared biogas would reduce NO_x emissions, in particular during lean biogas flaring.

Figure 14: Measured NO_x Emission Factors vs Flared Biogas NH_3 Content

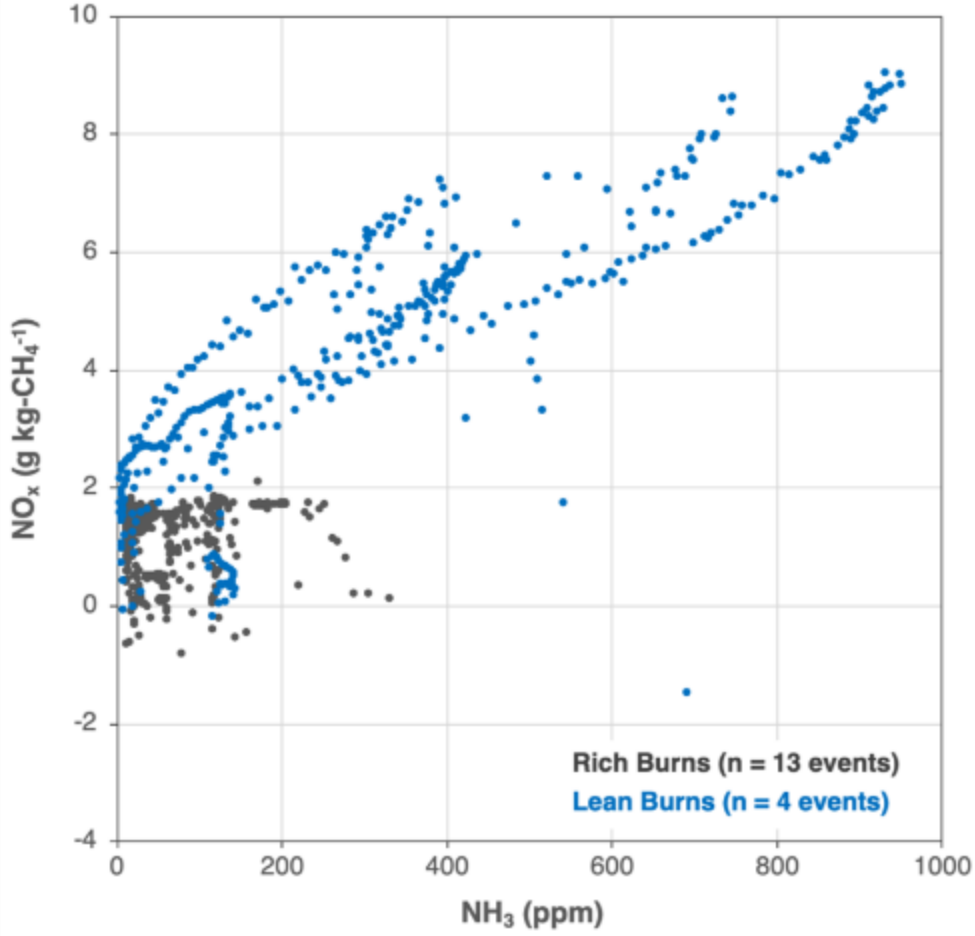

Minute-average measured NO_x emission factors from lean and rich biogas flaring events sampled in 2018 relative to sampled ammonia concentrations in flared biogas.

Source: Lawrence Berkeley National Laboratory

Fuel NO_x formation from nitrogen-containing compounds in fuel is thermodynamically favored under fuel-lean conditions, whereas formation of N_2 is favored when combustion is fuel-rich (Grcar et al. 2005; Flagan and Seinfeld 1988). In pre-mixed combustion, conversion of fuel nitrogen to NO_x can approach 100 percent at equivalence ratios near stoichiometric (Pfefferle and Churchill 1986). Biogas fuel and air are not pre-mixed before combustion in the ZWEDC flare, though. While the flare operates overall as fuel-lean, fuel-rich regions are also expected under these conditions as a result.

The non-zero intercept of the NO_x emission factor trend shown in Figure 14 suggests that the flare would emit NO_x even if there was no NH_3 in the biogas, thereby indicating the presence of thermal NO_x. While the measured flare temperature is very consistently

well below the temperature required for significant thermal NO_x formation (around 900 °C vs 1600 °C), the measured temperature is not indicative of the turbulent flame temperature everywhere. In such a turbulent flame, temperature differs with location and is likely higher than the temperature measured with the fixed thermocouples in some places. Table A-3 in the Appendix summarizes the average emission factors for NO_x and other pollutants quantified for lean and rich biogas flaring events.

Emissions from CHP Units

CHP Unit Design and Operation

ZWEDC employs two combined heat and power (CHP) units. These are lean burn internal combustion engines (2G Cenergy, model 2G-800 BG) that are each rated for 800 kW. Each unit is equipped with a selective catalytic reduction (SCR) system to control NO_x emissions, using ammonia to reduce exhaust NO_x to N_2. An iron sponge ahead of both the flare and CHP units controls sulfur dioxide (SO_2) emissions.

Operation of the CHP units is nominally continuous, with facility operations balancing the need to meet forecasted sales of electricity back to the grid with the production, consumption, and storage of biogas. ZWEDC generally operates each CHP unit around 500 kW, though they are capable of higher maximum power output. ZWEDC has found that operating at this lower output level reduces maintenance and breakdown issues. In late 2017 and early 2018, ZWEDC found it to be a challenge to keep both CHP units running. After routine maintenance of the digester sand traps, the microbial activity in Module 1 significantly dropped off and led to low quality biogas, thereby preventing CHP 1 from operating. Additionally, routine servicing of CHP 2 resulted in delays of several weeks. These issues led to several months of reduced and even no CHP operation, as reflected in Figure 9.

Measurements were taken both when the SCR was operational and when it was not. ZWEDC periodically makes spot measurements for compliance; the project team sampled with a larger suite of instruments over the course of a day to show the temporal variability over CHP operation.

Measurement of CHP Exhaust Emissions

Exhaust from CHP 2 was sampled over an afternoon as the unit operated continuously after a warm start-up. Sampling from CHP 1 was not possible because the heat exchanger suffered corrosive damage, making the exhaust from CHP 1 too hot to effectively measure. Emissions are assumed to be the same from both units.

Exhaust concentrations of CO_2, CH_4, NH_3, H_2S, N_2O, CO, NO_x, and O_2 were measured with the instruments listed in Table A-1. Figure 15 shows a schematic of the sampling setup. To prevent condensation losses of NH_3 in the sampling line and to bring the measured concentrations down to the operational ranges of these instruments, a factor of 7.9 dilution from a compressed nitrogen cylinder was introduced directly at the sampling inlet installed at the CHP exhaust chimney. The sample line extended down

from the exhaust stack to a condensate trap consisting of three 50 mL glass impingers connected in series and submerged in an ice water bath to ensure all analyzers sampled dry exhaust. Figure 16 shows this sampling inlet and dilution tee, as well as the analyzers set up in the mobile sampling platform.

Figure 15: Schematic of CHP Sampling Setup

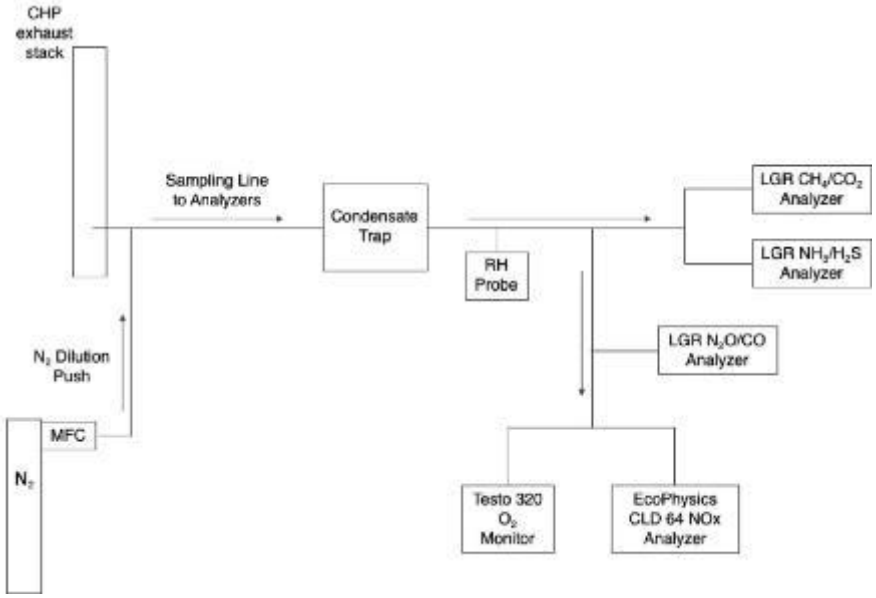

Real-time analyzers continuously sampled from the CHP exhaust stack, with dilution immediately introduced at the sampling port.

Source: Lawrence Berkeley National Laboratory

Figure 16: Sampling Setup at CHP Exhaust

The sampling port installed on the exhaust chimney of CHP 2, with dilution introduced at the tee (left). The analyzers housed in the mobile sampling platform, positioned at the base of the CHP exhaust chimney with sample lines running down from the sampling port (right).

Source: Lawrence Berkeley National Laboratory

Emission Rates

Figure 17 plots the corresponding time series of pollutant emission rates for the steady period of the CHP unit after start-up. These measurements were taken on a day when the SCR was not operating.

The Bay Area Air Quality Management District (BAAQMD) operational permit for ZWEDC limits emissions from each CHP unit to 12.4 ppm NO_x, 121 ppm CO, and 5 ppm NH_3, each corrected to 15 percent O_2. Using the stoichiometric relationship described in Appendix A, these limits equate to fuel-based emission factors of 1.3 g NO_x per kg, 7.9 g CO per kg, and 0.2 g NH_3 per kg. As shown in Figure 17, the measured emission rates of NO_x and CO exceed these permitted values by a factor of 6.3 and 1.4, respectively. The measured emission rate of ammonia, on the other hand, is less than 10 percent of the permitted value. The average CH_4 emission rate of 24 g per kg means 2.4 percent of methane is emitted rather than combusted and converted to CO_2.

Figure 17: Measured Emission Rates from Biogas-Fueled CHP Exhaust (without SCR)

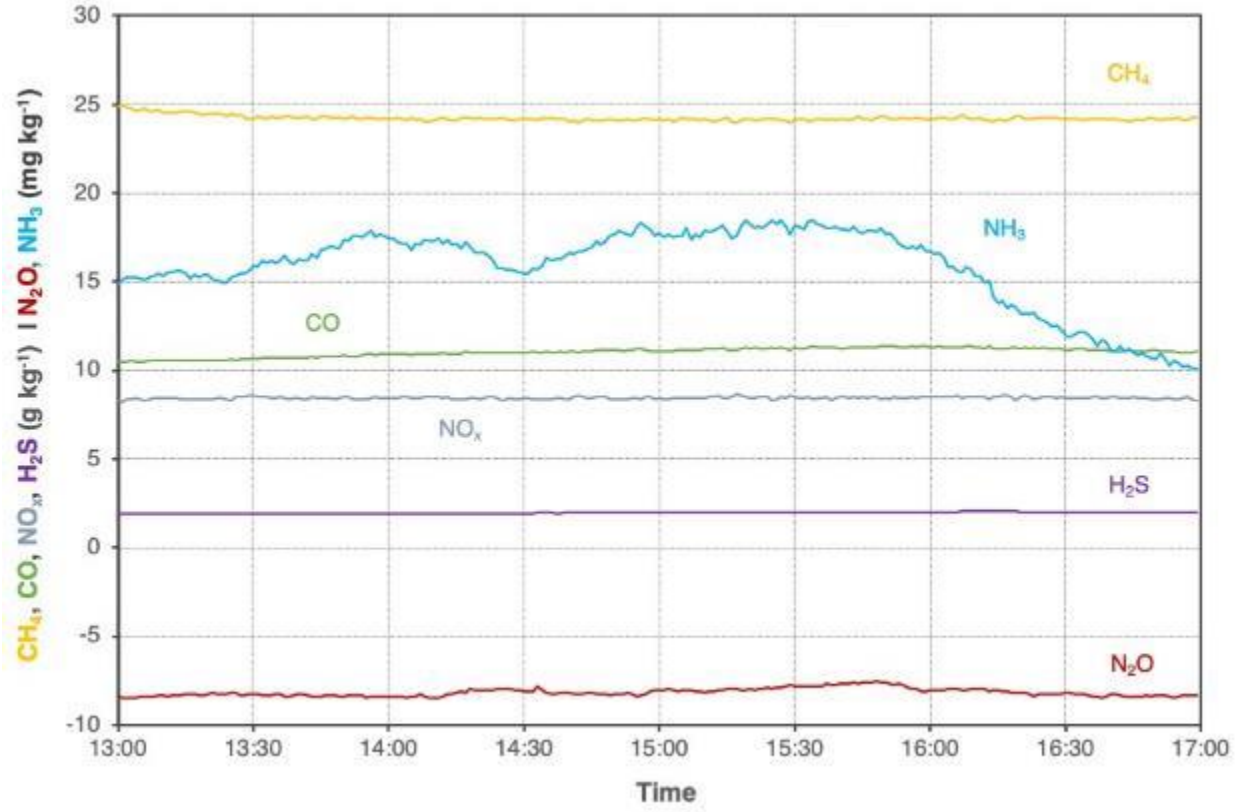

Calculated pollutant emission rates versus time for the steady period of CHP operation after the warm start-up phase. Note that the emission rate of N_2O is negative, which means that ambient nitrous oxide is consumed during combustion.

Source: Lawrence Berkeley National Laboratory

These measurements (Figure 17) were made on a day when the SCR system on CHP 2 was not operating. ZWEDC routinely measures the exhaust from their CHP units to verify that emissions are effectively controlled. Figure 18 plots the average NO_x emission rate (± 95 percent confidence interval) measured over time, with the pre-October 2018 measurements showing effective SCR performance. The results highlight the importance of incorporating a functional SCR system to control NO_x emissions from these CHP units. Without an operational SCR system, NO_x emission rates were 13 times greater than SCR-controlled emissions. The average exhaust concentrations during SCR operation in 2018 were 5.8 ppm NO_x and 36 ppm CO (both at 15 percent O_2), well below the permit limits. Additional CHP emission factors are reported in Table A-4 and Source: Lawrence Berkeley National Laboratory

Table A-5 in Appendix A.

Figure 18: NO_x Emission Rates from CHP Unit over Time

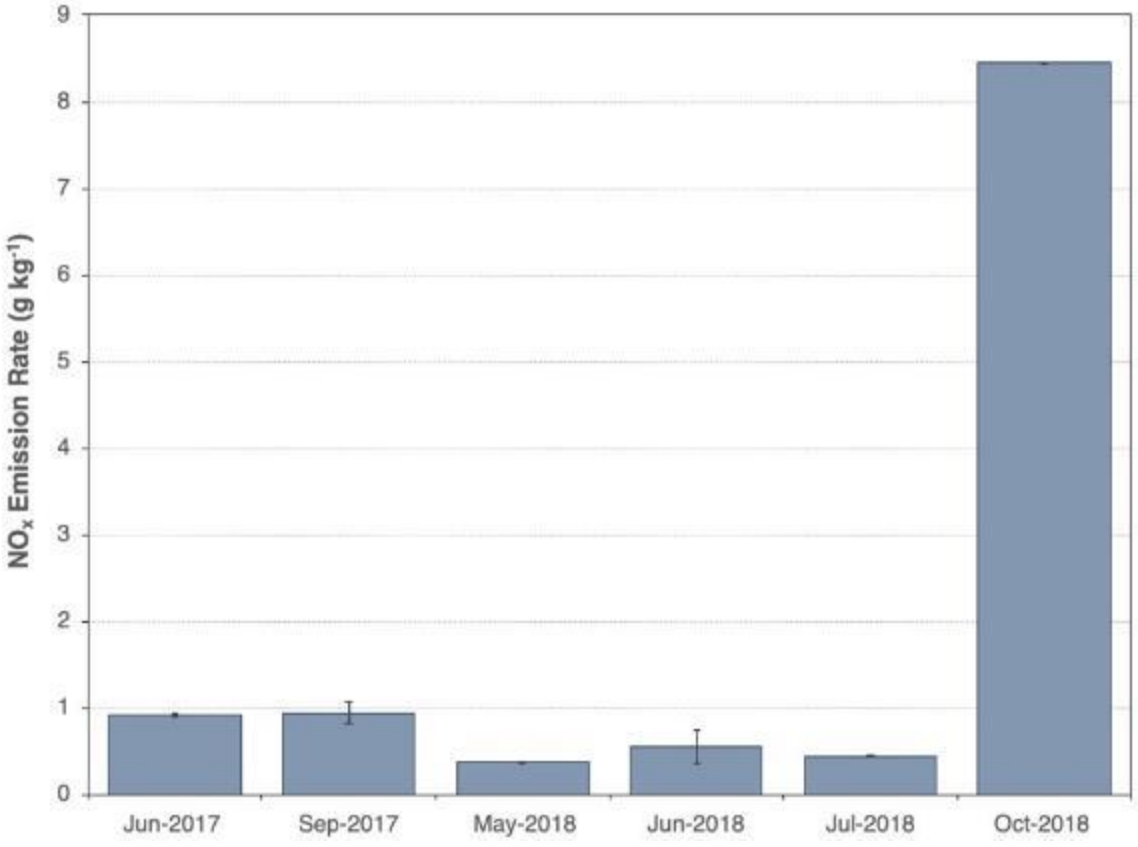

Measurements from June 2017 through July 2018 were made when the SCR system was operational, whereas the October 2018 measurement was made when the SCR system was not. The error bars show the 95 percent confidence intervals about each average value.

Source: Lawrence Berkeley National Laboratory

Emissions from Composting

To estimate greenhouse gas and odorous emissions of composting ZWEDC digestate material, two experimental systems were employed: (1) a laboratory-scale composting system to represent a full 14-week cycle, and (2) the measurement of emissions in-situ at the Z-Best composting facility. The former proved unsuccessful due to an inability to maintain biological activity and sufficient compost temperature at a laboratory scale. Though unsuccessful, a description of the laboratory-scale composting experiments is presented in Appendix A.

Design and Operation of Composting Windrows

Uncovered composting windrows were initially set up on-site at ZWEDC. After receiving numerous odor complaints, ZWEDC moved composting operations offsite in October 2015. Digestate material is now trucked to Z-Best Products in Gilroy, California, an industrial-scale composting facility that employs enclosed aerated static piles to compost MSW.

Each month, ZWEDC trucks approximately 4400 tons of digestate material to Z-Best. This material is placed into commercial composting bags that are approximately 100 meters long, 6 meters wide, and 3 meters tall when filled, as shown in Figure 19. A filled bag is referred to as a windrow. Each windrow is aerated using two blowers at the pile head that supply air into two perforated pipes that are buried longitudinally along the bottom of the pile. Vent holes are cut into each bag approximately 2.5 meters from the ground around every 5 meters on either side of the pile.

Figure 19: Encased Composting Windrows at Z-Best Products

Encased composting windrow at Z-Best Products in Gilroy, California, filled with ZWEDC digestate material and aerated by two blowers (left). Windrows are approximately 100 m × 6 m × 3 m when filled, and are placed in close proximity to one another (right).

Source: Lawrence Berkeley National Laboratory

Each windrow is left composting for approximately 14 weeks, during which time the two blowers independently and regularly cycle on and off. For example, a blower may be set with a total aeration cycle of 60 minutes, during which the blowers are on and active for 40 percent of that cycle. The piles are not turned or otherwise altered during the time. After 14 weeks, the plastic bag is opened and the remaining material is removed and screened for usable compost. Residual inorganic material is sent to the landfill. On average, a full-length windrow bag holds approximately 700 tons of material. After the 14-week composting cycle, about 500 tons of material typically remain.

In-Situ Measurements at Z-Best: GHGs and Odorous Compounds

A sampling procedure was designed to measure the spatial and temporal variability in emitted GHGs and odorous compounds across multiple windrows over the 14-week composting cycle. This method relied on simultaneously measuring the forced aeration flow provided to each pile and the corresponding concentrations of emitted gas from vent holes.

Aeration flows into each windrow from the two supply blowers were measured using differential pressure sensors. Pairs of integrating pitot tubes (Dwyer Instruments, Michigan City, IN; averaging flow sensor series PAFS-1005) were installed in the middle of two 6-inch diameter ducts that were then placed between each blower and its corresponding aeration pipe. Figure 20 shows an example of this continuous flow monitoring setup.

Figure 20: Measurements of Windrow Blower Flows

Measurements of blower flow delivered to each aeration pipe at the bottom of the windrow pile, monitored continuously by integrating pitot tubes.

Source: Lawrence Berkeley National Laboratory

The concentrations of the gases emitted from the windrow were measured by collecting spot gas samples at many locations across a pile, at several dates during a composting cycle, and from several windrows. Emitted gas was collected into metal-foil-lined sampling bags (Calibrated Instruments, McHenry, MD; Cali-5-Bond gas sampling bags), as shown in Figure 21.

Figure 21: Bag Sampling of Emitted Gas from Composting Windrow

Collection of emitted gas from into sampling bags by syringe. To ensure that the sampled volume was undiluted by ambient wind passing over the surface of the vent, the syringe sample was pulled from the base of a short chimney that was installed inside of the vent hole. This sampled volume was then pushed into the sampling bag and taken back to the lab for analysis.

Source: Lawrence Berkeley National Laboratory

The end of a 2-inch diameter, 12-inch long PVC pipe was inserted into openings of the plastic sheeting covering the composting pile. This chimney ensured that the sampled volume of gas was not diluted by ambient wind. The sampling point openings were either already cut into the windrow bag by Z-Best technicians as part of the regularly spaced vents described above, or were made by the researchers as ~2-inch wide cuts. Gas was drawn from within the PVC pipe using disposable syringes and then injected into the sampling bags. Typically, each sample bag was filled with 140 mL of emitted gas.

Bag samples were collected at ~35 locations on each windrow during a sampling event, including along the top and on each side of the pile. The bag samples were all taken within approximately one hour by three to six people, with the blower flow held constant for that sampling window. Bag samples were taken when the aeration blowers were both on and off. Field blanks and duplicate samples were collected. The team also verified the stability and repeatability of gas concentrations measured from the

sampling bags by analyzing the same sample bag multiple times over several days. Additional details are provided in Appendix A.

Results and Estimation of Emission Rates

For all compounds measured, there is not a discernible trend in the concentrations of the emitted gases as a function of windrow age. One might expect to see a trend over the composting cycle that relates to biological activity. Although there are noticeable differences shown in Figure 22 through Figure 24, it appears that the spatial variability is as significant, or more so, than any differences that might be attributable to the age of the composted material or stage of composting. There do seem to be some differences in emitted concentration that could be related to composition or windrow aeration; the distributions of CH_4, CO_2, and N_2O from windrow A-21 (shown in red) are shifted towards higher concentrations and/or have wider ranges than the other four piles, regardless of age. The significant levels of emitted CH_4 concentrations over the full 14-week cycle indicate that some anaerobic activity persists.

Figure 22: Distributions of Measured CH_4 Concentrations by Windrow

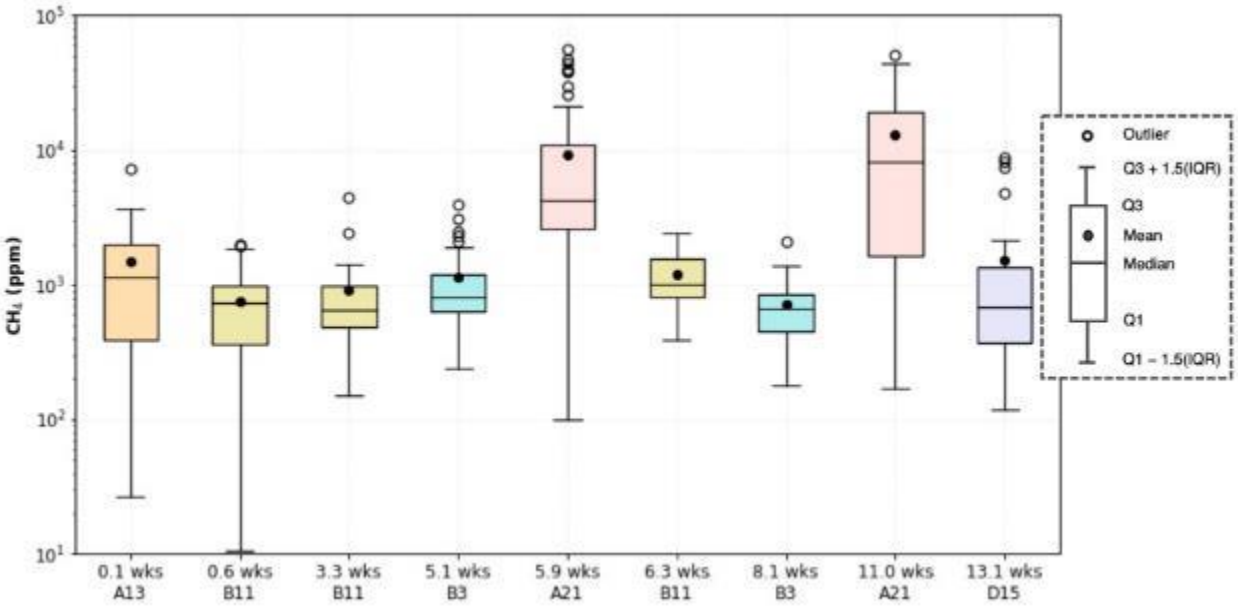

The horizontal axis shows unique identification names of the windrow sampled and the age of the windrow when samples were taken. Note that multiple windrows are listed in some cases. Windrows sampled multiple times during the 14-week composting process are color code matched. Note that the y-axis is a log scale.

Source: Lawrence Berkeley National Laboratory

Figure 23: Distributions of Measured CO_2 Concentrations by Windrow

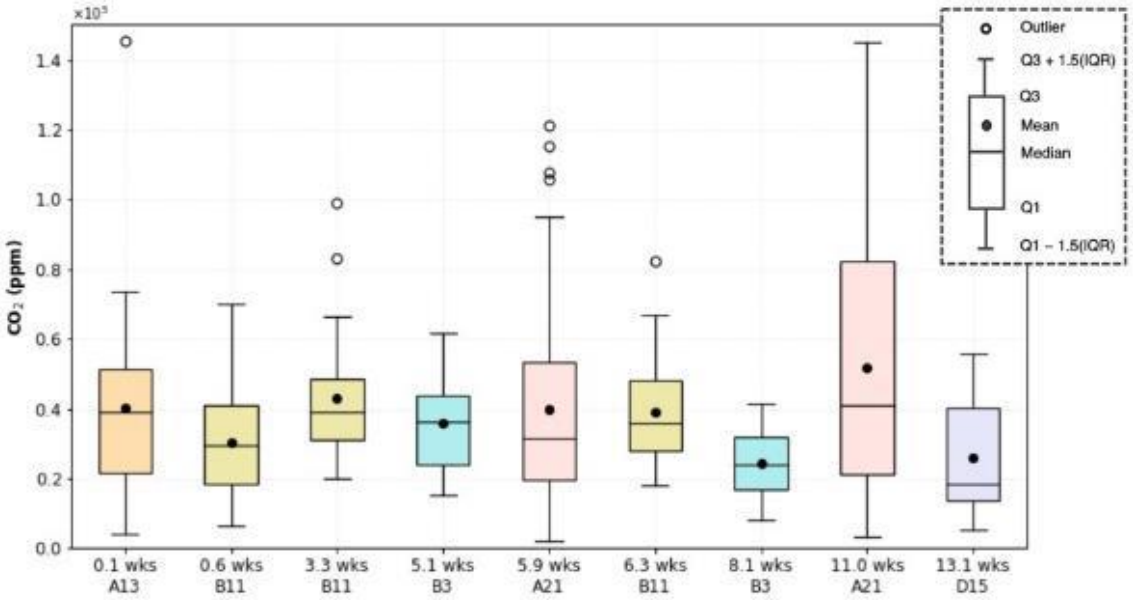

The horizontal axis shows unique identification names of the windrow sampled and the age of the windrow when samples were taken. Note that multiple windrows are listed in some cases. Windrows sampled multiple times during the 14-week composting process are color code matched.

Source: Lawrence Berkeley National Laboratory

Figure 24: Distributions of Measured N_2O Concentrations by Windrow

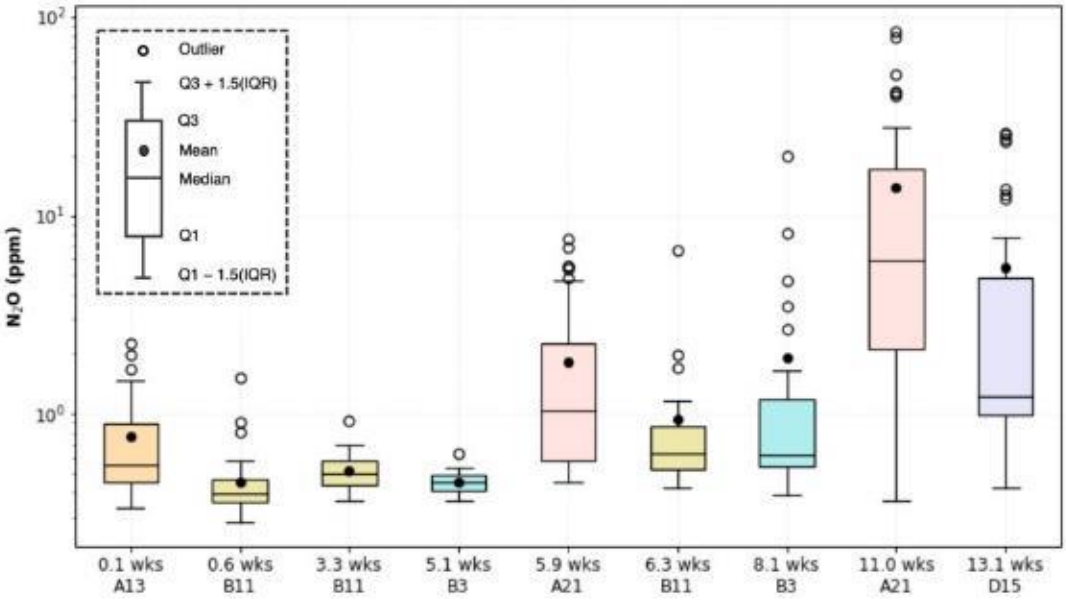

The horizontal axis shows unique identification names of the windrow sampled and the age of the windrow when samples were taken. Note that multiple windrows are listed in some cases. Windrows sampled multiple times during the 14-week composting process are color code matched. Note that the y-axis is a log scale.

Source: Lawrence Berkeley National Laboratory

For each sampled windrow, an average emission rate in units of mass of pollutant emitted per hour per windrow pile was calculated as the product of the average emitted concentration and the effective hourly aeration flow rate. The average concentration of emitted gas from each windrow was calculated as the average of all bag samples taken during a sampling window (about 1 hour) and converted to mass units. The effective hourly volumetric flow rate supplied to the pile was determined from the sum of the two measured blower flows during the sampling window and their cycle settings, as summarized in Table A-6 in Appendix A. The pollutant mass emitted when the blowers were off was assumed to be negligible relative to the amount of mass emitted when the blowers were active, as discussed above.

In-Situ Measurements at Z-Best: VOCs

The bag sampling method described above was not sufficient for measurements of the broader set of VOCs, as the collected volumes were too small and the stabilities and recoveries of some compounds in the sample bags were poor. Given these constraints, VOC samples were separately collected at Z-Best from two additional windrows using a separate integrated sampling approach that was designed to capture to the bulk of emissions from each enclosed composting pile.

The sampled windrows were both aged approximately 4 weeks, thus giving a snapshot in time of emissions rather than a time history. The aeration flow into each pile during the measurement period was held at a constant, time-averaged rate that was based on the two blower settings. This method assumes that the total volumetric emission flow out of the compost pile is equal to or greater than the amount of aeration flow provided.

A set of five dilution chambers were distributed along the windrow's top centerline over holes cut into the composting bag, with all other accessible vent holes sealed so that the bulk of emitted gases were captured by the chambers. Emissions from the compost pile into the chambers was first diluted with a high flow of ambient air to quickly reduce the sample humidity, with the ambient dilution rate estimated via a mass balance on water vapor concentration. Next, a fraction of the diluted exhaust was drawn from each dilution chamber into a sampling trunk line by vacuum, further diluted with dry air, and delivered to a sampling manifold. Integrated samples were collected on different sampling media, depending on the target chemical. Further details of the sampling method and sample analysis are provided in Appendix A.

Results and Estimation of Emission Rates

The targeted chemical analysis included 102 VOC species and used three different analytical methods that are described further in the Appendix. The target species were selected based on known odor causing chemicals and a screening analysis that compared mass spectra in collected samples to the NIST mass spectral library. All targeted species were quantified using calibrations prepared from pure standards. Figure 25 presents the average emission rates of these targeted VOC, where the 102

individual target species are categorized by chemical class based on structure and/or major functional groups. The number of individual species included in each VOC class is noted in the figure. These targeted species represented about 60 percent of the total VOC (TVOC) mass in these samples, and their emission rates varied by two orders of magnitude between phthalates and ketones.

A secondary non-targeted analysis identified 250 species that contribute to TVOC mass emissions. In this non-targeted analysis, mass spectra were compared to the NIST mass spectral library and chemicals were qualitatively identified. Rather than quantify each species using a pure standard, the chemicals were converted to toluene-equivalent concentrations and similarly categorized by chemical class. The average contribution of each chemical class to TVOC in the non-targeted analysis is shown in Figure 26, with an average TVOC emission rate as toluene-equivalents of 17 g TVOC emitted per hour per windrow. Aromatics, alkenes, alkanes, and terpinoids comprise the largest fractions of emitted TVOC and together represent two-thirds of the total. On a mass and time integrated basis, this emission rate is equal to 63 mg TVOC emitted per kg of digestate material composted per 14-week cycle, assuming that the snapshot measurement applies over the entire composting cycle.

Figure 25: Composting VOC Emission Rates Based on Targeted Species Analysis

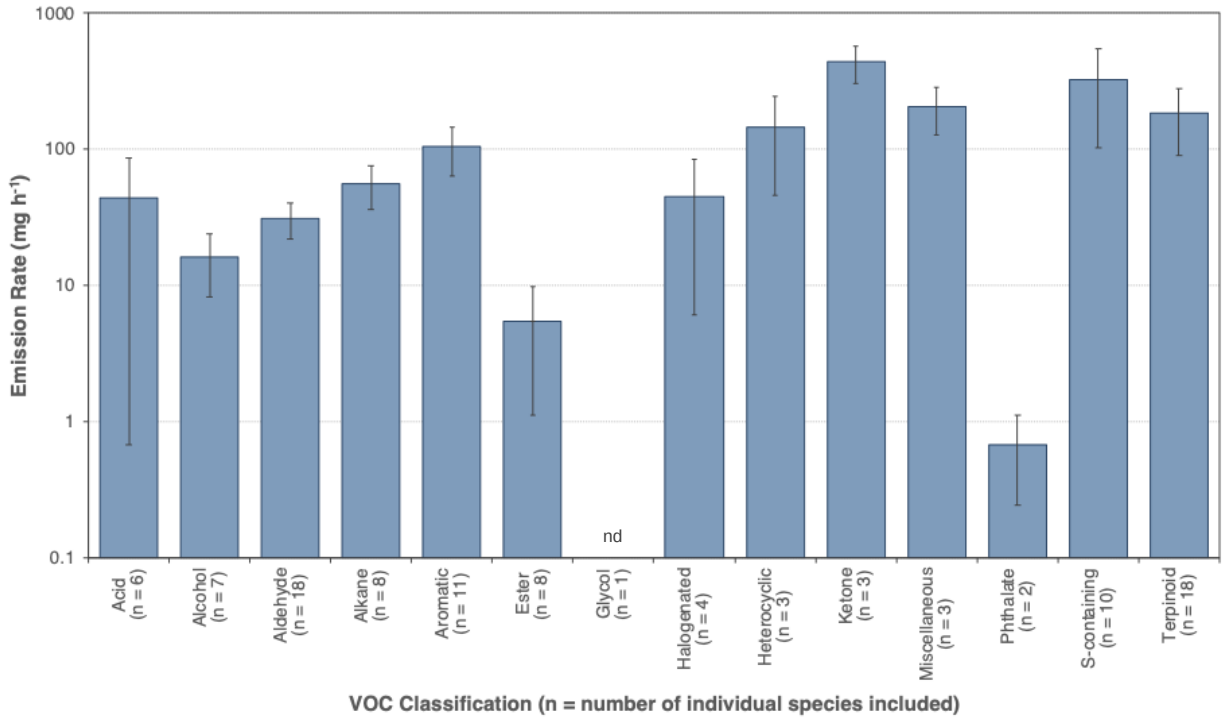

Average (± 95 percent confidence intervals) VOC emission rates from the composting windrows sampled at Z-Best, categorized by chemical class and based on a targeted VOC sample analysis. The concentration of emitted glycol species was below the limit of detection, indicated with *nd*. The number of individual species (*n*) included in each class is noted on the x-axis. The y-axis is presented as a log-scale.

Source: Lawrence Berkeley National Laboratory

Figure 26: Speciated Total VOC Emissions from Composting

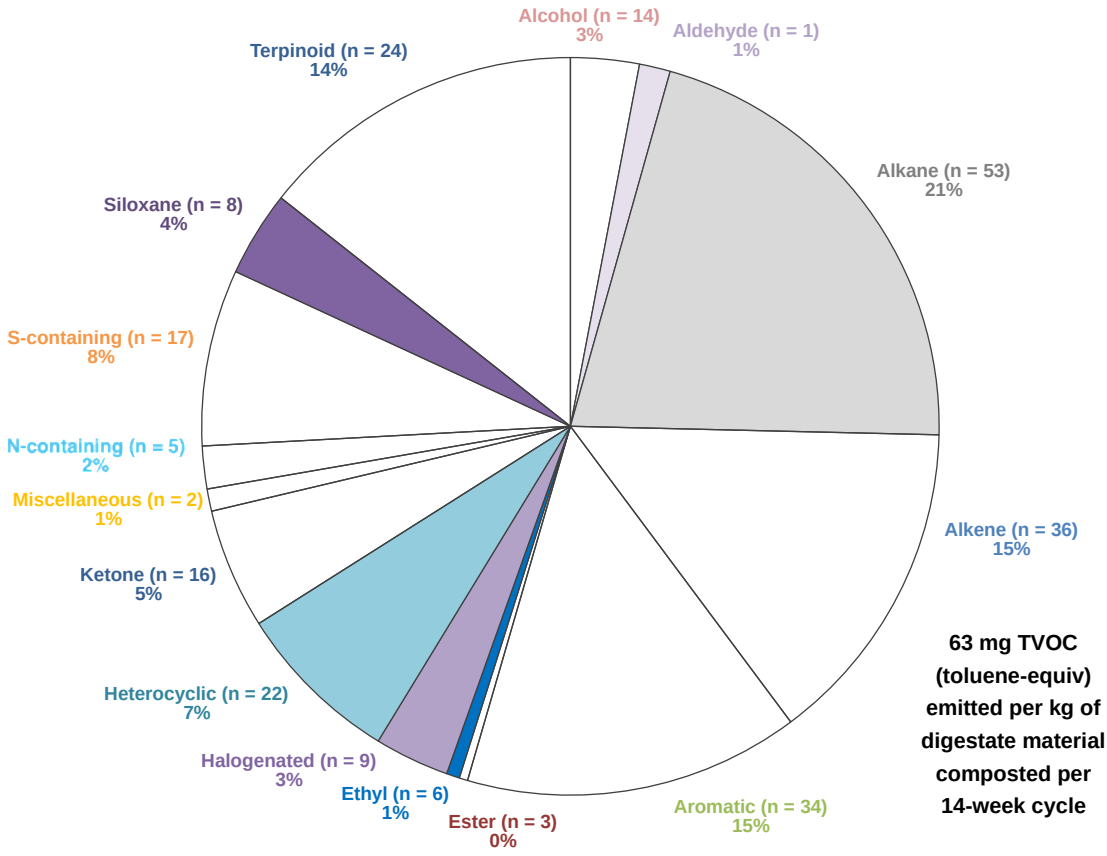

Speciated fraction of total VOC (TVOC) emitted from the composting windrows sampled at Z-Best, based on a non-targeted sample analysis that identified 250 species that were then categorized by chemical class. The number (*n*) of individual species in each class is noted along with each category's percent contribution to the toluene-equivalent TVOC emission rate.

Source: Lawrence Berkeley National Laboratory

Emissions from Biofilters

Biofilter Design and Operation

ZWEDC operates four biofilters that are downstream of two acid scrubbers. Together, these systems serve to remove pollutants from the facility's exhaust air system. They continuously process approximately 53,000 m^3 per hour of air that collectively comes from the negatively pressurized receiving hall, ultra-lean biogas containing less than 3 percent CH_4 from digester start-up and shutdown phases, and effluent from the IVC tunnels that aerate digestate material prior to being trucked to Z-Best for composting. Each biofilter is 25 feet in diameter and paired to an acid scrubber: Biofilters 1 and 2 are paired to one acid scrubber and Biofilters 3 and 4 are paired to the other. The biofilter substrate is kept sufficiently wet to promote a viable biofilm via a sprinkler system atop each biofilter surface. Figure 27 shows the facility's exhaust air system

feeding into the two acid scrubber units, the paired biofilters in series, and the sprinkler systems on top of the biofilters.

Figure 27: Acid Scrubbers and Biofilters

Facility air exhaust system, downstream acid scrubbers, and biofilters. Each acid scrubber is paired to two biofilters (left). Each biofilter substrate is kept sufficiently wet for effective control of odorous air pollutants via sprinkler systems (right).

Source: Lawrence Berkeley National Laboratory

Temporal Measurements of Emissions

Concentrations of CO_2, CH_4, NH_3, and H_2S were measured continuously from a single location on the surface of one of the four biofilters over a period of four days, as shown in Figure 28. Concentrations were then measured continuously from the biofilter inlet, just downstream of the acid scrubber, over a subsequent five-day period. Though these measurements were not made concurrently, they provide an estimate of the pollutant removal of these emission controls over various modes of ZWEDC's operations including digester shutdowns, IVC activity, and treatment of air from the indoor waste receiving hall.

Figure 28: Real-time Sampling on Biofilter Surface

Ultraportable spectrometers continuously measured concentrations of CO_2, CH_4, NH_3, and H_2S from just above the biofilter surface for a period of four days.

Source: Lawrence Berkeley National Laboratory

Concentration time series from these measurements at the biofilter inlet and exhaust are shown in Appendix A (Figure A-32 and Figure A-33). Figure A-33 includes periods when digesters were shut down and ultra-lean biogas was sent to the biofilters. The time period shown in Figure A-32 did not include a digester shutdown, which is a possible reason for the lack of these peaks. However, the magnitudes of these peaks are an order of magnitude lower than the concentrations of NH_3 found in the biogas during shutdowns (average of approximately 300 ppm NH_3; see Figure 13). Exhaust concentrations of CO_2 and CH_4 exceed ambient concentrations, meaning these GHGs should be considered in the LCA (Task 3).

Average concentrations of odorous NH_3 and H_2S measured at the biofilter inlet and exhaust are summarized in Figure 29, with 95 percent confidence intervals included as bars around the plotted mean values. The average NH_3 concentration at the biofilter inlet is two orders of magnitude greater than the average concentration measured in the biofilter exhaust. The average biofilter inlet H_2S concentration is an order of magnitude greater than the average exhaust concentration. These observations indicate that the biofilter and acid scrubbers effectively control NH_3 emissions.

Figure 29: Biofilter Inlet vs Exhaust NH_3 and H_2S Concentrations

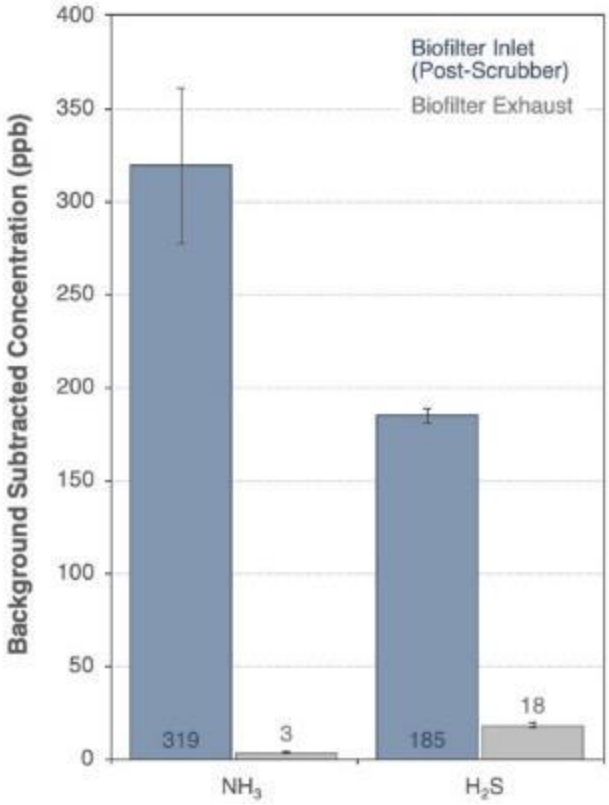

Average concentrations (± 95 percent confidence intervals) of odorous NH_3 and H_2S measured at the biofilter inlet and exhaust. Though these measurements were not made concurrently, they provide an estimate of the pollutant removal of these emission controls.

Source: Lawrence Berkeley National Laboratory

Spot Measurements to Estimate Spatial Variability

In addition to the above continuous measurements at a single location, samples of emitted GHGs and toxic/odorous compounds were collected across the surface of all four biofilters to characterize the spatial variability of emissions and determine pollutant emission rates. As shown in Figure 30, spot measurements were made by inserting the end of an approximately 16-inch long and 6-inch diameter aluminum duct into the surface of the biofilter. Gas was drawn from within this chimney using disposable syringes. The gas samples were then injected into metal-foil-lined sampling bags (Calibrated Instruments, McHenry, MD; Cali-5-Bond gas sampling bags). Typically, each bag was filled with 420 mL of emitted gas. Sample bags were brought back to the laboratory, and compressed nitrogen was added to each to dilute the sample by a factor of 4.8. The dilution enabled sufficient sampling volume for a steady-state response by the analyzers and reduced the relative humidity of the sample (<30 percent) as required by the analyzers. The analyzers used are outlined in Table A-1. Bag samples were collected at the same sampling locations on each biofilter surface three times in the course of one day of operation.

Figure 30: Biofilter Exhaust Spot Sampling

Sampling locations are noted by pink flags (top). Samples were collected into syringes from the base of chimneys that were inserted into the biofilter surface, and then pushed into gas sample bags for subsequent analysis in the lab (bottom).

Source: Lawrence Berkeley National Laboratory

Figure 31 shows the sampling locations on Biofilter 3 and the average emitted concentrations of CH_4, CO_2, N_2O, and CO measured at each sampling spot over the three sampling periods. Similar concentration gradient plots are shown for all four biofilters as Figure A-34 through Figure A-37 in the Appendix. Spatial plots of NH_3 and H_2S concentrations are not shown as they were limited in sample number. The team sampled Biofilter 3 more heavily than the other three biofilters to observe the spatial variability in surface concentration.

Concentrations of CO_2 above background were highly correlated with excess CH_4 concentrations ($R^2 = 0.91$), as shown in Figure A-38 in the Appendix. Exhaust CO_2 was also correlated with above-background N_2O concentrations ($R^2 = 0.57$). The NH_3 and H_2S sample sizes were small but the resulting concentrations were very correlated to one another ($R^2 = 0.91$). The high degree of correlation indicates that three GHG species are co-emitted by the same sources. The same can be said of the two toxic/odorous species.

Figure 31: Spatial Gradients of Measured Concentrations

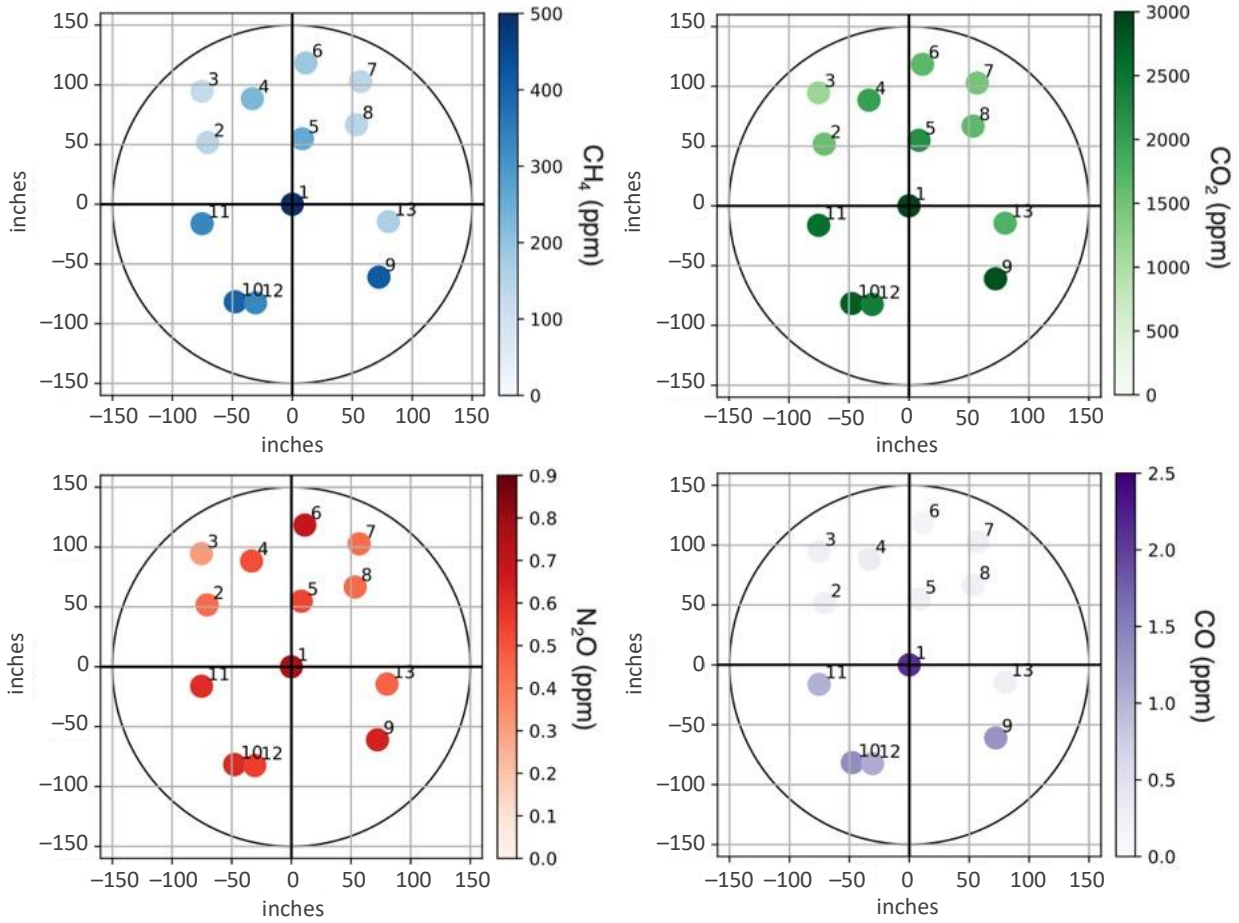

The axes show the relative locations of samples taken across the surface of Biofilter 3, which is 25 feet in diameter. The marker color represents the average exhaust concentration measured at that location, as indicated by the scale bar for each pollutant species. Plotted concentrations have been corrected for the factor of 4.8 dilution, but are not background subtracted. The numbers adjacent to each marker note the sample location number.

Source: Lawrence Berkeley National Laboratory

VOC Measurements

When the above-described spot measurements were made, VOC samples were also taken using a series of flux chambers across the surface of Biofilter 3. These chambers were connected to a trunk line that delivered diluted exhaust to a sampling manifold. Samples were simultaneously collected directly from the upstream supply line for the biofilter being tested, post-acid scrubber. Samples were collected sequentially from the supply line and in parallel from the surface sampler manifold. The VOC concentrations in the biofilter exhaust and upstream supply line were measured using four integrated sampling methods that targeted different compounds: (i) volatile carbonyls collected on adsorbent cartridges (USEPA Method TO-11); (ii) volatile amines collected on sulfuric acid coated filters followed by derivatization; (iii) volatile acids collected on silica gel cartridges; and (iv) volatile organic compounds collected on thermal desorption sorbent

tubes (USEPA Method TO-17). The sampling was conducted for a full day capturing normal operation of the facility, including a digester shutdown. Additional details about the sampling and analysis methods are included in Appendix A.

The average concentrations by chemical classification measured at the biofilter supply line and across the biofilter surface are shown in Figure 32. The 102 species included in this targeted analysis were categorized by chemical class. The number of individual species in each VOC class is indicated in the figure. With the exception of the halogenated and miscellaneous species (77 percent and 91 percent removal efficiency, respectively), the biofilters remove 95–99 percent of each VOC class on average and TVOC removal efficiency exceeded 98 percent.

Figure 32: Biofilter Inlet vs. Exhaust VOC Concentrations

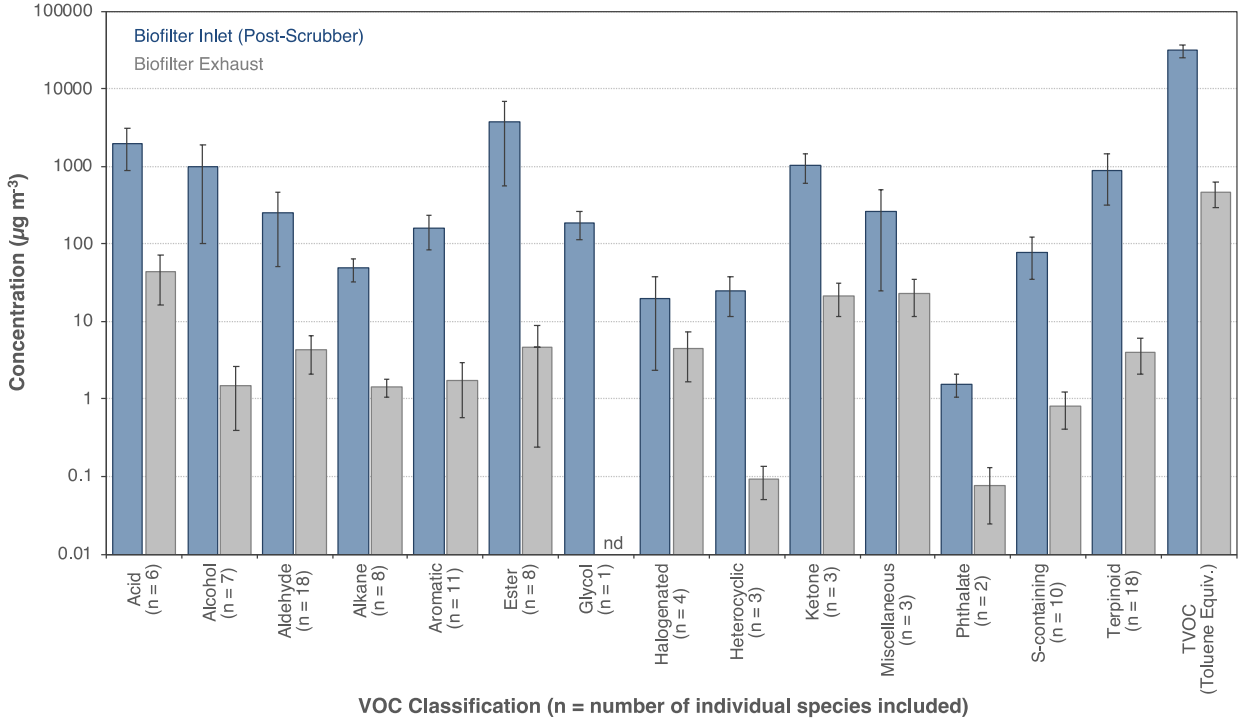

Average (± 95 percent confidence intervals) VOC concentrations in the biofilter supply line and emitted from the biofilter surface, categorized by VOC class. The concentration of glycol species in the biofilter exhaust is below the limit of detection, indicated with *nd*. The number of individual species (*n*) included in each class is noted on the x-axis. The y-axis is presented as a log-scale.

Source: Lawrence Berkeley National Laboratory

The collective TVOC emission rate from all four biofilters operating at once is estimated as 25 g of toluene-equivalent TVOC emitted per hour. This value is 1.5 times greater than the emission rate (17 g TVOC emitted per hour per windrow) measured for a typical composting windrow at Z-Best (Figure 26). When normalized to the mass of organic waste placed into digesters at ZWEDC, though, the TVOC emission rate for a windrow's 14-week composting cycle is an order of magnitude greater than the emission rate by the four biofilters (47 mg TVOC per kg vs 3 mg TVOC per kg).

Venting of Rich Biogas from Bladders

Bladder Function and Unplanned Venting

Biogas produced by the anaerobic digestion of organic municipal solid waste at ZWEDC is stored in two bladders before it is used for CHP production, flared, or vented to the atmosphere. Accumulation in the storage bladders depends on rates of biogas production and consumption via one of these three pathways. As noted earlier, the first pathway that produces energy is preferred but if the consumption rate is lower than the production rate, the bladder biogas pressure rises. Consumption at the CHP units can be low due to a number of reasons, including routine or sporadically required maintenance of the engine. To avoid over-pressurizing and rupturing the flexible membrane that encapsulates the biogas, the biogas must either be flared or vented directly to the atmosphere. Flaring is preferred over venting because flaring converts methane to carbon dioxide and the iron sponge upstream of the flare removes hydrogen sulfide. Thus, flaring reduces the emission of a potent greenhouse gas and a toxic gas from the facility compared to atmospheric venting. At the ZWEDC facility, a pressure relief valve (PRV) connected to the bladder prevents venting of biogas to the atmosphere until the stored biogas pressure exceeds the setpoint of the PRV.

The PRV is a column of water (Figure 33), and the water column height dictates the pressure threshold. The designated water height H in cm equates to the threshold bladder pressure in mbar at which biogas will be vented to the atmosphere. Until late 2017, ZWEDC's practice was to maintain a water column of 10 cm. By early 2018, ZWEDC had amended their BAAQMD permit to increase this threshold to 11.5 cm so as to further prevent venting. To avoid exceeding this pressure and releasing biogas to the atmosphere, the flare is activated to consume biogas when the measured bladder pressure reaches 7 mbar. Sometimes, the flare's biogas consumption rate is not sufficient to prevent the release of biogas to the atmosphere through the PRV.

ZWEDC does not directly measure vented biogas. Rather the facility assumes that venting occurs whenever the measured bladder pressure exceeds the water column threshold of 10 or 11.5 mbar. ZWEDC reports occurrences of venting to the BAAQMD, as is required by its operating permit. The BAAQMD assumes a biogas vent rate of 8 lbs of CH_4 emitted per hour with each occurrence. This study of biogas venting was conducted at the request of ZWEDC and the BAAQMD to verify that biogas venting occurs as expected in terms of frequency and biogas emission rate.

Figure 33: Schematic of the Biogas Storage Bladder Pressure Relief Valve

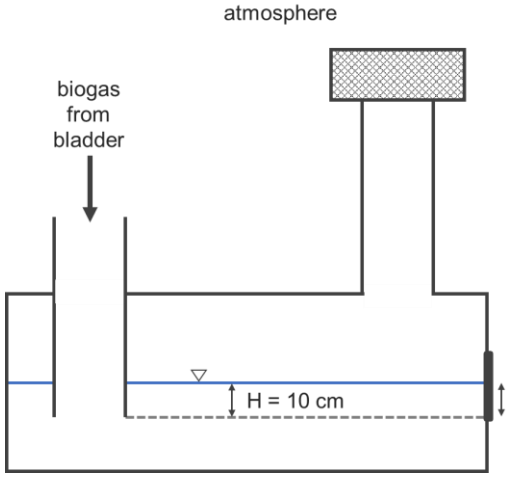

The PRV is a column of water, where the water height *H* determines the bladder pressure threshold beyond which biogas is vented to the atmosphere.

Source: Lawrence Berkeley National Laboratory

Experimental Method to Quantify Venting Frequency and Emission Rates

To measure the frequency and duration of biogas venting and estimate the volume of biogas released to the atmosphere, instrumentation was installed at the Module 1 PRV (PRV1) on 2017-Aug-31. Carbon dioxide (CO_2) concentration (LI-COR, model LI-820), gas temperature (Type T thermocouple with HOBO UX120 Thermocouple Data Logger), and gas velocity (The Energy Conservatory, model DG-700) were measured within the PRV chimney. The analyzers measured the environment inside the pressure relief valve chimney via a Teflon sampling line, thermocouple wire, and plastic tubing, respectively. Figure 34 shows the Module 1 biogas storage bladder and PRV, as well as the control room ~10 meters away that housed the analyzers.

Figure 34: Sampling Setup at Pressure Relief Valve

Measurements were made for approximately nine months (August 2017–May 2018) within the Module 1 PRV, with analyzers housed in a control room approximately 10 meters away. Data collection was continuous, with the exception of a few periods of unanticipated data loss.

Source: Lawrence Berkeley National Laboratory

Gas volume flow rate was calculated from velocity. Gas temperature and CO_2 concentration were measured because it was anticipated that a release of stored biogas that is ~50 percent CO_2 by volume would cause detectable and large changes, respectively, in the gas temperature and CO_2 concentration inside the PRV chimney. In addition to recording these data, bladder pressure, CHP power output, and biogas flows to the flare were downloaded from the ZWEDC Teamviewer operational data platform.

Results and Discussion

A total of 12 distinct venting events were measured over the sampling period at PRV1: 10 events between 2017-Aug-31 and 2017-Oct-24 and 2 events between 2017-Dec-07 and 2018-May-23 (Table A-12 and

Source: Lawrence Berkeley National Laboratory

Figure A-40 in the Appendix). Data collection was continuous, with the exception of unanticipated data loss that is indicated in Table A-12. Significant increases in CO_2

concentration and air velocity (when data was available) in the PRV chimney marked each event. Figure 35 shows an example time series of a venting event, in which there are clear responses from the temperature, CO_2, and air velocity analyzers that correspond to the previously rising storage bladder pressure.

Figure 35: Confirmed Venting Event from 2017-Oct-05 at PRV1

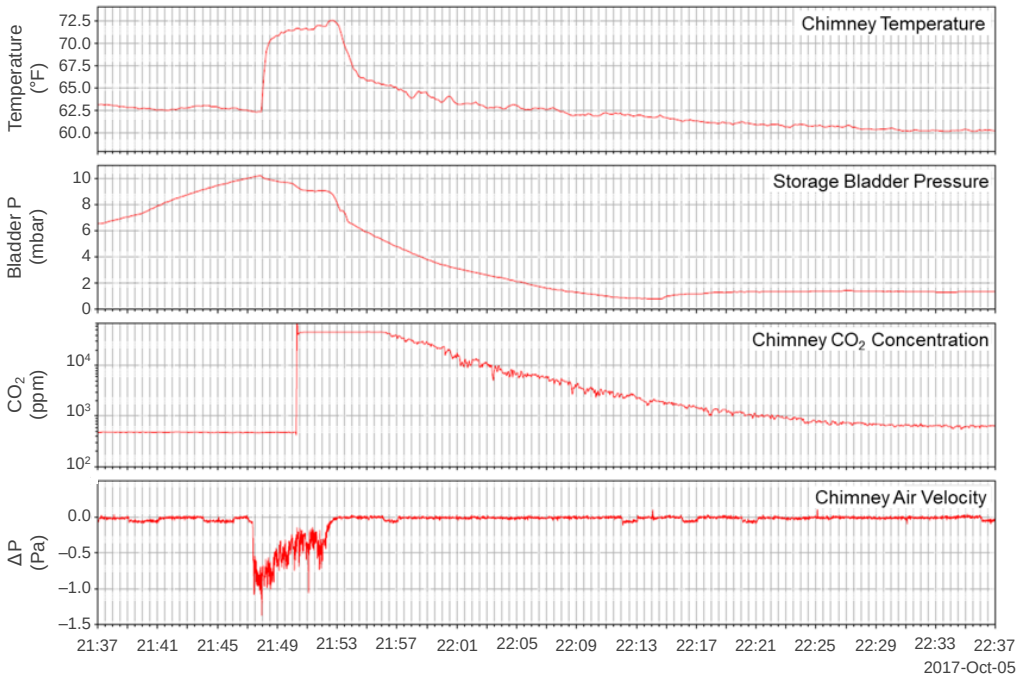

Time series of venting indicator parameters, showing a steady rise in bladder pressure that briefly exceeds 10 mbar and triggers a venting event.

Source: Lawrence Berkeley National Laboratory

The pressure measured at PRV1 did not reach the original water column threshold of 10 mbar on eight of the twelve observed events of biogas venting (events 1–5 and 9–11). Thus, biogas venting had been occurring unknowingly. One plausible explanation that arose after speaking with the ZWEDC facility managers is that the water column in the PRV was lower than intended, which would allow biogas venting to occur at pressures lower than 10 mbar. If this is correct, then it is possible that the venting of biogas could have been prevented if the water reservoir in PRV1 was filled to the intended 10 cm column height. After evidence of unknown venting was confirmed, the water column height was better maintained and venting emissions ceased.

For a majority of the venting events, the bladder pressure momentarily peaked (<1 minute) before dropping. Yet the measured air velocity, CO_2 concentrations, and temperature in the PRV1 chimney indicate that the duration of venting events lasted much longer (5–60 minutes). This further indicates that relying on bladder pressure alone to report venting is insufficient. As summarized in Table A-12 and Figure A-40, 8 out of the 12 observed venting events have air velocity data available and 5 of the 8

venting events occurred on the second and third day of monitoring. These daily events are presented together as cumulative daily volumes in Figure 36. Over the 163 days of active measurements with volume data available, 404 m^3 of biogas were directly vented to the atmosphere. This equates to an overall emission rate of 2.5 m^3 of biogas vented per day.

Figure 36: Cumulative Volume of Vented Biogas

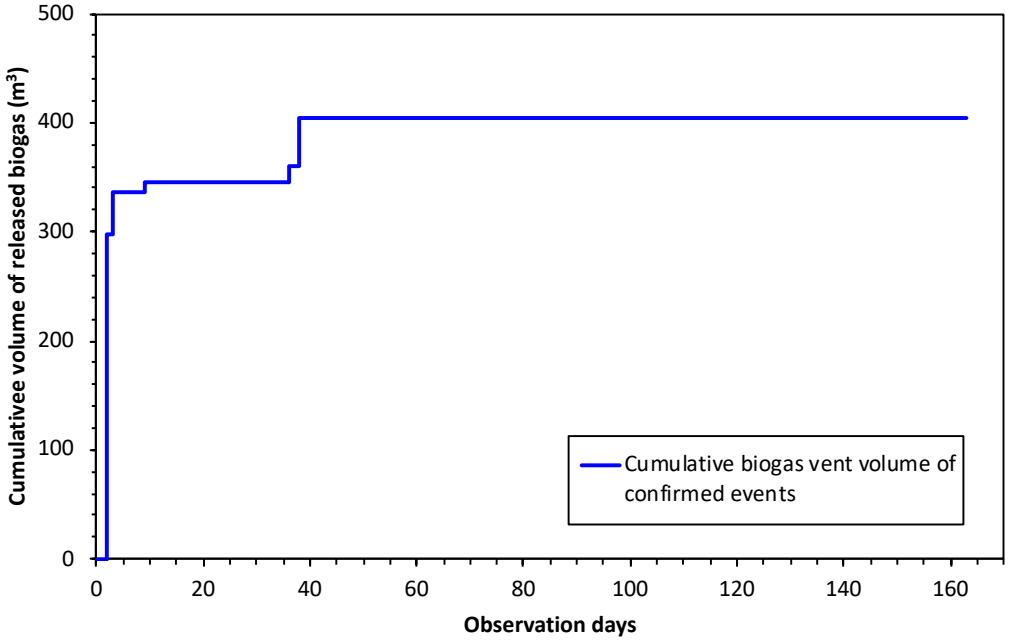

Cumulative daily volume of vented biogas at PRV1 for all observation days with available air velocity data. Three venting events occurred on day 2 and two events occurred on day 3. Eight of the twelve observed venting events included air velocity data.

Source: Lawrence Berkeley National Laboratory

Figure 37 shows the cumulative volume of methane emitted over all observed venting hours. Only those venting events with estimates of emitted volume are included (8 out of 12 events). These venting events occurred over a total of 2.6 hours and released a total of 204 m^3 of CH_4, based on the biogas composition data reported in Teamviewer (typically 50 percent methane by volume). Overall, this equals an emission rate of 78 m^3 of methane per hour or 113 lbs CH_4 per hour. The BAAQMD assumes a methane emission rate of 8 lbs per hour when the facility reports bladder pressures that exceed the specified threshold. The overall emission rate measured over this sampling period is 14 times greater than the assumed rate, while the observed event-by-event emission rates summarized in Table A-12 are 7 to 17 times larger than the assumed rate.

Figure 37: Cumulative Volume of Methane Released During Venting Events

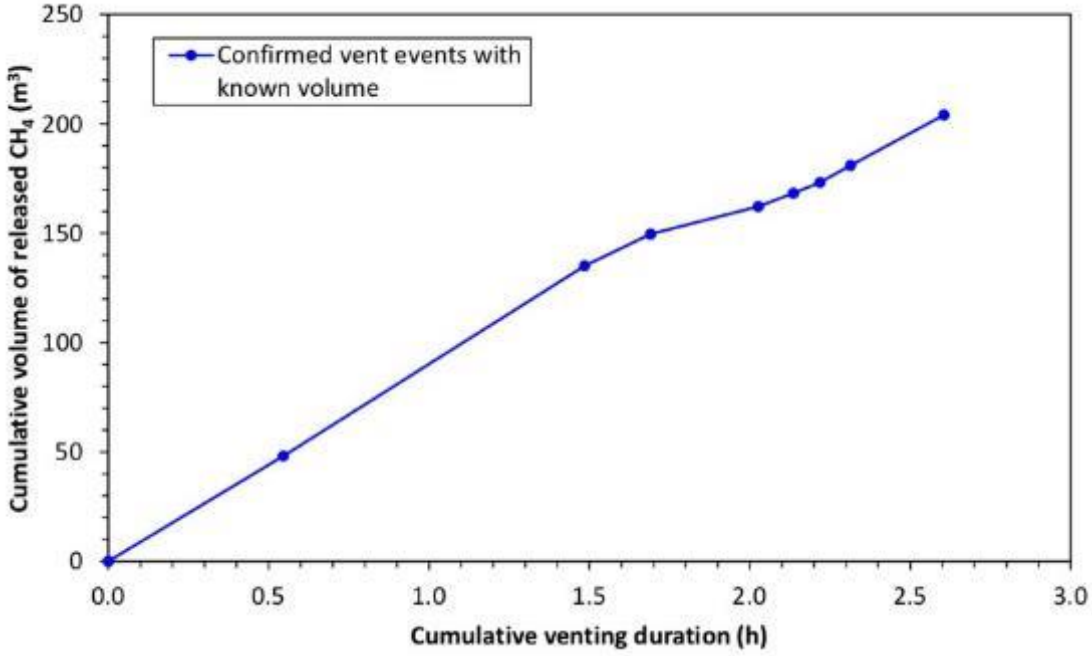

Cumulative volume of methane released during observed venting events with air velocity data available at PRV1 (8 out of 12 observed events).

Source: Lawrence Berkeley National Laboratory

To put the volume of vented biogas into perspective, the overall emission rate of 2.5 m^3 of biogas vented per day at PRV1 is ~0.02 percent of the average total volume of biogas consumed daily at the facility. The global warming potential of this vented biogas is ~0.7 percent of the daily CO_2 emissions from biogas consumption at the flare and CHP units, based on a 20-year global warming potential for methane (GWP = 86). A majority of the volume vented at PRV1 over the study period was emitted in September 2017 (346 m^3 of the total 404 m^3). During this outlier month, the total vented volume was equivalent to ~0.08 percent of monthly-average total biogas consumption at the facility and ~3.5 percent of monthly-average CO_2 emissions from flare and CHP operations.

Survey of VOC Emissions at ZWEDC

A survey of VOC concentrations in the effluent from the biofilters, in the waste receiving hall (with and without yard waste present), in the indoor break room, and over outdoor composting windrows at ZWEDC was performed. Figure 38 shows this sampling on top of the biofilter surface and on top of the outdoor composting windrow. Note that these measurements over the outdoor ZWEDC windrows were made before composting operations were moved to Z-Best; thus, there are operational differences in how these windrows were maintained. For example, the ZWEDC composting windrows were uncovered, turned, and smaller scale. Direct comparisons cannot be made to the previous section.

Figure 38: VOC Survey of Biofilter and Outdoor Composting at ZWEDC

Survey sampling of VOC concentrations atop the biofilter (left) and the outdoor composting windrow (right) at the ZWEDC facility, prior to composting activity being moved offsite.

Source: Lawrence Berkeley National Laboratory

Air samples were collected with DNPH cartridges, analyzed by high performance liquid chromatography (HPLC) with UV detection for carbonyls (aldehydes and ketones). Figure 39 and Figure 40 summarize the results of this survey.

In Figure 39, results are averaged over three samples for the biofilters and presented for a single sample for the other locations. "Waste Receiving Hall 1" was a sample taken when the majority of waste inside the hall was food waste, while "Waste Receiving Hall 2" was a sample taken when the majority of waste was yard waste. In Figure 40, measurements at the biofilters were taken before and after a digester shutdown, with the "after shutdown" samples including both the facility's air exhaust and ultra-lean biogas from the purged digester.

In the waste receiving hall, the measured acetaldehyde concentration ranged between 140–200 ppb. These concentrations were well below the OSHA enforced limit of 200 ppm but exceeded the 8-hour reference exposure level of 160 ppb set by OEHHA. The total VOC concentration in the waste receiving hall was two times higher on 2015-Oct-26 than 2015-Nov-18, with greater levels of 2-butanone and mathecrolein present (Figure 40). The difference by day is likely because yard waste was present in the receiving hall on 2015-Oct-26, while mostly food waste was present on 2015-Nov-18.

Concentrations above the biofilters were much lower than in the waste receiving hall, which can be attributed to removal by the acid scrubbers and biofilter controls, consistent with the results presented above for NH_3 and H_2S (in Figure 29). Concentrations above the outdoor composting windrows were also lower than in the waste receiving hall, but higher than the concentrations in the biofilter effluent. The employee break room had the lowest concentrations of the four locations.

Figure 39: VOC Composition and Concentration around ZWEDC Facility

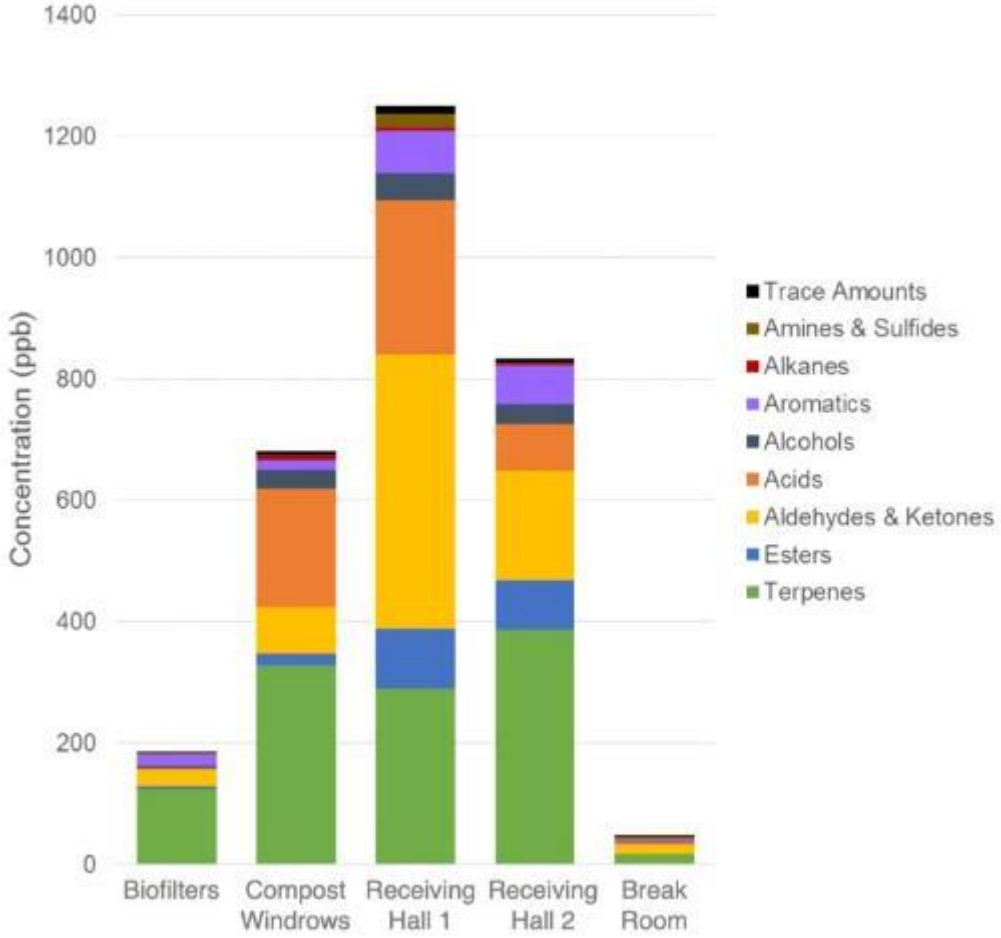

Results are averaged over three samples for the biofilters and presented for a single sample for the other locations. Waste Receiving Hall 1 refers to when the majority of waste inside the hall was food waste, while Waste Receiving Hall 2 refers to when the majority of waste was yard waste.

Source: Lawrence Berkeley National Laboratory

Figure 40: Aldehyde and Ketone Concentrations around ZWEDC

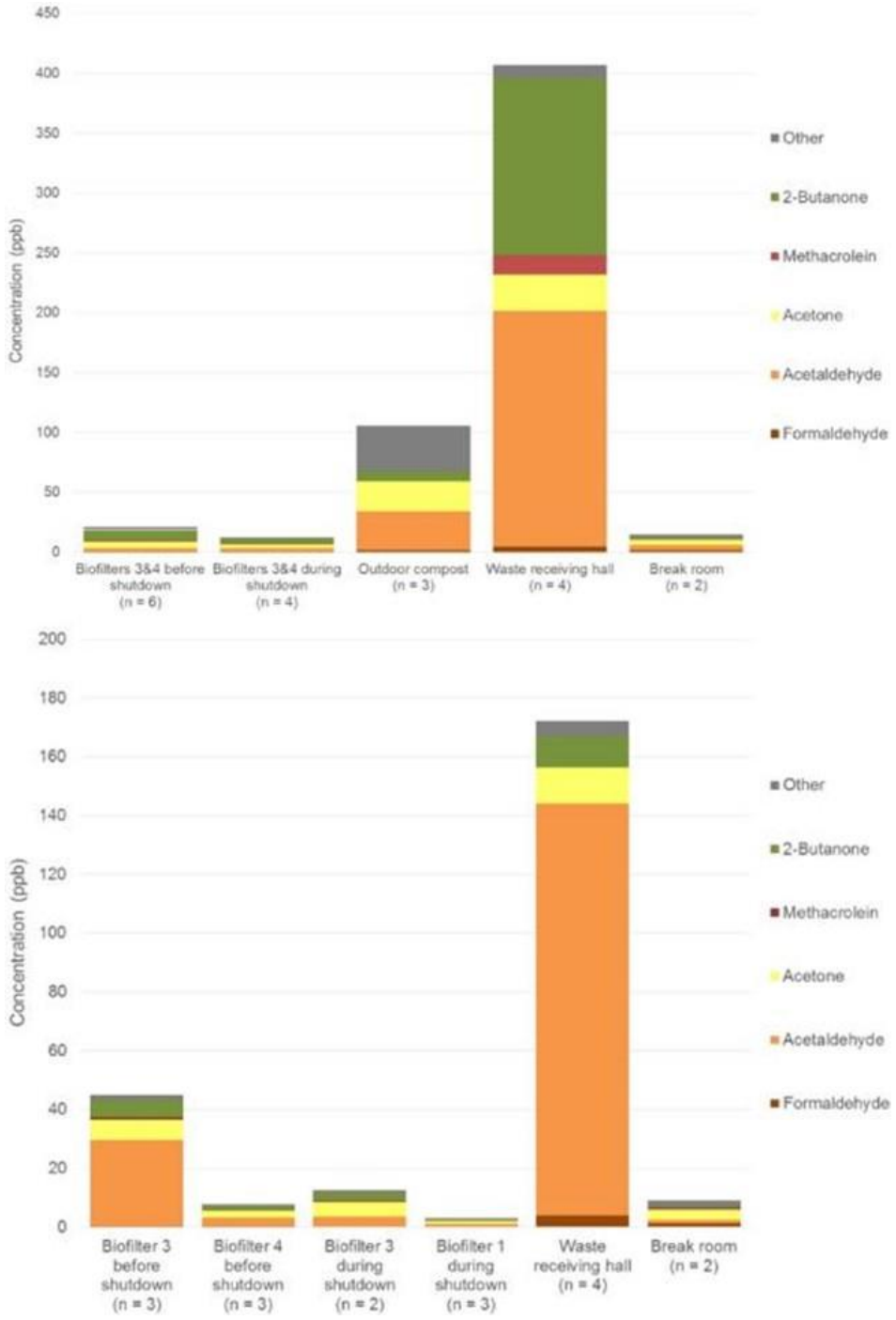

Survey sampling results of VOC concentrations around ZWEDC facility, with (top) and without (bottom) yard waste present in the waste receiving hall. Measurements at the biofilters included before and after a digester shutdown, when ultra-lean biogas is sent through the biofilters for treatment before being exhausted to the atmosphere.

Source: Lawrence Berkeley National Laboratory

Conclusions

Emissions of greenhouse gases, criteria air pollutants, and odorous compounds were measured at different points along the process of anaerobic digestion and composting of MSW. Outcomes of this task include:

- Pollutant emission rates that can be used to develop emission inventories and serve as inputs to odor modeling and a lifecycle analysis of net GHG benefits of the AD/composting of MSW over landfilling at current and scaled-up capacity (discussed below and in the following chapter)
- Strong relationship established between biogas ammonia content and flare NO_x emissions, which can help inform the permitting of other facilities
- Confirmed venting of rich biogas that resulted in subsequent control measures
- Pollutant characterization methods developed for relatively new sources

Comparison of Emission Factors by Source

Figure 41 through Figure 43 aggregate the CH_4, CO_2, N_2O, NO_x, NH_3, and H_2S results discussed above and summarize the average pollutant emission factors for each source in terms of grams emitted per kilogram of MSW digested at ZWEDC. These emission factors are also reported in Table A-13 in the Appendix. Composting emissions measured at Z-Best dominate the overall AD process for emissions of CH_4, CO_2, NH_3, and H_2S. CO_2 emissions have the highest magnitude of mass emissions per kg of MSW digested. N_2O emissions at the biofilters and from composting are both elevated relative to the combustion sources but small in magnitude.

The CO_2-equivalent emission rate for each pollutant and by each source studied were determined using 20-year global warming potential (GWP) values. These GWP-weighted emission factors have units of grams of equivalent CO_2 emitted per kilogram of MSW digested at ZWEDC and are presented in Figure 44. An analysis using the 100-year GWP values is also presented in Figure A-41 of the Appendix. Here, rich and lean biogas flaring events have been combined into one category to represent all CO_2-equivalent emissions from biogas combustion at the flare. Unknown venting from the biogas storage bladders was not included in this analysis because it was anomalous and ceased to occur during our study. The CO_2 emission rate reported for the flare and CHP units was not measured but instead calculated using a carbon balance of the combustion of 1 kg of methane:

$$E_{CO_2} = 10^3 g\ CH_4 \cdot \frac{w_C}{w_{CH_4}} \cdot \frac{MW_{CO_2}}{MW_C} = 5488\ g\ CO_2\ kg^{-1}$$

Figure 41: CH_4 and CO_2 Emission Factors by Source

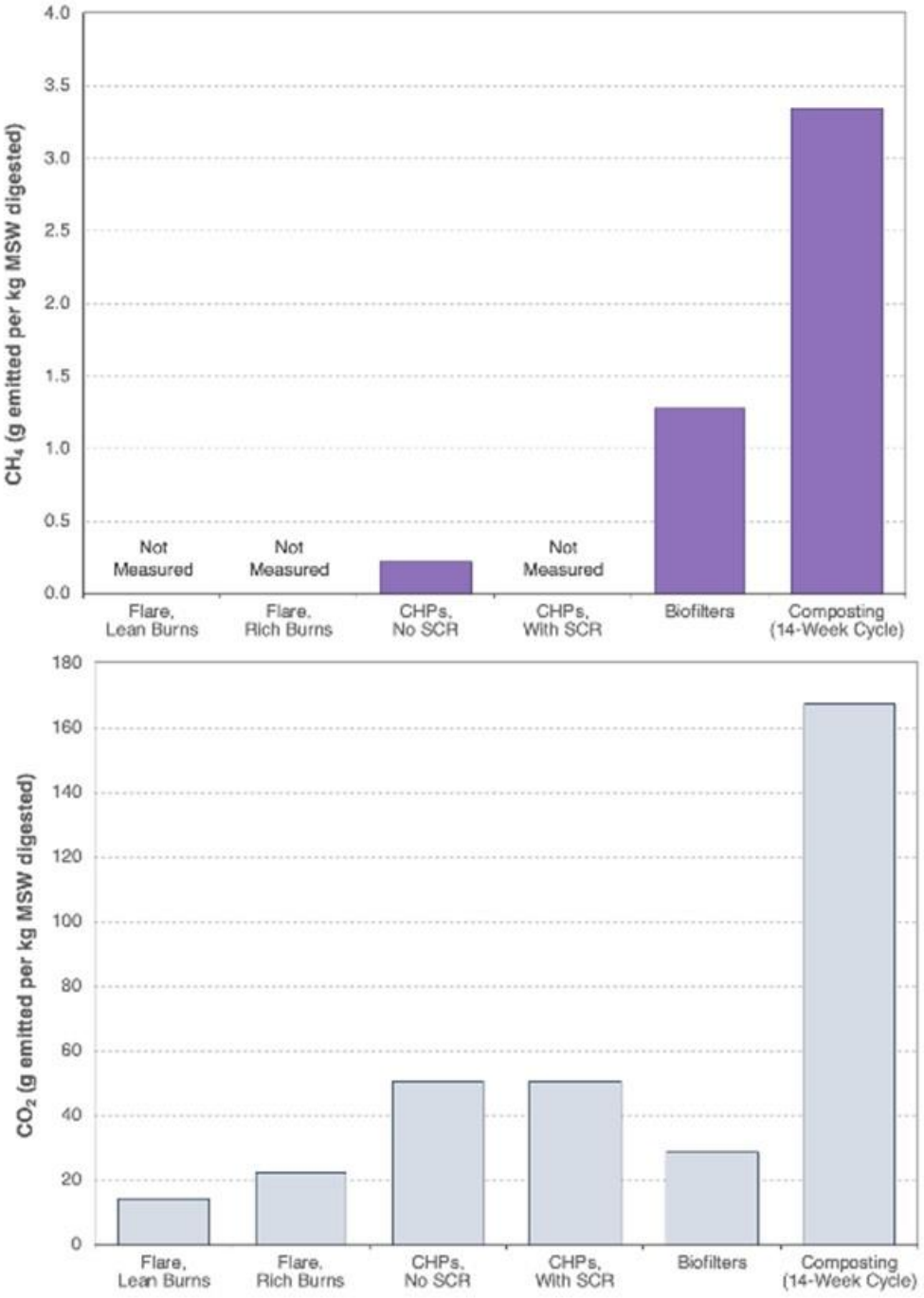

Average mass of CH_4 and CO_2 emitted per kg of MSW digested at ZWEDC for each measured source.

Source: Lawrence Berkeley National Laboratory

Figure 42: NO_x and N_2O Emission Factors by Source

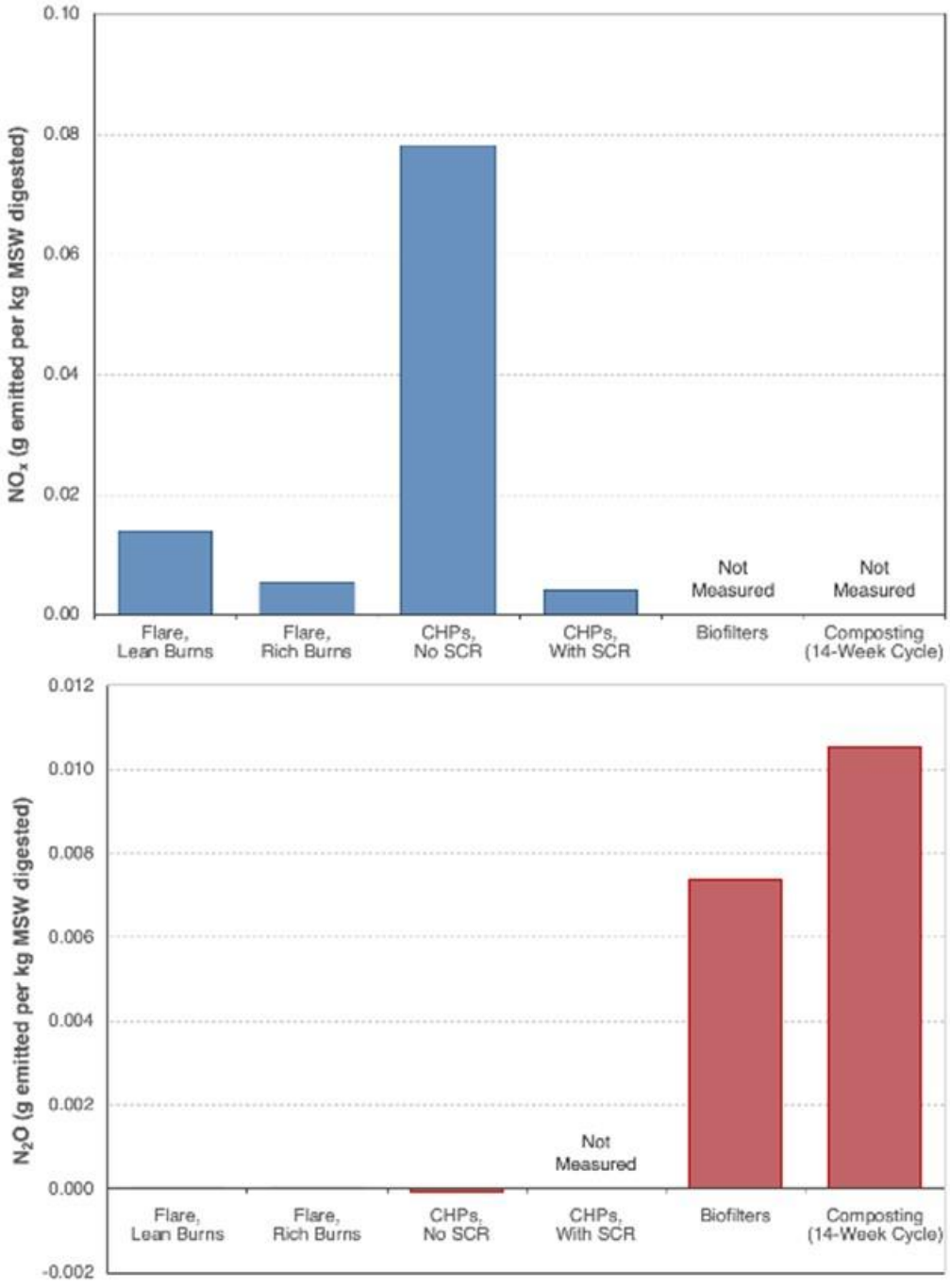

Average mass of NO_x and N_2O emitted per kg of MSW digested at ZWEDC for each measured source.

Source: Lawrence Berkeley National Laboratory

Figure 43: NH_3 and H_2S Emission Factors by Source

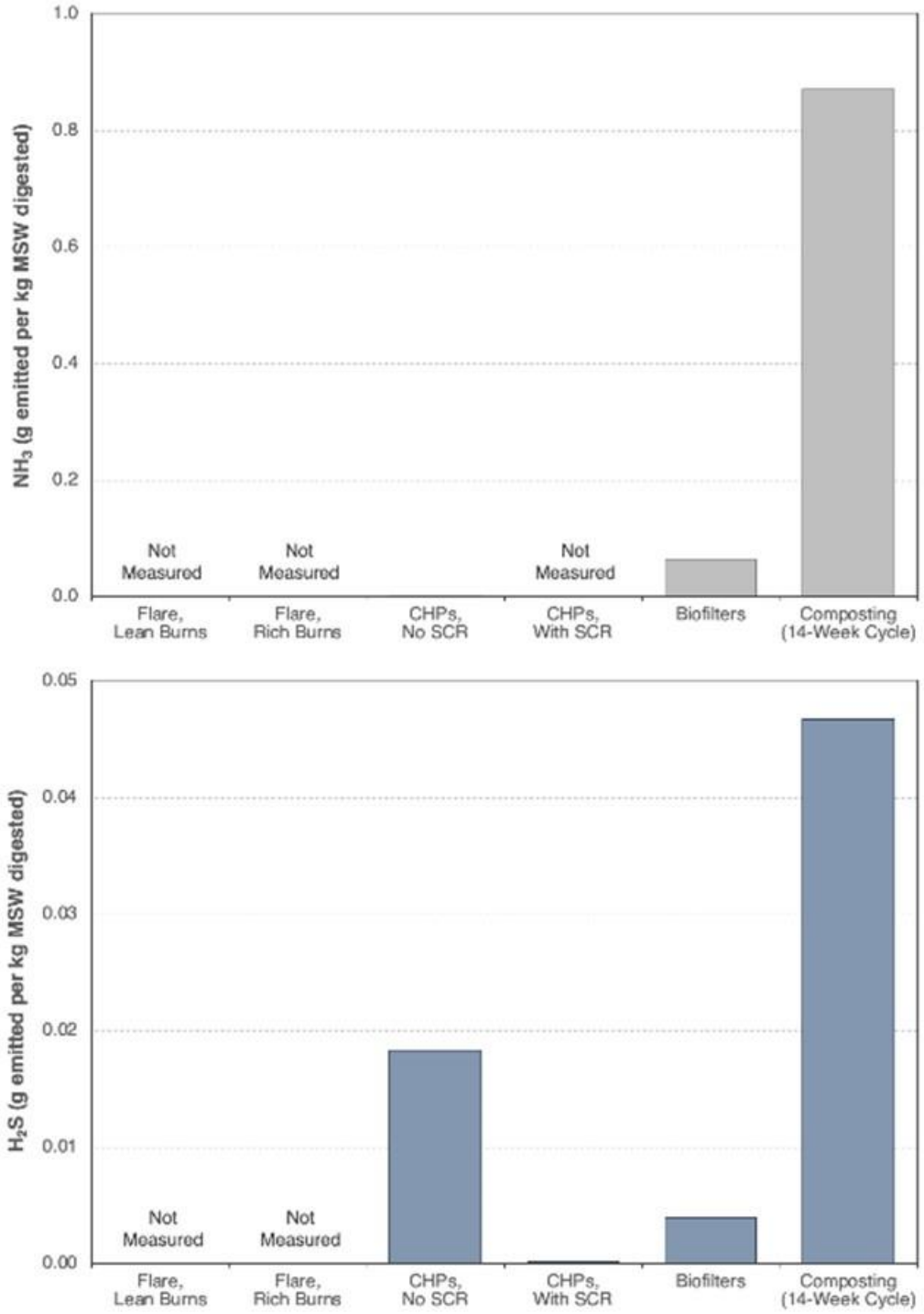

Average mass of NH_3 and H_2S emitted per kg of MSW digested at ZWEDC for each measured source.

Source: Lawrence Berkeley National Laboratory

Figure 44: CO_2-Equivalent Emission Factors by Source (20-Year GWP)

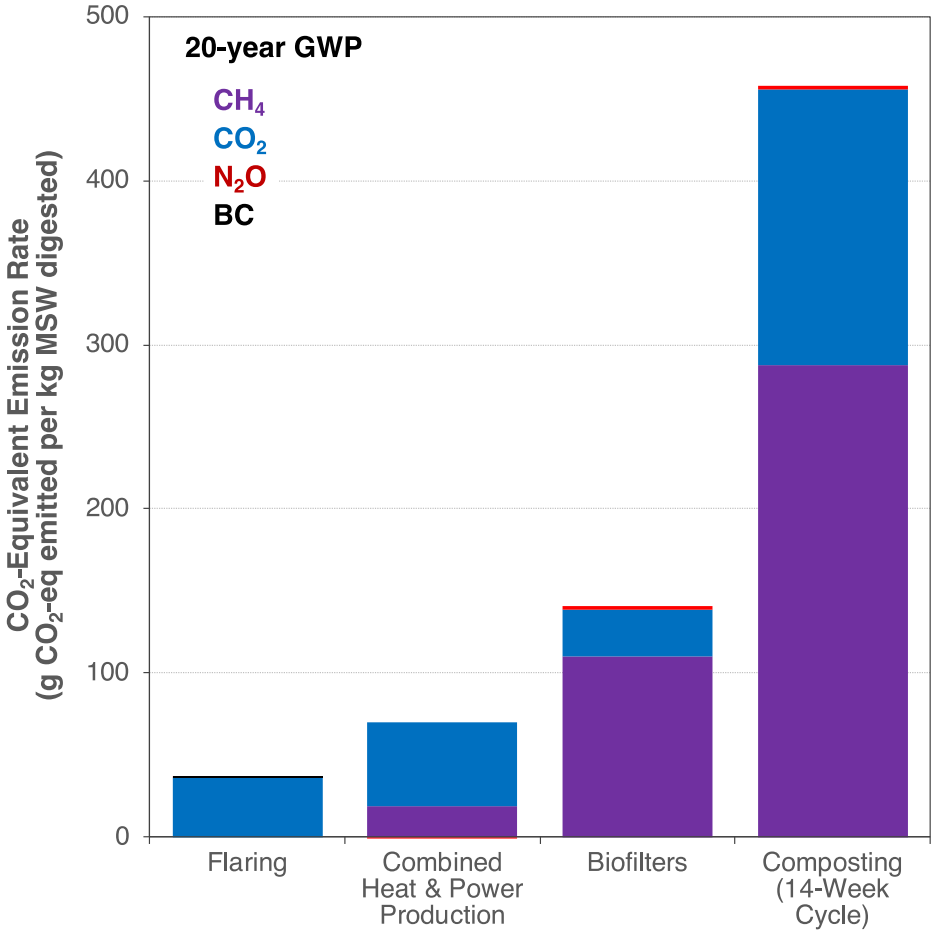

Average mass of equivalent CO_2 emitted per kg of MSW digested by each source, based on 20-year GWP values for CH_4, N_2O, and BC.

Source: Lawrence Berkeley National Laboratory

Between the four sources of emissions presented, composting is again the dominate source of emissions. On a 20-year time horizon, flaring and CHP production respectively account for 5 percent and 10 percent of total CO_2-equivalent emissions per kg of MSW digested. The GWP for these activities is dominated by CO_2 emissions that come from the near-complete conversion of methane in the biogas to carbon dioxide during combustion, as intended. CH_4 emissions were not measured in the flare exhaust and may be non-zero. BC emissions from rich burns at the flare had little impact on the GWP-weighted emission rate. Twenty percent of the total CO_2-equivalent emissions are from the biofilters and 78 percent of those emissions were methane. The 14-week composting cycle was responsible for 65 percent of the total CO_2-equivalent emissions per kg of MSW digested; methane comprised 63 percent of those emissions from composting, with CO_2 emissions making up most of the remaining fraction. The high methane contribution suggests that the composting of piles is not completely aerobic, and that some CH_4-producing anaerobic digestion continues.

Part 2: Odor Management via Dispersion Modeling

Odor is a challenging problem associated with waste conversion facilities, and often limits its scale-up and adoption as an energy source. It acts as a major barrier to further development in anaerobic digesters (AD) and composting facilities. All AD facilities generate odor at all process stages including delivery, waste sorting, composting, and curing, where the last two processes usually contribute the most odorous emissions (Epstein and Alix 2001). The major odor-causing compounds are sulfur-, nitrogen-, and carbon-based. For example, hydrogen sulfide (H_2S), which smells like rotten eggs, and ammonia (NH_3), which is pungent, sharp and eye-watering, could be the major cause of complaints from neighbors. Decomposition of organic matter is never odor-free, even under optimal conditions. Failure to achieve near- and optimal conditions is guaranteed to exacerbate odors, particularly those odorants that people find most annoying or unpleasant. Hence, a successful waste treatment facility requires careful consideration of factors like site layout, prevailing wind directions and speeds as well as locations of sensitive receptors. All the odor management practices mentioned above will not eliminate odors but will greatly reduce the potential for odor episodes that will cause problems. To minimize odor impacts on the public from these facilities, it is important to understand the identity of sources and transport of the odor compounds to the impacted areas.

Field measurements to characterize odor sources are insufficient to account for the effective impact of odors on citizens. Odorant concentrations at the receptor locations are needed for the assessment of their impacts on public. Dispersion modeling uses mathematical equations, describing the atmosphere, pollutant dispersion and their chemical and physical processes within the plume, to estimate the ambient concentrations associated with specific source releases (Holmes and Morawska 2006). This assessment of odor dispersion from the ZWEDC facility provides information on the average and seasonal patterns in local circulation by critically reviewing prior assessments of odor and analyzing local multi-year meteorological data. This assessment provides information to determine temporal and spatial characteristics of odor dispersion, and delineate separation distances for odor annoyance at current and future operation scales of the ZWEDC facility.

Odor Problems at ZWEDC

In this section, the project team (1) characterizes past odor complaints to ZWEDC; and (2) analyzes the odor complaints in relation to the local circulation patterns and onsite operations to (3) identify important odor sources and data requirements for subsequent dispersion modeling.

Past Odor Complaints

ZWEDC has taken precautions to minimize odor release by housing the waste sorting, AD, and in-vessel composting in a fully enclosed and negatively pressurized building. The exhausted air from the building is treated in series with an acid scrubber to remove

ammonia and four biofilters made of moist wood chips. Despite these precautionary measures, 69 odor complaints were reported to the local air district between March 2014 and October 2015. All these complaints came from the San José-Santa Clara Regional Wastewater Facility (RWF) (personal communication with the staff at ZWEDC) located across street southeast of ZWEDC. The project team used data from Oct 2014 to Sep 2015 to explore the seasonal and day-of-week distributions of odor complaints (Figure 45).

The data indicate a number of complaints occurred in all seasons with higher numbers in spring (March-April-May) and lower numbers in winter (Dec-Jan-Feb). The day-of-week distribution suggested that complaints mostly occurred in the first half of the week especially Mondays. Monday is most likely unusual because facility personnel tend not to be present for the weekend period. Onsite operations including waste receiving, anaerobic digesting, digester shutting down, in-vessel composting, and outdoor curing take place on a continuous basis (personal communication with the staff at ZWEDC) with waste receiving and digester shutting down processes limited to the weekdays when staff are onsite. This does not suggest weekday-only processes are the main causes of odor complaints. Since odor complaints came from the waste water facility, perception of odor may be associated with the weekday when workers were present. To further explore the causes of odor complaints, the project team analyzed the complaints in relation to local circulation patterns and onsite operations to identify important odor sources and data requirements for subsequent dispersion modeling.

Figure 45: Number of Odor complaints by Season and by Day of Week

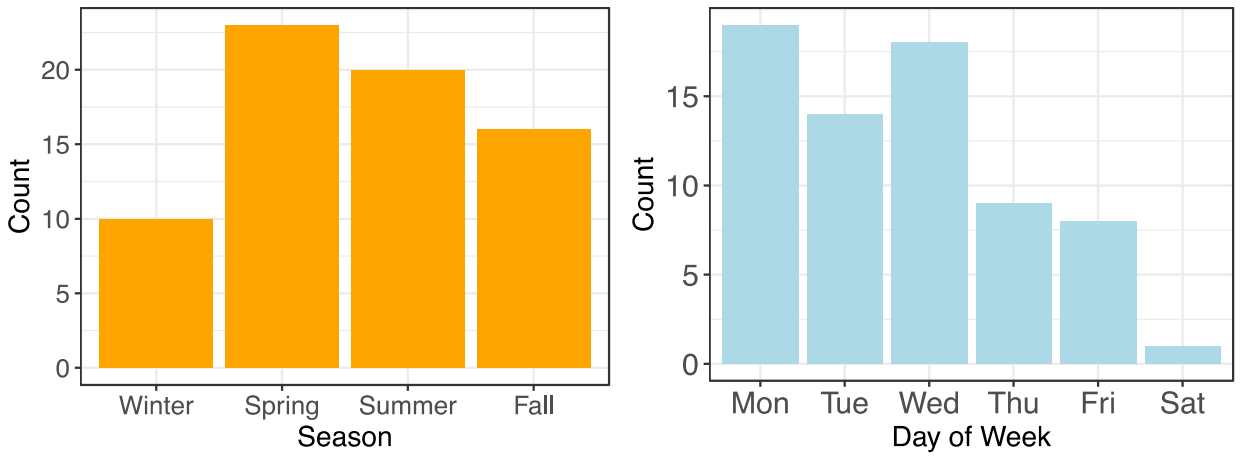

Source: Lawrence Berkeley National Laboratory

Local Meteorology

Meteorology acts as a significant factor in odor dispersion with atmospheric stability affecting the dilution of odorants and flow patterns affecting the direction and extent of impacted areas (Coker 2012). In this section, we discuss the analysis of meteorological data collected at the facility and nearby at 7 weather stations. The project team

presented the circulation patterns and identified the appropriate meteorological input data that were required for subsequent dispersion modeling.

We first analyze the meteorological data from the two facility-operated weather stations that are on or near ZWEDC to derive flow patterns. Due to the data quality problems, we determine the ZWEDC onsite meteorology data is not suited for deriving local circulation patterns and for subsequent odor dispersion modeling (see Appendix B).

To understand the circulation pattern around ZWEDC with reliable and longer-term data, we further analyze multi-year (2000-2014) meteorological measurements collected at seven National Weather Service (NWS) stations from the National Climatic Data Center (NCDC) Integrated Surface Hourly (ISH) database site, (ftp://ftp.ncdc.noaa.gov/pub/data/noaa/) (Appendix B). Seasonal average flow patterns and diurnal variations are investigated (Appendix B). Among all 7 NWS stations, the Mountain View site best resembles the wind directions observed at ZWEDC for the same time period (Figure B-6). Similar to ZWEDC, this site is located close to the San Francisco Bay and is about 9 km away from ZWEDC. Note the wind speeds recorded at ZWEDC are generally slower than those at the Mountain View site, which may be due to the lower reception rate discussed earlier. Therefore, we will use long-term meteorological records at the Mountain View site for subsequent analysis and dispersion modeling.

The meteorological patterns established with the long-term records (2000-2014) at the Mountain View station are shown in Figure 46. The predominant winds from spring to fall seasons are consistently from the northwestern directions. This northwesterly flow for the spring-fall months can be explained by the bay-land thermal contrast that creates consistent northwesterly flow over the area. As the thermal contrast between bay and land decreases in the winter, the winds become weak and variable. It was also found that wind speeds are slowest during the night and early morning hours and increase to their highest speed in the late afternoon, which is mainly due to surface heating.

Figure 46: Long-term Wind Patterns around ZWEDC

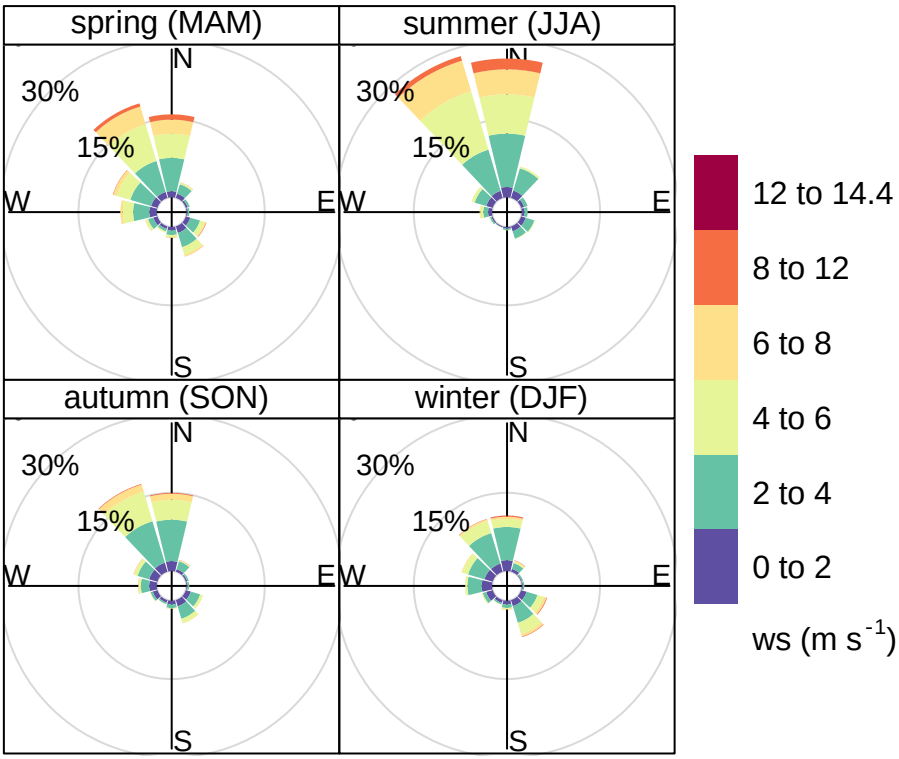

Source: Lawrence Berkeley National Laboratory

Role of Meteorology vs Onsite Operations

As seen previously, the longer-term data indicate a predominant northwesterly flow from spring to fall. This flow transports odorant compounds to locations southeast of ZWEDC, where the wastewater treatment plant is located. Winter winds become weaker and more variable which allow the odorant compounds to accumulate. Winter is the rainy season, and odorants can be removed by wet deposition. Winter season (Dec, Jan, and Feb) contains the holiday season and two holiday weekends and has fewer onsite activities and less worker presence at the odor receiving location (RWF). Together, these may explain the lower number of odor complaints in the winter season as seen in Figure 45.

At sub-seasonal time scale, we examine differences in meteorology (wind patterns and wind speed) of days with and without odor complaints. We use the onsite data focusing on the summer season with its better data quality for this short-term analysis because the results are sensitive to day-to-day changes in meteorology. For wind speed comparisons, both business hours (8 AM to 5 PM when workers at the RWF are present) and the night before (< 8 AM) are examined. This is because windrow turning usually takes place at night (personal communication with the ZWEDC staff), and the likely low winds at night may favor accumulation of odor compounds associated with the turning process and cause odor problem during early business hours. The comparison indicates wind directions are consistently from north-northwesterly

directions for odor and non-odor days (Figure 47 left). Wind speeds were indeed slower during business hours (8 am to 5 pm) as well as the night before (< 8 am) for odor days than during non-odor days. However, the differences are not statistically significant (Figure 47 right).

In summary, meteorology, especially the long-term flow patterns established around ZWEDC, can explain the odor receptor, RWF that is located south-southwest of ZWEDC. The day-to-day meteorology analysis could only qualitatively suggest that days with lower winds on average are likely to result in more odor complaints. However, the differences are not statistically distinguishable within our existing data set. Fluctuation of waste composition could potentially contribute to the odor complaints but the supporting data needed to confirm this point is also lacking.

Figure 47: Comparison of Meteorology for Days with and without Odor Complaints

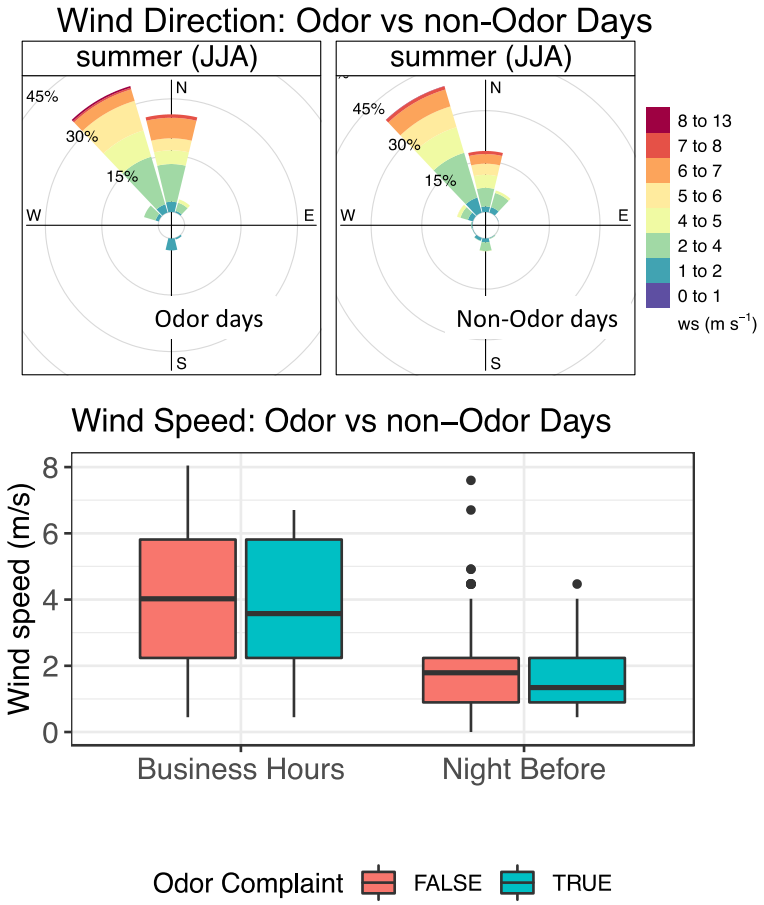

Source: Lawrence Berkeley National Laboratory

The majority of the processing stages are conducted indoors (Figure 48) with exhaust air treated with an acid scrubber before releasing to ambient environment through biofilters. The project team and ZWEDC considered two potential outdoor odor sources

at the ZWEDC facility in San José: biofilters and outdoor composting. Windrows. Also, untreated biogas concentrated with odorous compounds such as H_2S can be vented to the outdoor air through pressure release valves (PRV) from the storage bladders.

Figure 48: Potential Outdoor Odor Sources at the ZWEDC Facility

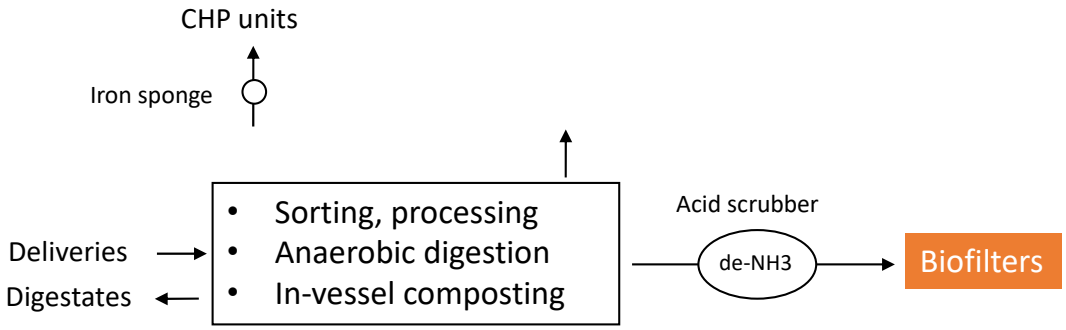

Major outdoor odor sources

Source: Lawrence Berkeley National Laboratory

ZWEDC made the following efforts to improve onsite operations to alleviate the odor annoyance.

Biofilter Sprinkler. Facility's biofilters are supposed to remove organic compounds from the facility air before the air is exhausted to the atmosphere. Between June and July 2015, ZWEDC learned that they were not keeping the biofilters wet enough to maintain a viable biofilm. To fix the problem, ZWEDC installed a sprinkler system atop the biofilters.

Compost Windrow Turner. ZWEDC initially attributed the main odor source to the outdoor composting windrows and purchased a windrow turner in June 2015 to improve aeration. ZWEDC also installed a sorting line to remove garbage from the organic waste prior to anaerobic digestion. In late 2015, the Local Enforcement Agency empowered by California Department of Resources Recycling and Recovery ("CalRecycle") to implement delegated CalRecycle programs and locally designated activities in the city of San Jose. In October 2015, the Enforcement Agency prohibited on-site composting at ZWEDC, and the digestate has since shipped to the Z-Best composting facility located in Gilroy.

These operational changes are marked along with the monthly counts of odor complaints in Figure 49. Both these measures helped reduce odor complaints and no more complaints were received after outdoor composting was relocated offsite. We can conclude that the major cause of downwind odor annoyance from ZWEDC is the outdoor composting processes. Inefficient operations of biofilters can also cause odor problems. Although the project team has no evidence of odor complaints from the

biogas PRV venting, the potential odor impact from this untreated source needs further investigation.

Figure 49: Monthly Odor Complaints and Onsite Operational Changes at ZWEDC

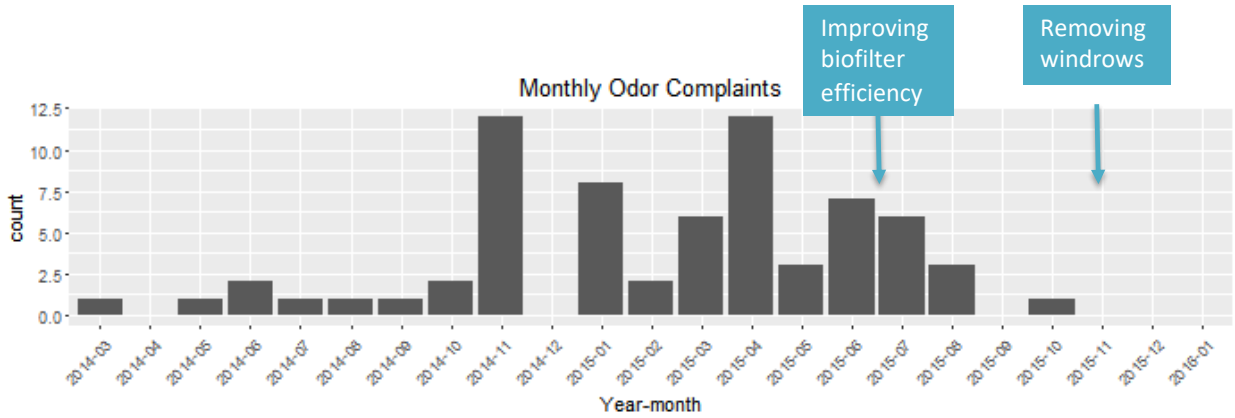

Source: Lawrence Berkeley National Laboratory

Odor Dispersion Modeling for Odor Impact Assessment

Current regulatory pressure from odor complaints has been alleviated by ceasing onsite compositing at ZWEDC. Offsite composting requires payments for trucking and tipping fees to another facility and decreases potential revenue from compost products. There may be unknown impacts from other odor sources (biofilters and PRV releases) at future increased processing capacities. Odor sources do not pose significant problems for ZWEDC currently but could be of concern for future facilities attempting to locate in urban areas where large waste streams are generated.

Odor dispersion modeling is an integral part of the framework to assess and mitigate odor impacts. Dispersion modeling uses mathematical equations, describing the atmosphere, plume dispersion and chemical and physical processes occurring within the plume, to predict offsite impacts from odor sources (Chirmata and Ichou 2016). It can be used to determine temporal and spatial characteristics of odor dispersion. In addition, it can help identify the most impacted receptor locations and delineate potential separation distances for odor annoyances at current and future operation scales of the ZWEDC facility, as well as provide general guidance to facilities in different geographic locations by identifying odor-constrained capacities and optimal siting insights.

In this section, the project team applies the US Environmental Protection Agency's (EPA) AERMOD dispersion model to the ZWEDC facility and develops odor impact assessment tools to characterize source - receptor relationships associated with potential important onsite odor sources.

Overview of AERMOD

Through the American Meteorological Society/Environmental Protection Agency Regulatory Model Improvement Committee (AERMIC), a steady-state plume model, the AERMOD modeling system, analyzes air dispersion based on the planetary boundary layer (PBL) turbulence structure and scaling concepts. AERMOD is Environmental Protection Agency (EPA)'s preferred dispersion model for regulatory modeling applications. AERMOD determines short-range impacts from a variety of sources in all types of terrain (US EPA 2004) and has been applied to odor impact assessment studies (e.g. Karageorgos et al. 2010; Chirmata and Ichou 2016; Vieira de Melo et al. 2012).

Odor dispersion is mostly influenced by meteorology, physical terrain, building downwash, and chemical and depositional removal (Coker 2013). Meteorology acts is a significant factor for odor dispersion. Atmospheric stability affects the dilution of odorants and flow patterns affect the direction and extent of impacted areas. Topography of the area is also another significant factor for odor dispersion. Coastal areas are prone to onshore and offshore breezes from pressure differences between land and ocean. Mountain ranges reduce airflow because of increased surface roughness, and also create atmospheric instability. Buildings are disruptive to odor dispersion. When odor plumes flow over buildings, small eddies are created which can result in vertical turbulence. The closer buildings are to a composting facility, the more likely an odorant plume will be forced downward toward the surface than it would be otherwise. This suggests that buildings should not be constructed close to the facility property. Deposition removes pollutants from the atmosphere, and can affect odor dispersion via two pathways: dry and wet deposition. Dry deposition occurs when an odor pollutant comes into contact with surfaces and wet deposition occurs when it comes into contact with precipitation.

Air pollutant dispersion models such as AERMOD integrate aforementioned physical and chemical processes and are able to determine odor dispersion by mathematically describing plume dispersion reliably and by using inputs of local meteorology and physical terrain data. The AERMOD modeling system consists of one main program, AERMOD, and two pre-processors, AERMET and AERMAP. Figure 50 shows the data flow and processing of information in AERMOD (US EPA 2004). The detailed model input preparation can be found in Appendix B.

Figure 50: Data Flow in the AERMOD Modeling System

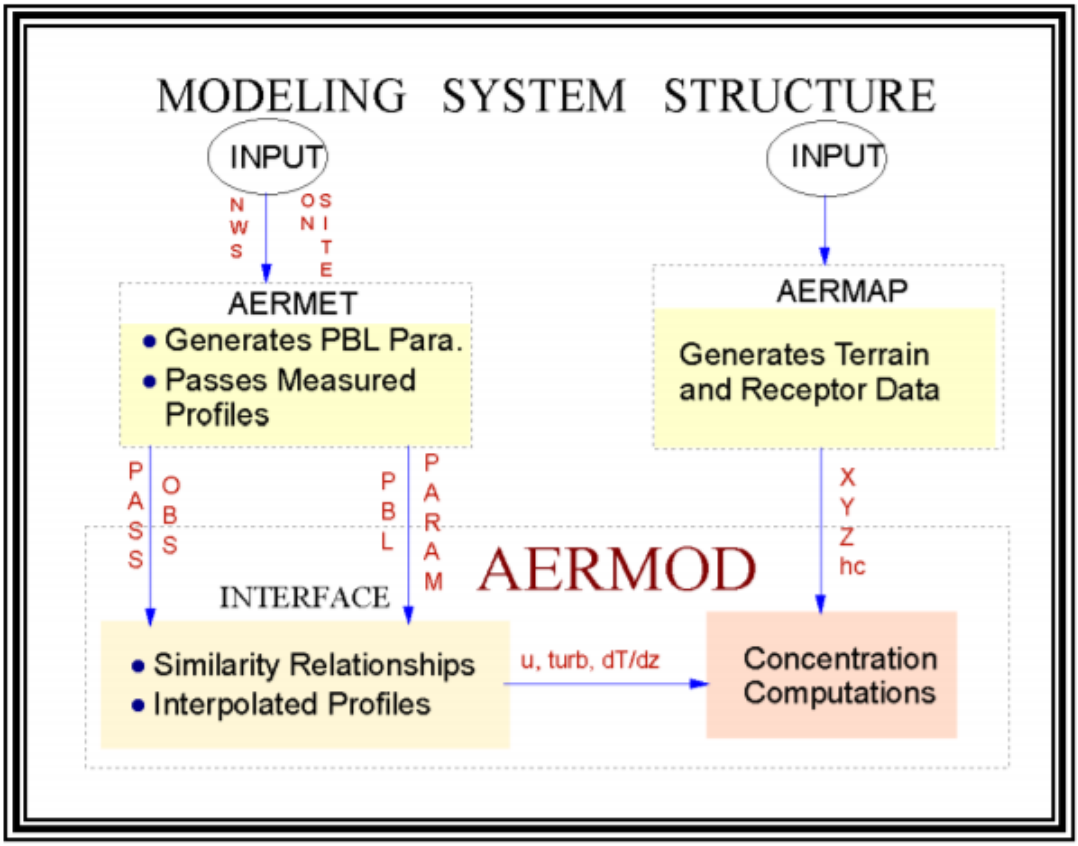

AERMOD Modeling System (US EPA 2004)

Source: Lawrence Berkeley National Laboratory

There are three main outdoor odor emission sources at ZWEDC. Two are area sources: the biofilters and outdoor composting windrows. One is a point source: the release of biogas from the PRV.

In addition, waste delivery may release odors. There are on-road waste-filled trucking activities and the receiving hall is open from the west end for incoming and the east end for outgoing trucks. The trucks and the hall are potential odor sources with emissions emitted on an intermittent basis. Receiving waste and trash storage are located in the west part of the logistic hall (indicated by "Receiving_Storage1" in Figure 51), while digestate storage is located in the east end of the logistic hall (indicated by "Storage2" in Figure 51). To account for their fugitive emissions, we include two more area sources to represent the receiving/storage of inbound wastes and the storage of the outbound digestates. The project team modeled the trucking activities as a line source on the nearby road with a 3 m width. The line source modeled in AERMOD is equivalent to an elongated area source with dimensions of 3 m by 30 m. dimension, using the maximum 10:1 aspect ratio recommended by AERMOD. This is equivalent to two large or three median sized trucks driving in tandem. The layout of the emission sources described above are illustrated in Figure 51.

Figure 51: Odor Source Location and Layout

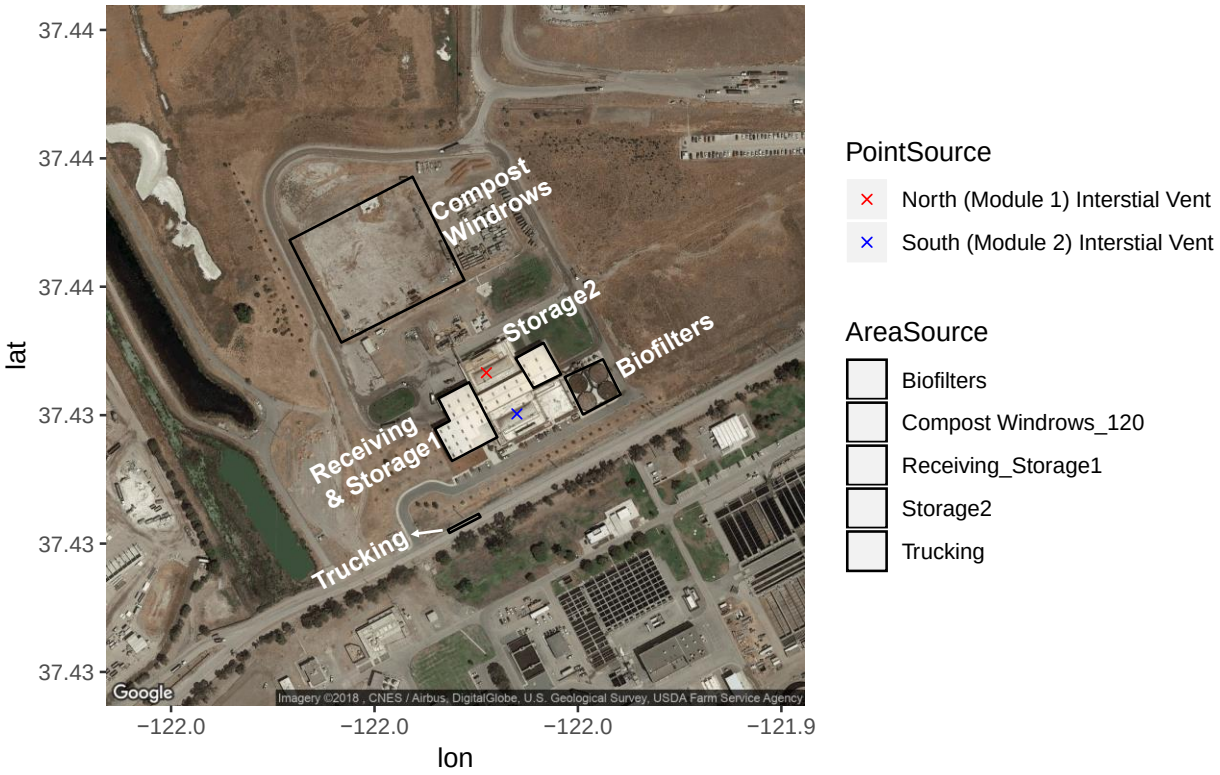

Source: Lawrence Berkeley National Laboratory

Source parameters used for simulation are summarized in Table 2.

Table 2: Summary of Source Parameters

Process Group	Process Description	Source Location / Starting Location (UTM Coordinates)		Point Source			
		Easting (X) (m)	Northing (Y) (m)	Stack Height (m)	Temp (K)	Exit V (m/s)	Stack Diameter (m)
PRV	Bladder pressure release	592812.5	4143572.3	4.9	294.3	7.2	0.6
PRV	ventng	592839.5	4143537.1	4.9	294.3	7.2	0.6
				Area Source			
				Release Height (m)		N Vertices	
Logistic Hall	Waste Receiving and Storage	592783.6	4143496	4.1		6	
Logistic Hall	Digestate Storage	592853.7	4143560	4.1		4	
Biofilter	Exhaust Air Treatment	592880.71	4143569.41	2.0		4	
Composting	Composting Windrows for digestate curing	592686	4143597	1.8		4	
				Line Source			
				Release Height (m)		Line Width (m)	
Trucking	Waste Transport	592782	4143434	3.0		3	

Source: Lawrence Berkeley National Laboratory

Odor Emission Rates for Sources

Odor associated with one or more compounds can be perceived by individuals only when the odorous compounds are present in sufficiently high concentrations to trigger olfactory responses. The intensity of odor is measured by odor units, which are the number of dilutions required to reduce odor detection to a level that would occur in only

50 percent of the exposed population. Since we do not directly measure odor concentrations in odor units (ou), the odor unit emission rates are either obtained from the literature or estimated from the measurements of individual odorous compounds (Appendix B).

The base case emission rates as well as the high and low cases are summarized in Table 2**.** Note that the emission rate from composting is esimated for an industrial-scale composting facility that employs enclosed aerated static piles to compost MSW similar to the system used by Z-Best.

Table 3: Source Emission Summary at Current Operation Scale

Process Group	Process Description	Source Type	Estimated Odor Emission Rate (ou/s)			Emission Category	Emission Frequency
			Base Case	Low Case	High Case		
PRV	Bladder pressure release ventng (PRV)	Point	5.0E+04	2.0E+04	8.0E+04	intermittent	Unknown
Logistic Hall	Western Part: Waste Receiving and Storage (RecStor1)	Area	2.8E+03	5.7E+02	5.7E+03	Intermittent	3 am to midnight (Inbound 6am-2pm; outbound to landfill 3am-8am and to ZBest 3pm-midnight)
Logistic Hall	Eastern Part: Digestate Storage (Stor2)	Area	1.5E+02	3.0E+01	3.0E+02	Intermittent	
Biofilter	Exhaust Air Treatment (Biofilter)	Area	1.9E+04	1.2E+04	2.8E+04	Continuous	
Composting	Composting Windrows for digestate curing (Compost)	Area	2.2E+05	8.4E+04	3.8E+05	Continuous	
Trucking	Waste Transport (Trucking)	Line	5.7E+02	1.1E+02	1.1E+03	Intermittent	same as Logistic Hall
Total without Compost (less PRV)			2.3E+04	1.3E+04	3.5E+04		
Total with Compost (less PRV)			2.4E+05	9.6E+04	4.2E+05		

Source: Lawrence Berkeley National Laboratory

Methods for Odor Impact Assessment

Peak-to-mean factors to scale hourly model outputs

Odor perception and sensation by humans are proportional to the instantaneous peak concentration of the odorant rather than to mean values (Schulte et al. 2007). The project team applied a recent peak-to-mean approach to scale the hourly modeled concentrations to more realistic shorter-time periods that odor is experienced.

This approach follows Piringer et al. (2016) to account for the influence of atmospheric stability and distance from the source. The project team examined separation distances determined at different times of day, seasons, and operational conditions with a range of assessment parameters to understand influential and sensitive conditions that require mitigation to limit odor impact. The analysis procedure is detailed in Appendix B.

Determination of Separation Distance

Separation distance to avoid odor nuisance is a simple metric that links odor generating sources to their impact on downwind communities, and it has been widely used in odor regulations around the world (Brancher et al. 2017). Odor dispersion modeling is the

most common method to determine separation distance. This method develops dispersion maps indicating the distance from an odor generating source where an odor is likely to exceed acceptable limits (Piringer et al. 2007).

Odor dispersion models simulate the atmospheric dilution of the odor source flow and predict ambient odor concentrations on an hourly basis. The peak-to-mean factor is applied to scale the hourly concentration to short-time peak concentrations to mimic odor sensation of the human nose. The time series of odor concentrations are evaluated for proximity to individual receptor locations to determine the exceedance probability of the threshold concentration (C_T) and compared to the allowable probability (P_T) of a given odor impact criteria (OIC). The directional dependent separation distances are usually presented on a dispersion map. In this study we report the maximum separation distances among all directions as a conservative metric for evaluating offsite odor impacts (refer to Appendix B for detailed description).

Model Simulations and Odor Impact Assessment

PRV venting

Meteorology-induced temporal patterns in separation distances

The project team first examined the spatial and temporal patterns under the fixed base case emission rate to understand the meteorological drivers of separation distances at diurnal and seasonal time scales in relation to assessment parameters. The separation distances derived here are for the worst-case (hypothetical) emission case when venting is constant.

The seasonal spatial patterns in top 2 percent odor concentrations over the "active hours" are shown in Figure 52. Odor concentrations generally present elongation in the northwest to southeast directions, corresponding to the predominant wind patterns observed in this region. There is also significant seasonal variability. The summer season (June-July-August) has the most narrow spatial extent while fall and winter seasons have more spread-out patterns when winds are weaker and more variable. Using the hourly concentrations without peak to mean scaling and aggregated over all the active hours, the separation distances from the source are generally from 200 meters in the summer to about 500 meters in the winter.

Figure 52: Seasonal Spatial Patterns over the Active Hours in Top 2 Percent Odor Concentrations

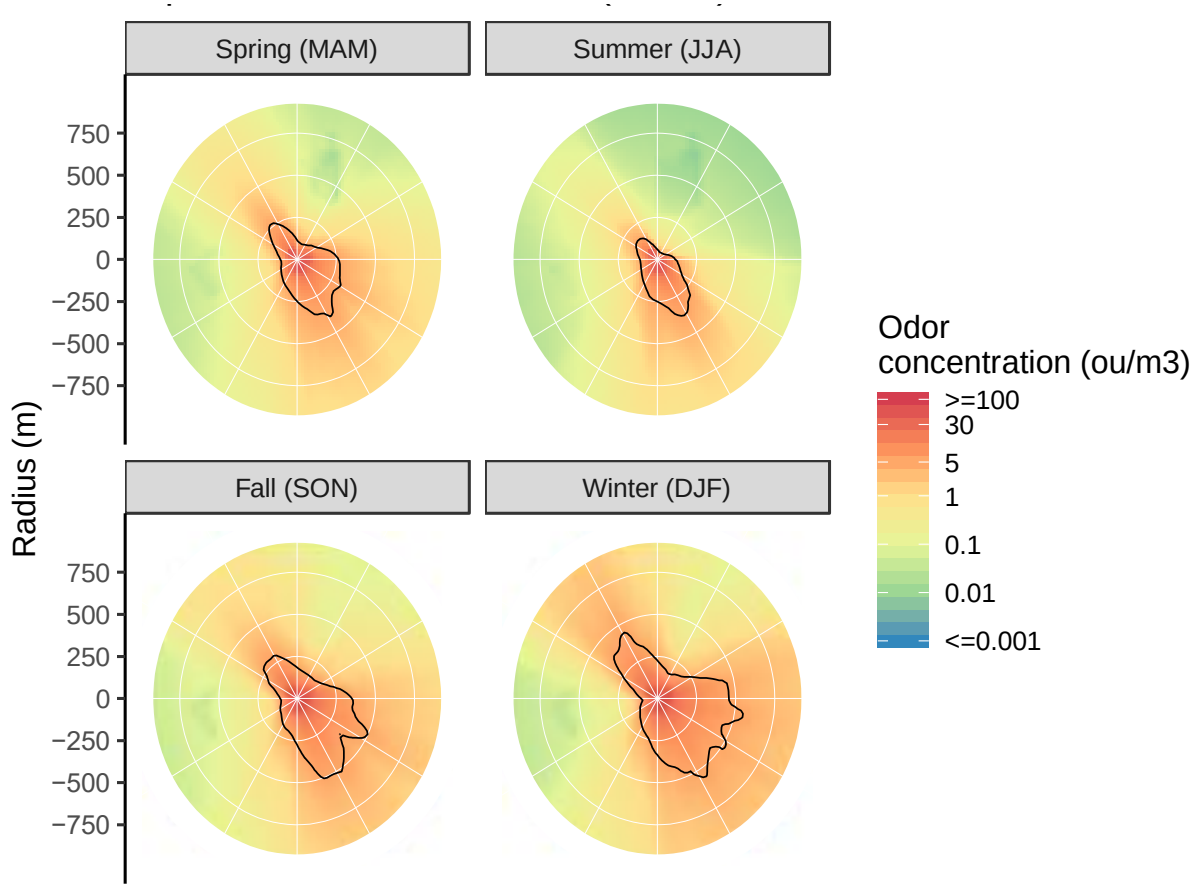

Source: Lawrence Berkeley National Laboratory

There are significant variations in separation distances. The separation distances are low (around 200–400 meters range) in the middle of the day and there is a noticeable increase (to > 500-meter range) in separation distance in the early morning and late afternoon regardless of the choice of averaging time or impact criteria (details in Appendix B). According to the time of day patterns, we can now stratify the analysis period into "high mixing hours" and "low mixing hours" when the separation distances behave more similarly with respect to each of the categories.

Influential operational conditions

Operation conditions such as venting frequency and emission rate (determined by the H_2S levels in biogas and biogas emission rates) were jointly linked to the offsite odor impacts. Figure 56 shows a two-dimensional heat map of separation distances as a function of both H_2S concentrations in biogas and venting frequencies for the worst-case scenario (during low mixing hours in the winter season) under the stringent impact criteria (not to exceed 5 ou/m^3 by 2 percent). The H_2S concentrations are varied from 100 to 2000 ppm at 100 ppb intervals. The venting frequencies in the model are varied

from 5 percent (one twentieth of the hours with venting) to 100 percent (constant venting) at 5 percent intervals.

For low mixing hours, fall and winter seasons are more challenging for limiting odor impacts. There are a number of conditions that will result in offsite impacts at distances greater than 2000 meters from the source, such as a venting frequency greater than 50% when H_2S is greater than 1500 ppm in winter (Figure 53). Therefore, at high H_2S levels (>1500 ppm) during low mixing hours in winter, the facility should take measures to reduce the likelihood of biogas venting to avoid odor nuisance in the downwind populated communities. Such measures should include proper maintenance of the water column for PRV and/or having a lower threshold for flare to avoid over pressurized bladder. For high mixing hours, the separation distances are less than 1,000 meters in all operational cases under the most stringent criteria across all seasons (see Appendix B for details).

Sensitive operational conditions can be determined by setting a "target" impact limit measured by separation distances. If the H_2S concentrations are variable or at high levels, to limit the separation distance to less than 1,000 meters, the venting frequency should be limited to less than 20 percent under the "stringent" criteria. For example, this means, on average, there should be no more than one venting per day in fall and winter during these hours. If the impact distance is limited to 500 meters, both the high and low mixing hour cases impose some limitations to the operation parameters. For example, without knowing the H_2S contamination levels, it is generally safe from an odor perspective to limit the venting frequency to less than 10 percent at all times. In this case, venting should ideally be avoided for the low mixing hours, and on average no more than one venting incidence is allowed each day during the high mixing hours.

In summary, when the facility is properly operated with infrequent venting (<20 percent), populations located 1000 meters away from the facility are largely not impacted. When recipient populations are located closer such as 200 or 500 meters away, potential conditions with large H_2S or high venting frequencies as indicated in Figure 53 may require immediate attention. Increasing plant size usually does not change the emission rates per venting events, but will likely increase the venting frequency. For larger plants, special attention is needed to harmonize processes among biogas CHP combustion and the flare to avoid frequent venting.

Figure 53: Separation Distances as a Function of Operational Conditions under Stringent Odor Impact Criteria in Winter

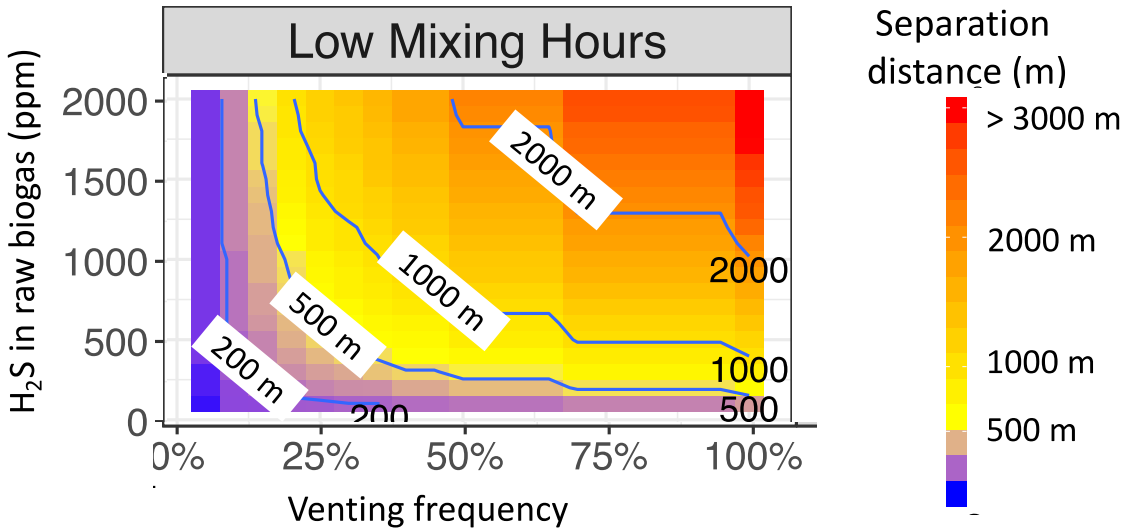

Source: Lawrence Berkeley National Laboratory

Area and Line Sources

For area and line source assessments, we aggregate the dispersion patterns based on "High" and "Low" mixing hours identified from previous analyses and report the results based on scaling hourly concentrations to a 6-minute peak to obtain a more realistic assessment. Separation distances based on the most stringent criteria (exceeding 5 ou/m^3 by 2 percent) are presented. All the results in this section are incorporated in an online tool at https://smelly.lbl.gov/zwedc.

Dispersion patterns and separation distance from area and line sources

The dispersion patterns by individual source types are aggregated over all seasons and all active hours (7am to 9pm), both the average and top 2 percent of the odor concentrations are considered. The emission sources in the logistic hall are aggregated into one category labeled as "Receiving".

The offsite impacts are dominated by the hypothetical composting windrow emissions, followed by those from the biofilters. Trucking and receiving hall emissions are insignificant when even evaluated by the most stringent odor impact criteria.

Figure 54: Maximum Separation Distances

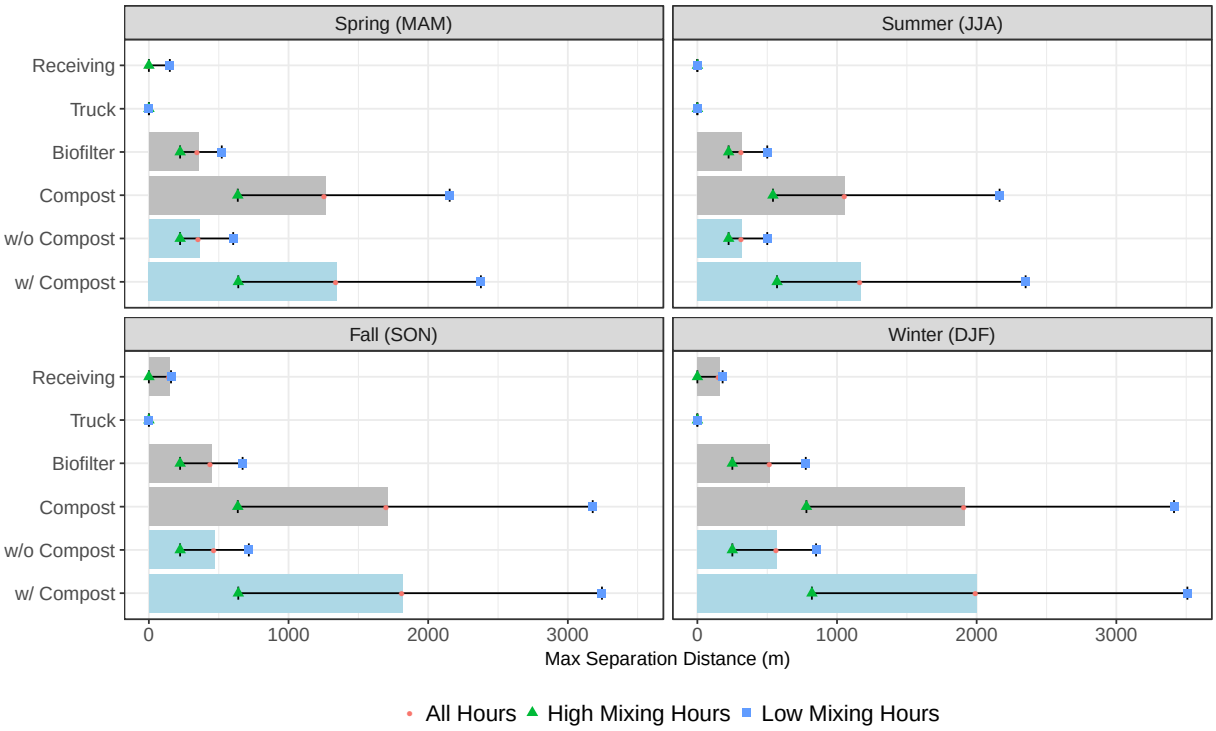

Atmospheric dispersion modeled for the ZWEDC location, with odor threshold of 5 ou/m^3 and exceedance probability of 2 percent. Grey bars indicate individual sources and blue bars indicate aggregated sources.

Source: Lawrence Berkeley National Laboratory

Odor Dispersion at Varying Operational Scales

To extend our analysis results to facilities with a wider range of waste processing capacities and atmospheric mixing conditions similar to the ZWEDC location, we simulated the odor dispersion for operation scales of 0.5, 1, 1.5, and 2 times the full scale ZWEDC capacity (90,000 ton of organic waste). The emission rates used are listed in Table 4. We consider a single biofilter or a single compost windrow as the fixed unit source, and assume the same per area emission rates and only vary the dimensions of the source layouts by plant scales.

Table 4. Odor Emission Rates (ou/s) by Sources and Facility Scales

Source	Full Scale (1x)	0.5x Scale	1.5x Scale	2x Scale
RecStor1	3.4E+03	1.7E+03	5.1E+03	6.7E+03
Stor2	1.8E+02	8.9E+01	2.7E+02	3.6E+02
Biofilter	2.2E+04	1.1E+04	3.4E+04	4.5E+04
Compost	2.9E+05	1.5E+05	4.4E+05	5.9E+05
Trucking	6.7E+02	3.4E+02	1.0E+03	1.3E+03

Source: Lawrence Berkeley National Laboratory

Considering all seasons and all active hours, we observe that areas beyond 1000 m away from the facility are not significantly affected by the facility's odor sources with no onsite composting. This is true considering all the operational scales from 45,000 tons to 180,000 tons of organic waste processing capacities and across all seasons (Figure 55).

Figure 55: Maximum Separation Distances for Each Source by Season and Facility Scale

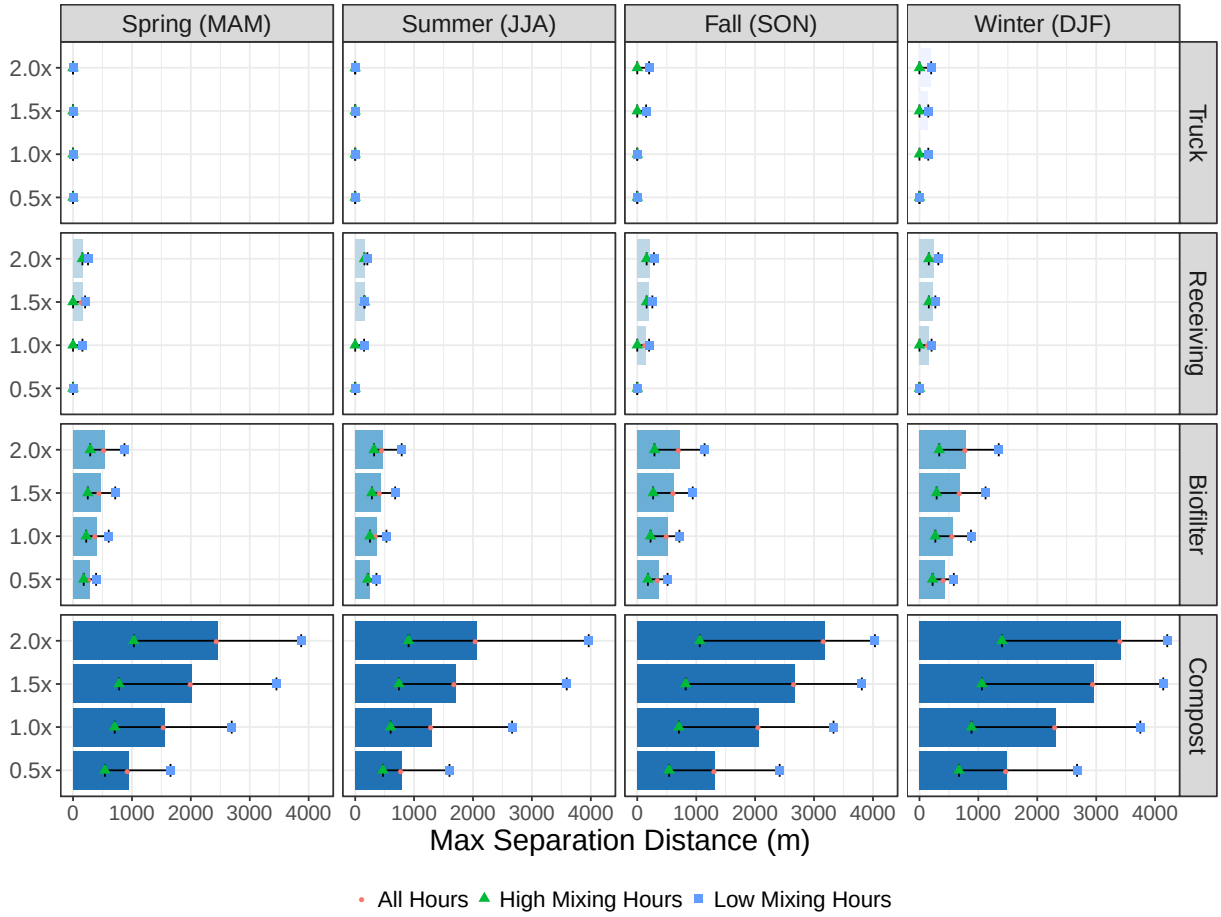

Atmospheric dispersion modeled for the ZWEDC location.

Source: Lawrence Berkeley National Laboratory

More generally, we also examined the relationship between odor unit emission rates and maximum separation distances for the range of emissions from 100 to 10^6 ou/m^3 and found a strong log-linear relationship between the two variables which are governed by atmospheric mixing conditions and seasonality (More details in Appendix B). Source geometry has a minor impact on the relationship after 500 m of separation distances. Odor emission rates below or around 10^5 ou/s generally have odor impacts limited within 2000 m away from ZWEDC, which is the case for all sources except composting at ZWEDC. This finding is useful to determine separation distance with

existing emission sources or to inform allowable emission limits within specific source-receptor distances.

Summary of Odor Dispersion and Impact Assessment

The modeling of potential odor source characterization using estimated emissions and atmospheric dispersion for the ZWEDC location revealed that the odor character and intensity vary greatly by sources. Modeled odor emissions are dominated by (hypothetical) compost windrows, followed by biofilter exhausts and biogas venting. Biogas venting is modeled as an intermittent source with unknown emission frequency. The model results indicate leakage from delivery trucks and the receiving hall is a minor contributor.

Dispersion modeling results revealed locations and times most sensitive to potential odors from the ZWEDC location. Odor transport is consistently in the southeast-ward direction with impacted areas largely within 2000 m of non-residence areas. Greater impacts were found during hours with low atmospheric mixing (early morning/evening and late afternoon) and in fall and winter seasons.

Modeled offsite odor impacts were found to be source dependent and were largely driven by hypothetical compost emissions (that could occur if onsite compost operations were returned to ZWEDC). Composting emissions are the most challenging of the potential odor sources considered. Separation distances of more than 3000 m are required (based on 2 percent exceedance probability of 5 ou/m^3 exposure) for the hypothetical onsite composting operation. Biofilters and other sources included in the model generally do not impose significant odor impacts on communities located 2000 m or farther downwind. The model results suggest these emission sources will not limit the facility scaleup to 1.5-2 times of current capacity.

The impact of biogas venting depends on operational conditions (contamination levels and venting frequency) and has potential impacts on local communities during hours with low atmospheric mixing.

Based on these findings, the project team recommends best practices include scheduling high-odor generating processes during high mixing hours (middle of the day) or outside of the human active hours (before 7 am or after 9 pm). In addition, the project team recommends maintaining the water column of the pressure release valve to reduce the probability of biogas venting during early morning hours and at the end of the day. Special attention is also needed to harmonize processes among biogas CHP combustion and the flare to avoid frequent venting of biogas.

Our analysis also revealed policy relevant findings. Separation distances required for siting a facility are highly dependent on the allowable odor impact criteria (allowable exceedance frequency and threshold concentration) set by policy makers. More research and data on community perceptions of odor would help inform development of odor impact criteria to ensure appropriate protection of nearby communities. This study

identified a strong log-linear relationship between separation distances and total odor emission rates. Knowledge of this relationship can be instrumental for future facility planning and siting. This model used atmospheric mixing for the ZWEDC location. Further investigation in other locations with different meteorological and terrain conditions would broaden the applicability of the odor dispersion model developed in this study.

CHAPTER 4:
Life-Cycle Energy, Greenhouse Gas, and Air Pollutant Assessment

In this chapter, we conduct a rigorous life-cycle assessment (LCA) that integrates the best available values across the scientific literature and newly-collected empirical data to explore the climate and human health tradeoffs between landfilling, composting, and dry AD of mixed municipal organic waste. Our choice to focus on dry AD (solids loading 22-40 percent (Ward et al. 2008)) rather than wet AD for waste-to-energy stems from its usefulness in processing solid organic waste streams, particularly those with appreciable inorganic contamination, in dedicated facilities and potential to reduce costs (De Bere 2000). This study also explores variations in the management of solid digestate remaining after AD, including landfilling, raw digestate application to land, and composting, including estimated net GHG impacts and fertilizer offset credits after the material is applied to working land. By establishing a system boundary that extends from waste collection through application of residual solids/compost to soils, this study provides a rigorous analysis of life-cycle GHG emissions (CO_2, CH_4, N_2O), air pollutant emissions (NO_x, non-methane volatile organic compounds or NMVOC, SO_2, CO, NH_3, and $PM_{2.5}$), and monetized climate and human health damages associated with organic waste management options.

Methodology

Clearly defined and sufficiently expansive system boundaries are essential to understanding the tradeoffs between different organic waste management and utilization strategies, along with input data that is as robust and representative as possible. Trucking distances, landfill emissions, composting emissions, and net emissions post-land application are all closely tied to the specifics of a location, waste composition, and detailed management strategy. Attempting to quantify a broadly applicable set of average values is of limited usefulness. We have chosen to begin with an existing set of operations in San Jose, California. Specific mass and energy balances, emission rates, and transportation distances are tied to a dry AD facility built and operated by Zero Waste Energy Development Company (ZWEDC), referred to simply as ZWEDC in the following sections (see Figure S1 for an aerial photo). In addition to the ZWEDC case, we evaluate alternative management options for the same material as variations on this scenario (see Figure 56). In the existing ZWEDC operations, mixed municipal organic waste is sent to a dry AD facility and raw biogas is combusted to generate electricity for on-site use and to export to the grid. The solid digestate is sent to a composting facility before it is ultimately applied to land as finished compost (Figure 57 shows detailed ZWEDC operations). The additional hypothetical alternatives include: landfilling all mixed organics, composting all mixed organics, variations on the

ZWEDC configuration in which digestate is either directly land-applied or landfilled, dry AD with biogas upgrading for pipeline injection to offset natural gas, and dry AD with biogas upgrading to fuel an otherwise diesel-powered truck fleet. Key details of these scenarios are discussed in following subsections.

Figure 56: System Boundary for Life-Cycle Assessment

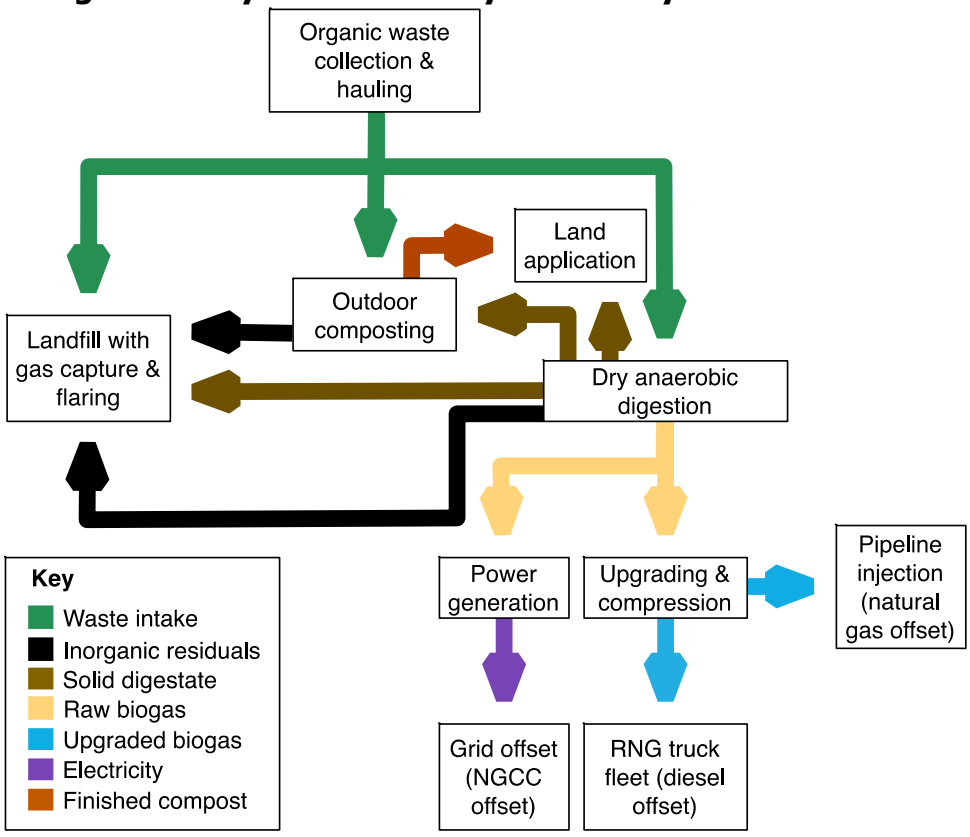

Source: Lawrence Berkeley National Laboratory

To compare these scenarios on a common basis, we express all emissions in term of one wet tonne of mixed organic waste processed. The question we seek to answer is: given a unit mass of organic waste, what management strategy results in the most favorable net GHG and human health impacts? The results are dependent on the waste composition, and for this analysis, the mixed commercial organics processed at ZWEDC are approximated as food waste. Visual inspection at ZWEDC indicated that the organics received by ZWEDC are, in large part, food and food-soiled paper products, although the exact composition varies day-to-day and is not characterized on a regular basis. For the landfilling and composting scenarios, as well as for hypothetical variations on ZWEDC operations such as biogas upgrading to RNG, best-available literature and industry values form the basis of our analysis. We expect these results to be generalizable in the U.S. national and international context for similar waste mixtures and technologies, with the exception of possible variations in composting and land

application emissions. Landfill emissions will also be higher in states and countries that do not tightly regulate fugitive emissions.

Landfilling Organic Waste

The most common basis for comparison in organic waste management is landfilling. This reflects "business as usual" practices for 76 percent of mixed organics across the U.S. (U.S. Environmental Protection Agency 2018). In the specific ZWEDC case, waste would be transported for disposal at the Newby Island Landfill. Large commercial waste streams (e.g. grocery stores and company cafeterias) are hauled directly, whereas municipal streams are sent first to material recovery facilities (MRFs) for initial sorting. Emissions sources in this scenario include trucks (modeled as all diesel as a simplifying assumption) hauling waste from commercial facilities and MRFs to the landfill, fugitive emissions from waste decomposition in the landfill not captured by the gas capture system, and emissions from the landfill gas flare. We account only for emissions that occur within 100 years of disposal. Fugitive landfill gas emissions and flaring emissions are based on California-specific data in the EPA Waste Reduction Model (WARM) (USEPA 2018). The mixed commercial organics processed at ZWEDC are approximated as food waste. Visual inspection at ZWEDC indicated that the organics received by ZWEDC are, in large part, food and food-soiled paper products, although the exact composition is not consistent day-to-day and has not been measured in detail. Food waste decays quickly before individual landfill cells can be capped and connected to the gas capture system, so more than half of total methane emitted over their lifetime is emitted to the atmosphere (USEPA 2018). Because WARM only includes GHGs, the emissions of NO_x, NH_3, SO_2, CO, NMVOCs, and $PM_{2.5}$ emissions from the landfill operation and flaring are estimated using data from Ecoinvent. We also account for landfills' potential to sequester biogenic carbon, although the global warming potential offset is fairly small compared to methane emitted; the sequestration of recalcitrant biogenic carbon offsets up to 7.5 percent of the methane emissions from landfills (USEPA 2018).

Composting Organic Waste

The most conventional alternative to landfilling is composting of raw organic waste. 61 percent of yard trimmings are composted in the U.S., although only 5 percent of mixed organics/food waste is composted (U.S. Environmental Protection Agency 2018). Composting can be a useful alternative for diverting either raw organic waste or further stabilizing solid digestate to make it more suitable for land application. That said, even a well-managed composting process can lead to releases of ammonia (NH_3), nitrous oxide (N_2O), CH_4, sulfur dioxide (SO_2), carbon monoxide (CO) and odor, but these emissions are not well studied across a range of starting materials, management techniques, and local climates (Amlinger et al. 2008; Boldrin et al. 2009; Saer et al. 2013; CEPA 2017). In this scenario, we model direct transportation of all raw organic waste to the Z-Best composting facility near the City of Gilroy (~ 70 km from ZWEDC), which is an outdoor composting operation capable of handling up to 1,180 tonnes of

organic waste per day. This longer driving distance will likely be representative of large-scale composting options for cities across the U.S., given odor and emissions concerns associated with such operations. In the scenario where all organic waste is shipped directly to Z-Best rather than ZWEDC, we assume it is bagged and composted for an additional 16 weeks. Finished compost is applied to cropland as a soil amendment and partial fertilizer replacement (Favoino and Hogg 2008; Martínez-Blanco et al. 2013; Martínez-Blanco et al. 2009). This compost ultimately displaces the need for urea fertilizer (46 percent nitrogen by mass), and the offset credit is calculated on the basis of nitrogen, using an assumption of 5.5 percent nitrogen content in the compost (Sullivan et al. 2015). The life-cycle of urea production is modeled assuming electricity, transportation (truck and rail), and natural gas production in the United States.

Dry Anaerobic Digestion of Organics with On-site Electricity Generation

Dry AD for conversion of solid organic waste to biogas under-studied relative to wet AD. The life-cycle impacts of wet AD systems used to process the municipal organic waste, manure, and biosolids have been explored in numerous papers (Scipioni et al. 2009; Möller and Müller 2012; Turconi et al. 2011; Tonini et al. 2013; Boesch et al. 2014). To populate our model, we were able to obtain operating data over multiple years from the ZWEDC dry AD facility in San José, CA. The facility is designed to accept approximately 81,650 tonnes (90,000 tons) of waste annually. Waste intake at ZWEDC is dominated by mixed organics, often accompanied by a substantial quantity of inorganic contamination that must be separated and landfilled. Our model relies on delivery logs that include the origin of each truckload of waste, some of which is delivered from MRFs while other loads are hauled directly from commercial sources including grocery stores and office parks. We modeled monthly average totals of 5,142 tonnes of commercial waste from Republic (a combination of direct-haul , 891 tonnes of processed organics from the SMaRT Station (a MRF in Sunnyvale, CA), 1,170 tonnes of commercial waste from locations around Palo Alto, 1,040 tonnes of yard waste from Palo Alto, and 35 tonnes from other sources.

At the ZWEDC facility, sorted organic waste is dewatered and loaded into 16 dry digesters that have a residence time of 21 days. Produced biogas is first sent to storage bladders located on the facility roof, which provide storage for a few hours' worth of biogas production, then biogas is treated to reduce H_2S concentrations using an iron sponge and fed to an on-site combined heat and power (CHP) facility comprised of two 800 kW generators, for a combined capacity of 1.6 MW. Approximately 30 percent of the biogas is flared due to gas storage limitations as well as the nature of batch digestion, which produces low-methane content (referred to as lean) gas at the start and end of each cycle that cannot be sent to CHP units (see Figure 57). Daily electricity consumption at ZWEDC averages 3,700 kWh/day (translating to an average load of 156 kW), including operation of the extruder, lighting, and fans. We assume net electricity exports offset marginal generation from natural gas combined cycle (NGCC) power plants in California. The solid digestate generated at ZWEDC (4,040 tonnes per month

on average) is aerated in four in-vessel composting tunnels on-site for 4-5 days before being sent to the Z-Best composting facility (72 km from ZWEDC).

After being trucked down to the Z-Best facility, solid digestate from ZWEDC is placed into commercial composting bags that are approximately 100 m × 6 m × 3 m when filled. Each encased windrow is filled with approximately 635 tonnes of material and undergoes a 14-week composting cycle, during which piles are force aerated but not turned. The finished compost is ultimately sold for agricultural and landscaping applications.

Figure 57: ZWEDC Dry Anaerobic Digestion Process

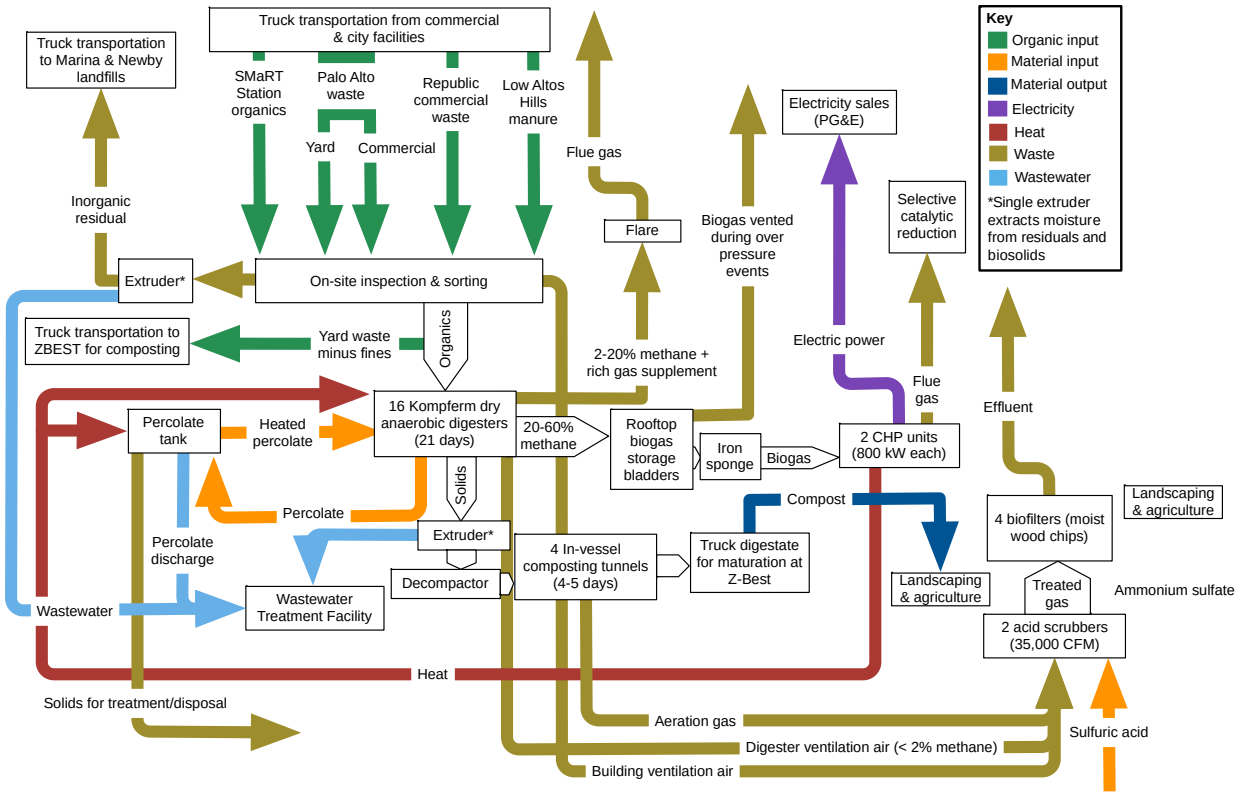

Source: Lawrence Berkeley National Laboratory

Solid Digestate Landfilling and Land Application

An alternative to the current ZWEDC operations as described above is a system in which all on-site operations are identical, but solid digestate is not sent to a composting facility. The first option is to landfill the digestate. Digestate can be handled as waste for landfilling or possibly used as alternative daily cover (ADC) to control insects, rodents, odors, fire. Because, in both cases, the same material is being placed in the landfill, we do not expect that the use of digestate as ADC would result in substantial differences in the GHG footprint or other emissions. For this case, we modeled outbound trucking of raw digestate to the Newby Island Landfill nearby, which captures and flares its landfill gas. Emissions associated with the landfilling of digestate are

highly uncertain and empirical data in the literature is inadequate. Thus, we conservatively assume the emission factor for landfilled digestate is equal to the emission factor for landfilling raw mixed organic waste. Another alternative fate for raw digestate is direct land application. In this case, we assume the raw digestate not only replaces inorganic fertilizers but also result in a higher nitrogen use efficiency by crops and contribute to soil organic matter turnover (Tambone et al. 2010; Brown and Leonard 2004). Land application of digestate in the form of biosolids can sequester 25 Mg CO_{2e} per 100 tons of dry biosolids thereby partially avoiding the use of synthetic fertilizers (Brown et al. 2010). Because of nutrient runoff concerns, land application of digestate only occurs for half of the year, with digestate being sent to landfills during the winter rainy season (California Association of Sanitation 2017; State Water Resources Control Board 2018).

Dry Anaerobic Digestion of Organics and Renewable Natural Gas Use for On-Site Truck Fleet

Understanding the tradeoffs between on-site combustion versus RNG applications is important for owners and operators of anaerobic digestion facilities, particularly when building new facilities or expanding existing ones. Without additional cleaning (primarily H_2S and water removal) and upgrading (where CO_2 is removed to increase the heating value), raw biogas cannot be compressed or used in pipelines or vehicles. This means raw biogas must either be flared or combusted for on-site heat and electricity generation, as is the case at ZWEDC. However, understanding the tradeoffs between onsite combustion versus RNG applications is important for owners and operators of anaerobic digestion facilities, particularly when building new facilities or expanding existing ones. In this scenario, we explore a hypothetical alternative scenario in which ZWEDC utilizes its biogas to fuel a retrofitted fleet of trucks rather than combusting it for electricity generation. Conversion of biogas to RNG is energy-intensive and reported mass/energy balances vary across the literature. Biogas is treated to remove moisture, particulates, contaminants and other gases (such as CO_2, O_2, N_2 and VOCs); this increases the methane content to 90 percent or more, depending on the upgrading technology. Commonly used biogas upgrading technologies include water scrubbing, pressure swing adsorption, and membrane separation. Some studies estimate membrane separation energy requirements around 0.3 kWh/m^3 (Makaruk et al. 2010; Pöschl et al. 2010) but the energy demand estimates can be as high as 0.5 kWh/m^3 (Pertl et al. 2010). Pressure swing adsorption and water scrubbing require around 0.2 kWh/m^3 and 0.27 kWh/m^3, respectively (Pertl et al. 2010). We use an approximate value of 0.32 kWh/m^3 with a 0.6 percent loss factor and methane content of upgraded biogas of 96 percent. Because the biogas is being compressed and thus longer-term storage (beyond a few hours' worth of production) is more feasible, we conservatively approximate that venting events can be cut by 50 percent relative to the base case. We assume produced RNG displaces diesel use in trucks that would be fueled on-site.

Dry Anaerobic Digestion of Organics and Renewable Natural Gas Pipeline Injection

Upgraded biogas with methane content more than 96 percent can also be used as renewable pipeline-injected natural gas. The upgrading process and associated energy demand is identical to the case described above for on-site RNG use in trucks. However, the offset credit is different because we assume the RNG displaces fossil natural gas (as opposed to offsetting diesel in the on-site truck fleet scenario) in unspecified end-uses and that the facility transports biogas via an interconnecting pipeline to an existing commercial pipeline located one mile away. In other words, end-use emissions are assumed to remain unchanged relative to a base case in which fossil natural gas is used. Emissions associated with the construction of the one-mile pipeline interconnection are assumed negligible when amortized over its lifetime, and thus are excluded.

Life-Cycle Emissions Inventory

The life-cycle inventory includes GHG emissions (CO_2, CH_4, and N_2O) on a 100-year CO_{2e} basis, NO_x, NH_3, NMVOC, SO_2, CO, and $PM_{2.5}$. These are all evaluated across a common functional unit of one wet tonne of organic waste processed (see Figure 56). To construct a life-cycle inventory for each scenario, we collected direct mass and energy flow data, using as much measured and facility-logged data as possible from the ZWEDC facility's four years of operation. This is particularly important given the lack of data on dry AD and solid digestate composting in the existing literature, as well as the gap between best practices in an idealized scenario and what is typical at organic waste management facilities that handle highly contaminated waste streams. Through a collaboration with the ZWEDC facility owners and operators, we accessed inbound and outbound logs, including organics by type, residuals (trash for landfilling), and solid digestate. The facility also provided total biogas production, biogas flared, and electricity production; venting frequency and duration at the storage bladders were measured by the co-authors on-site. Emission factors for digestate composting, biogas flaring, and biogas venting are all based on measured values at Z-Best and ZWEDC. Values that could not be or were not directly measured are assembled from literature sources, including peer-reviewed articles, GREET, and the Ecoinvent database (see Appendix C).

Direct mass and energy flows from waste source to final product(s) were incorporated into a physical units-based input-output life-cycle inventory model, Agile-C2G, which has been documented extensively in previous literature (Breunig et al. 2019; Neupane et al. 2017; Baral et al. 2019; Scown et al. 2014). This model was used to calculate indirect emissions associated with electricity generation, fertilizer production, diesel fuel production, and other minor material/energy inputs. California-based sources were considered wherever appropriate. To account for net CO_2, CH_4, and N_2O emissions after land application of composted organics, raw digestate, and composted digestate, we use GHG emission and sequestration factors documented in Breunig et al. (2019). Other

non-GHG air pollutant emission factors during the post-land-application phase are assumed to be negligible relative to the emissions during waste management, AD, and composting.

To capture parameter uncertainty, we established probability distributions for key parameters based on previous literature and used these in a Monte Carlo analysis (see Appendix C). The model was run for 10,000 trials drawing from these distributions to develop the box and whisker plots shown in the results. Although the distributions were developed based on wide-ranging literature values from both in and outside California, the expected values indicate values specific to the ZWEDC case study. At times, the specific study result may lie beyond the upper or lower quartile because the measured values at ZWEDC or Z-Best are not in the middle of the ranges published in previous literature. This text will focus its discussion on the expected-value results for ZWEDC/Z-Best.

Monetized Climate and Public Health Damages

Although monetized externality estimates are an imperfect measure of environmental impacts, converting GHG emissions and air pollutant impacts into social costs can serve a few purposes. First, these estimates provide a means of comparing different inventory metrics based on their relative importance to one another. Second, monetizing human health damages allows for differentiation between emissions that occur within or outside densely populated areas and thus the expected impact on the population. Third, the dollar values provide some guidance as to what governments may wish to pay in order to avoid undesirable externalities. To account for the human health damages associated with air pollutant emissions, we compare two common integrated assessment models: Air Pollution Emission Experiments and Policy analysis (APEEP, specifically version 3, hereafter referred to as AP3) and Estimating Air pollution Social Impact Using Regression (EASIUR) (Muller and Mendelsohn 2007; Heo, Peter J Adams, et al. 2016; Heo, Peter J. Adams, et al. 2016). Multipliers to convert emissions to social costs are provided in Appendix C. In these cases, we include only pollutants that occur locally, either at the ZWEDC facility, Z-Best compost facility, or nearby transportation routes, assuming ground-level emissions values. The damage factor most difficult to refine on a scientific basis is the social cost per tonne of CO_{2e} emitted, and the cost of carbon used in regulations can be highly politicized. We use a relatively conservative social cost of carbon of $42 per tonne CO_{2e}, which was established by the Interagency Working Group on the Social Cost of Greenhouse Gases for use in regulatory analyses (Interagency Working Group on the Social Cost of Greenhouse Gases 2016).

Life-Cycle Assessment Results

The results of our analysis are presented in three sections. First, we show life-cycle GHG emissions results, followed by results for all air pollutants (NO_x, NH_3, NMVOC, SO_2, CO and $PM_{2.5}$). Last, we convert these life-cycle inventory results into monetized

damages using the multipliers discussed in the Methods section and provided in Appendix C.

Life-Cycle Greenhouse Gas Inventory

The life-cycle GHG results (see Figure 58), which include non-biogenic CO_2 as well as all CH_4 and N_2O emissions normalized using a 100-year global warming potential (GWP), indicate that landfilling organic waste is the most GHG-intensive option on a per-tonne basis, with a GHG footprint of 800 kg CO_{2e} per tonne of organic waste. Any option for diverting organic waste, particularly the higher-moisture material such as food waste that releases substantial fugitive methane, provides substantial GHG benefits. The footprint will be roughly doubled if organics are sent to a landfill without a functioning gas capture system in place. The next most GHG-intensive options are the dry AD configurations in which some or all of the solid digestate must be landfilled. If all digestate is landfilled, the GHG footprint is 87 kg CO_{2e} per tonne of organic waste. As mentioned in the Methods section, solid digestate can only be land applied for a portion of the year in California because of water quality/runoff concerns during the rainy season, so the land application scenario still results in large landfill emissions. Thus, the land application scenario reduces, but does not eliminate, landfill methane emissions, resulting in a net GHG footprint of 54 kg CO_{2e} per tonne of organic waste. Each of these scenarios is dominated by landfill methane emissions. Some facilities may choose to avoid this seasonal limitation by trucking digestate long distances to locations that do not regulate digestate land application in the winter. In that case, the avoided landfill GHG emissions are likely to be larger than the increased trucking emissions. However, depending on the local climate where digestate is land-applied, there may be other concerns such as increased nitrogen runoff and N_2O emissions (Breunig et al. 2019).

The GHG footprints of composting raw organics and the three dry AD scenarios that do not require any landfilling of solid digestate all have much lower GHG footprints than scenarios that involve landfilling. The emissions for these scenarios are net negative and on the same order of magnitude as one another, and the factors driving the differences between them, such as the net soil carbon impacts of compost application, are nuanced and uncertain. This finding is consistent with previous literature, as shown in the meta-analysis by Morris et al. (2013). Composting results in the lowest GHG footprint, totaling -76 kg CO_{2e} per tonne of organic waste. A large GHG sequestration credit and a more limited fertilizer offset credit are both based on expected benefits from land application of the compost. The scenario that combines dry AD, electricity generation, and composting digestate (ZWEDC current operations) results in a net GHG footprint of -12 kg CO_{2e} per tonne of organic waste. If biogas is upgraded to RNG and used to offset diesel fuel use in a fleet of new or retrofitted trucks, the net GHG footprint is reduced to -56 kg CO_{2e} per tonne of organic waste. This demonstrates that offsetting diesel can avoid a larger quantity of fossil CO_{2e} emissions than offsetting NGCC electricity, as is assumed in the biogas-to-electricity scenarios. Upgrading biogas to RNG and injecting it into the pipeline for use in place of fossil natural gas results in

reduced GHG mitigation (-22 kg CO_{2e} per tonne of organic waste) relative to the scenario in which RNG offsets diesel use.

Figure 58: Life-Cycle Greenhouse Gas Footprints by Scenario

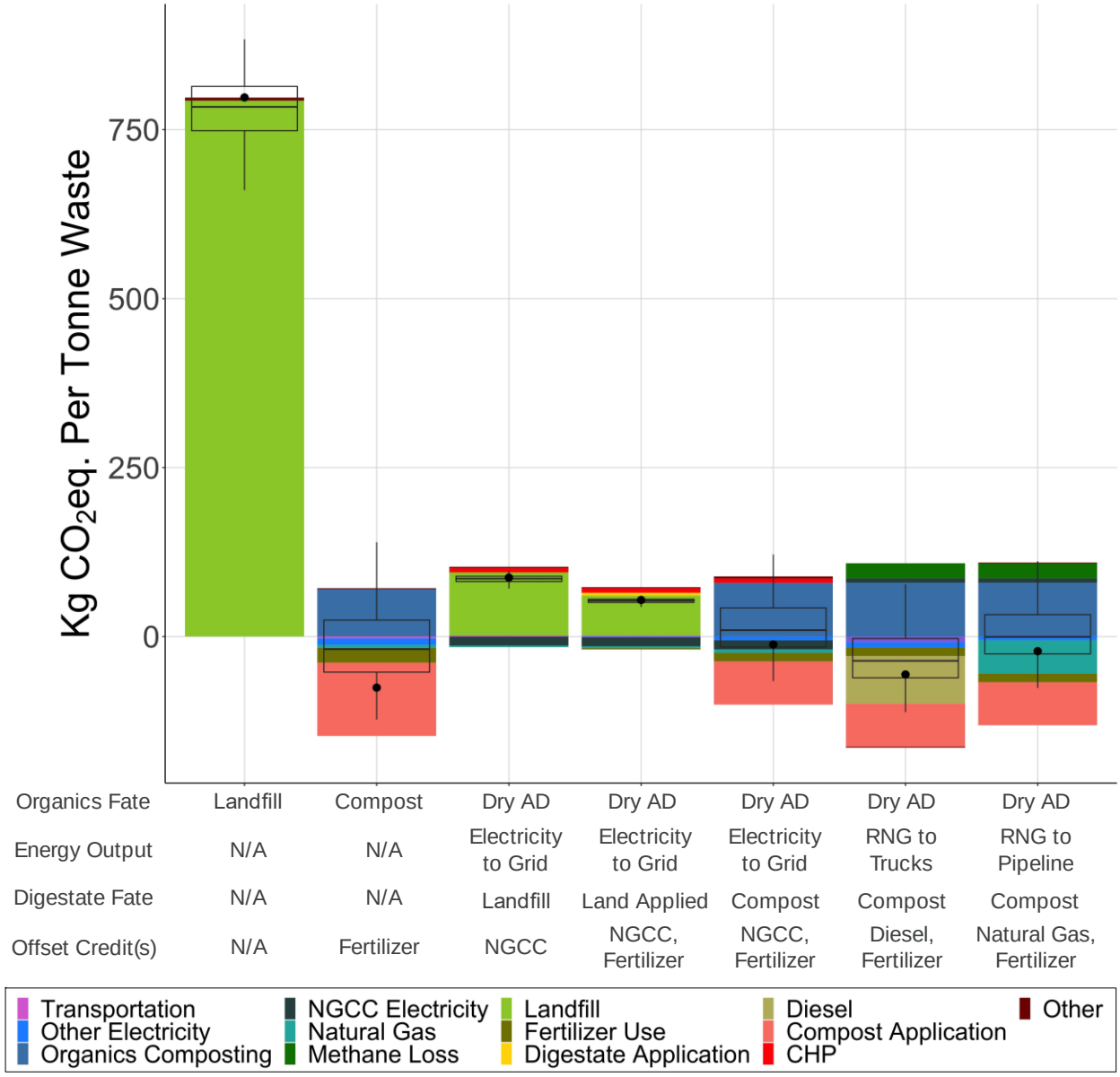

The black dot indicate net. Contributors less than 1 percent are categorized as "Other."

Source: Lawrence Berkeley National Laboratory

A point of confusion may be the fact that cleaning up biogas and injecting it into the pipeline to be combusted in place of fossil natural gas (at a power plant or otherwise) is preferable to combusting raw biogas on-site for electricity and heat. The process of cleaning and upgrading biogas does, after all, involve energy inputs and methane losses. ZWEDC operates two 800 kW engines at approximately 40 percent efficiency, not accounting for rich biogas that must be flared or vented when units are down for

maintenance or are otherwise not able to utilize all available biogas. Aside from heat losses during electricity generation, 30 percent of rich biogas is flared at ZWEDC and a negligible fraction is vented. By comparison, NGCC plants are able to use waste heat in a secondary steam cycle to generate additional electricity, resulting in an average NGCC plant efficiency across California of 47 percent. We also assume that, once the facility invests in a gas cleanup/upgrading system and pressurized storage, flaring and venting will be cut in half, resulting in only a 15 percent loss. Thus, even after accounting for beneficial waste heat recovery for use in the digesters, the choice to clean and upgrade the biogas for use as a drop-in replacement for natural gas results in greater GHG reductions. If instead power exports to the electricity grid displace the average California grid mix, given its high share of renewable energy, the disparity is likely to become more pronounced. Furthermore, if pipeline-injected RNG is used for vehicles in place of diesel, the GHG advantage will grow. In short, the benefits of biogas upgrading to RNG are likely to be greater, no matter the end use of the RNG, relative to using biogas for on-site, small-scale electricity generation and export to the electricity grid in California or any other location in which the grid is relatively clean.

Life-Cycle Air Pollutant Inventory

The life-cycle air pollutant emissions vary dramatically across the different scenarios, as shown in Figure 59. $PM_{2.5}$ is generally recognized as the air pollutant primarily responsible for human health damages and it is primarily released as a result of combustion (Cohon et al. 2010). $PM_{2.5}$ can be emitted directly (primary $PM_{2.5}$) or formed in the atmosphere as the product of chemical reactions of precursors including NO_X, SO_2, VOCs, and NH_3 (referred to as secondary $PM_{2.5}$). Landfills are estimated to release the greatest primary $PM_{2.5}$ per tonne of organic waste across all options, and these emissions are dominated by the on-site flaring of landfill gas. Flares generally do not have emissions control technology and, given varying methane concentrations and imperfect mixing, they tend to emit more PM than biogas-fired power generators. The two dry AD cases in which some or all solid digestate must be landfilled are the next highest-emitting options in terms of primary $PM_{2.5}$. In contrast, the dry AD case in which RNG is used in place of diesel fuel for trucks is a net-negative because of the avoided $PM_{2.5}$ associated with operating diesel trucks (and the relatively negligible $PM_{2.5}$ emissions from RNG trucks). We do not account for potential non-combustion sources of $PM_{2.5}$ because they are expected to emit particles larger than 2.5 μm in diameter, such as dust.

Nitrogen oxides (NO_x), accounted for as mass of NO_2, and SO_2 are respiratory irritants for humans and precursors to secondary PM and ozone. Both pollutants are the product of combustion. Flares at landfills and AD facilities are the dominant source of SO_2. Flaring also emits NO_x, and because flares do not have NO_x emissions controls, the emissions per unit of fuel input are higher than for biogas and natural gas combustion in power generators, as reflected in Figure 59. Composting results in net-negative NO_x and SO_2 emissions because direct emissions are negligible and applying finished

compost to soil can reduce the need for nitrogenous fertilizer, which is energy- and emissions-intensive to produce. In the case where biogas is cleaned and upgraded to RNG, the distinction between RNG used to offset diesel in a fleet of trucks versus use in pipelines to offset fossil natural gas is critical. NO_x and SO_2 emissions are net negative if RNG is used in vehicles because of the avoided tailpipe emissions from diesel combustion. If RNG is used to offset fossil natural gas (through pipeline injection), net emissions are positive but still lower than most other scenarios.

NMVOC and NH_3 emissions are both challenging to quantify because of limited data. However, the life-cycle emissions for both are likely dominated by emissions from composting operations. NH_3 is produced during microbial decomposition, which occurs in both the digesters and during the composting process, as a way to discard excess nitrogen not required as a nutrient for the microbes. Thus, NH_3 is present in rich and lean biogas at the facility as well, but is largely removed by the acid scrubber or oxidized to NO_x through combustion. In the case of NMVOCs, small negative values are owed to the fact that offsetting fossil natural gas use reduces fugitive emissions (a small fraction of which are non-methane compounds such as ethane and propane). CO emissions are also dominated by composting operations, although incomplete combustion during flaring and biogas-fired electricity generation also contribute to the total emissions.

Greenhouse Gas and Air Pollutant Social Costs

To compare the social cost of primary and secondary $PM_{2.5}$ exposure and GHG emissions across waste management scenarios, we used two different integrated assessment models, APEEP and EASIUR, in combination with a $42 per tonne CO_{2e} social cost for GHG emissions (see Figure 60). The results indicate that the social cost of landfilling wet organic waste is approximately $40-50 per tonne (this does not include odor externalities or non-emissions related costs such as impacts on local property values). Because GHG-related damages make up the largest fraction of the overall monetized damages for landfilling, this value will change depending on the assumed social cost of carbon. For comparison, the median landfill tipping fee in California, as of 2015, was $50/tonne while countries that landfill very little of their waste, including Germany and Sweden, have tipping fees around $200/tonne (CalRecycle 2015), suggesting that incorporating even a fraction of the estimated social cost into tipping fees could greatly encourage diversion from landfills. Both AP3 and EASIUER indicate that NH_3 emissions are the dominant contributor to social costs in every case where some or all organic material is composted. This is because NH_3 emissions per tonne of organic waste processed are at least two orders of magnitude greater than any other non-GHG pollutant in each scenario that includes composting and the damages per tonne of NH_3 are four orders of magnitude larger than for CO_{2e} (see Figure 59). However, AP3 and EASIUR disagree in some cases by more than a factor of three, with AP3 estimating greater NH_3-related damages than EASIUR. An additional caveat is that there is very little known about NH_3 emissions from landfills

before cells are capped off and gas capture/flaring systems are in place, particularly for specific waste types, such as nitrogen-rich food wastes. Similarly, very little is known about NH_3 emissions from land application of raw or composted digestate.

Figure 59: Life-Cycle $PM_{2.5}$, NO_x, NMVOC, SO_2, NH_3, and CO

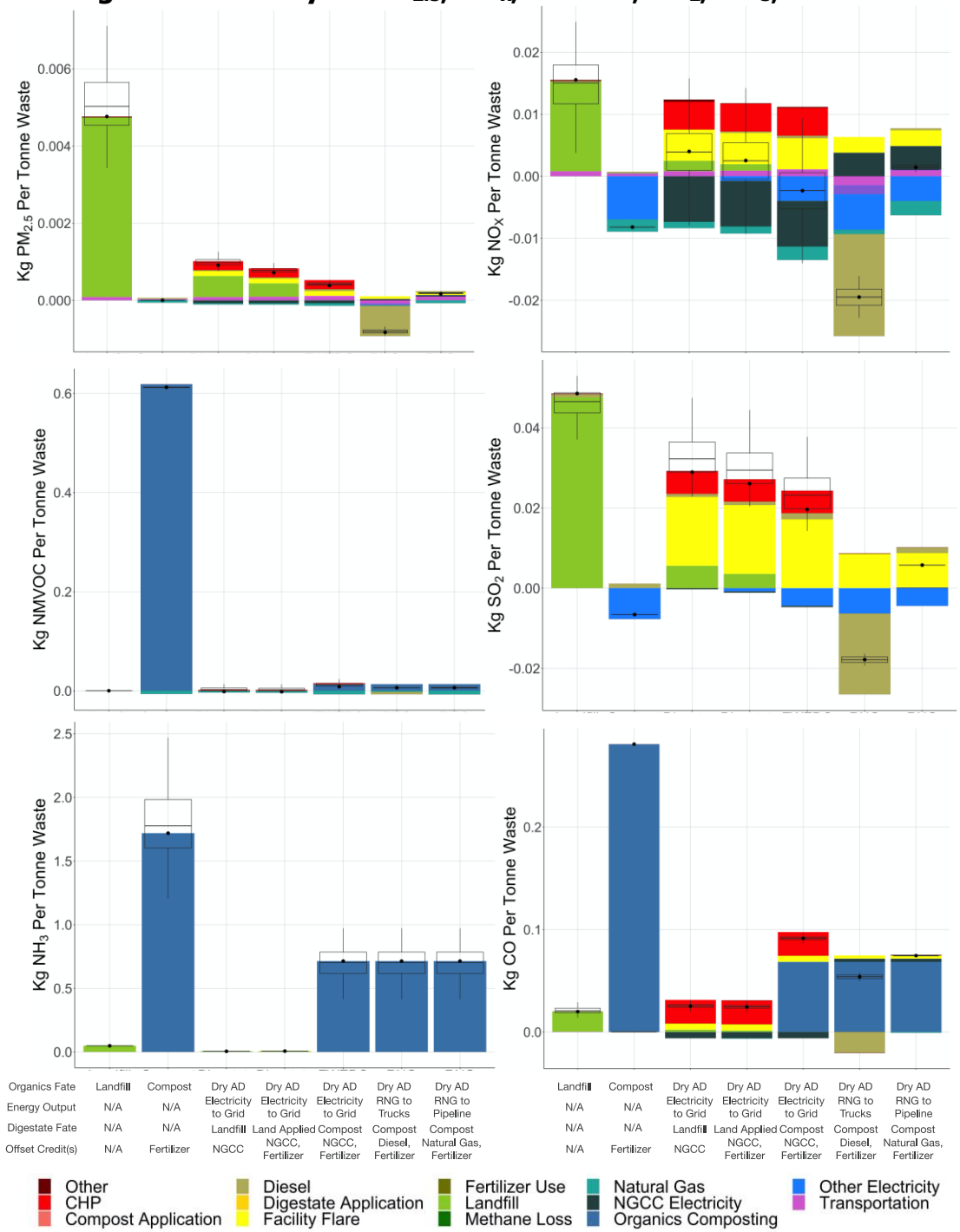

The black dot indicate net. Contributors less than 1 percent are categorized as "Others."

Source: Lawrence Berkeley National Laboratory

NH_3 plays an important role in the formation of secondary $PM_{2.5}$ by reacting with nitric acid (HNO_3) and sulfuric acid (H_2SO_4), resulting from NO_x and SO_x emissions, to form ammonium nitrate (NH_4NO_3) and ammonium sulfate ($(NH_4)_2SO_4$) aerosols. The recent inter-comparison of integrated assessment models by Gilmore et al. (2019) confirmed the relatively high social cost of NH_3 in all three models evaluated, especially when compared to NO_x. Since the molecular weight of NO_x is nearly three times larger than NH_3 per unit mass, NH_3 will generate more NH_4NO_3 molecules than will NO_x. Also, NH_3 reacts faster than SO_2 and NO_x to form secondary $PM_{2.5}$ such that the secondary $PM_{2.5}$ plume is smaller and more concentrated at ground level near people. Both EASIUR and AP3 indicate that composting has a greater social cost than landfilling. Both assessments also predict that landfilling and land applying digestate are the least damaging options among all scenarios considered in this study. However, the models yield contrasting estimates of the relative health impacts of the ZWEDC and two RNG scenarios versus landfilling: AP3 indicates that landfilling is the preferred option while EASIUR indicates that landfilling is the most damaging of these scenarios.

It is important to note the difficulty of accurately predicting secondary $PM_{2.5}$ formation in integrated assessment models; this is especially true for California. While sulfate formation is most important in the Eastern U.S., in California, secondary inorganic $PM_{2.5}$ is largely dominated by NH_4NO_3 due to use of low sulfur fuels in the power and transportation sectors (Chow et al. 2006). As discussed in Heo et al. (2016), NH_4NO_3 is a more difficult component to model than others in $PM_{2.5}$ due to greater uncertainties in emissions and atmospheric processes. Furthermore, the impact of NH_3 on particle formation is dependent on the relative abundance of NH_3 versus HNO_3 in the atmosphere, so the effect is location dependent. Both EASIUR and AP3 have been calibrated using data in the Eastern U.S., where the meteorology and atmospheric chemistry are different from the Western U.S. As such, further modeling for specific locations, particularly in the Western U.S., is warranted before making definitive conclusions. Additionally, care should be taken when comparing studies using different APEEP versions, as substantial changes to the model have occurred, particularly with respect to damage multipliers for NH_3.

Figure 60: Climate and Public Health Damages

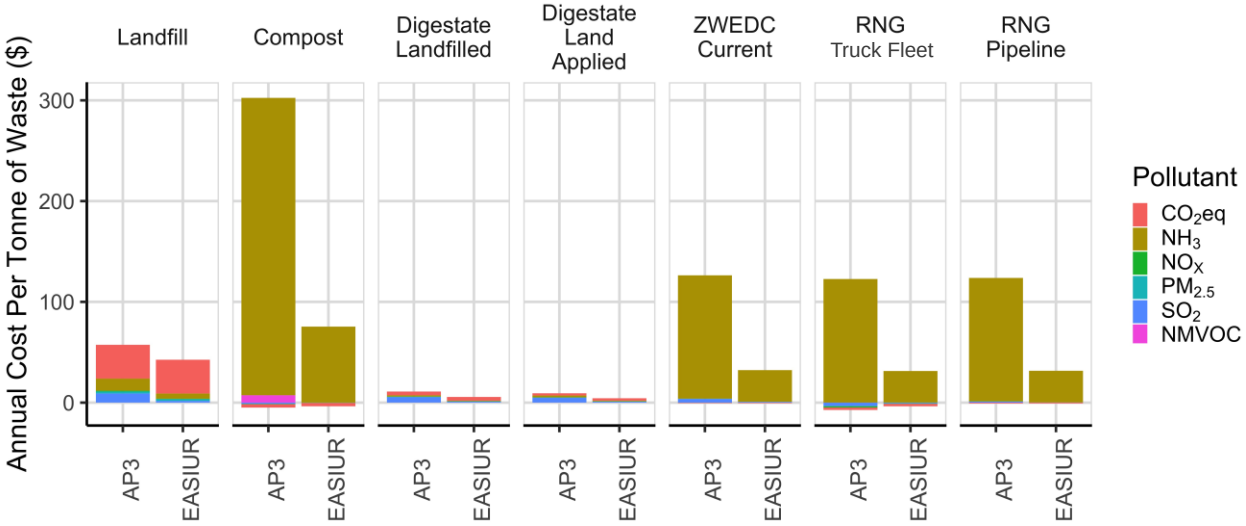

Source: Lawrence Berkeley National Laboratory

This study reveals the complexity of estimating environmental tradeoffs in organic waste management systems, and the difficulty of making broadly applicable recommendations for how organic waste should be handled. Previous literature has indicated consistently that landfilling is the least attractive option, even in more tightly regulated states like California that require efficient gas-capture systems (Morris et al. 2013). Our GHG emissions results reinforce this conclusion. Fugitive methane emissions are the key driver in the GHG footprint of organic waste, and any scenario in which organics are landfilled will result in higher GHG emissions. The offset credits for electricity, RNG, and finished compost are also important for determining both net GHG emissions and other air pollutant emissions. If, for example, compost application does not cause a net reduction in nitrogenous fertilizer use, the net negative values for NMVOCs, NO_x, SO_2, and GHGs will be eliminated. The question of whether RNG offsets diesel or fossil natural gas will have a substantial impact on net NO_x emissions. However, on a social cost basis, none of these changes to the assumptions would alter the basic conclusions.

If NH_3 emissions are confirmed to be a driving factor in social costs of organic waste management options and are indeed greater on average at composting sites relative to landfills, the larger question is how and to what degree those emissions can be reduced. Because large composting windrows are not well-mixed controlled environments, some pockets of excess nitrogen are inevitable, particularly when nitrogen-rich food waste or digestate serves as the input. However, maximizing microbial activity and thus increasing demand for nitrogen through improved monitoring and control of pH, temperature, and aeration level during the composting process can reduce NH_3 emissions (Jiang et al. 2011). Another alternative for minimizing total social cost is to locate large composting operations in sparsely populated areas, although this may result in environmental justice/inequity issues if rural populations are

socioeconomically disadvantaged relative to urban populations. Further empirical research, exploring a range of material types and composting practices, will be essential to better understanding which options for diverting organic waste from landfills provides the greatest public good.

CHAPTER 5:
Policy and Economic Barrier Assessment

Overview of Policy and Economic Barriers

The regulatory and policy barriers identified and discussed in this section are organized into three major process stages: (1) waste sorting, delivery, and processing; (2) AD/biogas management and utilization; and (3) outputs and residuals processing (see Figure 61). The chapter describes specific barriers and challenges within the major process stages supplemented with operational and financial data from the ZWEDC facility, where appropriate. The chapter concludes with implications for policymakers and regulators seeking to broaden the use of solid waste biomass technologies such as AD.

Figure 61: Three Major Anaerobic Digestion (AD) Process Stages

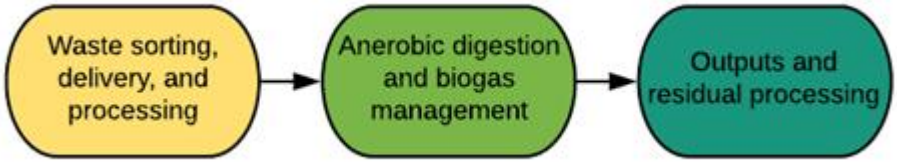

Source: Lawrence Berkeley National Laboratory

Waste Sorting, Delivery, and Processing Barriers

Sorting waste streams, including food waste, recyclables, and green materials, is a major process stage upstream of AD facilities impacting the efficacy of AD to meet public policy goals. Current material recovery infrastructure is streamlined to maximize throughput of high value recyclables, such as aluminum, dried paper, polyethylene, and high-density polyethylene plastics. Evaluating how the current infrastructure and practices impact the ability to recover and use organics is the first step to improving organic waste diversion from landfills. The upstream barriers fall into two broad areas: waste collection and feedstock quality.

First, shifts from multi-stream and drop-off center recycling processing to single-stream collection over the last several decades across much of U.S. has resulted in contaminated waste streams for AD facilities. In 2014, 80 percent of California's jurisdictions reported the use of single-stream collection services for both residential and commercial sectors (CalRecycle 2016). With California's collection infrastructure streamlined to capture high-value recyclables, organic waste is contaminated by the commingled stream of garbage and recyclables. Of the approximately 108 thousand tons of organic MSW accepted by ZWEDC in 2016 (much of which has been pre-

processed), almost 27 thousand tons (or approximately 25 percent) were inorganic residuals that had to be sorted, removed, and sent to alternate disposal sites.

Second, current California statewide waste quality standards and educational efforts do not target the organic waste stream, even in jurisdictions with separate composting bins for organic MSW collection. This causes variations in feedstock quality for AD facilities in California. While CalRecycle allocates and distributes funding to support public education, the funds are almost entirely dedicated to beverage container recycling.

Anaerobic Digestion and Biogas Management Barriers

AD facility operations that emit air pollutants are regulated via operating permits identifying sources of possible air emissions, specific equipment and methodologies for abating those sources, and maximum allowable emissions. These permits include emissions of greenhouse gases, criteria and toxic air pollutants and their precursors, and odorous compounds. When AD facilities operate in excess of permitted levels, they may receive citations or fines, or they can be shutdown. In ZWEDC's case, the Bay Area Air Quality Management District (BAAQMD) granted a permit to operate the AD facility that included requirements for its waste processing area, digesters, flare, biofilter, biogas storage bladders, outdoor compositing activities, and CHP section.

While air permits by themselves are not a barrier to enabling broader use of AD, several factors can lead to more citations, fines, and degraded operational efficiency. Many of the abatement technologies are not new, but the equipment can be complex and outside the expertise of smaller-scale facility managers. Similarly, managing the range of abatement equipment and following the required testing and operational procedures specified in air permits may overextend a facility's compliance staff that had not factored in more technical and numerous air monitoring requirements. Air permits are also inherently inflexible in how they establish specific operational thresholds instead of ranges.

AD and aerobic composting facilities, which utilize biological processes that produce ammonia, hydrogen sulfide, and odorous organic compounds, must also manage the generation of odors and health and safety concerns from bioenergy production. Adverse publicity and regulatory pressure are associated with failure to control and manage odors in the organic recycling industries (Coker 2012). At AD facilities, odor generation is associated with all three major process stages (see Figure 61), though outdoor composting and curing typically contribute most to the odorous emissions (Epstein and Alix 2001). ZWEDC invested substantial resources to address odor concerns, including purchasing compost windrow turners, aerating equipment, and an odor control misting system totaling more than $330,000 in capital equipment, yet was unable to satisfactorily reduce odorous emissions. The facility now sends digestate more than 70 miles away to another company for offsite composting, which imposes additional costs for trucking and tipping fee payments.

Beyond the common odor problems associated with organic waste facilities, there are additional health and safety concerns specific to the ZWEDC facility in its bioenergy production. First, the venting of biogas and odor compounds directly to the atmosphere without passing through abatement systems such as a flare—which is a safety measure to prevent over-pressurization of the biogas storage units—poses public health concerns. This biogas can include high concentrations of hydrogen sulfide, which is both an odorous compound and an air toxin. In addition, the high quantities of methane within the biogas make the venting an explosion hazard. Second, a small amount of ammonia used to control NOx emissions from the CHP engines can "slip" past the selective catalytic reduction (SCR) system. This released ammonia contributes to the atmospheric formation of particulate matter. These emissions scale with the facility size and could require safety training and protective equipment, potentially contributing to the operational and compliance costs during the facility scale up.

Output and Residuals Barriers

A range of co-products from typical AD processes could potentially have high economic and environmental value, including compost, fertilizer, as well as conversion of biogas to heat and electricity. In addition, biogas has the potential to be cleaned of impurities and upgraded to biomethane for use in compressed natural gas (CNG) vehicles or injection into natural gas pipelines. Yet, realizing the full value of these products requires addressing several issues, including contamination of compost products, interconnection requirements, and net electricity export compensation.

Digestate, in this case, refers to the solid and liquid material remaining after the AD process is complete and has several applications for agriculture, including compost (the solid portion of the digestate) and fertilizer. The quality of digestate is dependent on two key factors: (1) the types of feedstocks used in the AD process, and (2) the level of contamination in waste collection and processing.

Enabling the sale of electricity from biogas powered generation sources (e.g., CHP), as well as the purchase of backup power, requires interconnection to the utility's network. The standards governing technical and contractual terms between generating system owners (the AD facility in this case) and the utility are generally established by state utility regulators and can pose a costly and complex barrier (Costello 2014). Interconnection procedures and requirements may delay project development and add significant expenses to complete technical analyses, even more so in the case of newer technologies and applications such as AD. In ZWEDC's case, the interconnection process took many months and the utility over-estimated the costs to install electrical equipment to export electricity by about $1 million.

In 2015, the California Public Utilities Commission established a bioenergy feed-in-tariff (FiT) program (Bioenergy Market Adjusting Tariff or BioMAT), mandated by SB 1122 (California Public Utilities Commission (CPUC) 2014). FiT programs provide small-scale bioenergy facilities the opportunity to obtain competitive fixed-price standard contracts

with investor-owned utilities (IOUs). For example, PG&E is required to accept 30.5 MW of biogas from the following sources: wastewater treatment, municipal organic waste diversion, food processing, codigestion.[2] FITs have proven effective at increasing adoption of renewable energy (Couture et al. 2010). ZWEDC was the first facility to enroll successfully in California's BioMAT FiT program, which provides electricity price compensation to eligible generators of waste-derived electricity at about $130 per MWh, significantly above the 2016–2017 wholesale electricity market prices in California (e.g., $30 to $40 per MWh, depending on the time of day and time of year). Prior to enrollment, ZWEDC was essentially selling electricity to the utility at wholesale market prices. Participation in the BioMAT program has noticeably increased the facility's monthly exported electricity revenues from a few thousand dollars to more than $50,000.

While FiT programs have largely been successful, they present a number of implementation challenges for policymakers and utilities. FiT programs tend to be somewhat broadly defined in terms of the resources they support and may result in less cost-effective siting of projects on the grid (Couture and Cory 2009). ZWEDC's enrollment and participation in the BioMAT program has proved to be time-consuming and costly. BioMAT enrollment requirements are the same for facilities of any size up to 5 MW of generation (provided not more than 3 MW is delivered to the grid at any time) and many of the enrollment requirements are set to meet the complexity of the largest facilities. For example, facilities must provide numerous design and operational certifications that presume sophisticated understanding of power engineering and power generating facility technical criteria (e.g., testing, re-powering). This puts the facilities at the smaller end of the range, like ZWEDC (1.6 MW of generating capacity), at a disadvantage.

Implications for Regulators and Policymakers

In response to recent legislation mandating waste diversion, California will face a steep increase in accessible organic waste supply within a decade. Both AB 1826 and SB 1383 mandate a high degree of organic waste diversion and processing for commercial and public sectors; specifically, 75 percent of organic waste disposed each year will need to be diverted.

The increasing supply of organic waste requiring diversion due to upcoming regulatory mandates will likely be met with a lack of processing infrastructure. At the end of 2015, CalRecycle's Facility Information Toolbox estimated that California's organic waste processing sector had 5.7 million tons of processing capacity available (CalRecycle 2016). To meet the Short Lived Climate Pollutant Act's diversion mandate, 9.7 million more tons of processing capacity will be required in order to process this newly diverted

[2] CPUC. December 18, 2014. Decision 14-12-081 in Rulemaking 11-05-005. Decision Implementing Senate Bill 1122. Ordering Paragraph 1.

material. Current AD facilities, therefore, may need to be expanded, and new facilities built.

The barriers faced by the bioenergy sector in California are multi-faceted and involve several agencies. The report offers several considerations for policymakers and regulators across California state agencies—CalRecycle, CARB, CPUC, and CEC—to address the challenges and develop more adaptive policy solutions:

California's waste infrastructure is designed to primarily capture high-value recyclables, but the waste diversion goals in SB 1383 suggest an equal or greater value needs to be placed on organic waste. State mandates specifying organics separation may improve feedstock quality for solid waste biomass facilities. Additionally, major investments in waste infrastructure may be required to optimize the collection and processing of organic waste, which otherwise is considered a low-value contaminant relative to other recyclable residential collection streams.

Similarly, historical education efforts and current franchise agreements reflect this focus on recyclables over organic waste and may need to be reconsidered in light of increasing needs for organic waste separation. For example, source separation practices could be incorporated statewide in the K-12 curriculum.

AD facilities must conform to air permitting and regulatory standards largely through abatement technologies requiring dedicated staff and expertise, which may be lacking at smaller-scale facilities. Air permits may also establish operating parameters based on non-similar technologies that can constrain AD operations. The 2012 CEC Bioenergy Action Plan identified several recommendations regarding the permitting of bioenergy facilities that would address many of the challenges discussed in this report.

In addition to permitting, AD processes generate odorous compounds and facilities must manage public odor concerns. These odor sources and their impacts are difficult to characterize and quantify due to their sporadic nature. More research and measurement efforts are needed to characterize the odor sources associated with AD facilities and air permitting agencies could work with first adopters of AD to better understand emissions prior to enforcing monetary penalties.

Many of California's investor-owned utility interconnection processes are unnecessarily costly and technically burdensome. State utility regulators can address interconnection barriers and establish rules that do not unduly burden AD facility generating systems. Several states (e.g., Ohio and Oregon) have successfully implemented interconnection standards that promote broad participation of customer generators (Interstate Renewable Energy Council (IREC) 2013). Additionally, AD facility planners should take into account the additional time and cost implications of interconnection standards, as well as the details of the standards when making decisions about facility design and project budgets.

Current BioMAT enrollment requirements can be lengthy and limit participation by smaller generators. Additionally, BioMAT includes penalty provisions that, while intended to produce consistent generation output, may be unnecessarily large and limit generator profitability. Price levels and rules for BioMAT, and other similar biomass FiT programs, could incentivize additional municipal organic waste diversion if they consider the environmental benefits of solid waste biomass technologies, particularly benefits of diverting waste from landfills and align with timing of state policies for bioenergy (SB 1122) and methane reductions (SB 1383), among other state environmental policies.

CHAPTER 6:
Implementation in Scale-Up of Waste Intake and Power Production

Introduction

At the outset of this project, the ZWEDC facility's throughput was approximately half of its 90,000 tons/year capacity. The solid digestate was composted on-site and the facility faced a range of challenges, including odor complaints and exceedances in allowable emissions from the flare. ZWEDC, Lawrence Berkeley National Laboratory, and the City of San José formed a partnership to conduct research in support of scaling up operations at ZWEDC and addressing the most pressing technical challenges faced by the facility.

The goals for scaling up ZWEDC were established in terms of both tons of waste intake and on-site electricity generation. At the beginning of the project, ZWEDC established the following schedule for scale-up:

- End of year 1: waste intake to 50,000 tons organic waste/year
- End of year 2: waste intake to 70,000 tons organic waste/year and 1 MW generation
- End of year 3: waste intake to 90,000 tons organic waste/year and 1.6 MW generation
- Double total capacity; install 90,000 tons/year of additional anaerobic digestion capacity and corresponding composting capacity, possibly increasing net CHP capacity to 4 MW

This chapter describes ZWEDC's progress to meet major scale-up milestones, as well as the barriers and challenges limiting the waste intake and power production for the foreseeable future. The project team used monthly operational data to explore financial barriers through a *pro forma* financial model. The chapter concludes with recommendations to mitigate barriers for larger scale dry AD deployments in California.

Data and Feedback Provided

This analysis uses ZWEDC operational data to assess facility costs and revenues at increasing waste intake levels. Waste intake data were captured through daily waste delivery logs and aggregated to monthly totals by major waste source. Electricity production data were recorded on a 15-minute timescale and aggregated to monthly values. Other operational and financial data used in this analysis were provided on a monthly basis.

The project team discussed preliminary findings and conclusions with ZWEDC staff. ZWEDC staff provided valuable feedback and context to improve the project team's understanding of trends. The project team aggregated and summarized information to protect commercially sensitive data.

Completion of Phase 1

ZWEDC achieved its Phase 1 goal of 90,000 tons/year of organic waste intake and 1.6MW of nameplate CHP capacity by the end of 2015. This chapter describes trends in monthly waste intake, biogas production, electricity generation, and net electricity export from January 2016 through June 2018 with a focus on factors leading to significant monthly variations.

Waste Intake up to 90,000 Tons per Year

From January 2016 to June 2018, monthly waste ranged from about 6,700 tons to about 10,600 tons, though most months are well above the 7,500 ton per month minimum necessary to achieve the 90,000-ton annual goal (see Figure 62). Residual amounts similarly showed significant variation, ranging from less than 12 percent to more than 41 percent. ZWEDC invested in an extruder in June 2016 to remove water weight from residual waste to reduce disposal costs. The effect of this is evident by a decline in residual waste weight beginning in July 2016.

Figure 62: Monthly Waste Intake Levels by Source with Residual Percentage

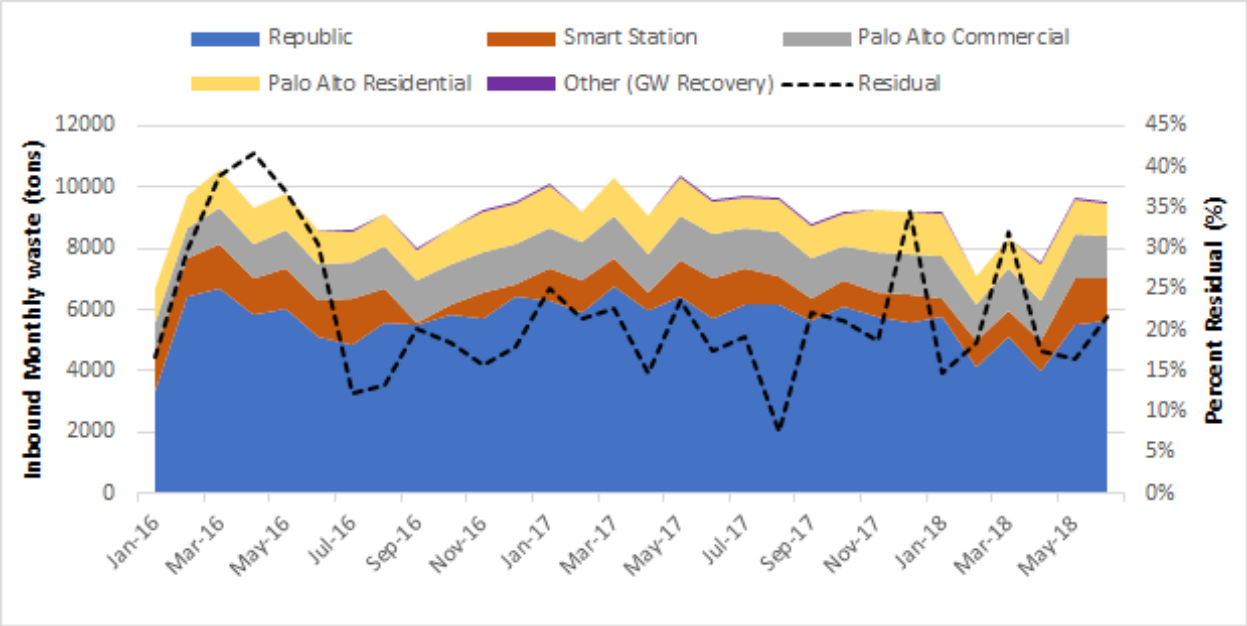

Left axis shows monthly waste intake in total tons and right axis shows the corresponding residual content as percentage of total waste.

Source: Lawrence Berkeley National Laboratory

Figure 63 shows on-site biogas consumption at the ZWEDC facility and the percent of produced gas that went to the CHP units. Total gas production is impacted by the amount of organic waste being processed through the digesters, though there is not a perfect match-up between waste intake and biogas production due to staggered schedules for loading digesters and 21-day residency times. In late 2018, gas production significantly decreased due to the death of the bacteria in one of the two digester percolate tanks. "Lean burn" flaring events occur for the low-methane gas that is produced at the start and end of each digester bay's cycle, and therefore a small but consistent portion of gas goes to this purpose. "Rich burn" flaring events occur when the biogas storage bladders are full and additional gas cannot be sent to the CHP units. In Fall of 2016, CHP shutdowns caused significant rich burns, while the aforementioned bacterial shutdown and (possibly related) shutdown of CHP 2 caused higher-than-usual rich burns while the system was stabilized and CHP 2 was brought back online. In stable operating months, around 80 percent of the produced biogas by volume is sent to electricity production, though this fraction can be as low as 10 percent depending on operational challenges.

Figure 63: Monthly On-site Biogas Consumption by Use with Percent Used by CHP Units Noted

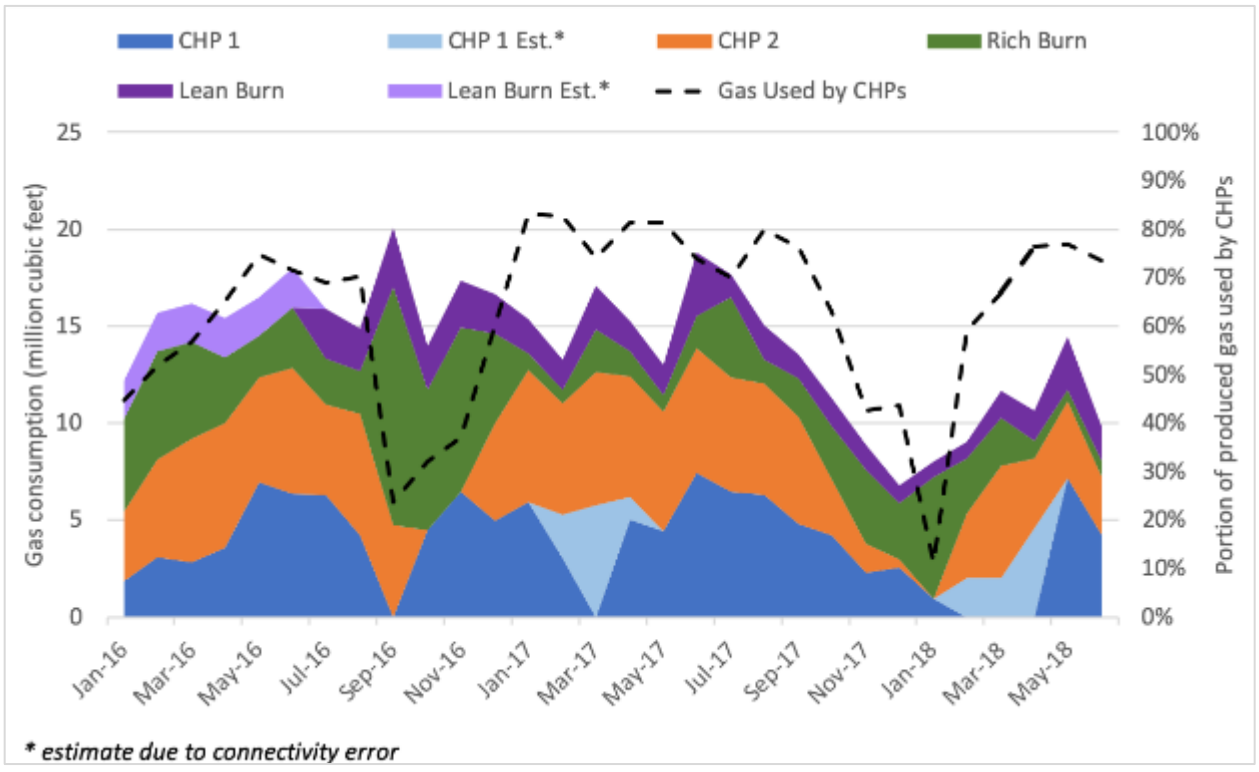

Left axis shows monthly biogas consumption and right axis shows the percent of biogas produced used by the CHP section.

Source: Lawrence Berkeley National Laboratory

Power Generation to 1.6 MW

Figure 64 shows monthly CHP production for each of the two 800 kW CHP units from April 2014 through June 2018. During that period, monthly CHP capacity factors ranged from less than 10 percent in earlier years to more than 70 percent in more recent periods.

Notwithstanding a general trend of improving capacity factors over time, the CHP is operating at capacity factors lower than ZWEDC's expected maximum of 80 percent. Low capacity factors are typically due to low biogas production or CHP unit shutdowns as described in the section above.

Figure 64: Monthly CHP Production by Unit with Total CHP Capacity Factor

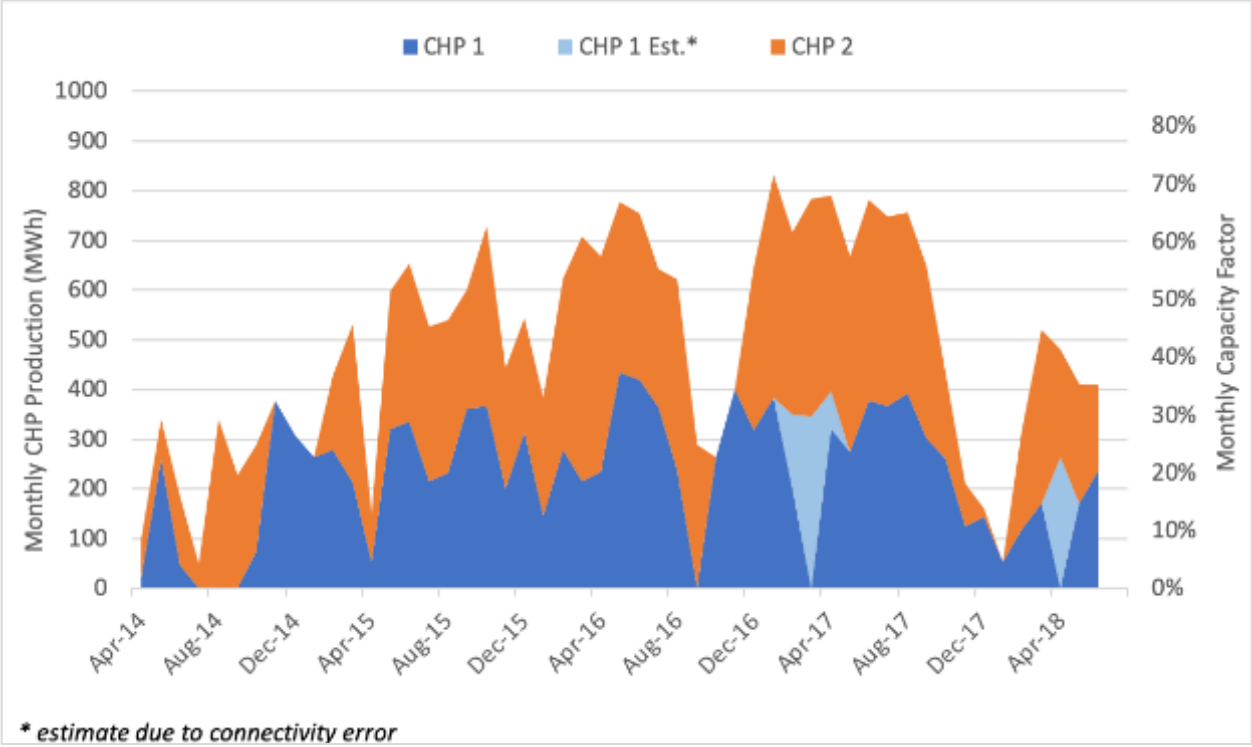

Left axis shows monthly CHP production at each unit in MWh and right axis shows corresponding total CHP capacity factor.

Source: Lawrence Berkeley National Laboratory

Figure 65 shows monthly CHP production against ZWEDC's on-site electricity use and the resulting net electricity export for July 2016 through June 2018, the months for which metered electricity use data is available. In general, ZWEDC metered on-site usage is relatively flat, and therefore net electricity exports are driven by total CHP generation. As discussed earlier, CHP production is affected by many factors. Thus, net electricity export is likewise impacted by waste intake levels, biogas production, and CHP maintenance (planned or unplanned). The increase in ZWEDC metered use (and subsequent decline in net electricity export) from November 2017 to January 2018 is due to the bacterial shutdown described above. Typically, waste heat from the CHP

units is used for heating the digester percolate tanks and in-vessel composting tunnels, however due to the low gas (and therefore heat) production during the shutdown electric boilers were rented and used to heat the necessary portions of the facility.

Figure 65: Monthly CHP Production, ZWEDC Consumption, and Net Electricity Exports

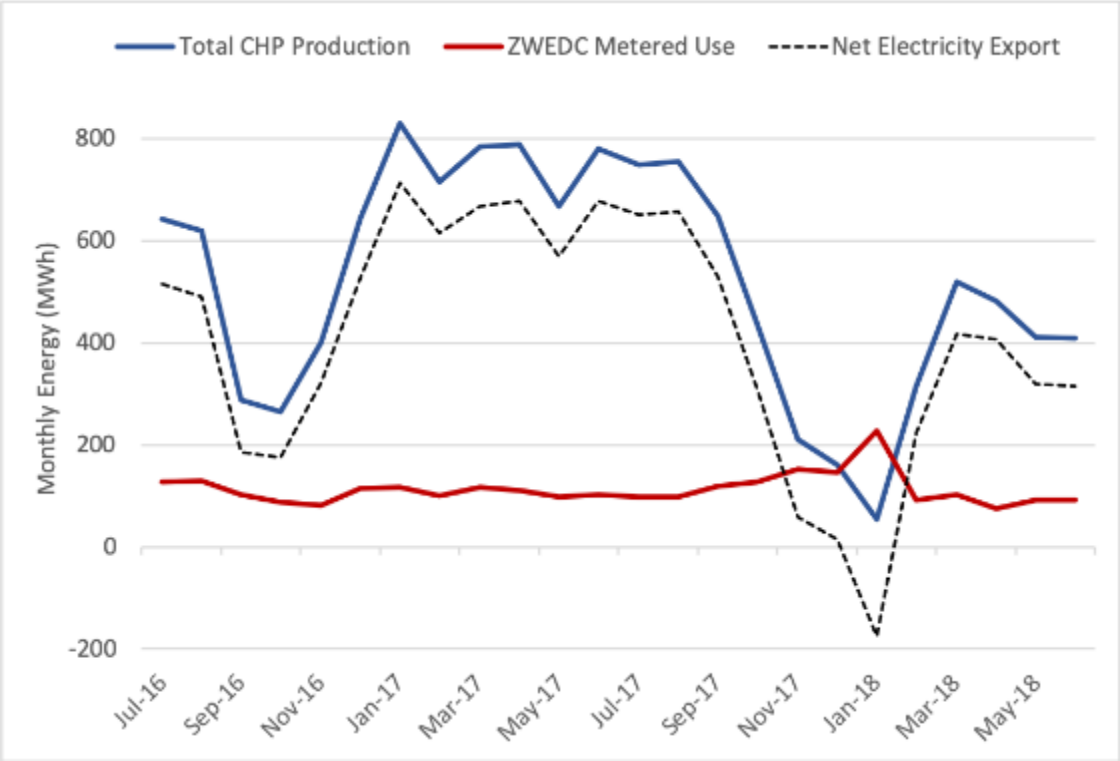

Source: Lawrence Berkeley National Laboratory

Further Scale-up

At the onset of this project, ZWEDC scheduled a final scale-up to approximately double its Phase I capacity (90,000 tons/year of additional anaerobic digestion capacity and corresponding composting capacity, possibly increasing net CHP capacity to 4 MW). Due to many operational challenges at Phase I capacity and regulatory barriers discussed earlier, ZWEDC has postponed further scale-up. ZWEDC also noted several financial factors in its decision to remain at Phase I capacity, including lack of consistent feedstock at increased scale to justify the high capital and construction costs.

Financial Analysis

Complexities faced by the ZWEDC facility make it challenging to assess the financial performance of the facility including how individual factors influence overall profitability and how desirable (or viable) a scaling-up of operations is. Therefore, an economic model of the ZWEDC AD facility was developed based on past financial and operational data. This model allows the project team to understand how economic and policy

barriers discussed above have impacted the facility's past profitability and the likelihood that it could successfully scale-up operations. Additionally, the project team used this model to understand the potential financial situation of the facility under various sizes and operational scenarios, and what scenarios may make a future scale-up more desirable.

Methodology

The ZWEDC economic model ("the model") calculates the annual costs and revenues for the facility at a range of waste intake levels, under a number of various scenarios. The base scenario represents current facility design and operational arrangements, but with fewer feedstock and maintenance irregularities than have been seen in recent years. Empirical operational and financial data collected from the ZWEDC facility from 2014–2018, along with numerous conversations with ZWEDC leadership and staff, are used to inform this base scenario. This section describes the data, assumptions, and scenarios in the model, while Appendix D provides a detailed account of equations and metrics used.

Scenarios and Sensitivities

The "base" scenario in the model estimates the current operations of the ZWEDC facility across a range of waste processing levels. Organic waste tonnages from 60,000 tons per year (TPY) to 270,000 TPY are modeled in 5,000-ton increments. This range is chosen to span from the 2016-2018 organic waste intake levels of approximately 75,000 TPY to future plans of potentially tripling capacity to 270,000 TPY. In the base scenario, all waste intake, operational, and cost parameters match 2016-2018 facility operations.

An "OS1-only" scenario models ZWEDC operations if all incoming waste were to meet the OS1 distinction of 10 percent residuals or less, as opposed to the average of ~34 percent residuals observed in facility data from January 2016 to June 2018. This scenario examines what impact upstream policies such as improving customer sorting and instituting more rigorous hauler contracts may have on the facility. The hypothesis is that fewer residuals will improve ZWEDC's operations due to the sorting and disposal costs associated with the waste, though potentially reduce tipping fee revenues.

Two scenarios explore bringing composting back on-site. The "compost on-site" scenario assumes steady sales of compost at the $50 per ton price initially reported by ZWEDC staff, while the "compost on-site (low)" scenario assumes only 60 percent of the compost is sold, and at a much lower $12 per ton price. The low scenario is based on information obtained from ZWEDC's current composting partner, Z-Best.

Lastly, the project team performed a sensitivity analysis on this base scenario using the following parameters:

- A 20 percent increase or decrease in capital costs, due to fluctuating materials and skilled labor costs causing uncertainty in future construction costs.

- A 20 percent increase or decrease in tipping fees, due to the spread in tipping fees currently received and uncertainty in the ability of obtaining secure contracts with additional waste haulers.
- A 50 percent increase and decrease in electricity revenues, due to the disparity in current rates received through California's BioMAT program, lower wholesale rates previously received before BioMAT enrollment, and higher bioenergy-targeted rates seen in other parts of the country (VEPP Inc. 2018).

Results

Base Scenario

Figure 66 shows the facility's average annual costs and revenues, net cash flow, and net present value (NPV) at each waste intake level. NPV is calculated for a 25-year period with a 7 percent annual discount rate (See Appendix D). ZWEDC's financials first break-even in terms of NPV with a waste intake of ~75,000 organic TPY V (Figure 66) and annual average cash flow (Figure 66b, dashed line). The sawtooth pattern exhibited in the results is due to the modular design of the facility; the majority of the existing facility is built as two parallel 45,000 TPY modules, each with its own digesters, biogas storage bladder, and exhaust air biofilters. The model assumes any scale-up at the facility will occur in 45,000 TPY modular increments.

At the current facility scale, capital, O&M, labor, and digestate management costs are roughly equal, while at larger scales digestate management becomes relatively more significant and capital and labor costs experience some economies of scale. Economies of scale are limited for facility expansion, due to the modular nature of scale-up described above. Tipping fees dominate income, with electricity sales only accounting for 12 percent of annual revenue. This revenue structure incentivizes maximum throughput at the facility without much motivation to optimize biogas and electricity production.

Figure 66: Net Present Value and Costs and Revenues of ZWEDC Operating at 60–270 kTPY

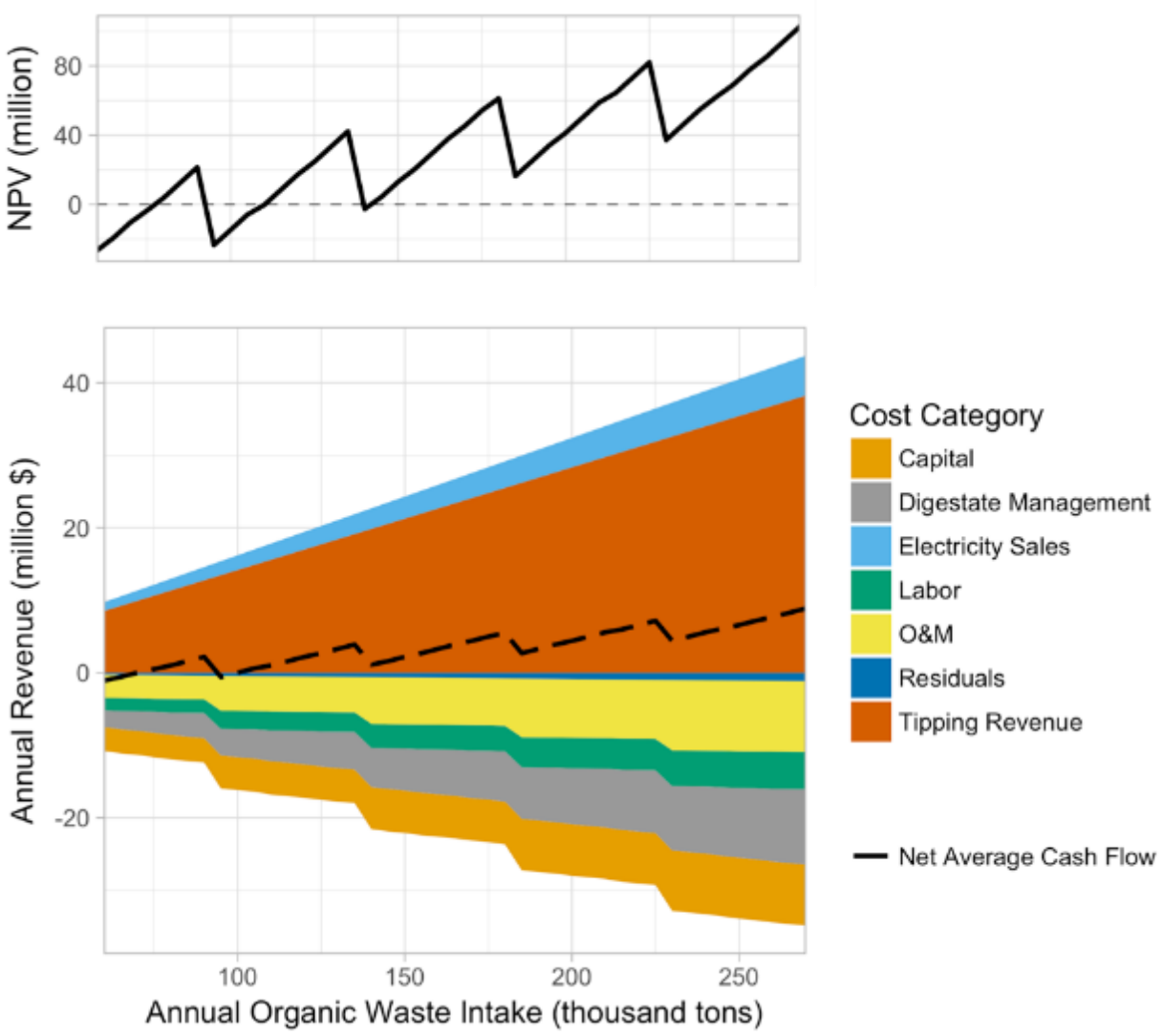

Top plot shows net present value and bottom plot shows costs and revenues associated with the ZWEDC facility operating at 60–270 thousand tons per year.

Source: Lawrence Berkeley National Laboratory

Costs follow a stepwise function as the facility is expanded, while revenues are linear with waste intake. Each peak in the net cash flow and NPV lines represents a facility that is operating at maximum capacity (90 kTPY, 135 kTPY, etc) with the point immediately following representing a facility expanded an additional 45 kTPY for only 5 kTPY more waste intake. This pattern in the NPV line highlights the risk of facility expansion and the need to secure strong feedstock contracts. For example, the current 90,000 TPY facility at maximum intake has a NPV of $20 million. If the facility were to expand to 135,000 TPY, the NPV without additional waste contracts would be -$25 million. The facility would need 125,000 TPY of waste contracts to reach a NPV greater than $20 million, and would therefore only realize the higher NPV benefits during the

last 10,000 TPY of capacity utilization. Similarly, a 180,000 TPY facility would need 160,000 TPY of incoming waste in order to improve upon the current facility's NPV.

Figure 67 shows the cost of processing one ton of organic waste at the current facility at the current intake level (75 kTPY), maximum capacity (90 kTPY) and double and triple capacity (180 and 270 kTPY). The net cost can be compared to the average per-ton tipping fee income to see the facility's per-ton profit. Note that these values are in terms of organic tons, so the tipping fee will be higher than in terms of total tons. While maximizing the current facility's waste intake results in a much more profitable facility (13 percent lower cost, 4x profit), economies of scale are more modest when expanding the facility to double and triple capacity (5 percent lower cost, 30 percent more profit). This is assuming the facility would be able to secure contracts at the current tipping fee levels, which are quite high relative to tipping fees at landfills and composting facilities.

Figure 67: Modeled Costs of Processing One Ton of Organic Waste at ZWEDC at Four Potential Intake Levels

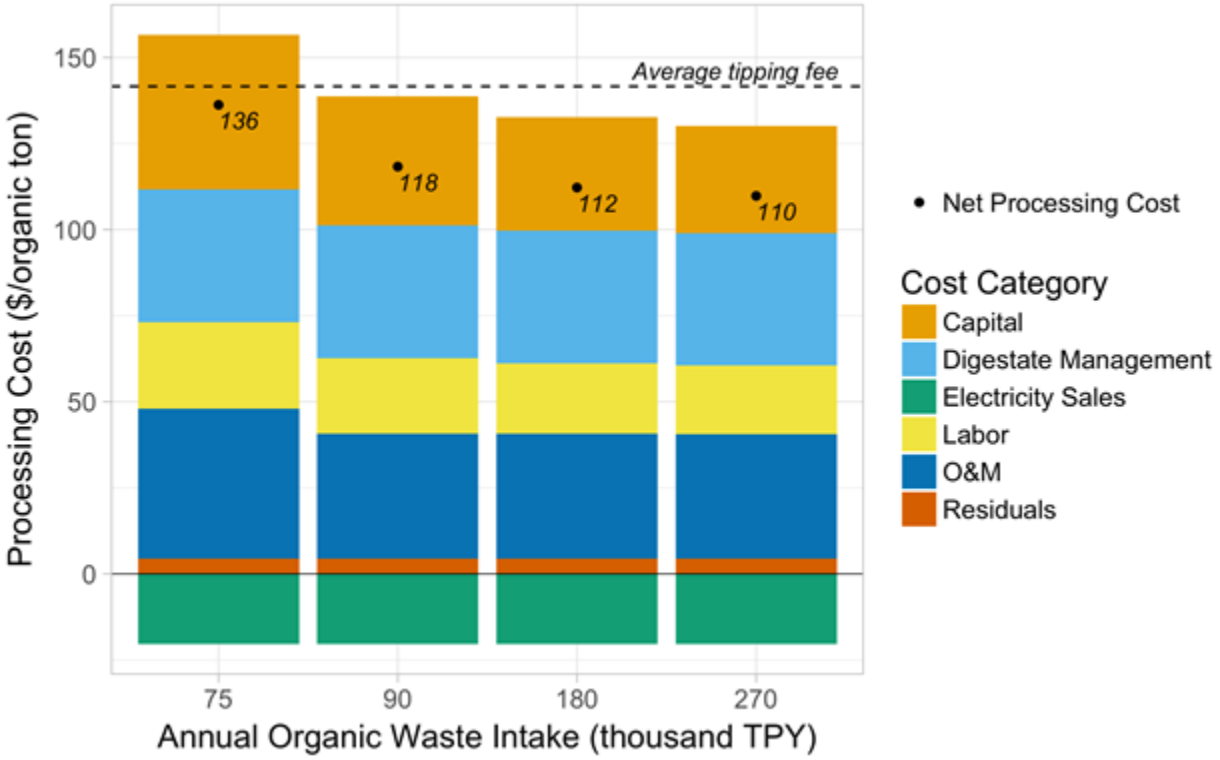

Source: Lawrence Berkeley National Laboratory

OS1 Scenario

This scenario explores the impact of having clean organic waste coming into the facility. Figure 68 shows per-ton processing costs and revenues, by category, for two waste scenarios (bars) and three facility scales (columns). Note that OS1 has an allowance of 5 percent residuals to which we add a 5 percent margin of error for the purposes of our modeling.

For all cases, results show the expected trend of decreasing costs (negative value bars) and increasing profit (points) with facility scale. Labor and residuals costs are lower for the OS1 scenario, which is expected, as there is less need to sort waste and truck it away. Capital, digestate management, and O&M costs as well as electricity revenues are the same between the two scenarios, as the modeled facility is still putting 90,000 TPY through the 90,000 TPY digesters and generating the same quantity of byproducts. Therefore, the cleaner waste coming in reduces per-ton processing cost by 8 percent. While costs are lower to process clean waste, revenues are also lower, significantly so. The facility receives tipping fees based on total tonnage, and actually receives a higher fee the more contaminated the waste is. Additionally, highly contaminated waste requires less facility capital than an equivalent ton of all-organic waste, as the contaminants are sent away to landfill. So, while contamination results in a slightly higher labor and residuals cost, this cost is dwarfed by the higher tipping fee revenue in terms of organic waste. Therefore, from the facility's perspective, there is an incentive to take in as much waste as possible (and therefore receive more tipping fee income), no matter how contaminated it is, and a move to cleaner organic streams would not help with the prospects of facility expansion.

It is important to note that this analysis only considers the impact of residuals in terms of additional labor and residual trucking costs. In reality, there may be many more costs and complications to having highly contaminated incoming waste streams. Successfully removing 100 percent of contamination through sorting as modeled here is unrealistic, and some will inevitably end up in the digesters and digestate. The impact of contaminants in the digesters is unknown, but hypothetically it could result in lower gas production or quality. Additionally, contaminated digestate requires additional sorting and could result in toxins and contaminants being present in the finished compost. Understanding the impact of various types of contaminants (metals, plastics, etc.) on digester performance is an area for further exploration, as we do not know how this is impacting the current facility. Impact on finished compost is an area of active research, but this aspect does not impact the current facility's operations, as it does not handle composting in-house.

Figure 68: Model of Per-Ton Processing Costs and Revenues for the Base Scenario and OS1 (Clean Organics) Scenario

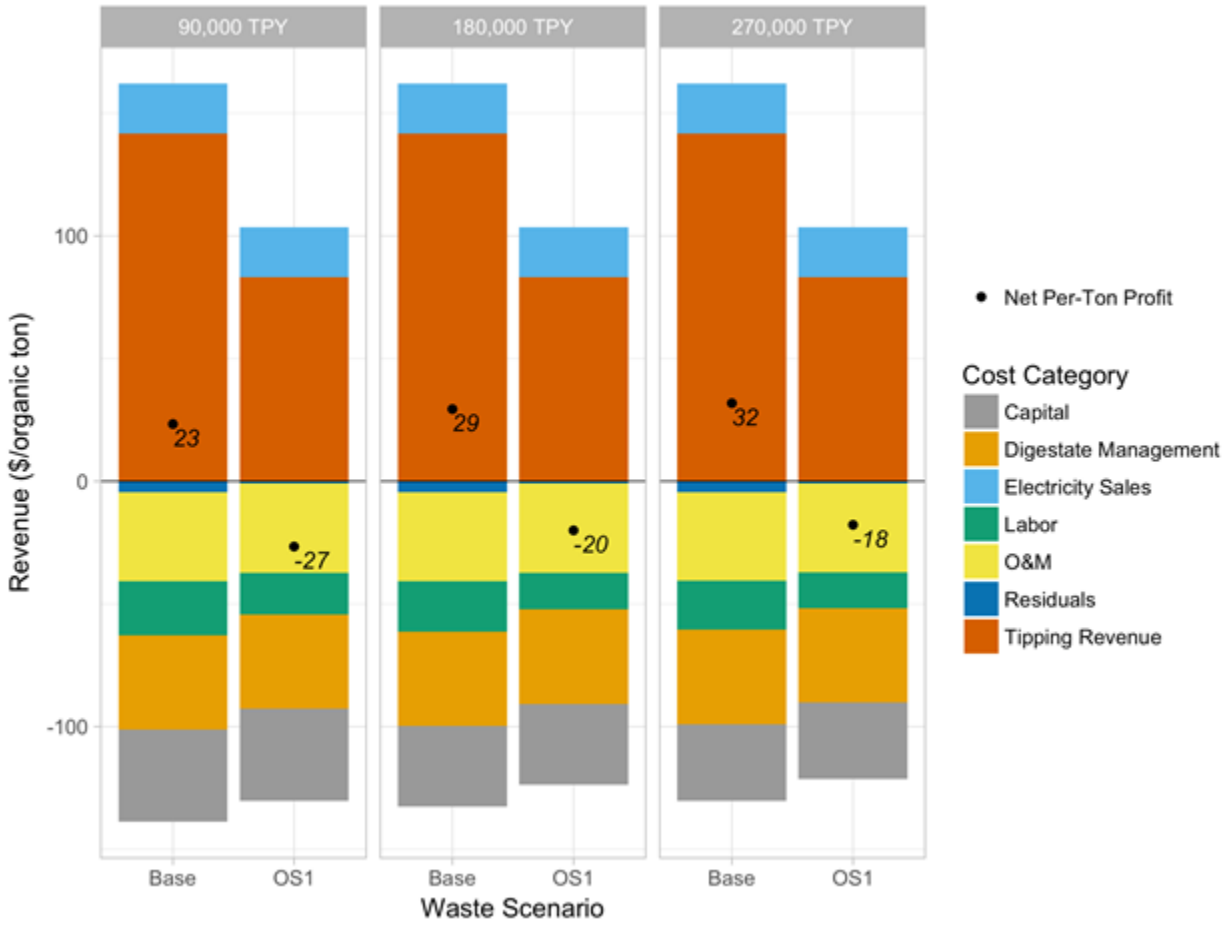

Source: Lawrence Berkeley National Laboratory

Compost Scenario

This scenario aims to quantify the economic impact of sending digestate to a third-party composting facility as opposed to composting on-site, as ZWEDC initially did. Figure 69 shows the categorized disposal costs for three composting scenarios for a 90,000 TPY facility. As shown, composting on-site removes all off-site digestate management costs and causes a very slight increase in labor and in an indiscernible increase in capital costs. Additionally, the compost revenues can either be extremely significant (double those of electricity sales), if using initial assumptions of $50/ton and 100 percent sales, or minor, if using current assumptions of $12/ton and 60 percent sales. In either case, per-ton profit is more than tripled over the base scenario. Note that the "On-Site (low)" scenario does not include the cost of landfilling the 40 percent of compost that is not sold.

This analysis includes costs consistent with the facility's previous on-site composting operations. At that time, the facility experienced many issues with odor complaints and air emissions that led to the ending of on-site composting. Investment in improved

composting equipment and odor abatement technologies would increase the total processing costs in these scenarios. Such costs should be compared against the potential decrease in off-site digestate management costs and increase in revenues.

Figure 69: Modeled Per-Ton Processing Costs and Revenues for 90,000 TPY Intake Under Three Composting Scenarios

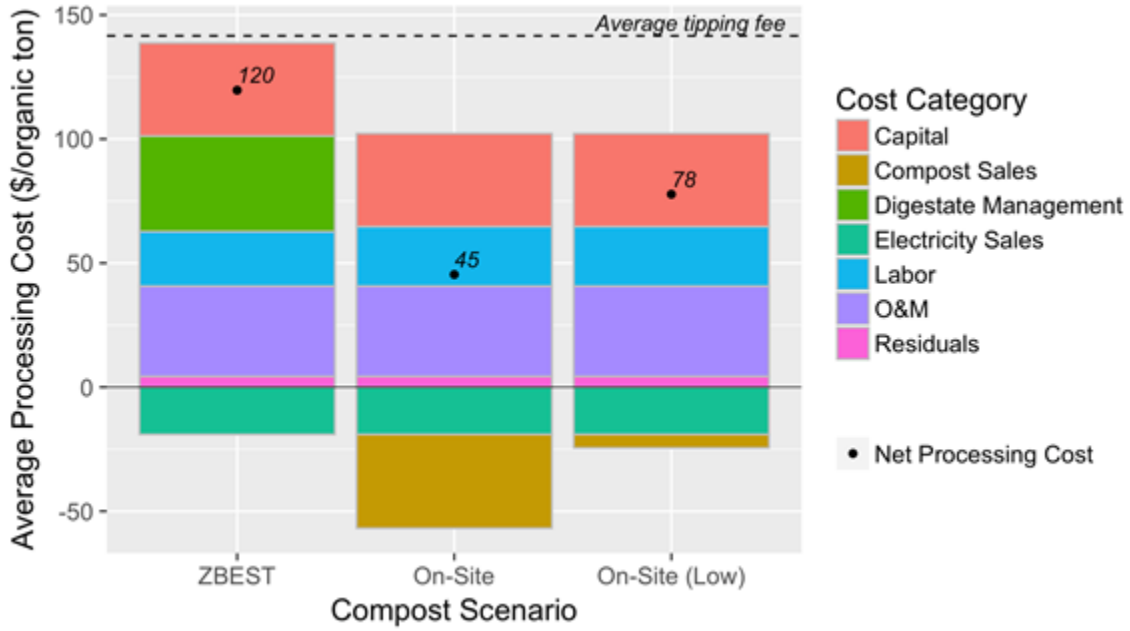

Source: Lawrence Berkeley National Laboratory

Sensitivity Analysis

Sensitivities of model results were analyzed for three metrics: electricity revenue (+/- 50 percent), tipping fee revenue (+/- 20 percent), and capital costs (+/- 20 percent). Results are shown in Table 5. In general, NPV and net cash flow results are sensitive to capital costs and electricity revenues, and extremely sensitive to tipping fees. Cash flow is slightly less sensitive with increasing scale, while NPV is more sensitive. Per-ton disposal processing costs are much less sensitive to these changes.

Sensitivity to electricity revenues indicates the importance of bioenergy feed-in-tariff programs for ZWEDC. The 50 percent lower closely resembles wholesale electricity rates, whereas 50 percent higher is on par with some other programs in the U.S. (VEPP Inc. 2018) These tariffs could have a large impact on the financial viability of municipal waste AD facilities, despite the seemingly low portion of revenue that comes from electricity sales. The project team expected the tipping fees to have a large impact in the sensitivity analysis, as they are the primary source of revenue for the facility. However, the impact was shocking: a 20 percent increase in per-ton rates nearly triples NPV and more than doubles annual cash flow for the 90,000 TPY facility. This is due to the facility's very low profit margins. With large expenses and revenues that roughly

cancel each other out, any change in the largest revenue stream has an outsized impact.

Table 5: Sensitivity Analysis Results Modeled for Three Parameters Across Three Potential Facility Sizes and Four Financial Metrics

Metric	Facility Size (TPY)	Capital Cost +/- 20 percent	Electricity Revenue +/- 20 percent	Tipping Fee Revenue +/- 20 percent
Avg annual cash flow	90,000	31 percent	42 percent	117 percent
Avg annual cash flow	180,000	22 percent	34 percent	93 percent
Avg annual cash flow	270,000	19 percent	31 percent	86 percent
Per-ton profit	90,000	31 percent	42 percent	117 percent
Per-ton profit	180,000	22 percent	34 percent	93 percent
Per-ton profit	270,000	19 percent	31 percent	86 percent
Per-ton disposal processing cost	90,000	6 percent	9 percent	--
Per-ton disposal processing cost	180,000	6 percent	9 percent	--
Per-ton disposal processing cost	270,000	6 percent	9 percent	--
Net Present Value	90,000	54 percent	53 percent	181 percent
Net Present Value	180,000	33 percent	37 percent	127 percent
Net Present Value	270,000	28 percent	33 percent	113 percent

Source: Lawrence Berkeley National Laboratory

Conclusions and Discussion

The ZWEDC facility is operating on narrow margins in ideal conditions, and at a loss any time they encounter operational issues. With revenues from both tipping fees and electricity prices established by long-term contracts, the facility must cut costs or increase biogas and electricity production to improve its economic situation. Digestate management (tipping fees paid to the compost facility) have been the largest unexpected cost since the facility began operation. While composting on-site would be much more profitable, the facility's windy, urban location and associated odor issues have essentially eliminated this option. Biogas production per ton of waste has been declining over the last year due to operational challenges and, possibly, the impact of high contamination levels (although additional studies would be required to determine the impact of contamination). Biogas yield, and therefore electricity production, could likely be improved with better contaminant removal, optimized mixing of yard and food waste, and digester operation improvements such as longer residence time and alternative percolate spraying strategies. As shown in the sensitivity analysis, a 20 percent increase in electricity sales revenue would increase their annual net cash flow and per-ton profit approximately 40 percent.

Though the facility initially considered scaling up to double or triple capacity, this seems unlikely in the current environment. While a facility with double or triple the current 90,000 TPY capacity could potentially result in 25 percent to 35 percent higher per-ton profits, this investment comes with significant risk. If the facility were to scale up without adequate feedstocks secured, it would be worse off. Additionally, it would lose its advantageous feed-in-tariff (as the BioMAT program is limited to generators less than 3 MW) and have to turn to a net-metering or wholesale electricity sales agreement. Scaling up the facility will lead to limited economies of scale due to the modular nature of the equipment, so until the current financial situation improves on a profit per-ton basis, there is likely little motivation to take on more capacity and waste feedstock.

This analysis underscores the importance of establishing favorable long-term feedstock, energy sales, and residual and digestate management contracts before an anaerobic digestion facility is constructed. Though multiple AD facilities have been operated successfully in urban areas, they will likely not be able to do on-site composting without significant investment in advanced odor control technologies. Therefore, the cost of transporting and disposing digestate at rural composting facilities must be considered. For cities or counties who wish to have their organic wastes managed through private AD facilities, offering high tipping fees and guaranteeing consistent feedstock is the best way to support development.

CHAPTER 7:
Project Impacts and Conclusions

Results Summary

A multidisciplinary research team at Lawrence Berkeley National Laboratory partnered with the Zero Waste Energy Development Company (ZWEDC) and the City of San José with three overarching objectives, namely: enabling ZWEDC and California to achieve economically and environmentally sustainable scale-up of waste processing and CHP production by overcoming key barriers; maximizing net life-cycle energy and GHG benefits to California ratepayers; and transferring the knowledge gained, experimental results, and lessons learned to the public and key decision makers.

Figure 70 illustrates the relationship between the major activities undertaken in this project. ZWEDC provided a unique opportunity to analyze its facility data (e.g., MSW intake, electricity production, capital and operating costs, and revenues) and physical site access and support to conduct measurements of air pollutant emissions.

Figure 70: Project Outcomes

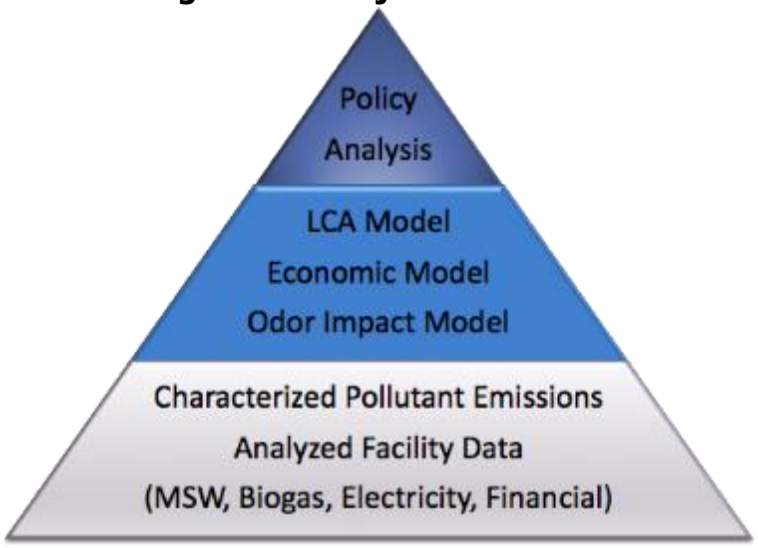

Source: Lawrence Berkeley National Laboratory

The team developed methods and quantified emission rates of greenhouse gases, ammonia, hydrogen sulfide, volatile organic compounds, and oxides of nitrogen from ZWEDC's on- and off-site activities. Together with the facility data, the emissions results provide a foundation for the odor transport framework and regional impact model and the environmental life-cycle and economic analysis models that were developed in this project to assess net environmental, societal, and financial impacts. With the knowledge gained through this project and an understanding of the policy and regulatory landscape, we articulate specific barriers and challenges among three major stages of

the anaerobic digestion process. Highlights from each of the major project activities follow.

Emissions

Pollutant emission rates were determined for multiple pollutants and from several sources: outdoor composting, biogas flaring, combined heat and power production, biogas venting, and the biofilter at the end of the facility air handling system. This study found that outdoor aerated composting activities contribute the most emissions of CH_4, CO_2, NH_3, and H_2S per kg of MSW digested. On a 20-year GWP time horizon, the 14-week composting cycle was responsible for 65 percent of the total CO_2-equivalent emissions per kg of MSW digested; methane comprised 63 percent of those emissions from composting, with CO_2 emissions making up most of the remaining fraction. Significant CH_4 emissions over the full 14-week composting cycle indicate that some anaerobic activity persists despite aeration. As it relates to compliance with permitted emissions of NO_x from biogas flaring, this study found a strong correlation between biogas NH_3 content and flare NO_x emission rate. It is conceivable that facilities that flare biogas can improve compliance with permitted air emissions by removing ammonia prior to combustion.

Odor Impact Modeling

Considering past odor complaints to ZWEDC, surface and upper atmosphere meteorological data, terrain characteristics, onsite operations, and relevant literature, the team characterized five odor generating sources at ZWEDC (odor emission rates, source geometry, and emitting frequency) and used EPA's AERMOD plume model to link odor sources to offsite, downwind receptor impacts. The result is an odor impact assessment framework that determines separation distances required to avoid odor annoyance. We use separation distance as an impact metric to determine that: (1) odor impacts vary significantly by time of day from a few hundred meters to more than 2000 m downwind of the facility; (2) onsite composting is the most significant source to cause offsite odor impacts extending more than 2000 m downwind of the facility; (3) bladder venting has potential odor impacts during hours with low atmospheric mixing; (4) odor impacts vary by facility waste processing capacities with a strong log linear relationship between odor emission rates and separation distances. These findings can guide mitigation priorities and strategies for ZWEDC and have policy implications for future facility siting and planning.

Life-Cycle Assessment

The results indicate that on the basis of 100-year global warming potential (GWP), emissions from decomposition of organics in landfills are dominant even for well-managed landfills in California with gas capture systems in place. Landfilling all organics results in approximately 156 kg CO_2-equivalent emitted per tonne of waste intake. If ZWEDC were to landfill their digestate, net GHG emissions would be nearly as high given the large quantity of residuals remaining at the end of the process, although

fugitive methane emissions from landfilling of digestate is not well-understood and may be lower than the estimates in this report. Land-applying digestate rather than undergoing compost cuts emissions approximately in half, because digestate can only be land-applied for a portion of the year and will likely still be landfilled for 6 months. Composting, current ZWEDC operations, and hypothetical ZWEDC scenarios in which gas is cleaned up for either transportation or pipeline injection all result in net-negative GHG emissions. This is largely due to three factors: (1) carbon sequestration in soil from compost application, (2) diesel offsets in the case of renewable natural gas (RNG) used for transportation, and (3) natural gas offsets resulting from grid-export of electricity or pipeline injection. These net emissions range from -45 to -83 kg CO_2-equivalent per tonne of waste intake. NO_x, VOCs, and $PM_{2.5}$ are more variable, depending on estimates of emissions from landfill gas flaring, which in itself is highly uncertain. However, current ZWEDC operations generally reduce emissions by at least half relative to landfilling.

Policy and Economic Barrier Assessment

The research team developed an economic model of the ZWEDC AD facility to understand how economic and policy barriers have impacted the facility's past profitability and to evaluate different operational scenarios. Our findings identified large and potentially highly variable digestate and residual management costs as a key concern for short-term AD facility financial viability. Improved biogas yields would increase electricity sales and profit, but require operational improvements. Three factors were identified to improve the business case for larger scale facilities: (i) Long-term feedstock and digestate management contracts, as well as net electricity compensation prior to facility construction; (ii) investment in waste recovery to support cleaner feedstocks; and (iii) financial mechanisms to overcome large, lumpy capital expenditures.

Scale-up

ZWEDC more than doubled its MSW intake during the project to 90,000 tons per year, achieving its Phase 1 goal of 90,000 tons per year of organic waste intake and 1.6 MW of nameplate CHP capacity by the end of 2015, though the CHP capacity was installed prior to the start of our project in 2014. ZWEDC has successfully operated at Phase 1 capacity, despite high residual content and unforeseen operational challenges. ZWEDC has postponed further scale-up and noted several financial factors in its decision to remain at Phase I capacity, most notably the lack of consistent feedstock at increased scale to justify the high capital and construction costs. ZWEDC was the first biomass generator to enroll in California's BioMAT program.

Research Contributions

Air Pollutant Emissions Characterization

New methods developed in this project to measure pollutant emission rates from multiple sources can be replicated or improved upon in future studies. The emission rates quantified contribute important new information that regulatory bodies can use when evaluating the impacts of increasing use of organic MSW for energy production in California. Further, the emission rates are used in this study in the odor transport model and net life-cycle environmental impacts assessment.

Odor Impact Assessment

We characterized and identified most influential odor generating sources across major AD processing stages. We developed a separation distance-based odor impact assessment framework to relate facility odor emissions to offsite annoyance on local communities. The findings were used to prioritize odor mitigations and guide best practices at ZWEDC. Our policy relevant findings highlight the importance of appropriate odor impact criteria, consistent and high frequency source and community monitoring. The data and tools developed in this study can be extended to facilities at other locations and of different capacities to inform optimal siting and facility planning.

Policy Analysis

We identified and discussed regulatory and policy barriers along three major AD process stages: 1) waste sorting, delivery, and processing; 2) AD/biogas management and utilization; and 3) outputs and residuals processing. Our analysis described specific barriers and challenges within the major process stages supplemented with operational and financial data from the ZWEDC facility, where appropriate. Finally, we concluded with implications for policymakers and regulators seeking to broaden the use of solid waste biomass technologies, like AD, and align them with public policy goals.

Economic Analysis

We developed an economic model of the ZWEDC AD facility to understand how economic and policy barriers discussed have impacted the facility's past profitability and the likelihood that they could successfully scale-up operations. Additionally, we used this model to understand the financial situation the facility may find themselves in under various facility sizes and operational scenarios, and what scenarios may make a future scale-up more desirable.

Life-Cycle Assessment

The team developed a physical input-output life-cycle assessment model and a geospatial truck routing tool, directly linked with operational data outputs from the ZWEDC facility, to analyze and automatically update results based on day-to-day mass and energy balances. The model generated results for carbon dioxide, methane, nitrous oxide, particulate matter, nitrogen oxides, sulfur dioxide, carbon monoxide, and volatile

organic compounds (VOCs). This modeling effort serves as the most complete effort to-date on quantifying the net life-cycle impacts of waste-to-energy systems, and is grounded in empirical data not incorporated in any previous studies.

Ratepayer Benefits Summary

This research is important to ratepayers because it provides information that can be used to increase diversion of organic waste for distributed generation (DG), waste heat utilization, and compost production, which will result in greater electricity reliability and lower costs, as well as environmental and public health benefits. The benefits to ratepayers from diversion of organic waste from landfills to distributed generation flow from three considerations. First, utilizing organic waste instead of fossil fuel can help insulate ratepayers from fluctuations in and long-term increases in fossil fuel prices and reduces life-cycle emissions of environmental pollutants. Second, utilizing waste heat reduces costs and increases safety by improving the overall efficiency of the waste-to-energy facilities, thus avoiding additional fossil fuel demand and environmental impacts. Third, distributed electricity generation can help reduce transmission and distribution costs and improve grid reliability.

Knowledge Transfer Activities and Feedback

The project team has been highly engaged with representatives from the waste management and bioenergy industrial sectors from the beginning of the project through the end. The nature of these communications in the early stages of the project was to gather information. As work progressed, outreach shifted toward sharing results and insights.

Technical Advisory Committee Meetings and Follow-Up Interactions

Throughout the course of this project, we have communicated with our Technical Advisory Committee (TAC) as both a resource and potential audience for our results. Our TAC includes a wide variety of key stakeholders and domain experts, as shown in Table 6. We held meetings with the TAC about a year into the project on May 3, 2016 and again at the end of the project on February 5, 2019. During the course of the project, we held meetings with many of the TAC members, including Julia Levin, who invited us to speak at a Bioenergy Association of California meeting, Todd Pray, who works with relevant companies such as Recology in his capacity as leader of the Advanced Biofuels/Bioproducts Process Demonstration Unit, Bill Monson, Don Lucas, and Phil Martien.

Table 6: Technical Advisory Committee Members

Name	Affiliation	Project Relevance/Expertise
Phil Martien	Bay Area Air Quality Management District	Manager in Planning & Climate Protection Division
Bill Monson	MRW Associates	Expert in tariff/rate analysis, market opportunities for wholesale, and large cities
Harry Beller	Lawrence Berkeley National Lab (LBNL)/Joint BioEnergy Institute (JBEI)	Expert in characterization of bacterial metabolic diversity in nature, including discovery of enzymes relevant to biosynthesis of fuel-related compounds and environmentally important biogeochemical cycling.
Julia Levin	Bioenergy Association of California (BAC)	BAC's Executive Director; expert in renewable energy policy
Fabrizio Adani	University of Milan, visitor at JBEI	Full Professor at University of Milan, expert in waste-to-energy systems
Todd Pray	Program Head, Advanced Biofuels (and Bioproducts) Process Demonstration Unit	Familiarity with the practical challenges of scaling biological waste-to-energy systems
Donald Lucas	LBNL	Developed measurement methods for chlorinated HCs, metals, and particles in combustion systems; authored SB521 report to Governor recommending MTBE removal from gasoline; with California EPA developed a multimedia review for pollutants; former Deputy Director of the EH&S Division at LBNL
Jack Brouwer	UC Irvine	Professor of Mechanical and Aerospace Engineering; Associate Director of the National Fuel Cell Research Center and Advanced Power and Energy Program at UCI

Source: Lawrence Berkeley National Laboratory

Expert, Regulatory, Industry, and Utility Outreach

The project team communicated results with and gathered feedback from research leaders, regulatory bodies, private companies, and regulated utilities. Also, the project team toured a number of wet and dry anaerobic digestion facilities located in California. Specific activities include:

- Presentation of our results at the CEC EPIC Symposium by Sarah Smith, February 2018
- Presentation of our results at the CEC EPIC Symposium by Jay Devkota, February 2019
- Presentation of our results at the Berkeley Energy and Resources Collaborative (BERC) Expo in February 2018 by Jahon Amirebrahimi
- Facility tour - Monterey Regional Waste Management District (Sarah Smith)
- Facility tour - Central Marin Sanitation Agency and Marin Sanitation Service (Sarah Smith)
- Facility tour - East Bay Municipal Utility District and lengthy discussion with John Hake and other EBMUD staff (Corinne Scown, Sarah Smith, Jay Devkota)
- Facility tour - City of San Mateo Wastewater Treatment Plant (Sarah Smith)
- Guest lecture - UC Berkeley CE 292 (Sarah Smith)
- Invited talk at the Bioenergy Association of California quarterly meeting in Oakland, CA (Corinne Scown)
- Attendance at the wet and gaseous waste to energy and products workshop hosted by DOE program manager Mark Philbrick in Berkeley, CA (Corinne Scown)
- Attendance at the Berkeley Energy & Resources Collaborative (BERC) 2018 Resources Roundtable on Waste, where stakeholders from EPA, CalRecycle, Closed Loop Partners, Recology, and other waste-related entities (Sarah Smith)
- Attendance at Second Meeting of Wastewater and Solid Waste Sectors in Sacramento, CA (Corinne Scown)
- Phone call with California Public Utilities Commission staff lead, James McGarry, on revisions to the BioMAT program (Andy Satchwell, Corinne Scown, Sarah Smith, and Jahon Amirebrahimi)
- The team had several meetings with TAC member Don Lucas to discuss the experimental plan to characterize NO_x emissions from ZWEDC's enclosed flare.
- Phone call with Zero Waste Energy, LLC, the developers of multiple dry anaerobic digestion facilities in California, to discuss their operations, challenges, and successes to incorporate into our analyses. (CEO Eric Herbert and Senior Project Manager Michael Hardy; Sarah Smith, Andy Satchwell and Corinne Scown). Follow-up meeting also conducted with ZWE at the ZWEDC facility to discuss odor control strategies with BAAQMD.

- Collaboration and eventual separate DOE-funded project with Anaergia on the GHG footprint of one of their California-based facilities (Rialto) that co-digests food waste (Corinne Scown)
- Presentation at the Society of Environmental Toxicology and Chemistry Annual Meeting 2018 in Sacramento, CA, where regulators and industry experts will be present (Corinne Scown)
- The team delivered three poster presentations to at the American Geophysical Union (AGU) meeting in Washington, DC, in December 2018, and in San Francisco, in December 2019, where domain experts and environmental regulators from across the U.S. and internationally gather
    - Environmental and Community Impact of Fugitive Emissions from an Organic Waste-to-Energy Facility, Ling Jin lead author
    - Greenhouse Gas and Toxic Air Pollutant Emission Rates from Industrial-Scale Composting of Municipal Solid Waste, Chelsea Preble lead author
    - Environmental and Community Impact Assessment of Operations at an Organic Waste-to-Energy Facility, Ling Jin lead presenter.
- Presentation at the 100th PERF Meeting with Liaison Members: Tech and Options for Efficient Environmental Protection and Risk Management, in Richmond, CA, on October 10th, 2019, where regulators and industry experts will be present (Ling Jin).
- We introduced fellow waste-to-energy researchers at other national labs NREL, ORNL, and PNNL to our datasets and tools by hosting a web-based tool demonstration and data discussion. Our presentation included our knowledge of waste-to-energy systems in California and feedstock heterogeneity, and incorporated insights from this project.
- The Bay Area Air Quality Management District (BAAQMD) is very interested in this project, which is located within their jurisdiction.
    - We hosted a well-attended teleconference with BAAQMD on May 19, 2017. In attendance were members of ZWEDC and LBNL teams and BAAQMD staff from six BAAQMD divisions: Rule Development (Idania Zamora and Robert Cave); Climate Protection - Policy (Yvette DiCarlo); Climate Protection Science (Abhinav Guha and Sally Newman); Emissions Inventory (Phil Martien, TAC member); Compliance and Enforcement (Ron Pilkington, Deepti Jain, Tracy Lee); and Engineering/Permitting (Snigdha Mehta, Arthur Valla).
    - Three BAAQMD staff attended the second TAC meeting including TAC member Phil Martien and two others interested in greenhouse gas emissions and odorous emissions from composting activities.

- Following our second TAC meeting, the project team was invited to present and discuss project results to a larger audience of BAAQMD staff at their headquarters in San Francisco.
- We provided material on emission measurements and quantification techniques to a BAAQMD presentation delivered to their stakeholder forum for "Developing a Sustainable Organic Waste Recovery Sector" in June 2018.
- Public workshop - BAAQMD Climate Protection and Organics Rule Development Efforts (Sarah Smith, Ling Jin) on Nov 1st 2018.
- Numerous conversations with BAAQMD staff about our emissions measurements and the need for better understanding and characterizing emissions from industrial-scale anaerobic digestion and composting operations.
- During our quarterly visits to ZWEDC, we presented our techniques to document the occurrence and volume of biogas venting from ZWEDC's storage bladder.
- We consulted with BAAQMD's source testing division about protocol for removing water from flare effluent and borrowed sampling equipment.

- Invited to meet with CalRecycle and the South Coast Air Quality Management District (SCAQMD) at the Rethink Methane Symposium on Feb. 27. SCAQMD is working on a new flare rule and the project team brought to their attention the findings of this project pertaining to the relationship between fuel-nitrogen content and NO_x emissions. The intention is that SCAQMD will report the project findings back to their Board.

Recommended Future Work

Air Emissions

This project provides new pollutant emission factors that can improve regional emission inventories for air quality models. Whereas this is a significant contribution to the field, additional measurements at other facilities that employ different emissions controls technologies will further improve regional emission inventories and assessments of environmental impacts.

This study found that outdoor aerated composting activities contribute the most emissions for most pollutants. Thus, the team recommends additional measurements from composting since there is a lot of diversity in composting activities and, therefore, there is possibly a lot of variability in the magnitude of emissions. The compost windrows measured in this study were wrapped in plastic and force aerated. Other practices, such as uncovered and turned, should be studied. Likewise, Zero Waste Energy informed us that future composting windrows at the Davis Street Resource Recovery Complex and Transfer Station in San Leandro will be "negatively aerated." As

described, air will be pulled through piles of compost, rather than pushed through, and then the air will be treated prior to atmospheric release. The emission rates of pollutants could be much lower than those measured in this study and should be measured.

This project's measurements showed strong correlation between biogas NH3 and flare NOx emissions. It is conceivable that facilities which flare biogas can improve compliance with permitted air emissions by removing ammonia prior to combustion. Further study at other facilities, including waste water treatment plants producing biogas from wet anaerobic digestion, may be warranted.

Odor Mitigation and Regulation

Findings from ZWEDC indicate strong relationship between odor emission rates and separation distances. The analysis framework needs to be extended to more California sites to verify and understand how such relationship vary by meteorology and terrain types. There is a pressing need to develop an integrated facility odor impact assessment and siting tool that accounts for location and source specific factors, time of day and seasonal influences, and facility sizes for future facility screening, planning and regulation.

Odor impact criteria (allowable odor threshold concentration and exceedance frequency) are shown to be critical for determining facility siting. Currently, the bay area air district sets the limit of 5 odor units at or beyond the facility fence line applied after at least 10 complaints within a 90-day period (Bay Area Air Quality Management District 1982), which translates to 2 to 6 percent exceedance frequencies depending on season during low atmospheric mixing conditions. Such criteria need to be verified whether to represent appropriate protection of a wide variety of exposed populations. This will require research linking ambient exposure levels to odor perception reflected by community odor complaints. Long-term and high frequency community-based monitoring and data collection are needed.

Lastly, standardized source monitoring and modeling protocols would help to identify important sources and conditions. More research is needed for not only continuous sources but also fugitive emissions to understand their odor contributions and develop and reinforce best practices.

Life-Cycle Emissions

Reducing greenhouse gas (GHG) emissions across California is one of the primary drivers of increased organics diversion from landfills. From a GHG standpoint, there is no question that pursuing any alternative to landfilling fast-degrading organics like food waste will reduce net GHG emissions. Further studies to understand how digestate behaves if/when landfilled will not alter this basic conclusion, but will fill a gap in the scientific knowledge regarding the carbon-intensity of landfilling digestate as compared to raw organic waste. Similarly, studies on the net impact of digestate and composted

digestate application to soils, and the resulting impacts on net primary productivity (NPP), soil carbon sequestration, and methane and nitrous oxide emissions, will provide valuable information that may alter the relative advantages of different composting and AD scenarios.

The most pressing gap in knowledge is related to air pollutant emissions, and specifically ammonia. Maintaining acceptable ambient air quality is also a particular challenge for the state, so solutions for diverting organic waste cannot place undue burden on local air quality relative to the status quo, particularly in disadvantaged communities. Our results indicate that composting of organics rich in nitrogen, such as food waste, may result in ammonia emissions that, when converted to estimated social damages, outweigh the GHG emissions advantages of composting over landfilling. It is critical to more thoroughly understand the relationship between material/waste type, management practices, and life-cycle ammonia emissions. This should be accomplished with additional empirical data collection and rigorous analysis to develop mechanistic and/or statistical models for estimating likely ammonia emissions. Furthermore, models that more accurately capture the formation of fine particulate matter as a result of ammonia emissions in California will be essential to weighing climate and air quality tradeoffs between different waste management strategies.

Also, because air pollutant emissions are so dependent on locally-permitted limits, compiling clear guidance on most likely permitted limits for key pollutants, by facility location, type, and size. Providing all this data in a transparent LCA tool will enable decision-making across agencies, including the CPUC, CalRecycle, Air Resources Board, and Energy Commission about which technologies and strategies to prioritize.

Additional Opportunities to Further Reduce Greenhouse Gas Emissions from Landfills

Organic Feedstock

State mandates specifying organics separation may improve feedstock quality for solid waste biomass facilities. Additionally, major investments in waste infrastructure may be required to optimize the collection and processing of organic waste, which otherwise is considered a low-value contaminant relative to other recyclable residential collection streams.

Net Electricity Export

Many of California's investor-owned utility interconnection processes are unnecessarily costly and technically burdensome. State utility regulators can address interconnection barriers and establish rules that do not unduly burden AD facility generating systems.

Current BioMAT enrollment requirements can be lengthy and limit participation by smaller generators. Additionally, BioMAT includes penalty provisions that, while intended to produce consistent generation output, may be unnecessarily large and limit generator profitability. Price levels and rules for BioMAT, and other similar biomass FiT

programs, should take into account the environmental benefits of solid waste biomass technologies, particularly benefits of diverting waste from landfills. Tariff program deadlines should also align with timing of state policies for bioenergy (SB 1122) and methane reductions (SB 1383), among other state environmental policies.

In addition to these, establishing long-term feedstock and digestate management contracts, as well as net electricity compensation prior to facility construction, and supportive financial mechanisms to overcome large, lumpy capital expenditures can be considered to help overcome barriers to increasing anaerobic digestion of municipal solid waste to energy in California.

REFERENCES

Amlinger, F., Peyr, S. and Cuhls, C. 2008. Green house gas emissions from composting and mechanical biological treatment. *Waste management & research : the journal of the International Solid Wastes and Public Cleansing Association, ISWA* 26(1), pp. 47–60.

Baral, N., Kavvada, O., Perez, D.M., et al. 2019. Greenhouse Gas Footprint, Water-Intensity, and, Production Cost of Bio-Based Isopentenol as a Renewable Transportation Fuel.

Bay Area Air Quality Management District 1982. *Regulation 7. Odorous Substances.*

Beychock, M.R. Fundamentals of Stack Gas Dispersion.

Boesch, M.E., Vadenbo, C., Saner, D., Huter, C. and Hellweg, S. 2014. An LCA model for waste incineration enhanced with new technologies for metal recovery and application to the case of Switzerland. *Waste management (New York, N.Y.)* 34(2), pp. 378–389.

Boldrin, A., Andersen, J.K., Møller, J., Christensen, T.H. and Favoino, E. 2009. Composting and compost utilization: accounting of greenhouse gases and global warming contributions. *Waste management & research : the journal of the International Solid Wastes and Public Cleansing Association, ISWA* 27(8), pp. 800–812.

Brancher, M., Griffiths, K.D., Franco, D. and de Melo Lisboa, H. 2017. A review of odour impact criteria in selected countries around the world. *Chemosphere* 168, pp. 1531–1570.

Breunig, H.M., Amirebrahimi, J., Smith, S. and Scown, C.D. 2019. Role of Digestate and Biochar in Carbon-Negative Bioenergy. *Environmental Science & Technology*.

Brown, S., Beecher, N. and Carpenter, A. 2010. Calculator tool for determining greenhouse gas emissions for biosolids processing and end use. *Environmental Science & Technology* 44(24), pp. 9509–9515.

Brown, S. and Leonard, P. 2004. Building carbon credits with biosolids recycling. *Biocycle* 45(9), pp. 25–29.

California Association of Sanitation, A. 2017. *An Evaluation of the Sustainability of Biosolids Use as Landfill Burial or Beneficial Cover Material*. CALIFORNIA ASSOCIATION of SANITATION AGENCIES.

California Public Utilities Commission (CPUC) 2014. *DECISION IMPLEMENTING SENATE BILL 1122*.

CalRecycle 2015. *Landfill Tipping Fees in California*. California Department of Resources Recycling and Recovery (CalRecycle).

CalRecycle 2016. *State of Recycling in California*.

CARB 2017. *Method for Estimating Greenhouse Gas Emission Reductions from Diversion of Organic Waste from Landfills to Compost Facilities*. California Environmental Protection Agency.

CEPA 2017. *Method for estimating greenhouse gas emission reductions from diversion of organic waste from landfills to compost facilities*. California Air Resources Board.

Chow, J.C., Chen, L. -W. A., Watson, J.G., et al. 2006. PM2.5 chemical composition and spatiotemporal variability during the California Regional PM10/PM2.5 Air Quality Study (CRPAQS). *Journal of Geophysical Research: Atmospheres*.

Cohon, J.L., Cropper, M.L., Cullen, M.R., et al. 2010. *Hidden costs of energy: unpriced consequences of energy production and use*. Washington, D.C.: National Academies Press.

Coker, C. 2012. Managing Odors in Organics Recycling. *BioCycle* 53(4), p. 25.

Costello, K. 2014. *Alternative Rate Mechanisms and Their Compatibility with State Utility Commission Objectives*. National Regulatory Research Institute.

Couture, T. and Cory, K. 2009. State Clean Energy Policies Analysis (SCEPA) Project: An Analysis of Renewable Energy Feed-in Tariffs in the United States. *National Renewable Energy Laboratory*.

Couture, T.D., Kreycik, K.C. and Williams, E. 2010. A Policymaker's Guide to Feed-in Tariff Policy Design. *National Renewable Energy Laboratory*.

De Bere, L. 2000. Anaerobic digestion of solid waste: state-of-the-art. *Water science and technology* 41(3), pp. 283–290.

ECN.TNO Phyllis2 - Database for (treated) biomass, algae, feedstocks for biogas production and biochar [Online]. Available at: https://phyllis.nl/ [Accessed: 26 November 2019].

ecoinvent 2018. *Ecoinvent v3.5*.

ecoinvent 2019. *Ecoinvent v3.6*.

eGRID2012 2012. *Emissions & Generation Resource Integrated Database (Version 1)*. U.S. Environmental Protection Agency.

eGRID2016 2018. *Emissions & Generation Resource Integrated Database* . U.S. Environmental Protection Agency.

EIA 2019. California Natural Gas Consumption by End Use [Online]. Available at: https://www.eia.gov/dnav/ng/ng_cons_sum_dcu_SCA_a.htm [Accessed: 1 February 2019].

EIA 1999. *Natural Gas 1998: Issues and Trends*. Washington, DC: Office of Oil and Gas, Energy Information Administration, U.S. Dept. of Energy.

EPA 1995. *AP 42, Fifth Edition Compilation of Air Pollutant Emissions Factors, Volume 1: Stationary Point and Area Sources*. EPA.

EPA 2013. *Inventory of U.S. Greenhouse Gas Emissions and Sinks: 1990 - 2011*. U.S. Environmental Protection Agency.

EPA 1993. Synthetic Ammonia, Chapter 8: Inorganic Chemical Industry. In: *AP-42: Compilation of Air Emissions Factors*. U.S. Environmental Protection Agency.

EPA 2009. *Technical Support Document for the Ammonia Production Sector: Proposed Rule for Mandatory Reporting of Greenhouse Gases*. U.S. Environmental Protection Agency.

Epstein, E. and Alix, C. 2001. Odor control at composting facilities. *Resource Recycling*, pp. 24–28.

Favoino, E. and Hogg, D. 2008. The potential role of compost in reducing greenhouse gases. *Waste management & research : the journal of the International Solid Wastes and Public Cleansing Association, ISWA* 26(1), pp. 61–69.

Flagan, R.C. and Seinfeld, J.H. 1988. *Fundamentals of air pollution engineering*. Englewood Cliffs, N.J: Prentice Hall.

Fournier, M., Lesage, J., Ostiguy, C. and Van Tra, H. 2008. Sampling and analytical methodology development for the determination of primary and secondary low molecular weight amines in ambient air. *Journal of Environmental Monitoring* 10(3), pp. 379–386.

Gilmore, E.A., Heo, J., Muller, N.Z., et al. 2019. An inter-comparison of the social costs of air quality from reduced-complexity models. *Environmental Research Letters* 14(7), p. 074016.

Golder, D. 1972. Relations among stability parameters in the surface layer. *Boundary-layer meteorology* 3(1), pp. 47–58.

Goldstein, N. 2018. High Solids Anaerobic Digestion + Composting In San Jose [Online]. Available at: https://www.biocycle.net/2014/03/28/high-solids-anaerobic-digestion-composting-in-san-jose/ [Accessed: 31 January 2019].

Grcar, J.F., Glarborg, P., Bell, J.B., Day, M.S., Loren, A. and Jensen, A.D. 2005. Effects of mixing on ammonia oxidation in combustion environments at intermediate temperatures. *Proceedings of the Combustion Institute* 30(1), pp. 1193–1200.

Hellebrand, H.J. and Schade, G.W. 2008. Carbon monoxide from composting due to thermal oxidation of biomass. *Journal of Environmental Quality* 37(2), pp. 592–598.

Heo, J., Adams, Peter J and Gao, H.O. 2016. Public health costs of primary PM2.5 and inorganic PM2.5 precursor emissions in the united states. *Environmental Science & Technology* 50(11), pp. 6061–6070.

Heo, J., Adams, Peter J. and Gao, H.O. 2016. Reduced-form modeling of public health impacts of inorganic PM2.5 and precursor emissions. *Atmospheric environment* 137(137), pp. 80–89.

Holly, M.A., Larson, R.A., Powell, J.M., Ruark, M.D. and Aguirre-Villegas, H. 2017. Greenhouse gas and ammonia emissions from digested and separated dairy manure during storage and after land application. *Agriculture, Ecosystems & Environment* 239, pp. 410–419.

Interagency Working Group on the Social Cost of Greenhouse Gases 2016. *Technical Update of the Social Cost of Carbon for Regulatory Impact Analysis*. Washington, DC: U.S. White House.

Interstate Renewable Energy Council (IREC) 2013. *Model Interconnection Procedures*.

Jiang, T., Schuchardt, F., Li, G., Guo, R. and Zhao, Y. 2011. Effect of C/N ratio, aeration rate and moisture content on ammonia and greenhouse gas emission during the composting. *Journal of Environmental Sciences* 23(10), pp. 1754–1760.

Jokela, J.P.Y. and Rintala, J.A. 2003. Anaerobic solubilisation of nitrogen from municipal solid waste (MSW). *Reviews in Environmental Science and Bio/Technology* 2(1), pp. 67–77.

Kirchmann, H. and Witter, E. 1989. Ammonia volatilization during aerobic and anaerobic manure decomposition. *Plant and soil* 115(1), pp. 35–41.

Kuo, J. and Dow, J. 2017. Biogas production from anaerobic digestion of food waste and relevant air quality implications. *Journal of the Air & Waste Management Association (1995)* 67(9), pp. 1000–1011.

Lenzen, M. 2008. Life cycle energy and greenhouse gas emissions of nuclear energy: A review. *Energy Conversion and Management* 49(8), pp. 2178–2199.

Makaruk, A., Miltner, M. and Harasek, M. 2010. Membrane biogas upgrading processes for the production of natural gas substitute. *Separation and Purification Technology* 74(1), pp. 83–92.

Martínez-Blanco, J., Lazcano, C., Christensen, T.H., et al. 2013. Compost benefits for agriculture evaluated by life cycle assessment. A review. *Agron. Sustain. Dev.* 33(4), pp. 721–732.

Martínez-Blanco, J., Muñoz, P., Antón, A. and Rieradevall, J. 2009. Life cycle assessment of the use of compost from municipal organic waste for fertilization of tomato crops. *Resour. Conserv. Recycl.* 53(6), pp. 340–351.

McDaniel, M. 1983. *Flare Efficiency Study*. Environmental Protection Agency.

McRae, G.J. 1980. A simple procedure for calculating atmospheric water vapor concentration. *Journal of the Air Pollution Control Association* 30(4), pp. 394–394.

Möller, K. and Müller, T. 2012. Effects of anaerobic digestion on digestate nutrient availability and crop growth: A review. *Engineering in life sciences* 12(3), pp. 242–257.

Morris, J., Scott Matthews, H. and Morawski, C. 2013. Review and meta-analysis of 82 studies on end-of-life management methods for source separated organics. *Waste management (New York, N.Y.)* 33(3), pp. 545–551.

Muller, N.Z. and Mendelsohn, R. 2007. Measuring the damages of air pollution in the United States. *Journal of Environmental Economics and Management* 54(1), pp. 1–14.

Neupane, B., Konda, N.V.S.N.M., Singh, S., Simmons, B.A. and Scown, C.D. 2017. Life-Cycle Greenhouse Gas and Water Intensity of Cellulosic Biofuel Production Using Cholinium Lysinate Ionic Liquid Pretreatment. *ACS sustainable chemistry & engineering* 5(11), pp. 10176–10185.

Pertl, A., Mostbauer, P. and Obersteiner, G. 2010. Climate balance of biogas upgrading systems. *Waste management (New York, N.Y.)* 30(1), pp. 92–99.

Pfefferle, L.D. and Churchill, S.W. 1986. NO_x Production from the Combustion of Ethane Doped with Ammonia in a Thermally Stabilized Plug Flow Burner. *Combustion Science and Technology* 49(5–6), pp. 235–249.

Piringer, M., Knauder, W. and Petz, E. 2014. Use of Ultrasonic Anemometer Data to Derive Local Odour related Peak-to-Mean Concentration Ratios. *Chemical Engineering Transactions*.

Piringer, M., Knauder, W., Petz, E. and Schauberger, G. 2015. A comparison of separation distances against odour annoyance calculated with two models. *Atmospheric environment* 116, pp. 22–35.

Piringer, M., Knauder, W., Petz, E. and Schauberger, G. 2016. Factors influencing separation distances against odour annoyance calculated by Gaussian and Lagrangian dispersion models. *Atmospheric environment* 140, pp. 69–83.

Piringer, M., Knauder, W., Petz, E. and Schauberger, G. 2014. Site-dependent decrease of odour-related peak-to-mean factors with distance. *Advances in Science and Research* 11(1), pp. 69–73.

Piringer, M., Petz, E., Groehn, I. and Schauberger, G. 2007. A sensitivity study of separation distances calculated with the Austrian Odour Dispersion Model (AODM). *Atmospheric Environment* 41(8), pp. 1725–1735.

Piringer, M., Petz, E., Groehn, I. and Schauberger, G. 2013. Corrigendum to "A sensitivity study of separation distances calculated with the Austrian Odour Dispersion Model (AODM)" [Atmos. Environ. 41 (2007) 1725–1735]. *Atmospheric environment* 67, pp. 461–462.

Pöschl, M., Ward, S. and Owende, P. 2010. Evaluation of energy efficiency of various biogas production and utilization pathways. *Applied energy* 87(11), pp. 3305–3321.

Preble, C.V., Cados, T.E., Harley, R.A. and Kirchstetter, T.W. 2018. In-Use Performance and Durability of Particle Filters on Heavy-Duty Diesel Trucks. *Environmental Science & Technology*.

Research Triangle Institute 2000. *Lime Production: Industry Profile*. U.S. Environmental Protection Agency.

Riber, C., Petersen, C. and Christensen, T.H. 2009. Chemical composition of material fractions in Danish household waste. *Waste management (New York, N.Y.)* 29(4), pp. 1251–1257.

Robins, A.G. 1979. The development and structure of simulated neutrally stable atmospheric boundary layers. *Journal of Industrial Aerodynamics* 4(1), pp. 71–100.

Roe, S., Spivey, M., Lindquist, H., Thesing, K., Strait, R. and E.H. Pechan & Associates, Inc. 2004. *Estimating Ammonia Emissions from Anthropogenic Non-Agricultural Sources*. Emission Inventory Improvement Program.

Saer, A., Lansing, S., Davitt, N.H. and Graves, R.E. 2013. Life cycle assessment of a food waste composting system: environmental impact hotspots. *Journal of Cleaner Production* 52, pp. 234–244.

Scipioni, A., Mazzi, A., Niero, M. and Boatto, T. 2009. LCA to choose among alternative design solutions: the case study of a new Italian incineration line. *Waste management (New York, N.Y.)* 29(9), pp. 2462–2474.

Scown, C.D., Gokhale, A.A., Willems, P.A., Horvath, A. and McKone, T.E. 2014. Role of lignin in reducing life-cycle carbon emissions, water use, and cost for United States cellulosic biofuels. *Environmental Science & Technology* 48(15), pp. 8446–8455.

Scown, C.D., Horvath, A. and McKone, T.E. 2011. Water footprint of U.S. transportation fuels. *Environmental Science & Technology* 45(7), pp. 2541–2553.

Sheehan, J., Camobreco, V., Duffield, J., Shapouri, H., Graboski, M. and Tyson, K.S. 1998. *An overview of biodiesel and petroleum diesel life cycles*. National Renewable Energy Laboratory (NREL).

Smet, E., Van Langenhove, H. and De Bo, I. 1999. The emission of volatile compounds during the aerobic and the combined anaerobic/aerobic composting of biowaste. *Atmospheric environment* 33(8), pp. 1295–1303.

Smith, M.E. Recommended Guide for the Prediction of the Dispersion of Airborne Effluents.

Spath, P. and Mann, M. 2001. *Life Cycle Assessment of Hydrogen Production via Natural Gas Steam Reforming*. National Renewable Energy Laboratory.

State Water Resources Control Board 2018. *General Waste Discharge Requirements for the Discharge of Biosolids to Land for Use as a Soil Amendment in Agricultural, Silvicultural, Horticultural, and Land Reclamation Activities*. STATE WATER RESOURCES CONTROL BOARD.

Strogen, B., Horvath, A. and McKone, T.E. 2012. Fuel miles and the blend wall: costs and emissions from ethanol distribution in the United States. *Environmental Science & Technology* 46(10), pp. 5285–5293.

Sullivan, D.M., Cogger, C.G. and Bary, A.I. 2015. *Fertilizing with Biosolids*. Oregon State University Extension.

Tambone, F., Scaglia, B., D'Imporzano, G., et al. 2010. Assessing amendment and fertilizing properties of digestates from anaerobic digestion through a comparative study with digested sludge and compost. *Chemosphere* 81(5), pp. 577–583.

Thinkstep 2018. *GaBi*.

Tonini, D., Martinez-Sanchez, V. and Astrup, T.F. 2013. Material resources, energy, and nutrient recovery from waste: are waste refineries the solution for the future? *Environ. Sci. Technol.* 47(15), pp. 8962–8969.

Turconi, R., Butera, S., Boldrin, A., Grosso, M., Rigamonti, L. and Astrup, T. 2011. Life cycle assessment of waste incineration in Denmark and Italy using two LCA models. *Waste management & research : the journal of the International Solid Wastes and Public Cleansing Association, ISWA* 29(10 Suppl), pp. 78–90.

U.S. Environmental Protection Agency 2018. *Advancing Sustainable Materials Management: 2015 Fact Sheet*. U.S. Environmental Protection Agency.

USEPA 2018. Waste Reduction Model (WARM). . Available at: https://www.epa.gov/warm.

Venkatesh, A., Jaramillo, P., Griffin, W.M. and Matthews, H.S. 2011. Uncertainty analysis of life cycle greenhouse gas emissions from petroleum-based fuels and impacts on low carbon fuel policies. *Environmental Science & Technology* 45(1), pp. 125–131.

VEPP Inc. 2018. 2018 Avoided Cost Caps.

Wang, M. 2008. *The Greenhouse Gases, Regulated Emissions, and Energy Use in Transportation (GREET) Model Version 1.5*. Center for Transportation Research, Argonne National Laboratory.

Ward, A.J., Hobbs, P.J., Holliman, P.J. and Jones, D.L. 2008. Optimisation of the anaerobic digestion of agricultural resources. *Bioresource Technology* 99(17), pp. 7928–7940.

Wernet, G., Bauer, C., Steubing, B., Reinhard, J., Moreno-Ruiz, E. and Weidema, B. 2016. The ecoinvent database version 3 (part I): overview and methodology. *The International Journal of Life Cycle Assessment* 21(9), pp. 1218–1230.

Wicke, B., Dornburg, V., Junginger, M. and Faaij, A. 2008. Different palm oil production systems for energy purposes and their greenhouse gas implications. *Biomass and Bioenergy* 32(12), pp. 1322–1337

APPENDIX A:
Emissions Measurements

Instrumentation and Emission Factor Calculations

Measurements of pollutant concentrations were made with a suite of fast-responding, high-grade instruments, which are summarized in Table A-1. Measured concentrations were then converted to fuel-based emission factors or time-based emission rates (E_P).

Table A-1: Instrumentation Used to Sample Pollutant Concentrations

Pollutant	Measurement Method/ Analyzer	Enclosed Flare	CHP	Outdoor Composting	Biofilter	Bladder Vent
CO_2, CH_4	cavity ring-down spectroscopy (LGR model 915-0011)	●	●	●	●	
N_2O, CO	cavity ring-down spectroscopy (LGR model N2OCM-919)	●	●	●	●	
H_2S, NH_3	cavity ring-down spectroscopy (LGR model 915-0039)	●	●	●	●	
CO_2	Nondispersive infrared absorption (LI-COR model LI-820)	●				●
O_2	Flue gas analyzer (Testo model 320, 350)	●	●			
NO_x	Chemiluminescence (Ecophysics model CLD64)	●	●			
BC	Aethalometry (Magee Sci. model AE16)	●				

Source: Lawrence Berkeley National Laboratory

For the sources of biogas combustion (i.e., the CHP units and flare), a carbon balance method was used to calculate fuel-based emission factors for each pollutant species, with units g of pollutant emitted per kg of methane combusted (g per kg, or g kg^{-1}):

$$E_P = \frac{\Delta[P]}{\Delta[CO_2]} \cdot \frac{MW_P}{MW_C} \cdot \frac{w_c}{w_{CH_4}} \cdot 10^3$$

Here, $\Delta[P]$ and $\Delta[CO_2]$ are the background subtracted concentrations of pollutant P and CO_2 measured in the exhaust of the CHP or flare and have molar concentrations of ppm. The molecular weights (MW) of pollutant P and carbon C are in units of g per mol. Finally, w_i is the weight fraction of species i in biogas fuel, with units of grams of species i per gram of biogas fuel. For methane, this constant equates to 0.27 g CH_4 per gram of biogas, assuming a typical 50/50 mixture of CO_2 and CH_4 by volume in the biogas. The weight fraction of carbon in biogas fuel (w_c = 0.4) assumes all carbon present in the biogas is present as CO_2 in the exhaust.

For the emission sources driven by aerated flow—composting, biofilters, and venting—time-based emission factors were calculated as the product of measured pollutant concentrations and flow rate:

$$E_P = C_P \cdot Q$$

Here, E_P has units of g of pollutant P emitted per hour (g per hour), C_P is the emitted pollutant concentration in mass concentration units (g per m^3), and Q is the volumetric flow rate for that source (m^3 per hour).

Additionally, we calculated emission factors for each species to relate the emitted pollutant mass to the amount of MSW handled and the volume of biogas produced at ZWEDC. Using the following expressions, we converted the measured g per kg emission factors:

$$\frac{g\ P}{X} = \frac{g\ P}{kg\ CH_4} \cdot \frac{w_{CH_4}}{10^3} \cdot \frac{(MW_{biogas})P_{amb}}{RT_{amb}} \cdot \frac{m^3 biogas\ consumed\ at\ source}{X}$$

where MW_{biogas} = 30 g per mol, P_{amb} is ambient pressure, T_{amb} is ambient temperature, R is the ideal gas constant, and X represents either kg MSW handled or m^3 of biogas produced. For the biofilter time-based emission rates, we converted from g per hour to g per X using:

$$\frac{g\ P}{X} = \frac{g\ P}{h} \cdot \frac{24\ h}{day} \cdot \frac{30\ days}{month} \cdot \frac{month}{X}$$

For composting time-based emission rates, we converted from g emitted per hour per windrow pile to g emitted per kg of MSW handled over a 14-week composting cycle:

$$\frac{g\ P}{kg\ MSW} = \frac{g\ P}{h \cdot pile} \cdot \frac{24\ h}{day} \cdot \frac{7\ days}{week} \cdot \frac{14\ weeks}{cycle} \cdot \frac{pile}{kg\ digestate} \cdot \frac{kg\ digestate\ trucked\ from\ ZWEDC}{kg\ MSW}$$

Table A-2 summarizes the monthly average MSW and digestate material flows, biogas production, and biogas consumption values for ZWEDC and Z-Best based on 2018 data from each facility that are used in the above emission factor calculations. These emission factor results are reported as a summary table in the Appendix for each subsection and are compared in the final subsection of Part 1 of this chapter.

Table A-2: Facility Operations Data for Emission Factor Calculations

Parameter	2018 Monthly Average Value
Mass of inbound MSW received at ZWEDC	7.76×10^6 kg
Mass of organic MSW digested at ZWEDC	5.35×10^6 kg
Volume of biogas produced at ZWEDC	210,954 m^3
Volume of biogas consumed during lean burns	42,921 m^3
Volume of biogas consumed during rich burns	66,191 m^3
Volume of biogas consumed by CHP units	150,656 m^3
Mass of digestate material trucked to Z-Best	4.02×10^6 kg
Mass of digestate per windrow at Z-Best	6.35×10^5 kg

Source: Lawrence Berkeley National Laboratory

Biogas Combustion Stoichiometry

For the purposes of local regulatory permitting, exhaust concentrations are typically expressed at a certain percent of O_2 (e.g., 15 percent O_2) to account for the effect of dilution on measured concentrations. Assuming the following biogas combustion stoichiometry, the adjusted concentration in ppm at Y percent O_2 relative to measured concentrations at exhaust Z percent O_2 is:

$$CH_4 + \frac{2}{\phi}(O_2 + 3.78\ N_2) + x\ NH_3 \rightarrow CO_2 + 2\ H_2O + \left(\frac{2}{\phi} - 2\right) O_2 + \frac{2}{\phi} 3.78\ N_2 + x\ NO_x$$

$$[P]\ at\ Y\ percent\ O_2 = [P] at\ Z\ percent \left(\frac{20.9 - X}{20.9 - Z}\right)$$

where Φ is the equivalence ratio and *20.9 percent* is the ambient O_2 concentration. To convert this concentration into a fuel-based emission factor, the number of moles of exhaust per mole of methane from the above combustion stoichiometry is used:

$$moles\ of\ exhaust\ per\ mole\ of\ CH_4 = 1 + \frac{9.56}{\Phi}$$

For 15 percent O_2, Φ is 0.263 and the number of moles of exhaust equals 37.3, such that:

$$\frac{g\ P}{kg\ CH_4} = \frac{mol\ P\ at\ 15\ percent\ O_2}{10^6\ mol\ exhaust} \cdot \frac{37.3\ mol\ exhaust}{1\ mol\ CH_4} \cdot \frac{MW_P}{MW_{CH4}}$$

where the molecular weights (*MW*) of pollutant *P* and CH_4 are in units of g per mol. The flare and CHP results presented below include a comparison to the permitted emission factor limit set by the Bay Area Air Quality Management District (BAAQMD), determined with this combustion stoichiometry for biogas.

Flare

Sampling Flared Biogas and Exhaust

Figure A-1: Schematic of the Automated System to Sample Flared Biogas

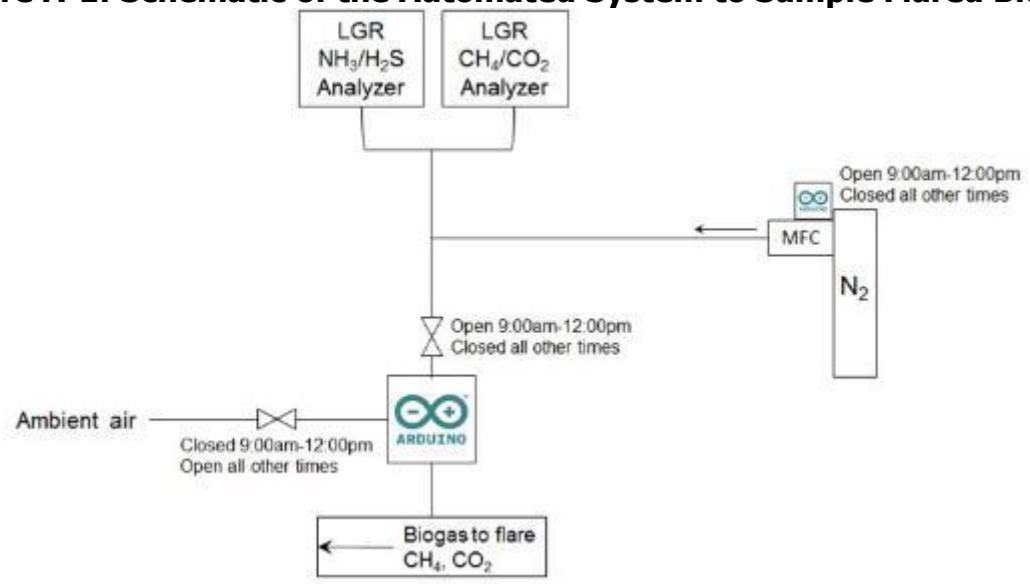

The automated sampling setup to measure flared biogas during lean burns in 2016 and 2017. LGR refers to the spectrometers, the Arduino symbol represents automation microcontrollers, and MFC refers to mass flow controller.

Source: Lawrence Berkeley National Laboratory

Figure A-2: Schematic of the Automated Flare Exhaust Sampling System

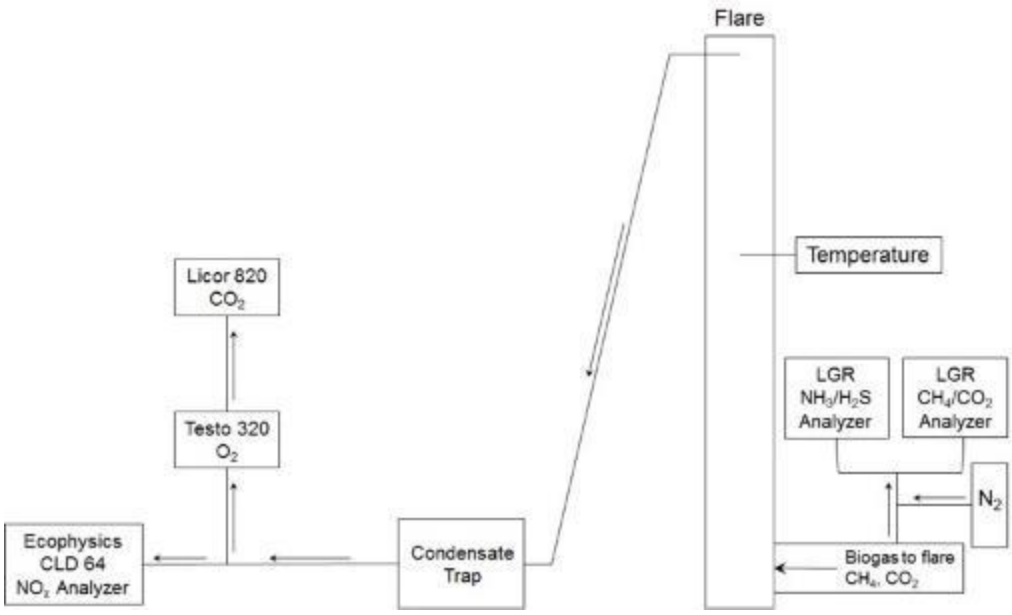

The corresponding sampling setup to the automated system to measure flare exhaust during lean biogas burns in 2016 and 2017. To prevent condensational losses in the sample line, sampled biogas was diluted with compressed nitrogen at a 3:1 ratio.

Source: Lawrence Berkeley National Laboratory

Emission Rates during Lean and Rich Biogas Burns

Using the carbon balance method outlined above, fuel-based emission factors (E_P) were calculated for each pollutant species in terms of mass of pollutant emitted per kg of methane combusted. Figure A-3 presents the minute-average emission rates calculated over the course of the typical lean and rich burns that are shown in Figure 10. Time series plots of the biogas flow rates, flare temperature, and pollutant emission rates for the four lean burns and thirteen rich burns sampled in 2018 are also individually reported in Figure A-4 through Figure 0-8.

Figure A-3: Emission Rates During Typical Flaring Events

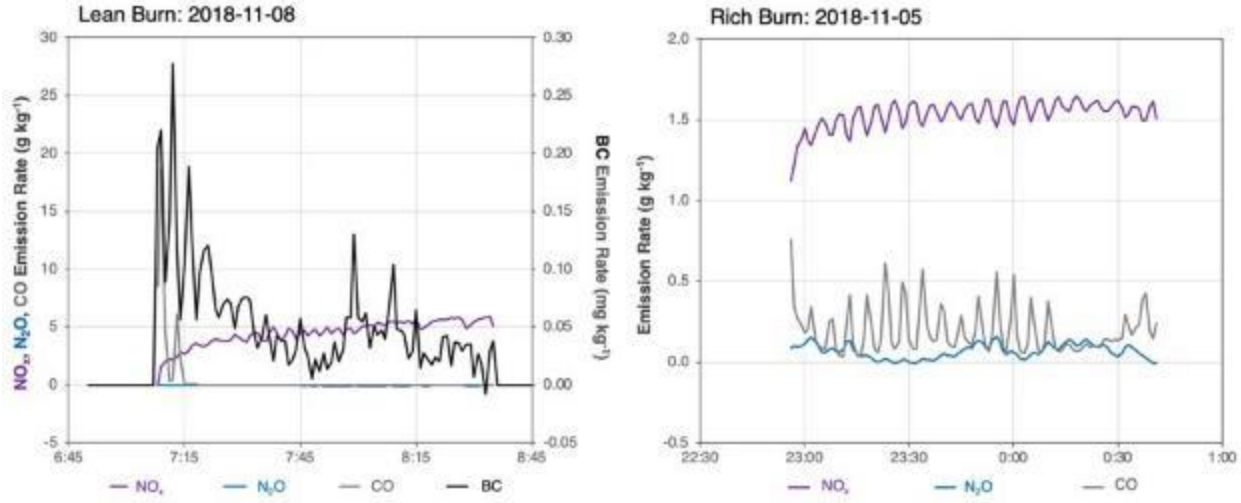

Minute-average emission rates of NO_x, N_2O, CO, and BC during the typical lean and rich biogas burns from Figure 10. BC data was not available during this rich biogas event.

Source: Lawrence Berkeley National Laboratory

Figure A-4: Lean Biogas Flaring Events 1–3

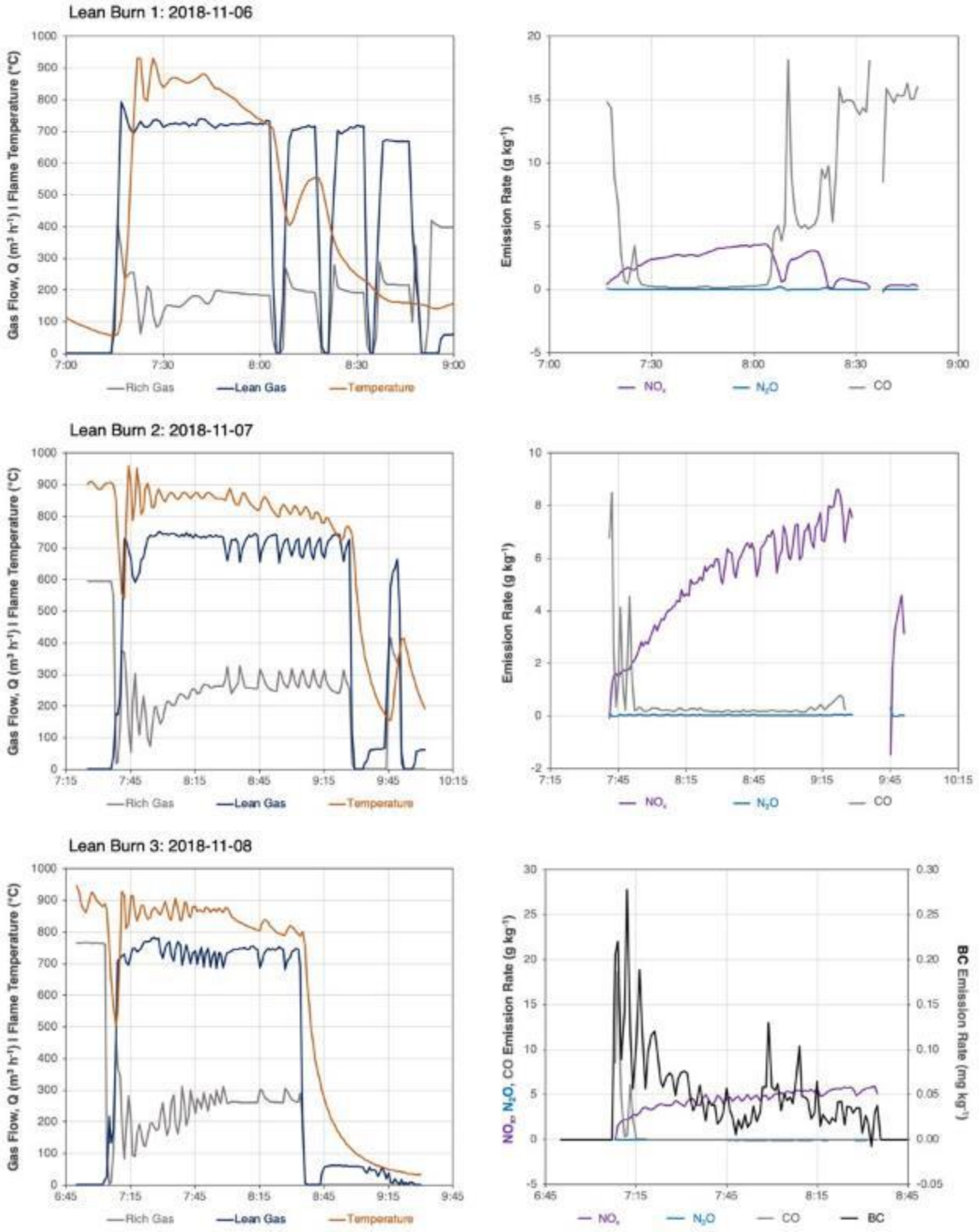

Source: Lawrence Berkeley National Laboratory

Figure A-5: Rich Biogas Flaring Events 1, 3, and 4

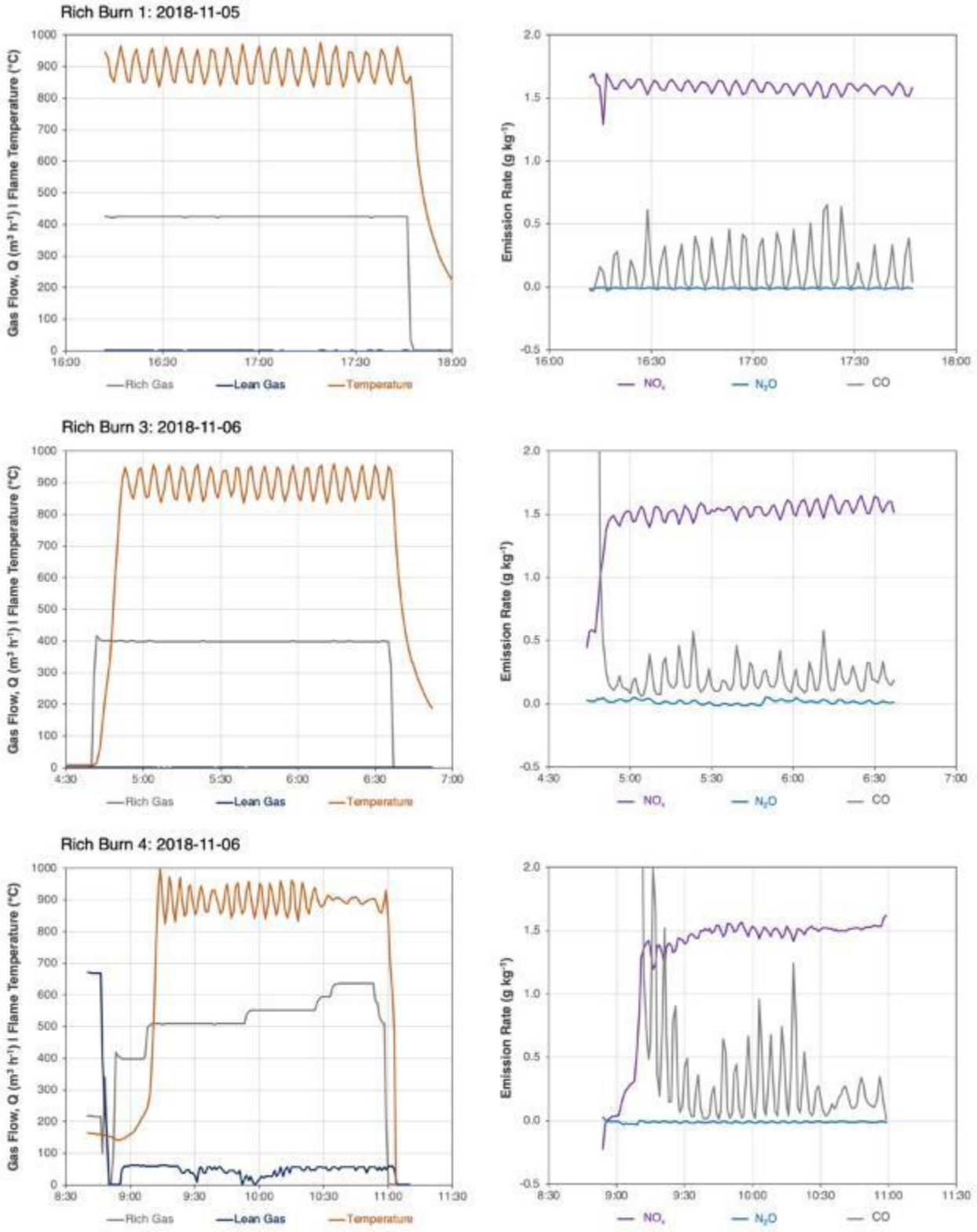

Source: Lawrence Berkeley National Laboratory

Figure A-6: Rich Biogas Flaring Events 5–7

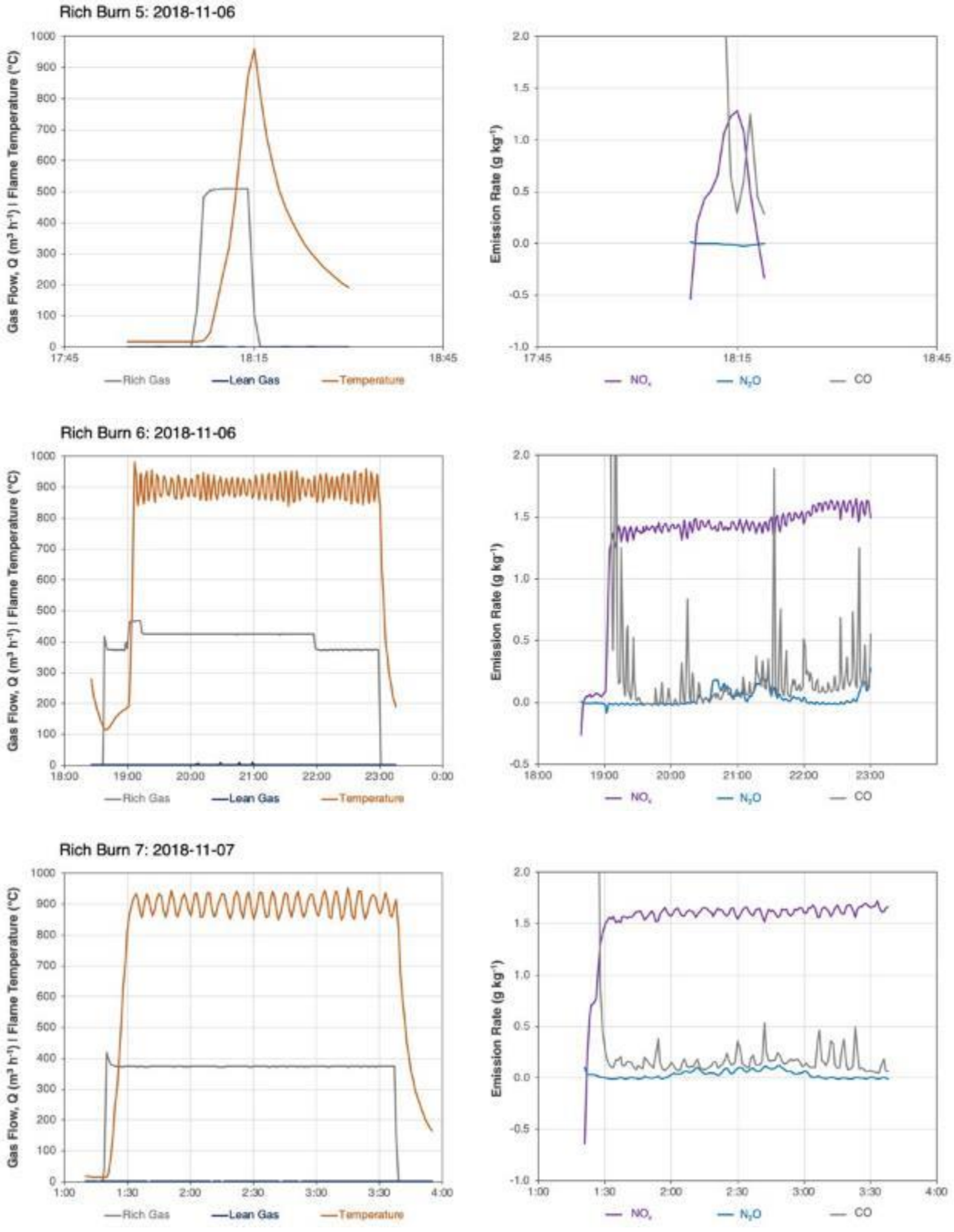

Source: Lawrence Berkeley National Laboratory

Figure A-7: Rich Biogas Flaring Events 8–10

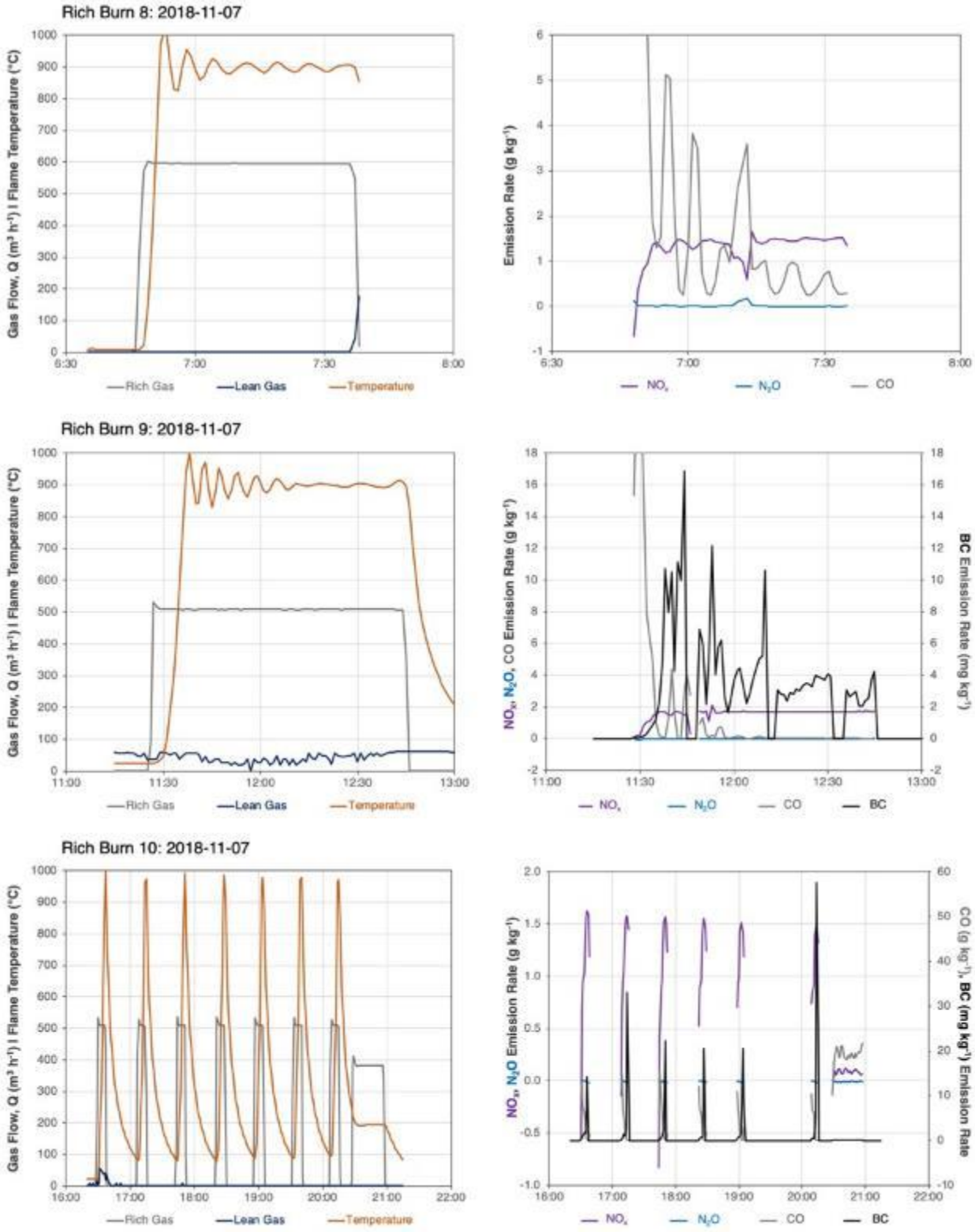

Source: Lawrence Berkeley National Laboratory

Figure 0-8: Rich Biogas Flaring Events 11–13

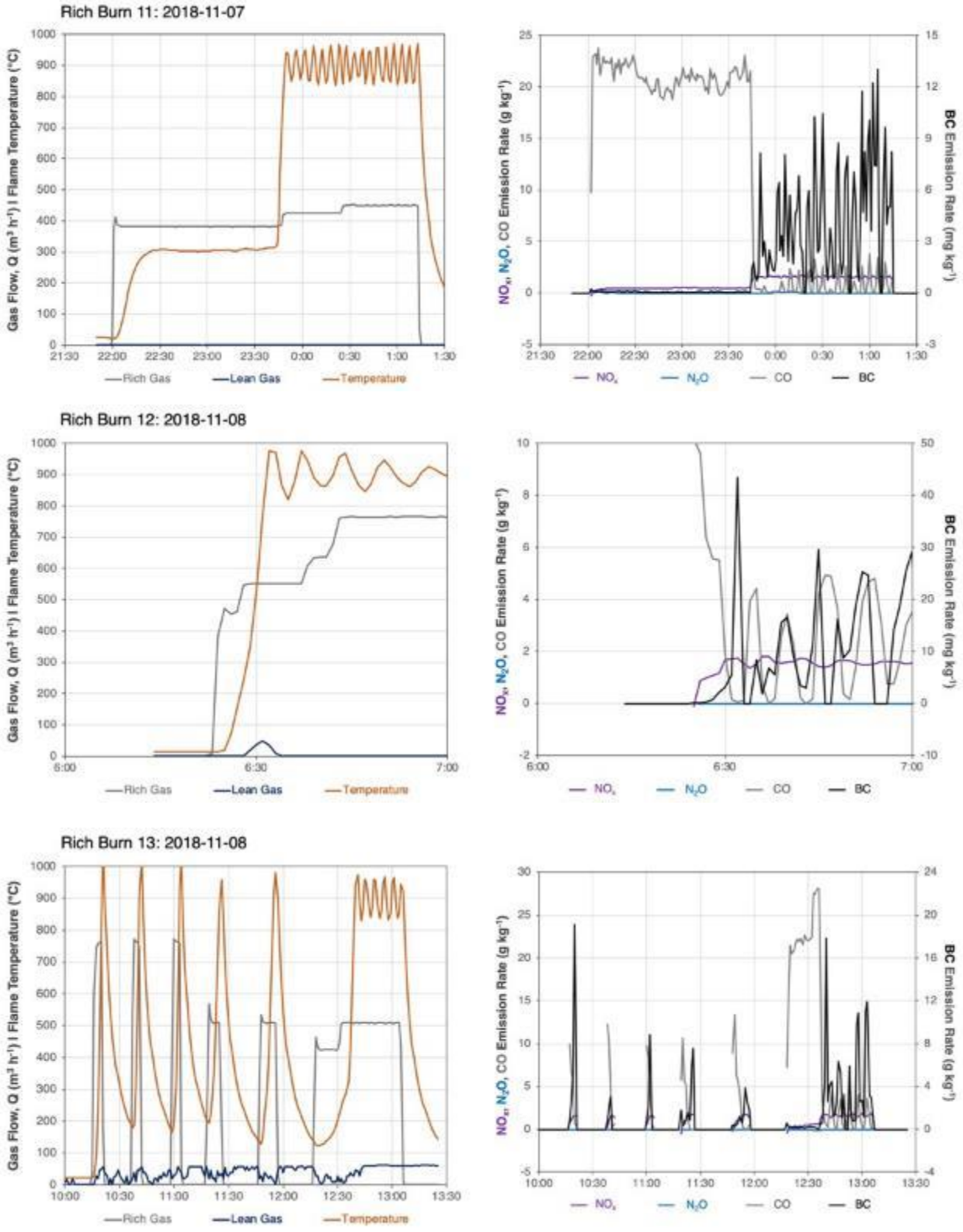

Source: Lawrence Berkeley National Laboratory

The emission rates of N_2O and CO are typically low and steady for the duration of lean and rich flaring events when there is an active flame. The NO_x emission rate mirrors the trend in emitted NO_x concentration from Figure 13, increasing over time during lean burns from zero to 5–10 g per kg versus remaining constant ~1.5 g per kg during rich burns. BC emissions during lean burns are near ambient concentrations (average exhaust concentration ~3 µg per m^3). BC concentrations are elevated during rich burns (average exhaust concentration ~80 µg per m^3), but the corresponding emission factors during those rich burns are small, with an average of 3.5 ± 0.6 mg per kg (± 95 percent confidence interval). The rich burns sampled during these measurements did not look to be as sooty as some that the project team visually observed in the past; it is possible that anomalous flaring conditions could result in greater BC emission rates than were measured in the present study.

Table A-3 summarizes the average emission factors for NO_x and other pollutants quantified for lean and rich biogas flaring events. On a per kg CH_4 burned basis, the lean NO_x emission rate is on average 3.3 times greater than that of rich burns, while the lean CO emission rate is on average half that of rich burns. Because more biogas is consumed during rich burns than lean burns, these lean-to-rich emission ratios are instead 2.2 and 0.3, respectively, when normalized to MSW mass or biogas production volume. Assuming the stoichiometric relationship presented above, the BAAQMD permitted limits of 118 ppm and 43 ppm at 15 percent O_2 for lean and rich burns, respectively, convert to 12.6 and 4.6 g per kg. The measured emission rates in this study were on average one-third lower than these permitted values in both cases. The BC emission rate from rich burns is an order of magnitude greater than that of lean burns, but overall low in magnitude relative to other important sources of BC emissions like heavy-duty diesel trucks (Preble et al. 2018).

Table A-3: Average Emission Rates from Flare During Lean and Rich Biogas Flaring Events (g emitted per X)

	Normalization Parameter, X	NO_x	N_2O	CO	BC
Lean Biogas Flaring Events	kg CH_4	4.38E+00	1.64E-02	1.94E+00	1.71E-04
	kg of inbound MSW received	7.94E-03	2.98E-05	3.52E-03	3.11E-07
	kg of organic MSW digested	1.15E-02	4.32E-05	5.11E-03	4.51E-07
	m^3 of biogas produced	2.92E-01	1.10E-03	1.30E-01	1.14E-05
Rich Biogas Flaring Events	kg CH_4	1.31E+00	1.29E-02	3.65E+00	3.46E-03
	kg of inbound MSW received	3.66E-03	3.60E-05	1.02E-02	9.67E-06
	kg of organic MSW digested	5.32E-03	5.23E-05	1.48E-02	1.40E-05
	m^3 of biogas produced	1.35E-01	1.33E-03	3.75E-01	3.56E-04

Source: Lawrence Berkeley National Laboratory

CHP Units

Measurement of CHP Emissions

Figure A-9 shows the exhaust concentrations (corrected for the factor of 7.9 dilution) measured at CHP 2 after a warm start-up at 12:40. The starting temperature of the CHP engine was 55 °C. Initially, there is a peak in emitted concentrations of all pollutants except N_2O. The exhaust nitrous oxide concentration dipped below background concentrations at start-up, meaning the CHP consumes ambient N_2O. The engine officially kicked on approximately 10 minutes after initial start-up, once temperature exceeded 75 °C. At this point, the measured exhaust concentrations are steady.

Figure A-9: Measured CHP Exhaust Concentrations

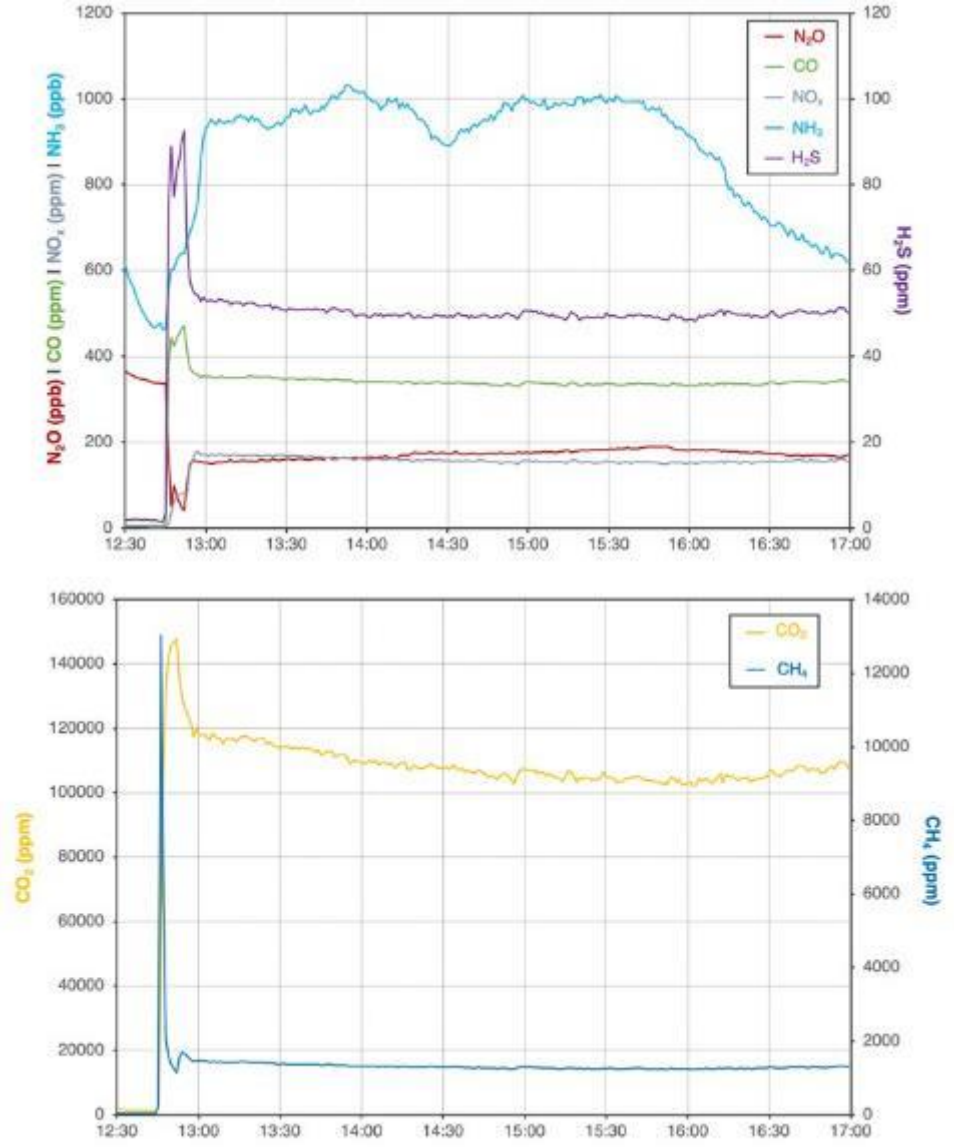

Plotted exhaust concentrations have been corrected for the factor of 7.9 dilution.

Source: Lawrence Berkeley National Laboratory

Table A-4: Average Emission Rates from CHP Units with Non-Operational SCR (g emitted per X)

Normalization Parameter, X	NO_x	CH_4	N_2O	CO	NH_3	H_2S
kg CH_4	8.45E+00	2.42E+01	-8.16E-03	1.10E+01	1.59E-02	1.98E+00
kg of inbound MSW received	5.38E-02	1.54E-01	-5.19E-05	7.02E-02	1.01E-04	1.26E-02
kg of organic MSW digested	7.80E-02	2.24E-01	-7.53E-05	1.02E-01	1.47E-04	1.83E-02
m^3 of biogas produced	1.98E+00	5.67E+00	-1.91E-03	2.58E+00	3.72E-03	4.63E-01

Source: Lawrence Berkeley National Laboratory

Table A-5: Average Emission Rates from CHP Units with Operational SCR (g emitted per X)

Normalization Parameter, X	NO_x	CO
kg CH_4	6.25E-01	2.35E+00
kg of inbound MSW received	3.98E-03	1.50E-02
kg of organic MSW digested	5.77E-03	2.17E-02
m^3 of biogas produced	1.46E-01	5.51E-01

Source: Lawrence Berkeley National Laboratory

Composting

Measurement Study: Laboratory-Scale Composting System

Under the guidance of technicians at Z-Best and Engineered Compost Systems (ECS), the project team constructed a laboratory-scale composting chamber at LBNL. A schematic of this system is shown in Figure A-10. The chamber represents a core taken from the middle of a composting windrow at Z-Best. The bottom of the chamber was connected to a pump that forced air through the core for aeration. Three thermocouples were placed along the chamber to monitor the sample's temperature. The chamber was filled with digestate material obtained from ZWEDC.

During the first experiment in this chamber, the sample initially entered the optimal temperature range (~60 °C) and remained there for three days. In the following week, the sample temperature dropped to nearly room temperature. Measured ammonia concentrations exceeded 10 ppm, a threshold indicated by ECS as an indication that composting may have been inhibited.

Figure A-10: Schematic of the Laboratory-Scale Composting Chamber

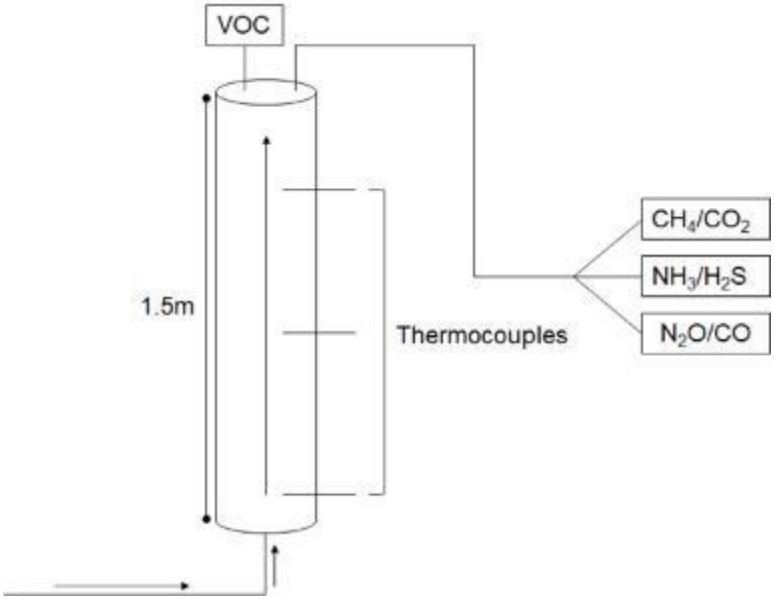

Source: Lawrence Berkeley National Laboratory

Additional experiments were run in the chamber, plus another experiment in a larger 200 L chamber that increased the surface area to volume ratio. The digestate was also amended with wood chips to create a mixture that was 75 percent wood chips by volume to increase the carbon to nitrogen ratio to 30:1, as recommended by ECS. The temperature exhibited the same trend, reaching the optimal temperature range for three days and cooling back to room temperature. It is likely that the chamber was not a suitable representation of the composting process at Z-Best, probably due to difficulties with scaling the large and diverse microbial activity in an industrial-scale windrow to a laboratory-scale setting. Although the size of the compost system can be scaled down, the microbial activity did not directly scale. As such, measurements were instead made in-situ at Z-Best on active composting windrows.

In-Situ Measurements at Z-Best: GHGs and Odorous Compounds

Sampling Method

The differential pressure between the pitot tubes was recorded using TECLOG (The Energy Conservancy, Minneapolis, MN), and the volumetric flow rate (Q, ft^3 per minute) was calculated using the following equations:

$$v = k\sqrt{\frac{2 \cdot \Delta P}{\rho}}$$

$$Q = v \cdot A$$

where v is the air velocity in m per second, k is an empirical factor for the sensor (equal to 1.39 for this system), ΔP is the measured differential pressure in Pa, ρ is the density of air, and A is the cross-sectional area of the duct. The resulting flow remained steady during each sampling period (Table A-6).

Table A-6: Summary of Aeration Flow Delivered to Each Sampled Windrow

Date Sampled	Pile ID	Blower 1 Measured Q (cfm)	Blower 1 percent On	Blower 1 Effective Q (cfm)	Blower 2 Measured Q (cfm)	Blower 2 percent On	Blower 2 Effective Q (cfm)	Total Measured Q (cfm)	Total Effective Q (cfm)
2018-07-12	A21	299	5	15	344	40	137	643	152
2018-08-17	A21	437	5	22	564	35	197	1001	219
2018-08-17	B11	696	40	278	815	70	571	1511	849
2018-09-05	B11	556	25	139	672	80	538	1229	677
2018-09-05	A13	696	40	278	668	70	468	1364	746
2018-09-05	B3	560	50	280	576	40	230	1136	510
2018-09-26	B11	599	10	60	769	70	538	1368	598
2018-09-26	B3	699	35	245	719	25	180	1418	424
2018-09-26	D15	564	50	282	811	75	609	1376	891

The measured flows have been adjusted by each blower's cycle settings to normalize the volumetric flow rate to an effective hourly flow rate.

Source: Lawrence Berkeley National Laboratory

Concentrations of gases in the bag samples were subsequently measured with analyzers in the laboratory, as described below. These concentrations are compared to a limited set of real-time measurements made in the field with the same analyzers, as shown in Figure A-11. Real-time measurements at multiple locations across a given windrow were restricted by: (1) a lack of accessible space to place instruments near sample locations, (2) difficulty in avoiding water condensation in the sampling lines due to the high temperature and water saturation of the emitted gas, and (3) the quantity of dilution gas needed to reach optimal concentration and relative humidity for the instruments. Spot measurements with the sample bags, on the other hand, provided greater spatial coverage across multiple windrows each sampling day, with bag analysis handled later in the laboratory.

Figure A-11: Real-Time vs Bag Sampling Measurements

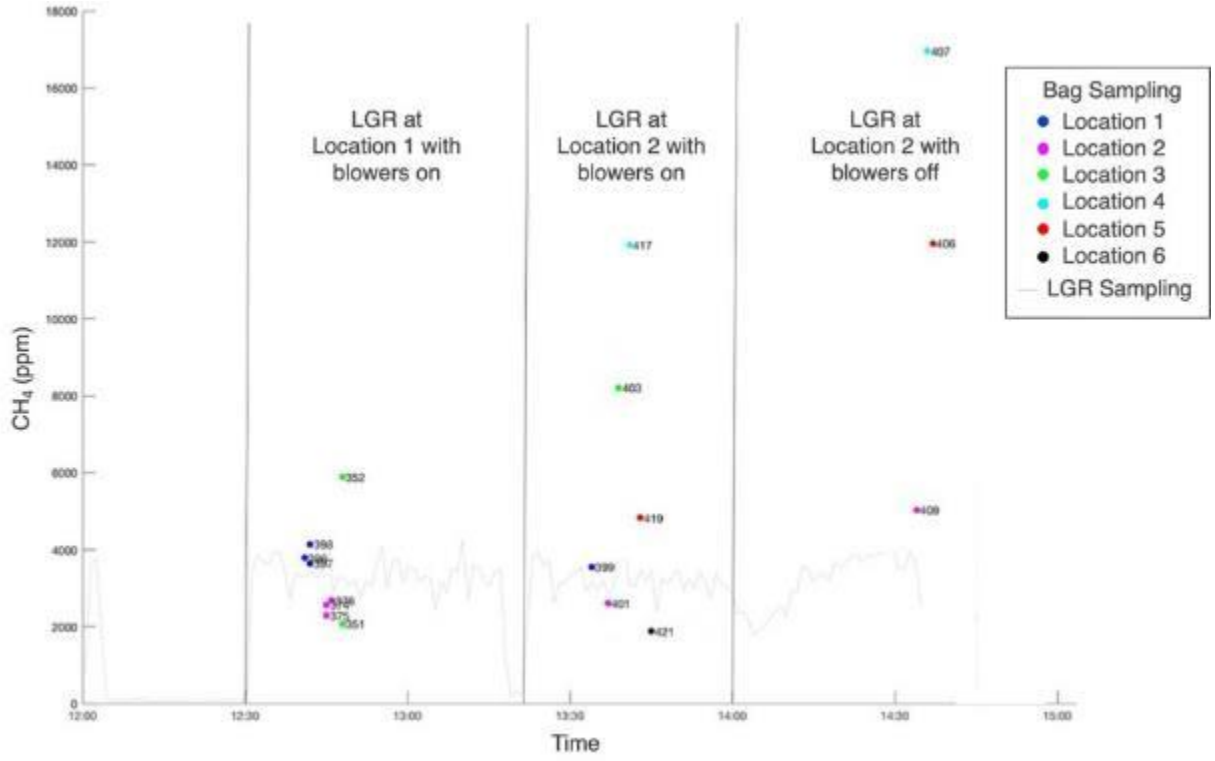

Comparison of concentrations in bag samples taken at six locations on a windrow relative to the concentrations measured in real-time at two of those locations. The six locations shown were equally spaced along the top centerline of the windrow. LGR refers to the ultraportable spectrometer that measured emitted concentrations in real-time at Location 1 during the 12:30 section and at Location 2 in the 13:30 and 14:00 sections of the time series. Note that the bag samples taken at Location 1 (shown in blue) during the 12:30 section and the bag samples taken at Location 2 (shown in pink) during the 13:30 section agree with the corresponding collocated real-time measurement for each. In this plot, we see no appreciable change in the gas concentration with the blowers on and off. Note, the numbers next to each bag sample point refer to a unique identifier rather than sampled methane concentration.

Source: Lawrence Berkeley National Laboratory

All sample bags were brought back to LBNL and compressed nitrogen was added to each to dilute the sample by a factor of 25. The dilution enabled sufficient sampling volume for a steady-state response by the analyzers, reduced the relative humidity of the sample (<30 percent) as required by the analyzers, and brought concentrations into the operational measurement range for the analyzers.

Measurement Results

As shown in Figure A-11, the bag sampled concentrations at multiple locations exhibit considerable variation. The concentrations at Locations 1 and 2 agree with the collocated real-time measurements, which adds validity to the bag sampling method we developed. Little temporal variability was observed over this sampling period, and there was no appreciable change in sampled concentration with the blowers on versus off. As such, this method assumes that the temporal variability within a bag sampling period (~1 hour) is small relative to the spatial variability and that the rate of emission to the atmosphere is heavily dominated by aeration periods.

Figure A-12: Measured Concentration Gradients across a Windrow

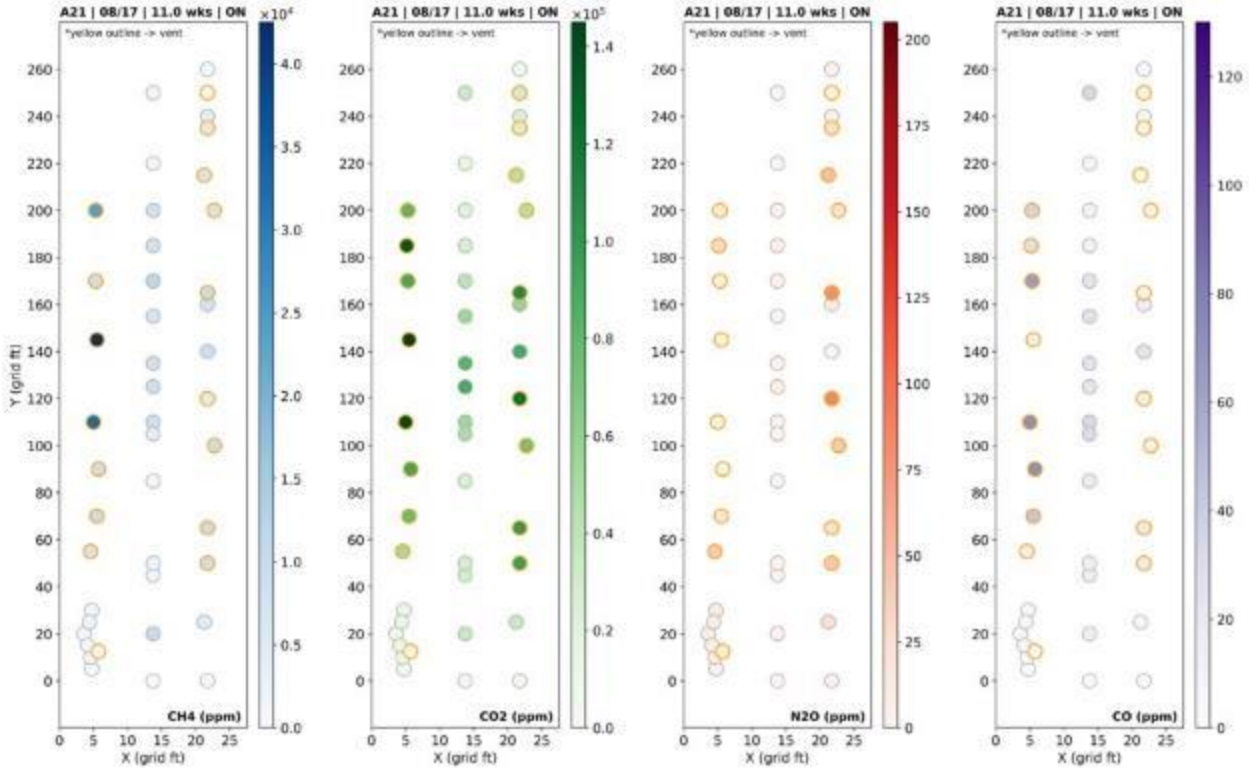

From left to right, measured concentrations of CH_4, CO_2, N_2O, and CO from bag sampling across the windrow surface are plotted. Samples were collected along the top and each side of the windrow (x-direction) and along the windrow length (y-direction). Pollutant concentrations are indicated by marker color, as identified in the corresponding scale bar.

Source: Lawrence Berkeley National Laboratory

Between 12-Jul-2018 and 26-Sep-2018, the project team measured emissions from five unique windrows. Three windrows were sampled more than once, at different periods in their composting cycles for a total of 9 samples. Figure A-12 shows an example of the density of bag sampling conducted across a given composting pile and the measured concentration gradients. Similar plots for each of the nine sampling periods are presented below (Figure A-13 through Figure A-20). Table A-7 summarizes the mean concentrations measured across each sampled windrow.

Figure A-13: Measured Concentration Gradients across Windrow A13 (0.1 Weeks)

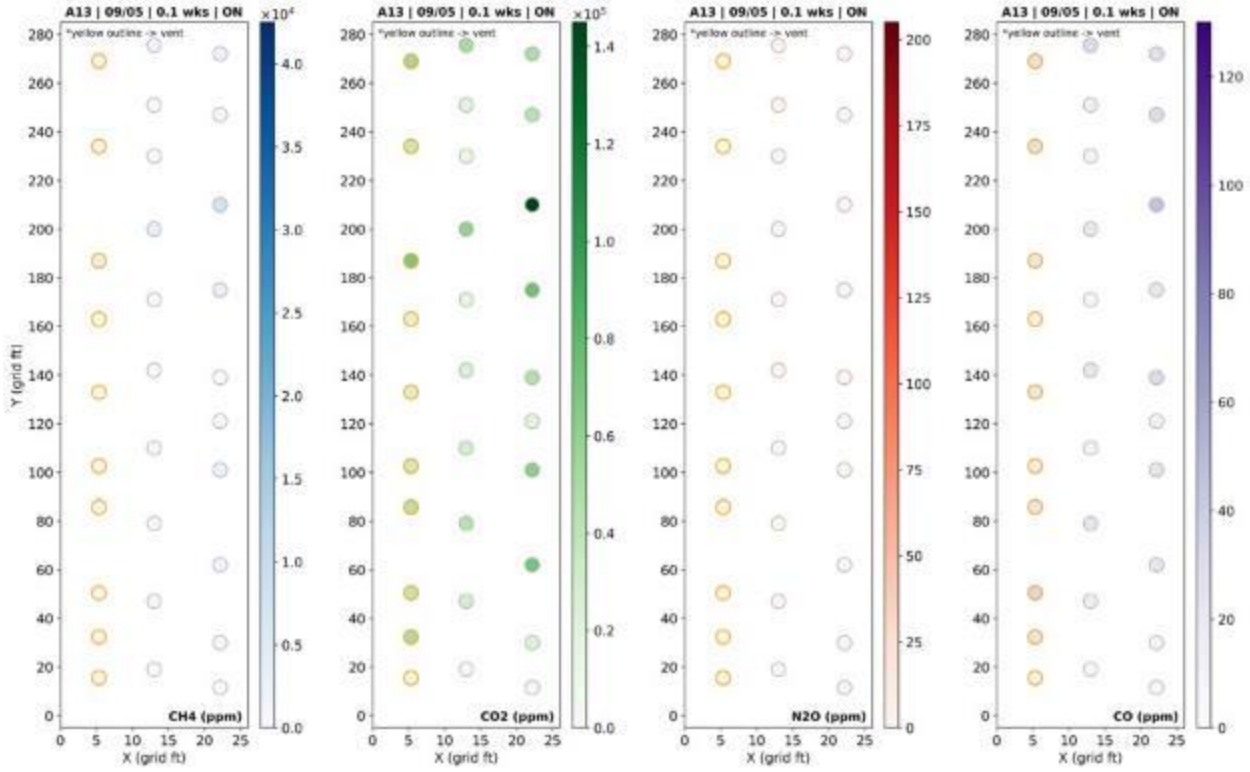

Source: Lawrence Berkeley National Laboratory

Figure A-14: Measured Concentration Gradients across Windrow B11 (0.6 Weeks)

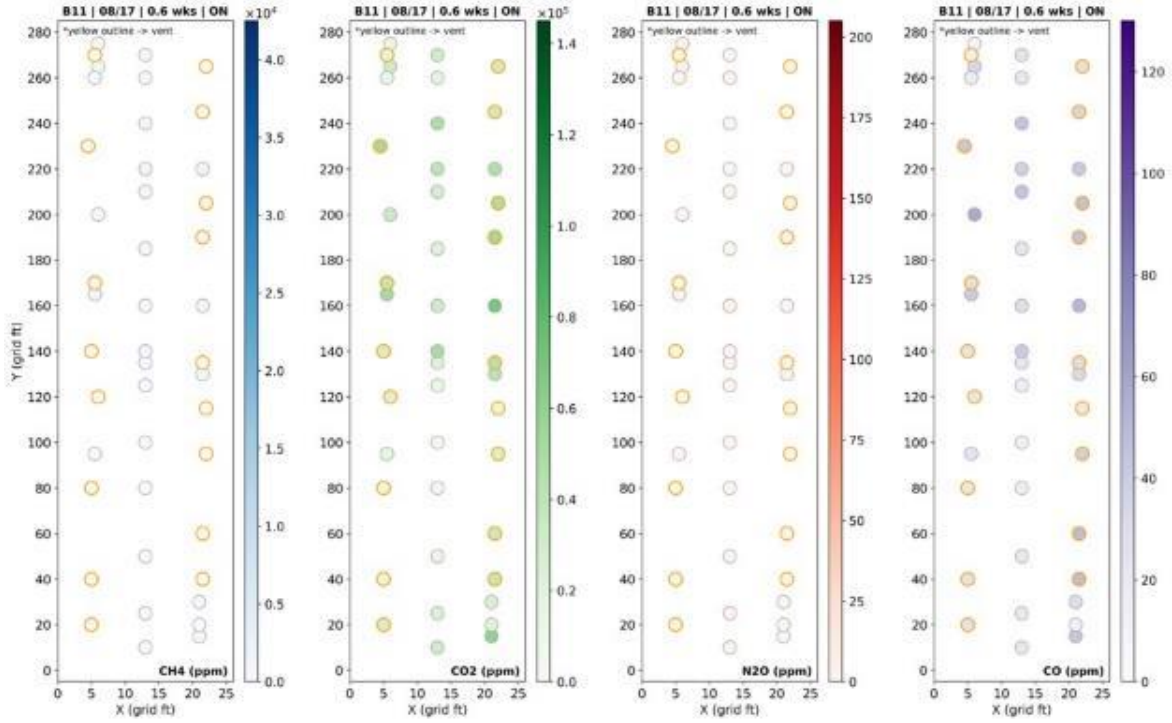

Source: Lawrence Berkeley National Laboratory

Figure A-15: Measured Concentration Gradients across Windrow B11 (3.3 Weeks)

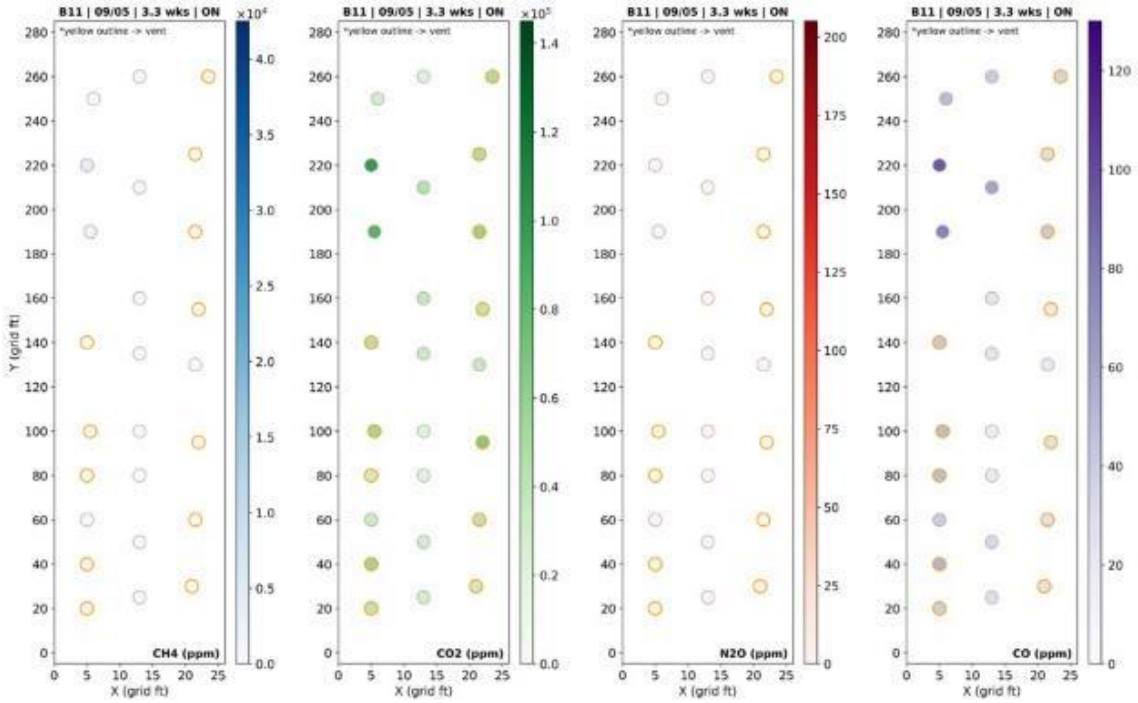

Source: Lawrence Berkeley National Laboratory

Figure A-16: Measured Concentration Gradients across Windrow B3 (5.1 Weeks)

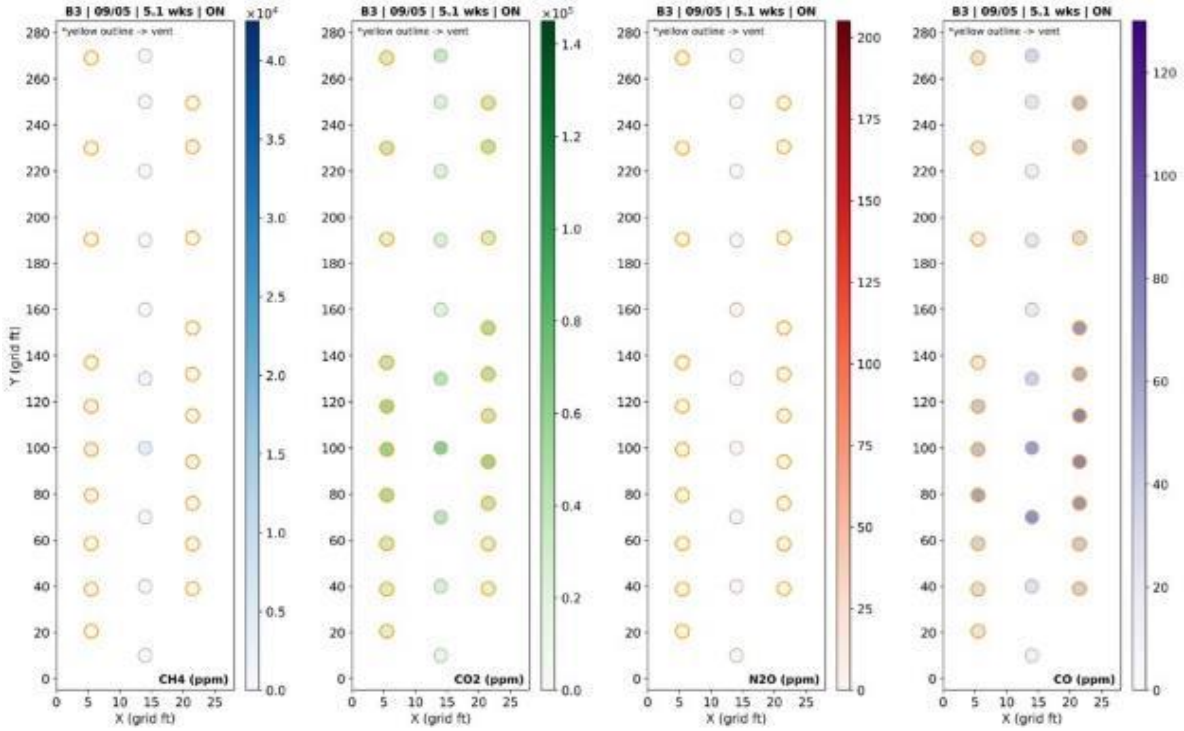

Source: Lawrence Berkeley National Laboratory

Figure A-17: Measured Concentration Gradients across Windrow A21 (5.9 Weeks)

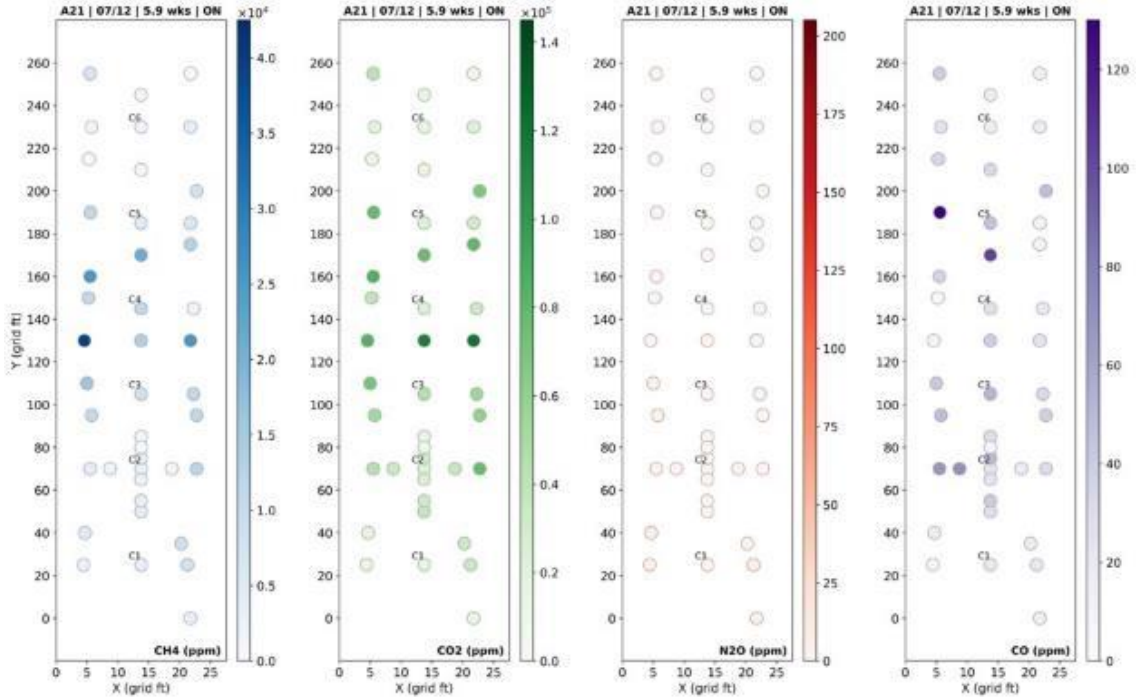

Source: Lawrence Berkeley National Laboratory

Figure A-18: Measured Concentration Gradients across Windrow B11 (6.3 Weeks)

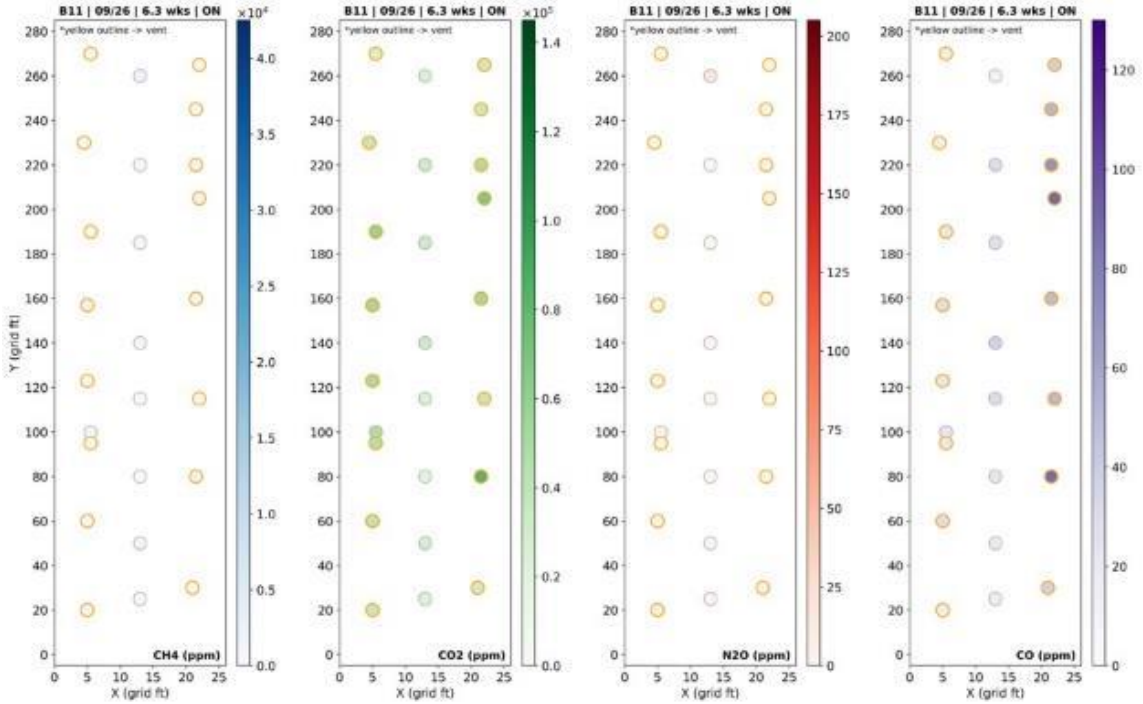

Source: Lawrence Berkeley National Laboratory

Figure A-19: Measured Concentration Gradients across Windrow B3 (8.1 Weeks)

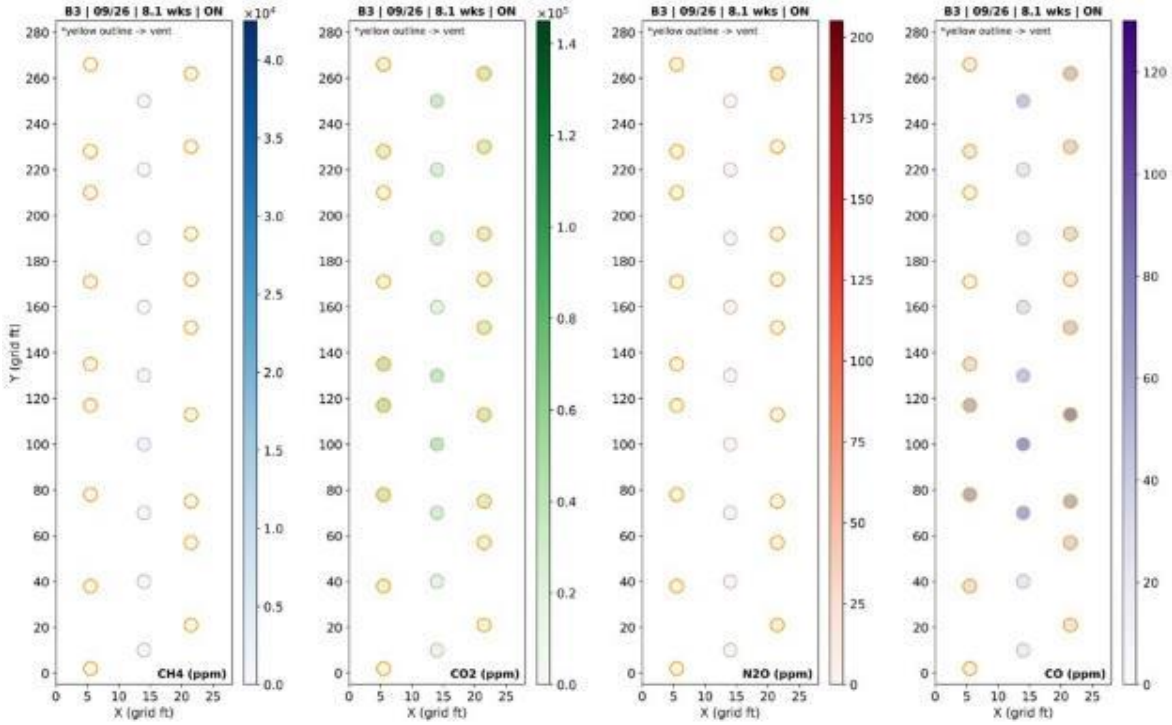

Source: Lawrence Berkeley National Laboratory

Figure A-20: Measured Concentration Gradients across Windrow D15 (13.1 Weeks)

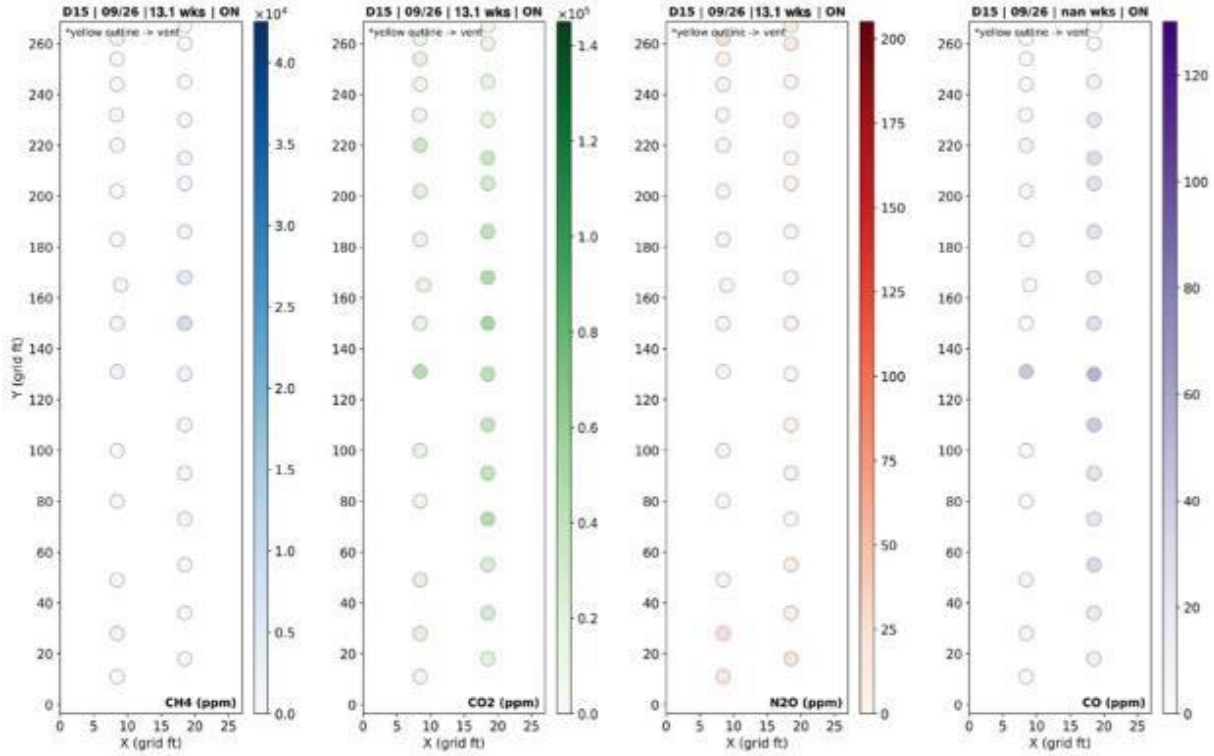

Source: Lawrence Berkeley National Laboratory

Table A-7: Summary of Windrow-Average Emitted Concentrations

Sampling Date	Pile ID	Pile Fill Date	Pile Age (Weeks)	CO_2 (ppm)	CH_4 (ppm)	N_2O (ppm)	NH_3 (ppm)	H_2S (ppm)
12-Jul	A21	01-Jun	5.9	39914 ± 6428	9268 ± 2754	1.81 ± 0.39	824 ± 155	15.6 ± 3.3
17-Aug	A21	01-Jun	11.0	53919 ± 11963	13506 ± 4206	14.22 ± 5.96	N/A	N/A
17-Aug	B11	13-Au	0.6	29586 ± 4965	750 ± 161	0.44 ± 0.07	N/A	N/A
05-Sep	B11	13-Aug	3.3	42842 ± 7178	923 ± 325	0.52 ± 0.05	N/A	N/A
05-Sep	A13	04-Sep	0.1	40430 ± 9997	1485 ± 533	0.77 ± 0.18	N/A	N/A
05-Sep	B3	31-Jul	5.1	35718 ± 4711	1148 ± 306	0.45 ± 0.02	N/A	N/A
26-Sep	B11	13-Aug	6.3	38934 ± 5523	1206 ± 203	0.94 ± 0.42	253 ± 85	8.0 ± 1.1
26-Sep	B3	31-Jul	8.1	24210 ± 3391	724 ± 154	1.91 ± 1.39	782 ± 120	20.4 ± 1
26-Sep	D15	26-Jun	13.1	25762 ± 5254	1528 ± 759	5.45 ± 2.7	502 ± 184	14.0 ± 3.1

Summary of measurements of emissions from composting windrows at Z-Best. All dates are from 2018. Average pollutant concentrations measured across each windrow at the specified sampling date are reported with 95 percent confidence intervals. Measurements of NH_3 and H_2S were not possible on all dates because of an issue with the analyzer; those sampling periods without NH_3 and H_2S measurements are marked as N/A.

Source: Lawrence Berkeley National Laboratory

Figure A-21 through Figure A-25 report the summary statistics of pollutant concentration distributions as box-and-whisker plots for all nine sampling periods.

Measured pollutant concentrations are variable both spatially across each sampled compost pile and between sampled windrows. Concentration gradients between pollutants tend to follow one another, as shown in Figure A-12. These differences in concentration both locally and between composting piles are likely due to variability in biological activity. This activity variance may be driven by compositional differences in the digestate material or by disparities in the amount of aeration actually provided across the windrow. A single windrow is filled by multiple truckloads of ZWEDC digestate material, which could result in different fill material along the pile. It is also possible that the pipes supplying air inside a windrow become clogged or plugged in certain areas.

The degree to which these differences in emitted concentrations are significant depends on the application of those measurements. For estimating an overall emission factor for the composting cycle, the variability in emitted concentration contributes to variability and uncertainty in the calculated emission factor; this variability can be important for subsequent life-cycle analyses or emission inventories. For studying odor and nuisance concerns, high concentrations are likely to incur greater odor concerns. In such analyses, quantifying regions of high concentration may be important, depending on the magnitude, compound, and emission rate. The analysis of odor is discussed in Part 2 of this chapter.

For all compounds measured, there is not a discernible trend in the concentrations of the emitted gases as a function of windrow age. One might expect to see a trend over the composting cycle that relates to biological activity. Although, there are noticeable differences shown in Figure A-21 through The horizontal axis shows unique identification names of the windrow sampled and the age of the windrow when samples were taken. Windrows sampled multiple times during the 14-week composting process are color code matched. Note that the y-axis is a log scale.

Source: Lawrence Berkeley National Laboratory

Figure A-25, it appears that the spatial variability is as significant, or more so, than any differences that might be attributable to the age of the composted material or stage of composting. There do seem to be some differences in emitted concentration that could be related to composition or windrow aeration; the distributions of CH_4, CO_2, and N_2O from windrow A-21 (shown in red) are shifted towards higher concentrations and/or have wider ranges than the other four piles, regardless of age.

Figure A-21: Distributions of Measured CH_4 Concentrations by Windrow

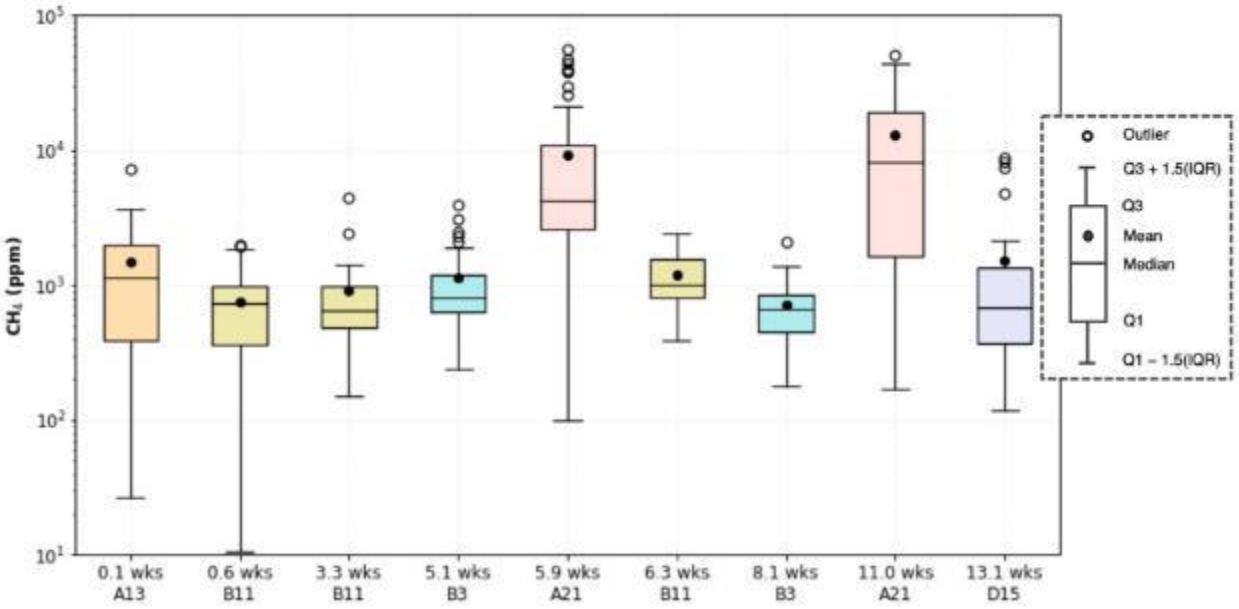

The horizontal axis shows unique identification names of the windrow sampled and the age of the windrow when samples were taken. Windrows sampled multiple times during the 14-week composting process are color code matched. Note that the y-axis is a log scale.

Source: Lawrence Berkeley National Laboratory

Figure A-22: Distributions of Measured CO_2 Concentrations by Windrow

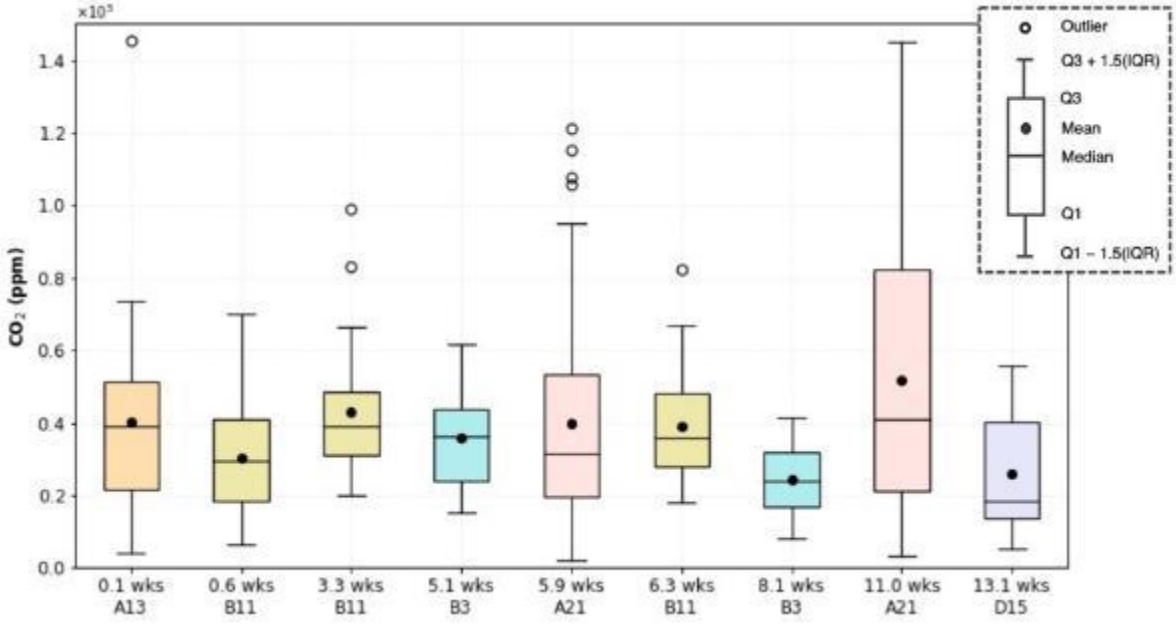

The horizontal axis shows unique identification names of the windrow sampled and the age of the windrow when samples were taken. Windrows sampled multiple times during the 14-week composting process are color code matched. Note that the y-axis is a log scale.

Source: Lawrence Berkeley National Laboratory

Figure A-23: Distributions of Measured N_2O Concentrations by Windrow

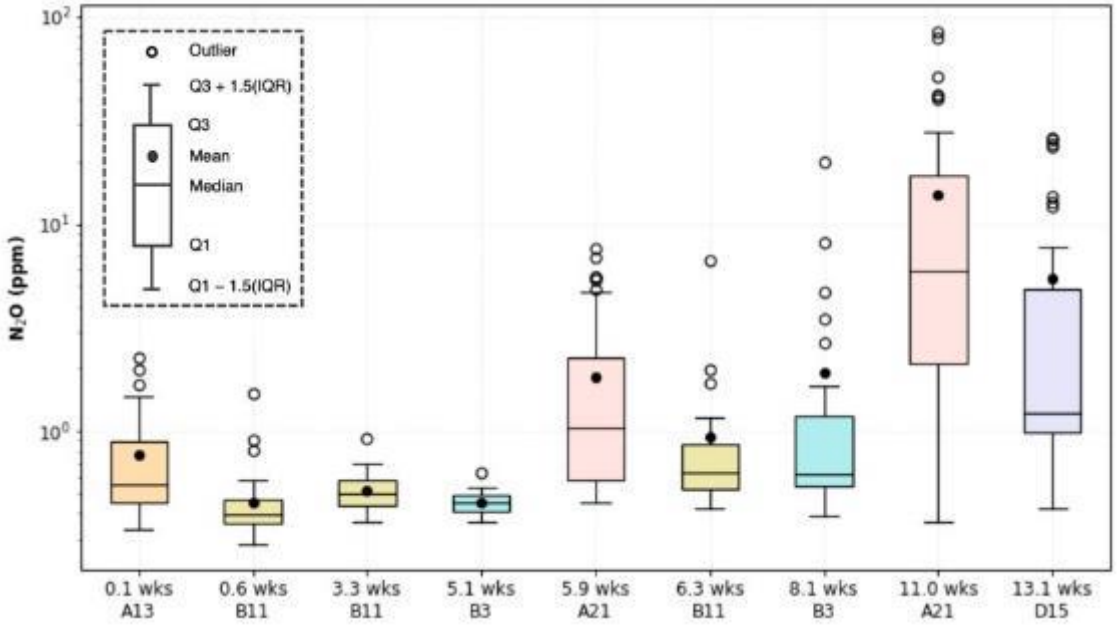

The horizontal axis shows unique identification names of the windrow sampled and the age of the windrow when samples were taken. Windrows sampled multiple times during the 14-week composting process are color code matched. Note that the y-axis is a log scale.

Source: Lawrence Berkeley National Laboratory

Figure A-24: Distributions of Measured CO Concentrations by Windrow

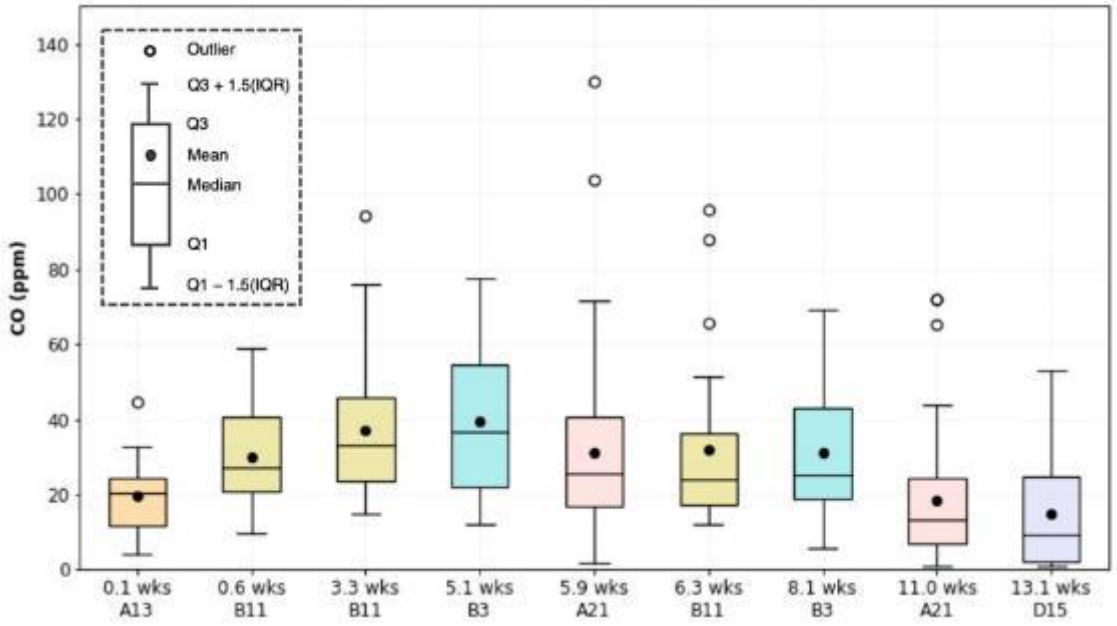

The horizontal axis shows unique identification names of the windrow sampled and the age of the windrow when samples were taken. Windrows sampled multiple times during the 14-week composting process are color code matched. Note that the y-axis is a log scale.

Source: Lawrence Berkeley National Laboratory

Figure A-25: Distributions of Measured NH_3 and H_2S Concentrations by Windrow

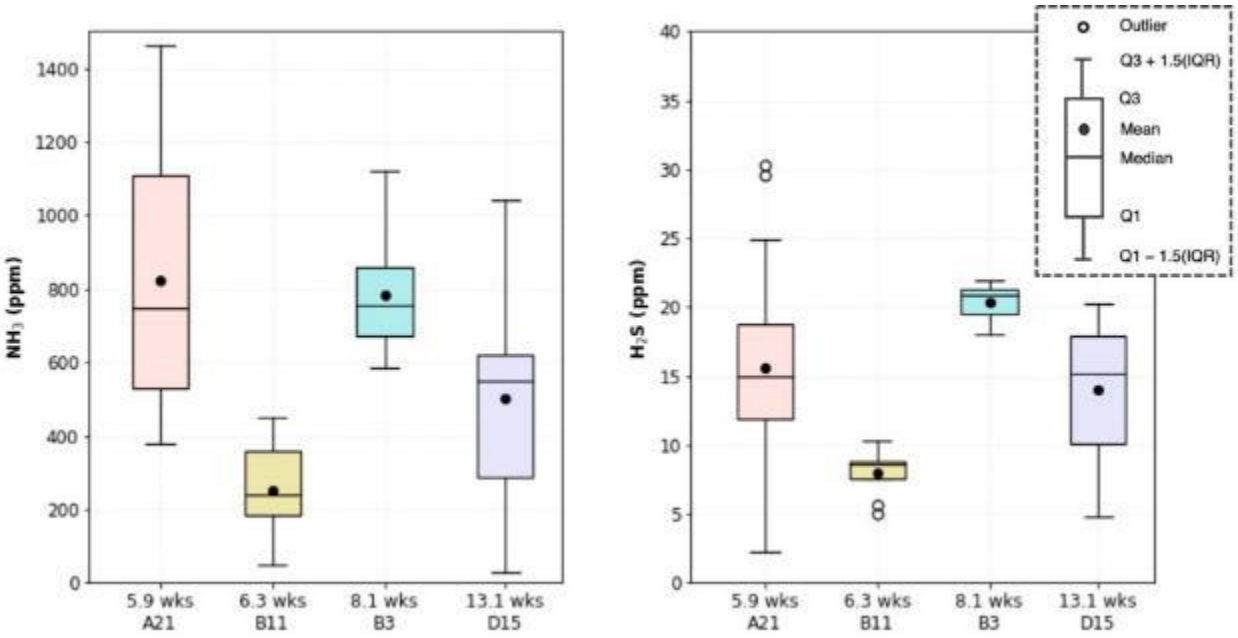

Distributions of measured NH_3 (left) and H_2S (right) concentrations. In both, the horizontal axis shows unique identification names of the windrow sampled and the age of the windrow when samples were taken. Windrows sampled multiple times during the 14-week composting process are color code matched.

Source: Lawrence Berkeley National Laboratory

Measured concentrations of NH_3 and H_2S show strong correlation to one another (R^2 = 0.80), as shown in Figure A-26. Emitted CO_2 and CH_4 concentrations are not as well correlated (R^2 = 0.39). These results suggest that the Z-Best facility provides aeration to the composting windrows at a rate sufficient to maintain required temperature and active biodegradation. However, the significant levels of emitted CH_4 concentrations over the full 14-week cycle indicate that some anaerobic activity persists.

Figure A-27 through The pile-average hourly mass emission rate is the product of the average emitted concentration (units of mass) measured across the composting windrow and the effective hourly volumetric aeration flow rate for that pile during the sampling window. The unique identification names of the sampled windrows are noted in the legend. Windrows sampled multiple times during the 14-week composting process are color code matched.

Source: Lawrence Berkeley National Laboratory

Figure A-29 show the pile-average hourly emission rates as a function of composting time in units of g pollutant emitted per hour per windrow. While there is no discernible trend in CO_2, CH_4, and CO as a function of windrow age, the emission rates of N_2O, NH_3, and H_2S appear to increase over the 14-week composting cycle. These trends are

not clear, though, and more work is needed to better characterize the relationship. Additional emission factors are summarized in Table A-8.

Given the above-described unknowns, the project team suggests future work focus on sampling the same windrow extensively for the entire 14-week composting cycle. Such an investigation could better characterize how composition, biological activity, aeration, and windrow age affect the spatiotemporal variability of emissions.

Figure A-26: Correlation of Emitted Concentrations

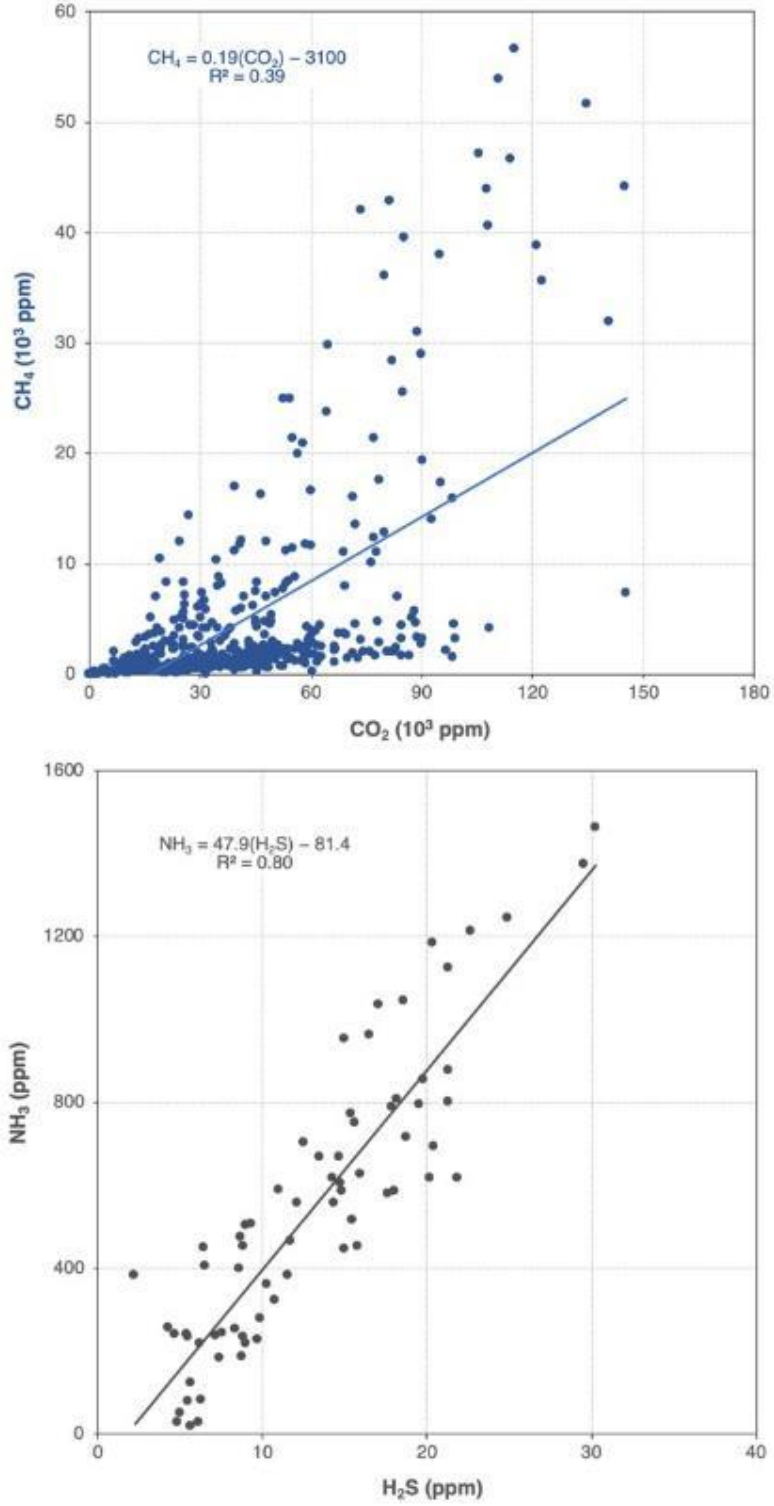

Individual sample bag concentrations from all composting windrow measurements, with best fit line and correlation noted.

Source: Lawrence Berkeley National Laboratory

Figure A-27: Hourly Emission Rates of CH_4 and CO_2 as a Function of Windrow Age

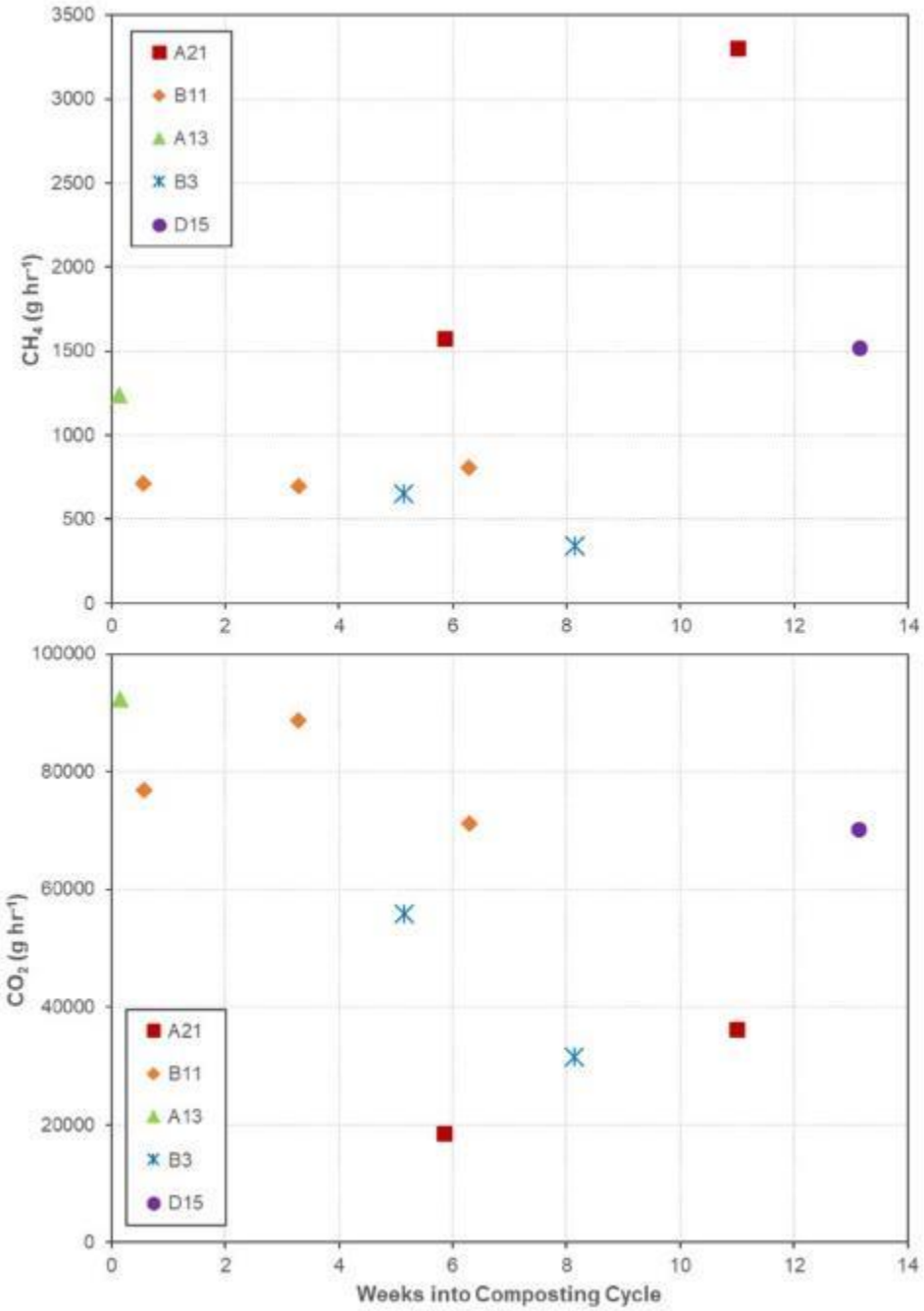

The pile-average hourly mass emission rate is the product of the average emitted concentration (units of mass) measured across the composting windrow and the effective hourly volumetric aeration flow rate for that pile during the sampling window. The unique identification names of the sampled windrows are noted in the legend. Windrows sampled multiple times during the 14-week composting process are color code matched.

Source: Lawrence Berkeley National Laboratory

Figure A-28: Hourly Emission Rates of N_2O and CO as a Function of Windrow Age

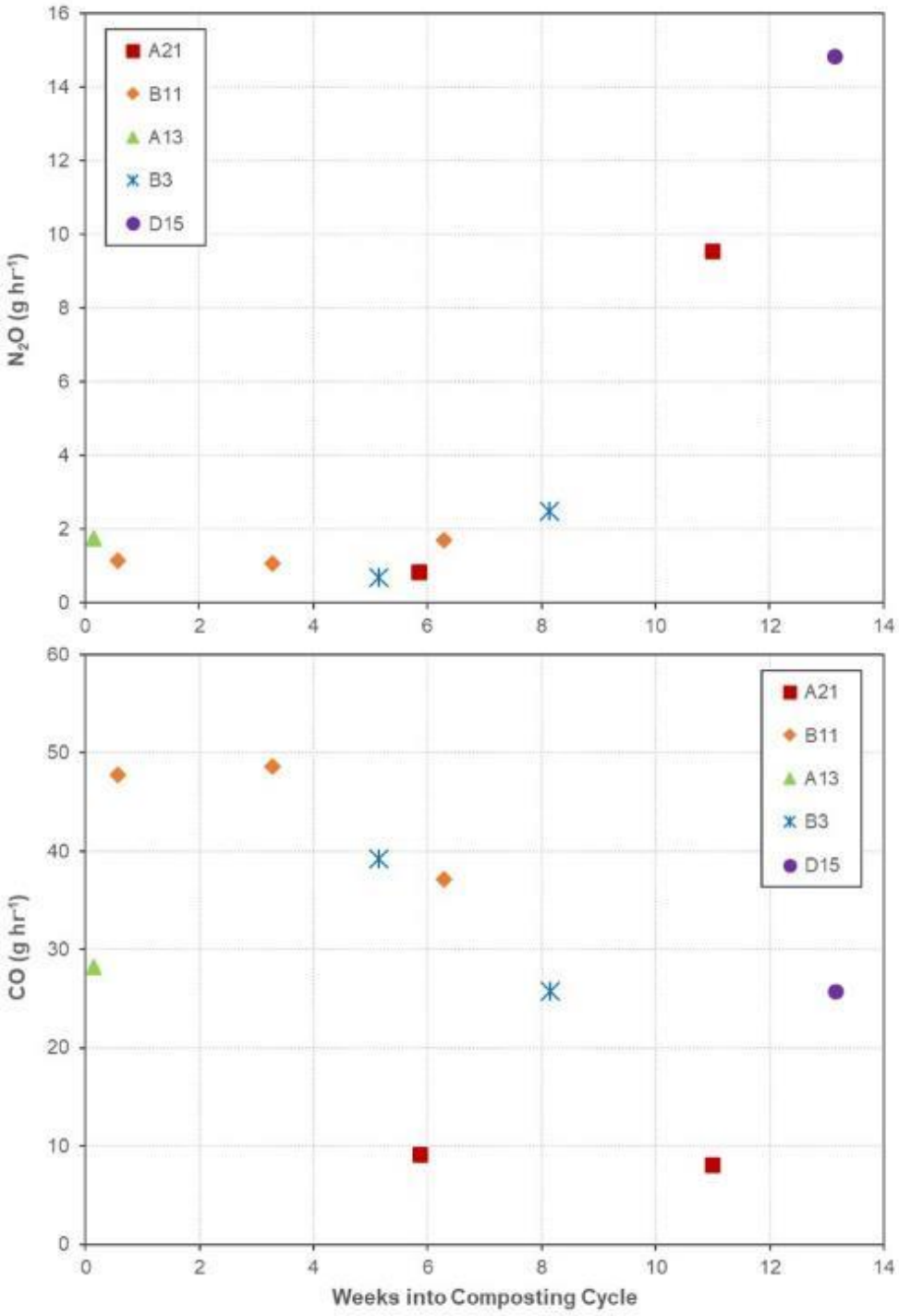

The pile-average hourly mass emission rate is the product of the average emitted concentration (units of mass) measured across the composting windrow and the effective hourly volumetric aeration flow rate for that pile during the sampling window. The unique identification names of the sampled windrows are noted in the legend. Windrows sampled multiple times during the 14-week composting process are color code matched.

Source: Lawrence Berkeley National Laboratory

Figure A-29: Hourly Emission Rates of NH_3 and H_2S as a Function of Windrow Age

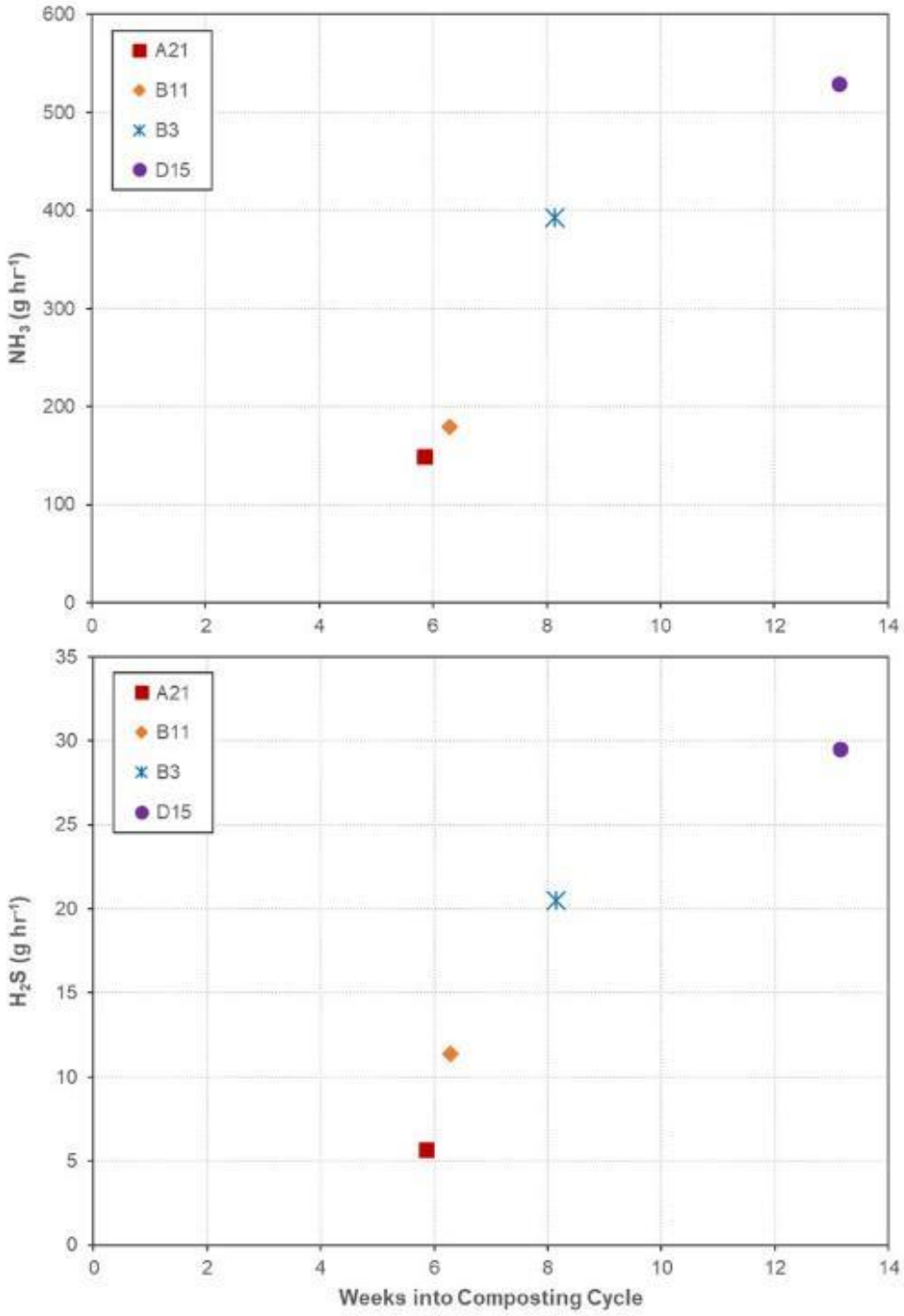

The pile-average hourly mass emission rate is the product of the average emitted concentration (units of mass) measured across the composting windrow and the effective hourly volumetric aeration flow rate for that pile during the sampling window. The unique identification names of the

sampled windrows are noted in the legend. Windrows sampled multiple times during the 14-week composting process are color code matched.

Source: Lawrence Berkeley National Laboratory

Table A-8: Average Emission Rates from the 14-Week Composting Cycle (g emitted per X)

Normalization Parameter, X	CH_4	CO_2	N_2O	CO	NH_3	H_2S
kg digestate composted	4.46E+00	2.23E+02	1.40E-02	1.11E-01	1.16E+00	6.22E-02
kg of inbound MSW received	3.35E+00	1.67E+02	1.05E-02	8.35E-02	8.71E-01	4.68E-02
kg of organic MSW digested	2.31E+00	1.15E+02	7.27E-03	5.76E-02	6.00E-01	3.22E-02

Source: Lawrence Berkeley National Laboratory

In-Situ Measurements at Z-Best: VOCs

Sampling Setup

Integrated samples of compost emissions were collected using five dilution chambers that were connected in series and distributed along the top centerline of the enclosed windrows at Z-Best. The goal of this approach was to capture a single stream of diluted emissions from the compost pile that represented the entire enclosed windrow. The dilution chambers were placed over holes cut into the composting bag, and all other accessible vent holes were sealed. A majority of exhaust flow from the pile was therefore released directly into the dilution chambers, assuming that the exhaust flow is mostly due to the aeration flow supplied to the pile. As with the above described sampling method, the two aeration blowers were set to a constant, effective flow rate during the sampling period.

As shown in Figure A-30, each dilution chamber was constructed from an inverted HDPE pail that was 12 inches in diameter and 10.25 inches in height. One-inch diameter dilution vent holes were drilled around the base of each chamber and a 100 ft^3 per minute blower was mounted to the top. The system operated at a slight vacuum (<15 Pa) to draw ambient dilution air into the chamber via the mounted blower without artificially increasing the emission rate from the compost pile. This diluted gas was exhausted through a 4-inch diameter duct that was fitted with an iris damper to adjust and continuously monitor total flow. A small sample was drawn continuously at 3.5–4 L per minute from the exhaust duct on each dilution chamber into a Teflon trunk line that was connected to a vacuum pump. Additional secondary dilution air was injected at a rate of 10 L per minute into the far end of the truck line using a portable zero-air

generator (PermaPure, model ZA-750-12). The combined flow of diluted sample air was drawn by vacuum through a Teflon manifold, where the integrated samples were collected (Figure A-31).

Figure A-30: Dilution Chamber for Sampling Compost VOC Emissions

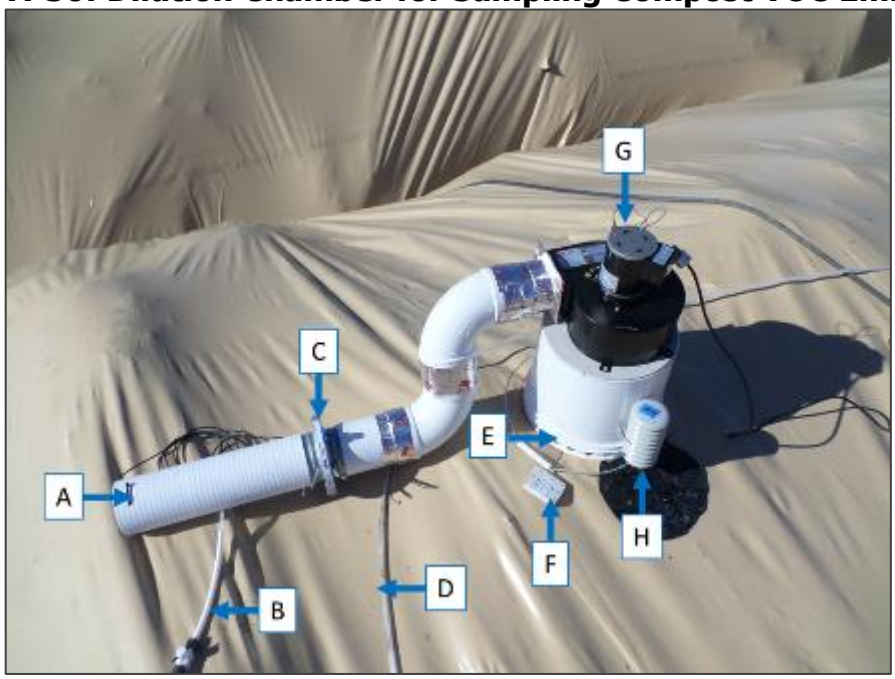

Dilution chamber showing: (A) exhaust duct with temperature and relative humidity sensor; (B) controlled flow sample line; (C) IRIS damper flow control and monitoring; (D) vacuum trunk line; (E) HDPE chamber with dilution air holes around base; (F) surface temperature probe; (G) 100 ft^3 per minute blower; and (H) ambient temperature and relative humidity sensor. The black disk shape underneath (H) is the underside of the flap from the hole cut in the compost bag; the vent is located under the dilution chamber.

Source: Lawrence Berkeley National Laboratory

Figure A-31: VOC Sample Collection Manifold

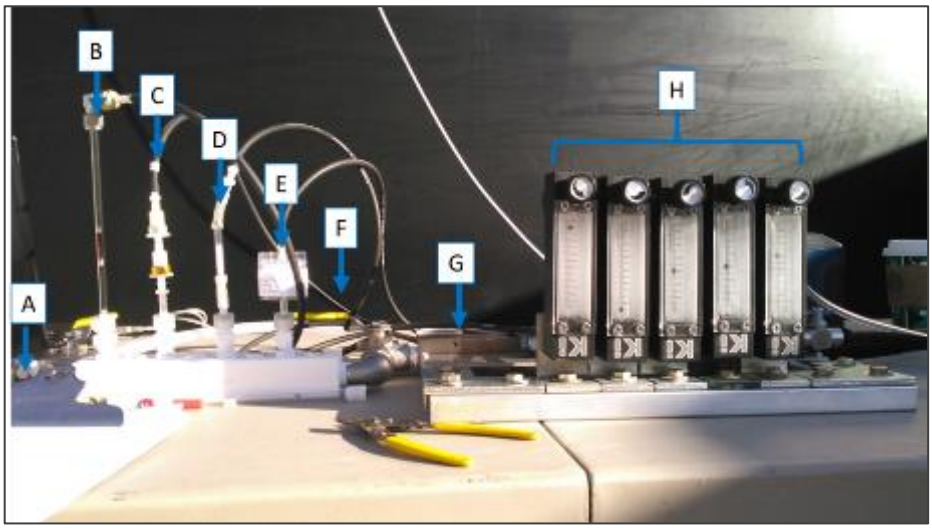

Integrated VOC sample collection, showing the Teflon manifold and: (A) trunk line from series of five dilution chambers; (B) VOC sample tube; (C) carbonyl sample cartridge; (D) acid sample tube; (E) volatile amine sample filter; (F) bypass line behind manifold used to direct flow around samples when switching sample tubes/cartridges; (G) vacuum line from manifold, and (H) bank of taper tube flow meters for sample collection.

Source: Lawrence Berkeley National Laboratory

The sampled stream of exhaust air from each dilution chamber included the gas directly emitted from the compost pile and ambient air that served as primary dilution. The primary dilution flow rate was not directly monitored but was instead calculated with a mass balance on measured water vapor concentration. The water balance was determined from continuous measurements of relative humidity and temperature in the ambient air and in the diluted emitted gas/ambient air mixture in the chamber exhaust duct, along with the temperature measured at the compost pile surface. This method assumes that the air from the compost pile is saturated at the measured temperature. Relative humidity is converted to water vapor concentration (McRae 1980).

Sample Collection

Ambient air concentrations were sampled alone through the dilution system prior to opening the holes under each dilution chamber. A set of two diluted emissions samples were collected at each composting windrow. Three different sample collection and analysis methods were used to quantify VOCs, volatile carbonyls, and volatile acids. All samples were collected using a vacuum pump, with air drawn through calibrated rotameters (taper-tube flow meters) at a nominal flow rate of 100 cm^3 per minute for VOCs and 1 L per minute for the carbonyls and acids (Figure A-31). Actual flow rates and sample durations were recorded on a tracking sheet for each sampling period to determine sample volumes.

Samples for VOC analysis were collected onto multibed glass thermal desorption tubes (Supelco, P/N 28286-U) custom-packed with a primary bed of Carbopack B sorbent (4

mm) and backed with a 2 mm section of Carbopack X. Prior to use, the sorbent tubes were conditioned at 345 °C for 30 minutes with a helium purge (30 cm^3 per minute) and then sealed in Teflon capped TDS3 storage containers (Sigma P/N 25045-U). Samples for volatile carbonyls (aldehydes and ketones) were collected onto single use silica gel cartridges coated with 2,4-dinitrophenylhydrazine (Waters Corp P/N WAT047205) with ozone scrubbers installed upstream (Waters Corp P/N WAT054420). Volatile acids were collected in the same way as the carbonyl samples but collected on single use silica gel sorbent tubes (SKC, P/N 22655). All samples were sealed after use and either analyzed the same day or stored on cold packs or in a freezer until analysis.

A fourth sample collection method was deployed to measure primary and secondary volatile amines using sulfuric acid impregnated filters followed by derivatization with dansyl chloride, as described by Fournier et al. (2008). Moderate to high levels of volatile amines were detected but could not be quantified because of unresolved sampling issues leading to high breakthrough.

Sample Analysis

Thermal Desorption Coupled with Gas Chromatography Mass Spectrometry (TD-GC/MS)

Before analysis, a gas-phase internal standard (120 ng of 1-bromo-4-fluorobenzene) was injected into each sorbent tube with a helium purge (30 cm^3 per minute) at room temperature for 4 minutes. Once prepared, the sorbent tubes were analyzed by gas chromatography (GC) and mass spectrometry (MS) using the following thermal desorption injection system: a ThermoDesorption Autosampler (Gerstel, model TDSA2), a thermal desorption oven (Gerstel, model TDS3) and a cryogenically cooled injection system (Gerstel, model CIS4). The cooled injection system contained a Tenax-TA©-packed glass injection liner (Gerstel, P/N 013247-005-00). The samples were desorbed at 50 cm^3 per minute (splitless), following a 60 °C per minute ramp from 25 °C (0.5 minute delay) to 330 °C with a 1 minute hold time. The cooled inlet was held at 1 °C and then heated after 0.1 minutes to 300 °C at a rate of 12 °C per second, followed by a 2-minute hold time. The GC was operated in the solvent vent mode with a splitless injection. Compounds were resolved on a GC (Agilent Technologies, Series 6890 Plus) equipped with a 30 meter by 0.25 mm diameter Restek Rxi-624Sil MS capillary column (P/N 13868) with 0.14 mm film thickness. The initial oven temperature was 1 °C, held for 2 minutes, then increased to 100 °C at 5 °C per minute (hold 2 minutes), increased to 140 °C at 3°C per minute, and finally increased to 300 °C at 10 °C per minute and held for 10 minutes. The helium flow through the column was held constant at 1.2 mL per minute (initial pressure 47 kilopascals, 39 cm per second). The resolved analytes were detected using 70 electron volts (eV) electron impact MS (Agilent Technologies, model 5973) operated in total ion current mode with target and qualifier ions specified for each target compound. The MS temperature settings were 240 °C, 230 °C, and 150 °C for the transfer line, MS source, and MS quad, respectively. The MS was operated in scan mode with a range of mass-to-charge ratios (m/z) of 34 to 450 m/z. Multipoint

calibrations were prepared from pure standards for all target VOCs. The response for each analyte was normalized to the internal standard response.

Low Molecular Weight Carbonyl Analysis by High Performance Liquid Chromatography (HPLC)

The DNPH-coated cartridges were extracted with 2 mL of high purity acetonitrile and analyzed for by HPLC. Target analytes were resolved on a 200 mm by 3.2 mm Allure AK column (Restek, P/N 9159523-700) and run with 60:40 acetonitrile/water mobile phase at 0.5 mL per minute with UV detection at 360 nm. Multipoint calibration curves were prepared from certified standard hydrazone derivatives of the target analytes (Sigma-Aldrich, CRM47651).

Measurement of Acetate by Ion Chromatography (IC)

The acid cartridges were extracted using 5 mL of 18 milliohm deionized water that was filtered through a 0.22 micron membrane. Extracts were analyzed by IC (Dionex, ICS 2000) equipped with an autosampler (Dionex, AS40), hydroxide ion generator (Dionex, EluGen cartridge P/N 058900), suppressor (Dionex, ASRS 300), and conductivity cell (Dionex, DS6). Samples were separated on a 4 mm by 200 mm AS11-HC column (Dionex, P/N 052960) at a flow rate of 1.0 mL per minute and 20 millimolar hydroxide ion concentration. The column was heated to 30 °C and a 25 microliter injection loop of was used to inject samples. A multipoint calibration was prepared from a 1.000 gram per liter chromatography standard.

Biofilters

Temporal Measurements of Emissions

Figure A-32: Temporal Variability of Biofilter Exhaust Concentrations

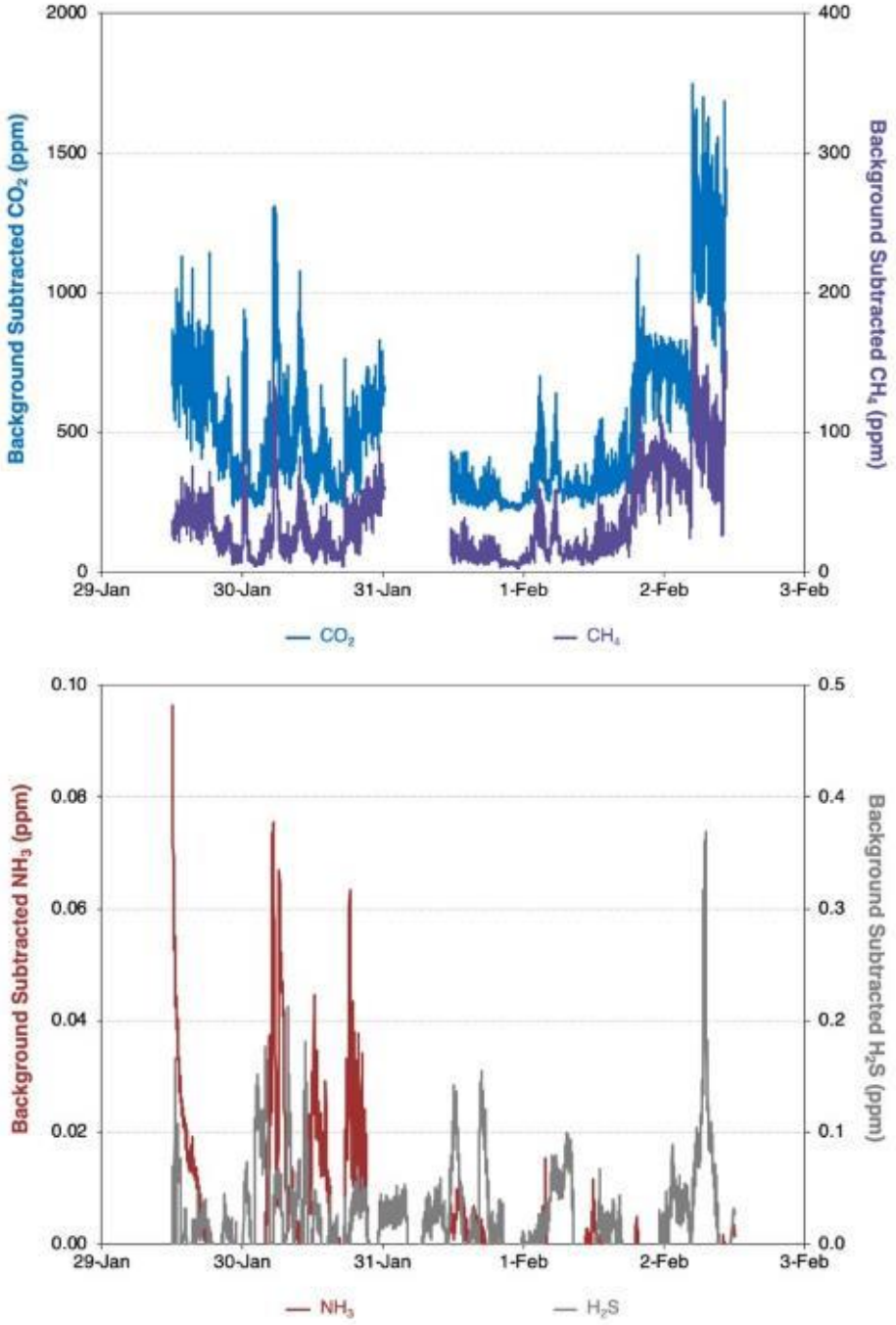

Time series of excess concentrations above background measured at a single location on the surface of a biofilter. Note, these measurements were not made over the same time period shown in Figure A-33.

Source: Lawrence Berkeley National Laboratory

Figure A-33: Temporal Variability of Biofilter Inlet Concentrations

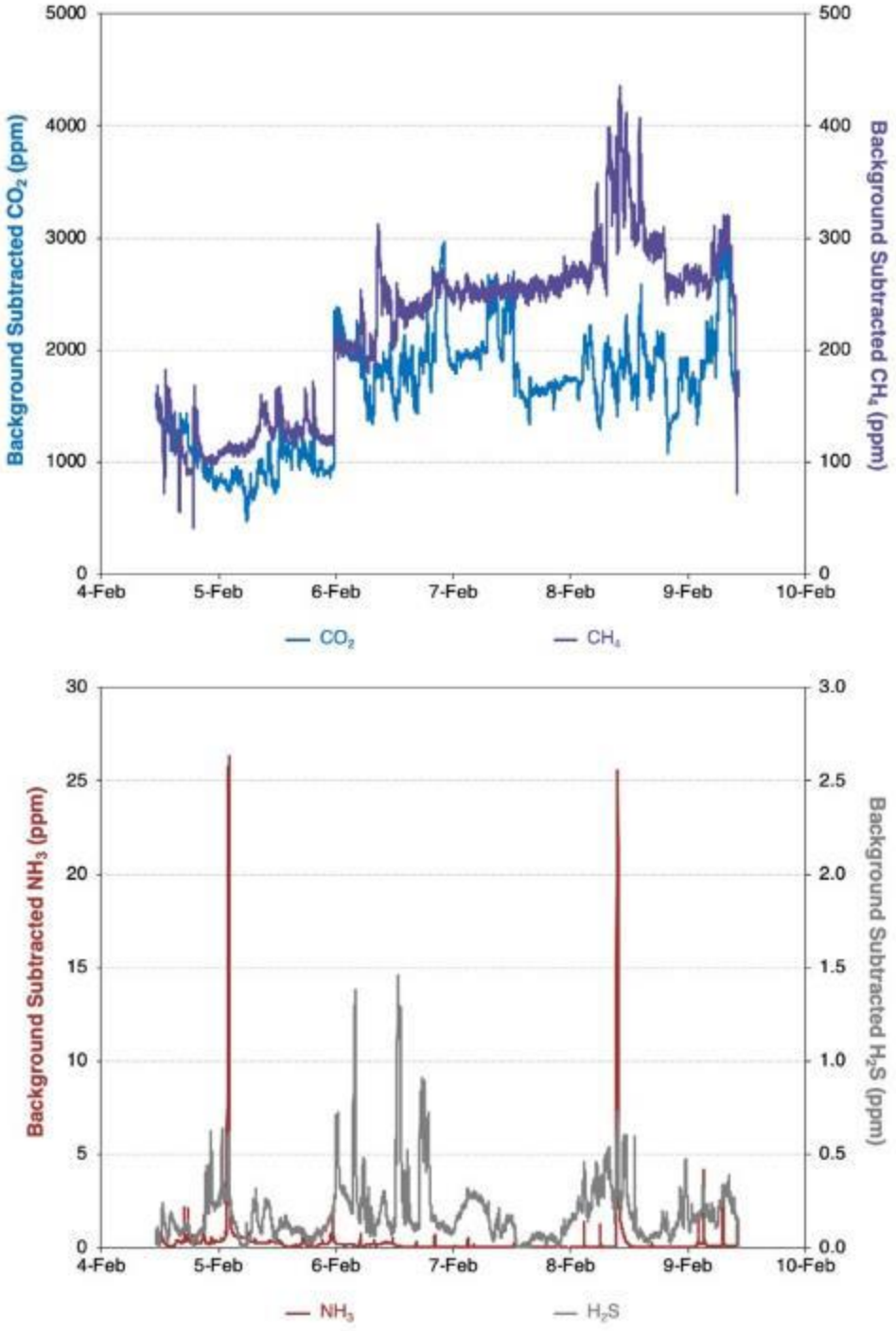

Time series of excess concentrations above background measured at the biofilter inlet, post-acid scrubber. Note, these measurements were not made over the same time period shown in Figure A-32.

Source: Lawrence Berkeley National Laboratory

Spot Measurements to Estimate Spatial Variability

Figure A-34: Biofilter Exhaust Concentrations of Methane

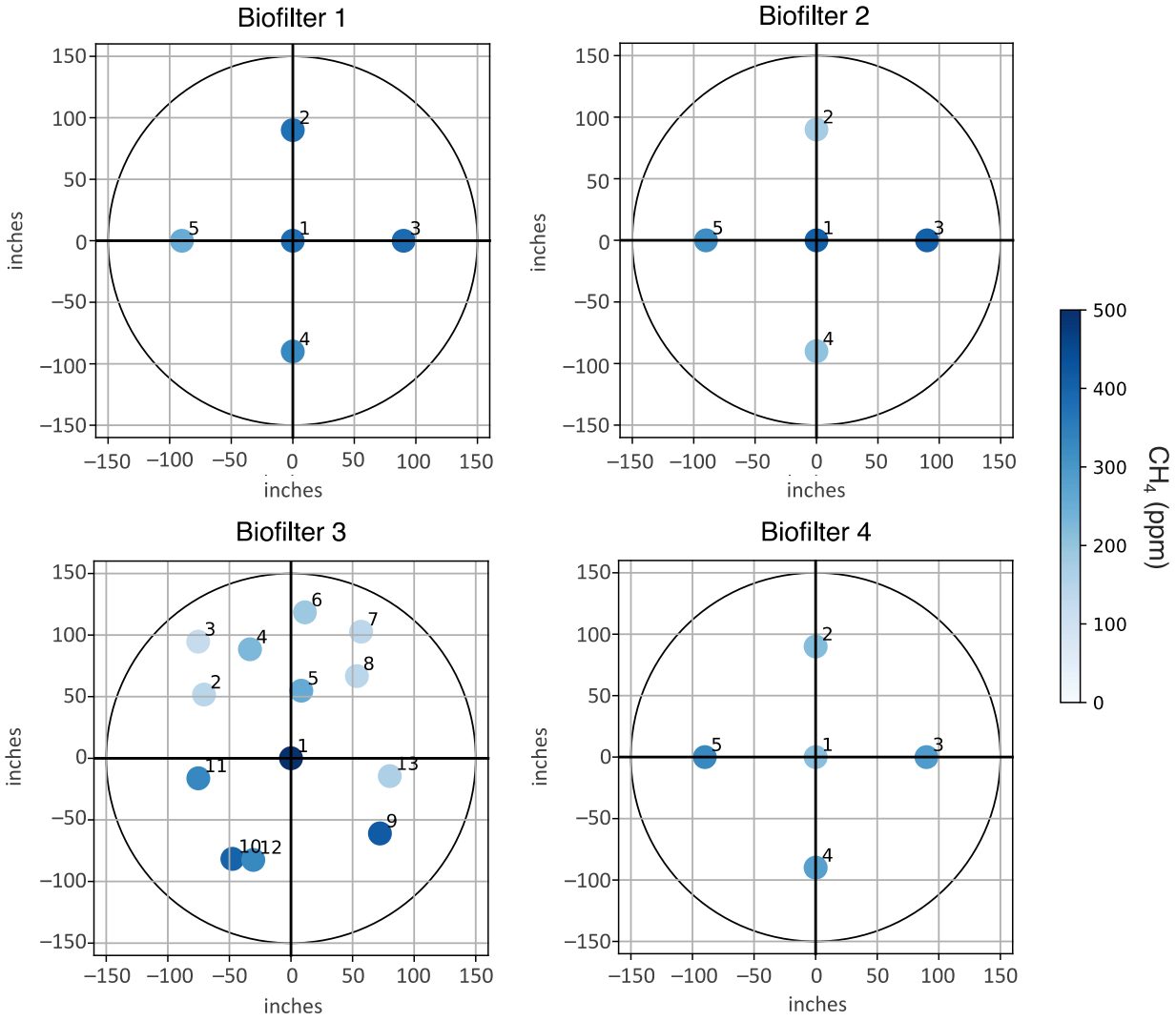

The axes show the relative locations of samples taken across each biofilter surface, which are 25 feet in diameter. The marker color represents the average exhaust concentration measured at that location, as indicated by the scale bar. Plotted concentrations have been corrected for the factor of 4.8 dilution but are not background subtracted. The numbers adjacent to each marker note the sample location number for that biofilter.

Source: Lawrence Berkeley National Laboratory

Figure A-35: Biofilter Exhaust Concentrations of Carbon Dioxide

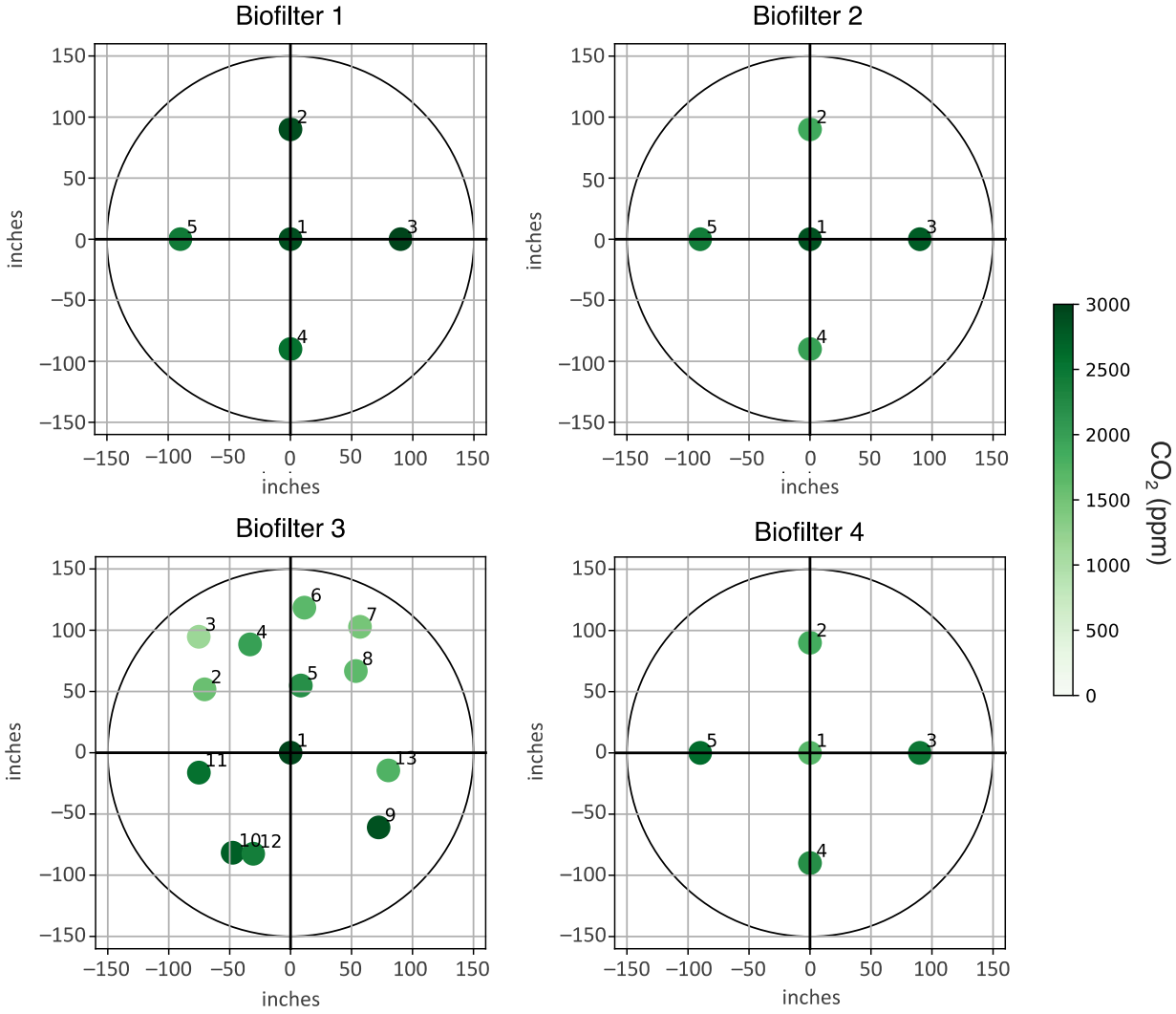

The axes show the relative locations of samples taken across each biofilter surface, which are 25 feet in diameter. The marker color represents the average exhaust concentration measured at that location, as indicated by the scale bar. Plotted concentrations have been corrected for the factor of 4.8 dilution but are not background subtracted. The numbers adjacent to each marker note the sample location number for that biofilter.

Source: Lawrence Berkeley National Laboratory

Figure A-36: Biofilter Exhaust Concentrations of Nitrous Oxide

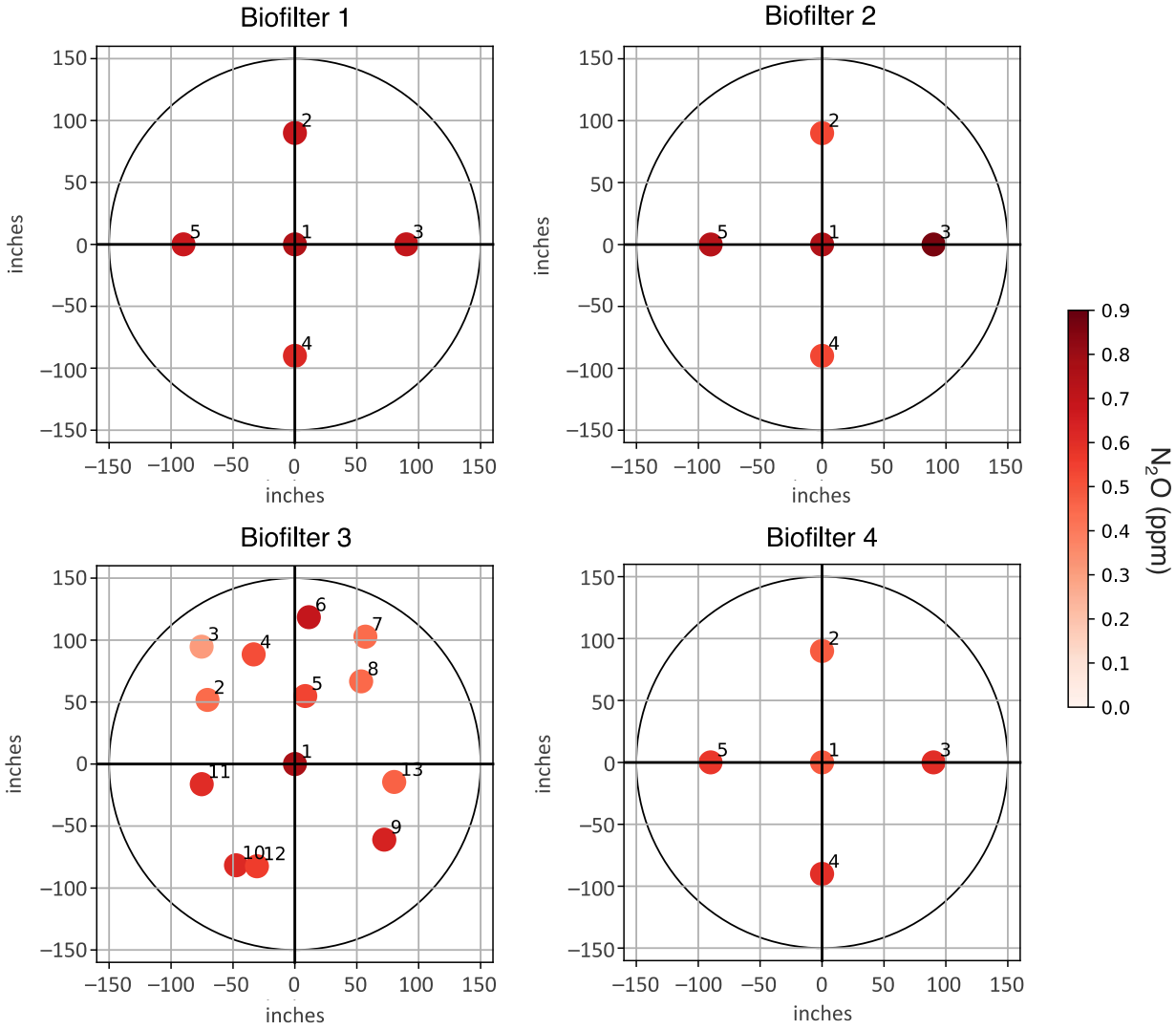

The axes show the relative locations of samples taken across each biofilter surface, which are 25 feet in diameter. The marker color represents the average exhaust concentration measured at that location, as indicated by the scale bar. Plotted concentrations have been corrected for the factor of 4.8 dilution but are not background subtracted. The numbers adjacent to each marker note the sample location number for that biofilter.

Source: Lawrence Berkeley National Laboratory

Figure A-37: Biofilter Exhaust Concentrations of Carbon Monoxide

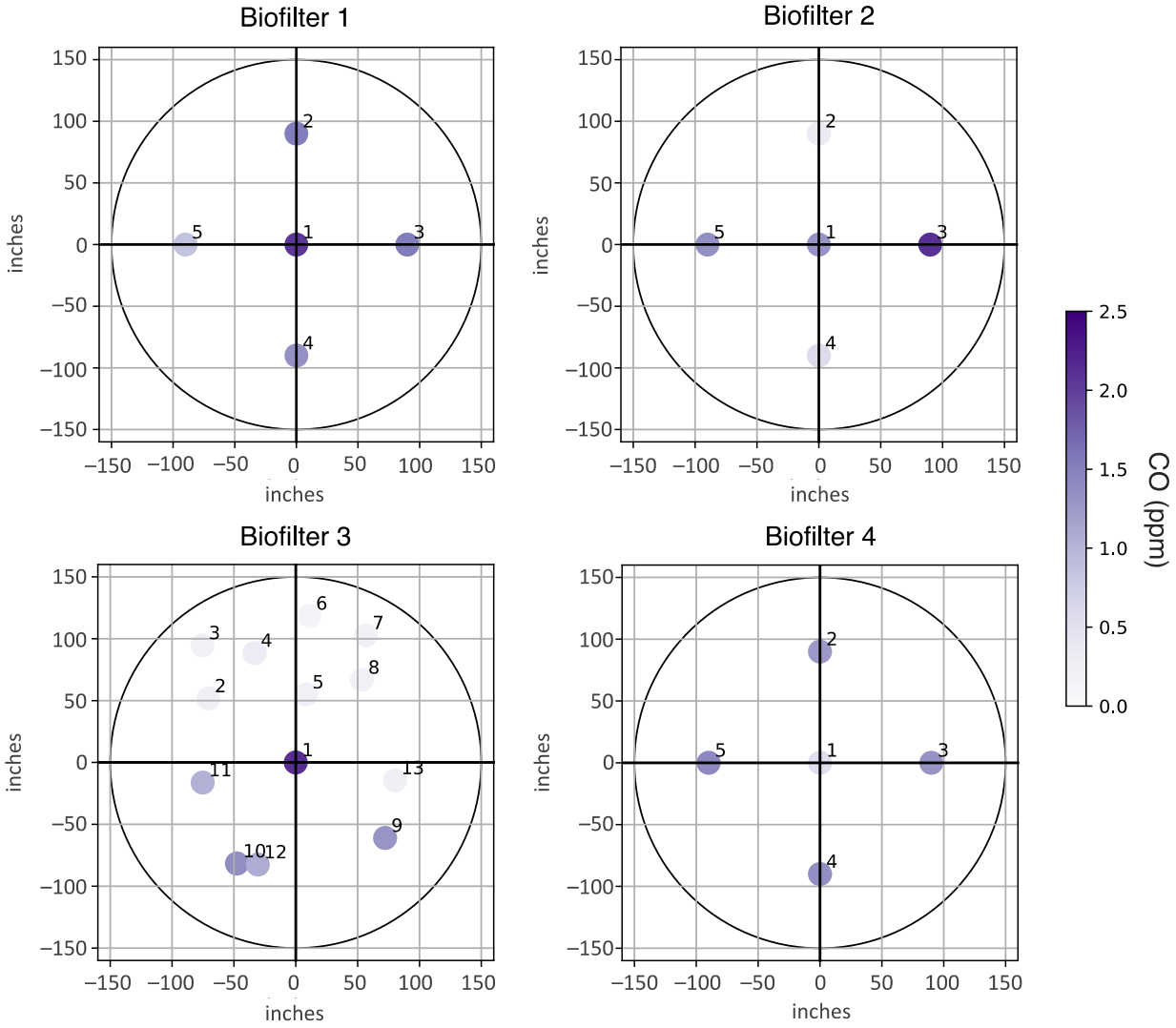

The axes show the relative locations of samples taken across each biofilter surface, which are 25 feet in diameter. The marker color represents the average exhaust concentration measured at that location, as indicated by the scale bar. Plotted concentrations have been corrected for the factor of 4.8 dilution but are not background subtracted. The numbers adjacent to each marker note the sample location number for that biofilter.

Source: Lawrence Berkeley National Laboratory

Figure A-38: Correlation of Emitted Biofilter Exhaust Concentrations

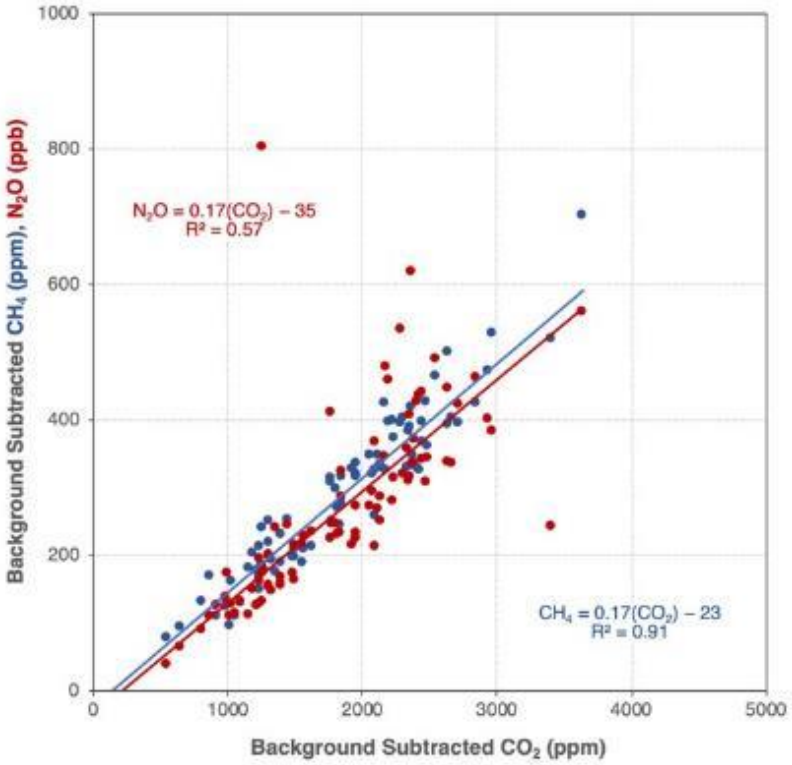

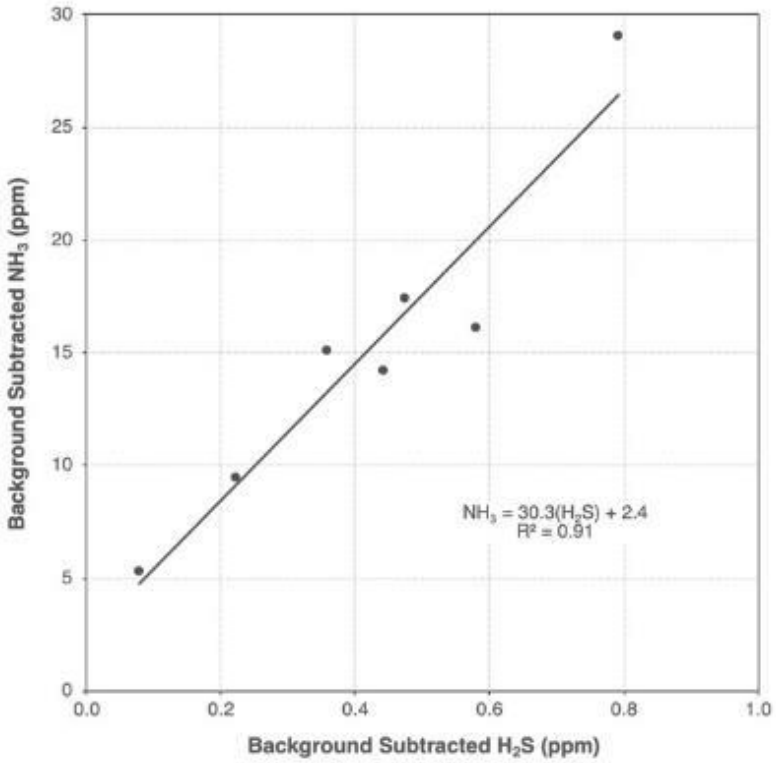

Individual bag sample concentrations measured across the four biofilter surfaces, background subtracted to show excess concentrations above ambient.

Source: Lawrence Berkeley National Laboratory

Estimation of Emission Rates from Biofilters

Table A-9 reports the mean concentration measured during each sampling period and across all sampling periods of spot measurements for each biofilter. To characterize the typical emitted concentration by the four biofilters, measured concentrations from all biofilters and sampling periods were combined and are summarized in Table A-10. The typical emitted concentration was used to estimate emission factors, which were calculated with the equations outlined above and are summarized in Table.

Table A-9: Mean Exhaust Concentrations by Biofilter and Sampling Period (ppm)

Biofilter	Sampling Period	CH_4	CO_2	N_2O	CO
1	1	329	2740	0.700	2.01
1	2	326	2770	0.663	1.35
1	3	362	2788	0.671	0.71
1	Overall	345	2778	0.688	1.48
2	1	300	2538	0.709	2.00
2	2	311	2366	0.637	0.93
2	3	300	2282	0.707	0.53
2	Overall	303	2395	0.684	1.16
3	1	349	2566	0.589	0.80
3	2	224	2058	0.545	1.06
3	3	242	1990	0.510	0.35
3	Overall	260	2114	0.545	0.70
4	1	279	2406	0.568	1.26
4	2	317	2650	0.626	1.96
4	3	265	2034	0.528	0.79
4	Overall	267	2183	0.553	1.19

Source: Lawrence Berkeley National Laboratory

Table A-10: Summary of Biofilter Exhaust Concentration Measurements for All Four Biofilters (ppm)

Statistic	CH_4	CO_2	N_2O	CO	NH_3	H_2S
Count	88	88	88	88	6	6
Mean	274	2220	0.575	0.98	13.01	0.400
Standard Deviation	128	763	0.183	0.82	4.62	0.183
Minimum	0.18	84	0.001	0.11	5.37	0.119
Maximum	704	4135	1.132	4.30	17.49	0.622
95 percent Confidence Interval	27	159	0.038	0.17	3.70	0.146

Source: Lawrence Berkeley National Laboratory

Table A-11: Average Emission Rates from Biofilters (g emitted per X)

Normalization Parameter, X	CH_4	CO_2	N_2O	CO	NH_3	H_2S
hour	9.52E+03	2.12E+05	5.49E+01	5.96E+01	4.80E+02	2.96E+01
kg of inbound MSW received	8.83E-01	1.97E+01	5.09E-03	5.53E-03	4.45E-02	2.75E-03
kg of organic MSW digested	1.28E+00	2.85E+01	7.39E-03	8.02E-03	6.46E-02	3.98E-03
m^3 of biogas produced	3.25E+01	7.23E+02	1.87E-01	2.03E-01	1.64E+00	1.01E-01

Emission rates reflect all four biofilters operating together.

Source: Lawrence Berkeley National Laboratory

VOC Sample Collection and Analysis

Integrated samples were collected using five surface flux chambers that were distributed across the surface of Biofilter 3 (Figure A-39). The chambers were run with vented tops, using dynamic air flow provided by the surface exhaust air from the biofilter itself. The exhaust air was assumed to be evenly distributed across the surface. The bottom edge of each flux chamber was pushed 2 to 5 cm into the biofilter surface, with the open area covering 0.05 m^2. Between the five chambers, 0.25 m^2 of total surface area was sampled. Air was metered from each chamber at approximately 3.5 L per minute into a Teflon trunk line for a total exhaust sample flow of 17.5 L per minute. An additional 10 L per minute of dry dilution air was injected into the far end of the trunk line using a portable zero-air generator (PermaPure, model ZA-750-12), resulting in a total sample flow of 27.5 L per minute. The diluted sample air was drawn through the same Teflon manifold described above (Figure A-31). This manifold allowed for simultaneous sample collection of VOCs, volatile carbonyls, volatile acids, and volatile amines. Samples of the supply air delivered biofilters from the building were simultaneously collected from the duct feeding the biofilters, at a point just after the acid scrubber. Supply air samples were collected using portable pumps (SKC, Universal), with flow calibration checked before and after each use. The three sample analysis methods that are described above in the Appendix section about composting VOC emissions were used to analyze these biofilter exhaust and supply air samples.

Figure A-39: Surface Flux Chamber for Sampling Biofilter VOC Emissions

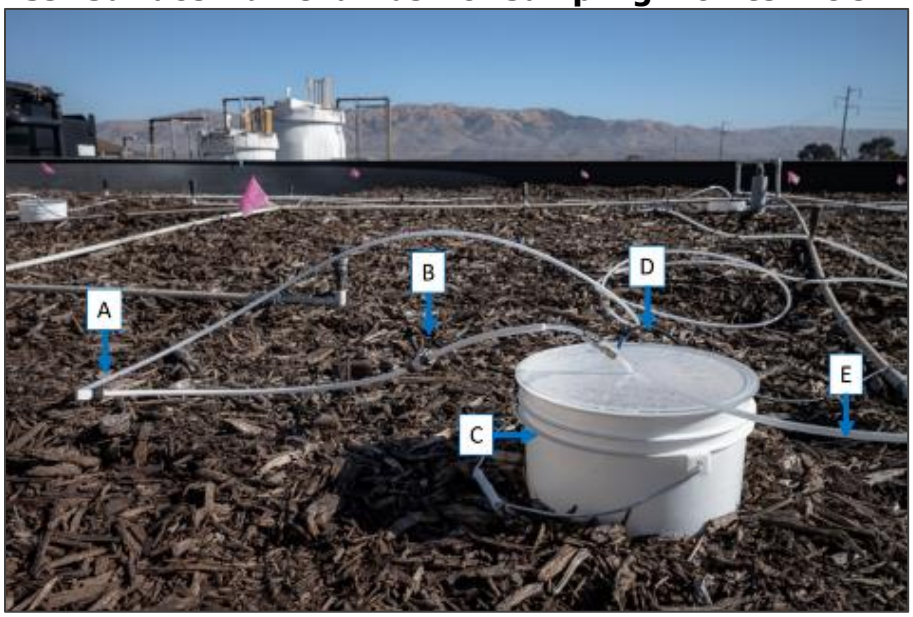

Surface flux sample collection system showing: (A) Teflon trunk line from flux chamber; (B) flow control valve for balancing sample rate; (C) one of five flux chambers set into surface; (D) test line to monitor pressure inside flux chamber; and (E) dry air dilution line from zero air generator. Note that the access hole in top of flux chamber is larger than sample line, allowing excess flow to vent to atmosphere during sampling.

Source: Lawrence Berkeley National Laboratory

Venting of Rich Biogas from Bladders

Results and Discussion

Table A-12: Summary of Venting Measured at PRV1

Event	Date	Duration (h)	Temp	Velocity	CO_2	Released Biogas (m^3)	Biogas EmissionRate (m^3 h^{-1})	CH_4 Emission Rate (lbs h^{-1})
1	2017-Sep-01	0.55	(a)	X	X	96	176	128
2	2017-Sep-01	0.94	(a)	X	X	173	185	134
3	2017-Sep-01	0.21	(a)	X	X	29	142	103
4	2017-Sep-02	0.34	(a)	X	X	25	76	55
5	2017-Sep-02	0.11	(a)	X	X	12	111	80
6	2018-Sep-08	0.08	(a)	X	X	10	120	86
7	2017-Oct-05	0.10	X	X	X	14	151	119
8	2017-Oct-07	0.29	X	X	X	44	150	114
9	2018-Oct-21	0.35	X	(a)	X			
10	2018-Oct-22	0.30	X	(a)	X			
11	2018-Jan-02	1.03	X	(a)	X			
12	2018-Jan-04	0.57	X	(a)	X			

(a) Gas temperature and velocity measurements were not available.

Source: Lawrence Berkeley National Laboratory

Figure A-40: Summary of Venting Measurements at PRV1

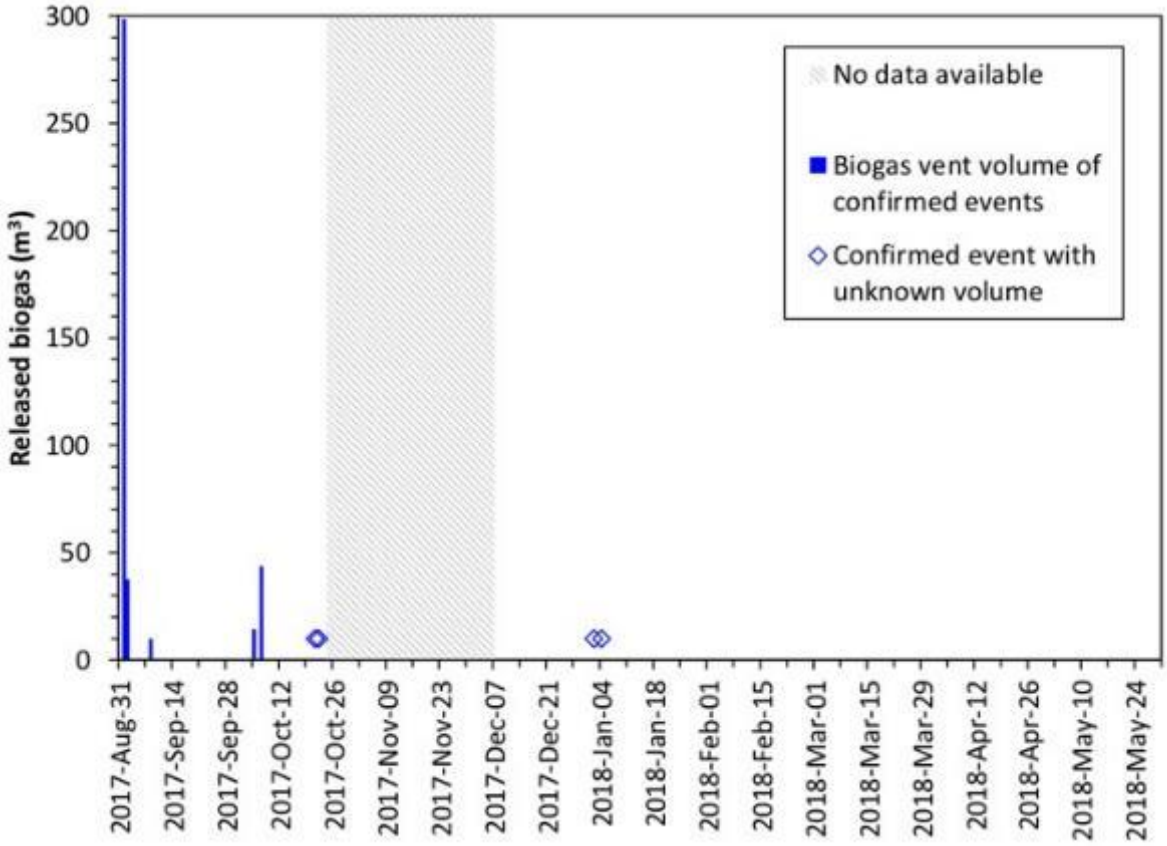

Volume of biogas released during each confirmed venting event; volume estimates were not available for four of the twelve events. Between 2017-Oct-25 and 2017-Dec-06, data was not available.

Source: Lawrence Berkeley National Laboratory

Conclusions

Table A-13: Summary of Emission Factors by Source (g emitted per kg MSW digested)

Source	CH_4	CO_2	N_2O	CO	NH_3	H_2S	NO_x	BC
Flare, Lean Biogas	N/A	1.44E+01	7.73E-06	6.03E-03	N/A	N/A	1.39E-02	-2.07E-06
Flare, Rich Biogas	N/A	2.23E+01	5.23E-05	1.48E-02	N/A	N/A	5.32E-03	1.40E-05

Source	CH_4	CO_2	N_2O	CO	NH_3	H_2S	NO_x	BC
CHPs, No SCR	2.24E-01	5.07E+01	-7.53E-05	1.02E-01	1.47E-04	1.83E-02	7.80E-02	N/A
CHPs, With SCR	N/A	5.07E+01	N/A	1.65E-02	N/A	1.85E-04	4.22E-03	N/A
Biofilters	1.28E+00	2.85E+01	7.39E-03	8.02E-03	6.46E-02	3.98E-03	N/A	N/A
Compost (14-Week Cycle)	3.35E+00	1.67E+02	1.05E-02	8.35E-02	8.71E-01	4.68E-02	N/A	N/A

Source: Lawrence Berkeley National Laboratory

Figure A-41: CO_2-Equivalent Emission Rates by Source (100-Year GWP)

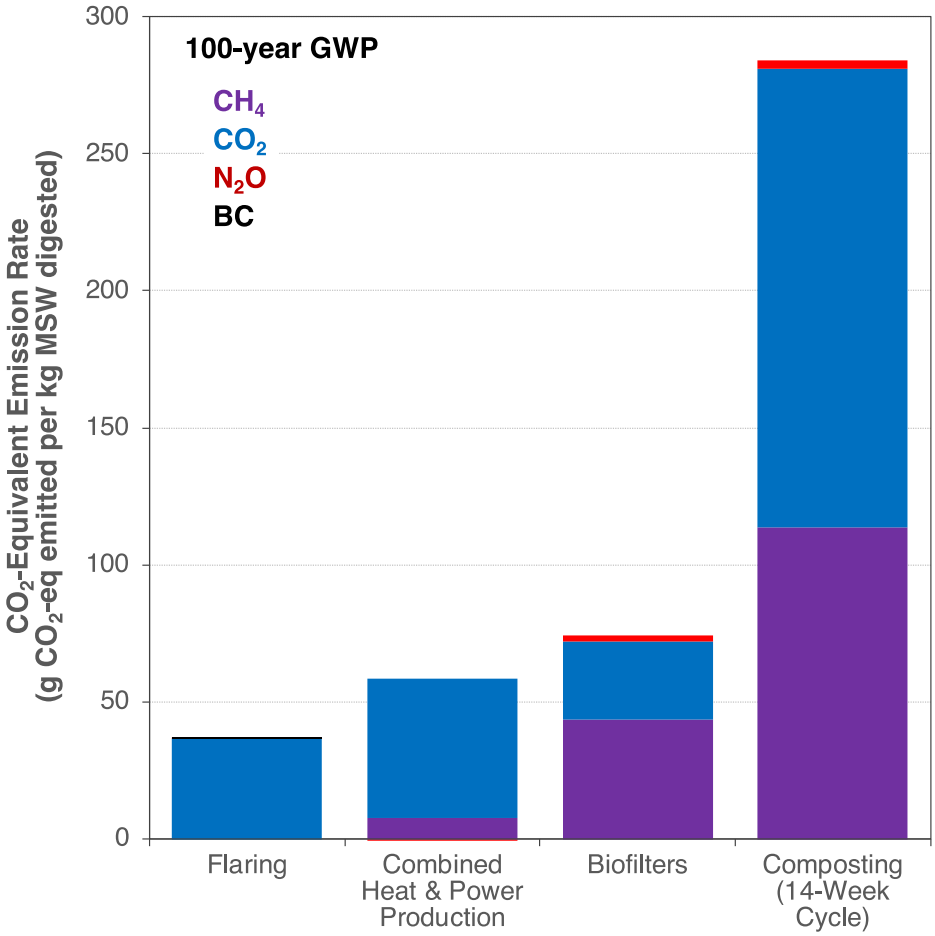

Average mass of equivalent CO_2 emitted per kg of MSW digested by each source, based on 100-year GWP values for CH_4, N_2O, and BC.

Source: Lawrence Berkeley National Laboratory

APPENDIX B:
Odor Management via Dispersion Modeling

Meteorological Data

We first analyze the meteorological data from the two facility-operated weather stations that are on or near ZWEDC to derive flow patterns. Due to the data quality problems, we determine the ZWEDC onsite meteorology data is not suited for deriving local circulation patterns and for subsequent odor dispersion modeling.

ZWEDC operates its own meteorological station to collect wind speed, wind direction, and air temperature. Data quality is found to vary significantly as indicated by the reception rate of the device (Figure B-1 blue color). More than half of the data has less than 50 percent of the reception rate recorded by the measurement device (indicated by the "ISS.Recept" variable). Windrose plots with wind data of different quality (cutoff values of ISS.Recep = 50 percent and 80 percent) showed different wind patterns in fall and winter (Figure B-2) over the business hours (8am to 5pm). Business hours were chosen because the odor complaints came from the nearby wastewater treatment plant when workers were present, according to official records. Summer time wind patterns are less sensitive to the reception rate and are more consistent across data quality categories (Figure B-2). In comparison, the meteorological data collected at the nearby facility, Republic Service at Newby Island (~3 km away, Figure B-1 red) was of higher quality because the majority of the data had a 100 percent reception rate. The predominant wind patterns of the two sites differ significantly (Figure B-1) due to their different locations to the nearby marshland. Examining the summer time data when wind patterns at ZWEDC are more consistent, regardless of data quality, we see that the predominant winds at Republic Services are more from the west instead of from the north as the ZWEDC patterns (Figure B-3). Wind measurements at Republic Services cannot be used to replace ZWEDC onsite data for the subsequent meteorological analysis and dispersion modeling.

Figure B-1: Data Quality of Onsite Meteorology Measurements

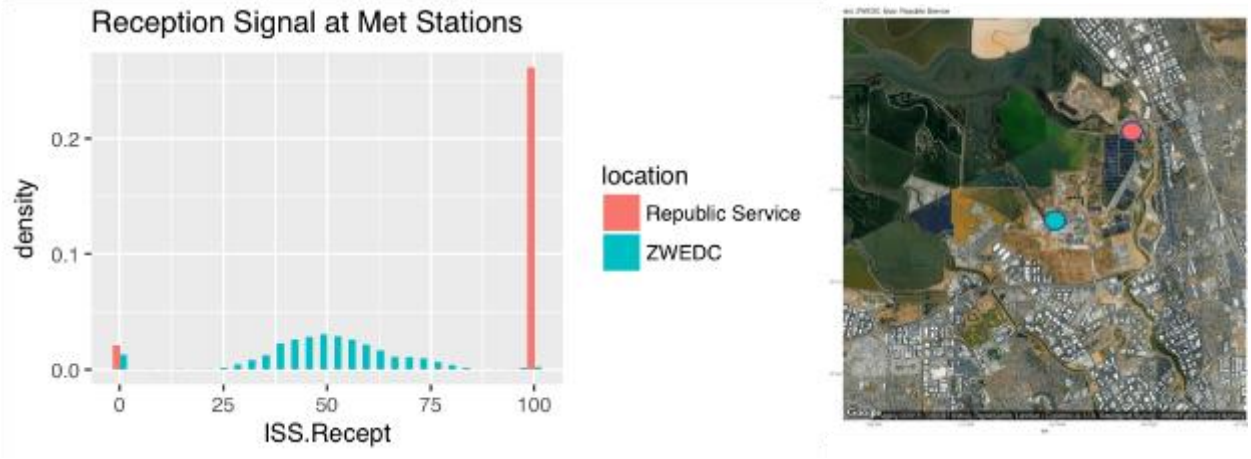

Data quality = ISS.Recept.

Source: Lawrence Berkeley National Laboratory

Figure B-2: Daytime Wind Roses at ZWEDC by Data Quality

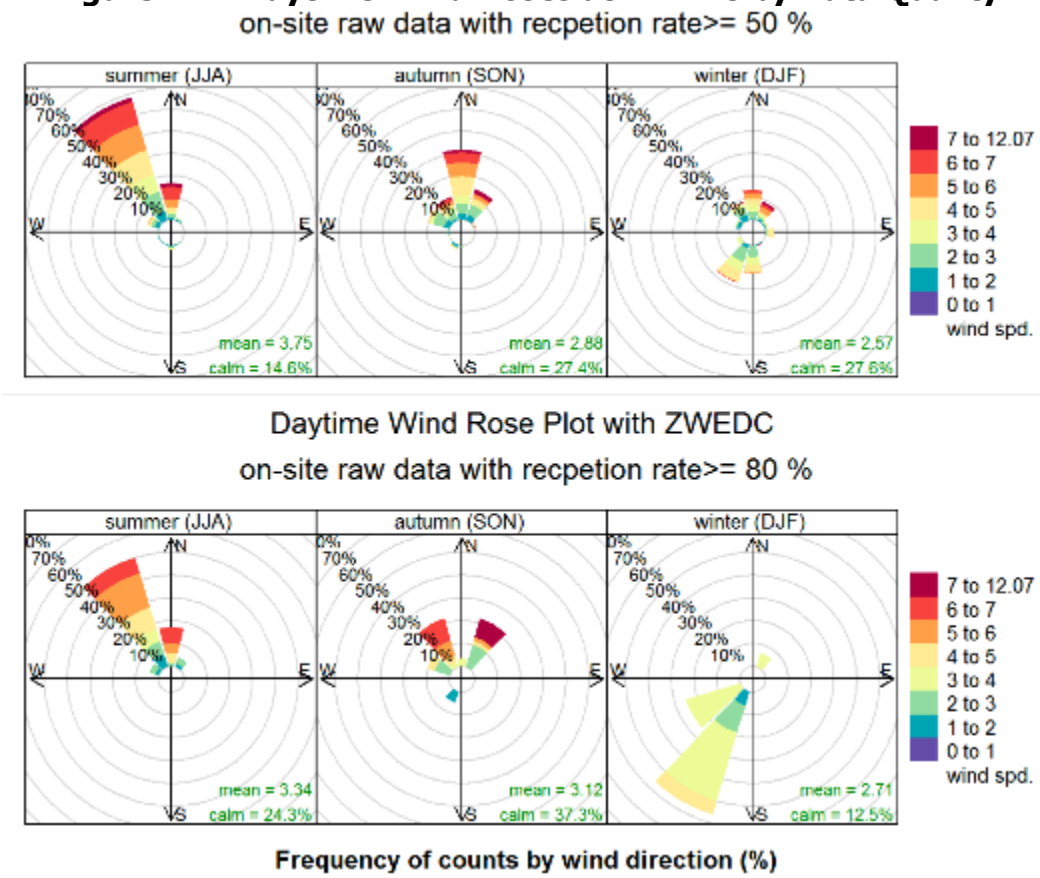

Source: Lawrence Berkeley National Laboratory

Figure B-3: Wind patterns at Republic and ZWEDC

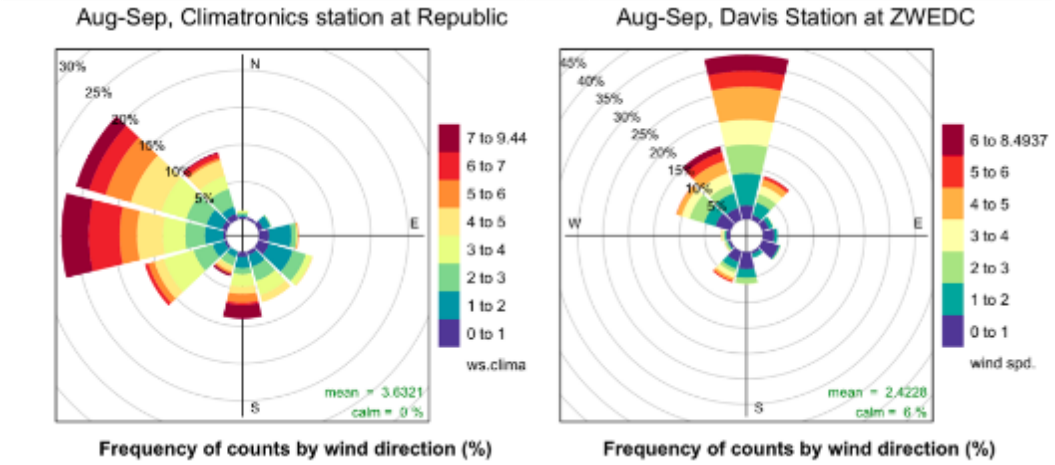

Source: Lawrence Berkeley National Laboratory

Table B-1: Weather Stations around ZWEDC

Station	USAF-WBAN	Latitude	Longitude	Start Year	End Year	Distance from ZWEDC (km)	Direction from ZWEDC
San Carlos	724938-99999	37.517	-122.250	2000	2014	27.78	NW
Redwood City	994041-99999	37.507	-122.200	2005	2014	23.46	NW
Palo Alto Airport	724937-99999	37.467	-122.117	2000	2014	14.79	NW
Mountain View	745090-23244	37.406	-122.408	2000	2014	9.114	WSW
San José Airport	724945-23293	37.359	-121.924	2000	2014	8.674	SSE
Reid-Hillview Airport	724946-99999	37.333	-121.817	2000	2014	16.32	SE
Hayward Airport	724935-93228	37.659	-122.120	2000	2014	28.51	NNW

Source: Lawrence Berkeley National Laboratory

Figure B-4: Diurnal Variation of Wind Speed by Season

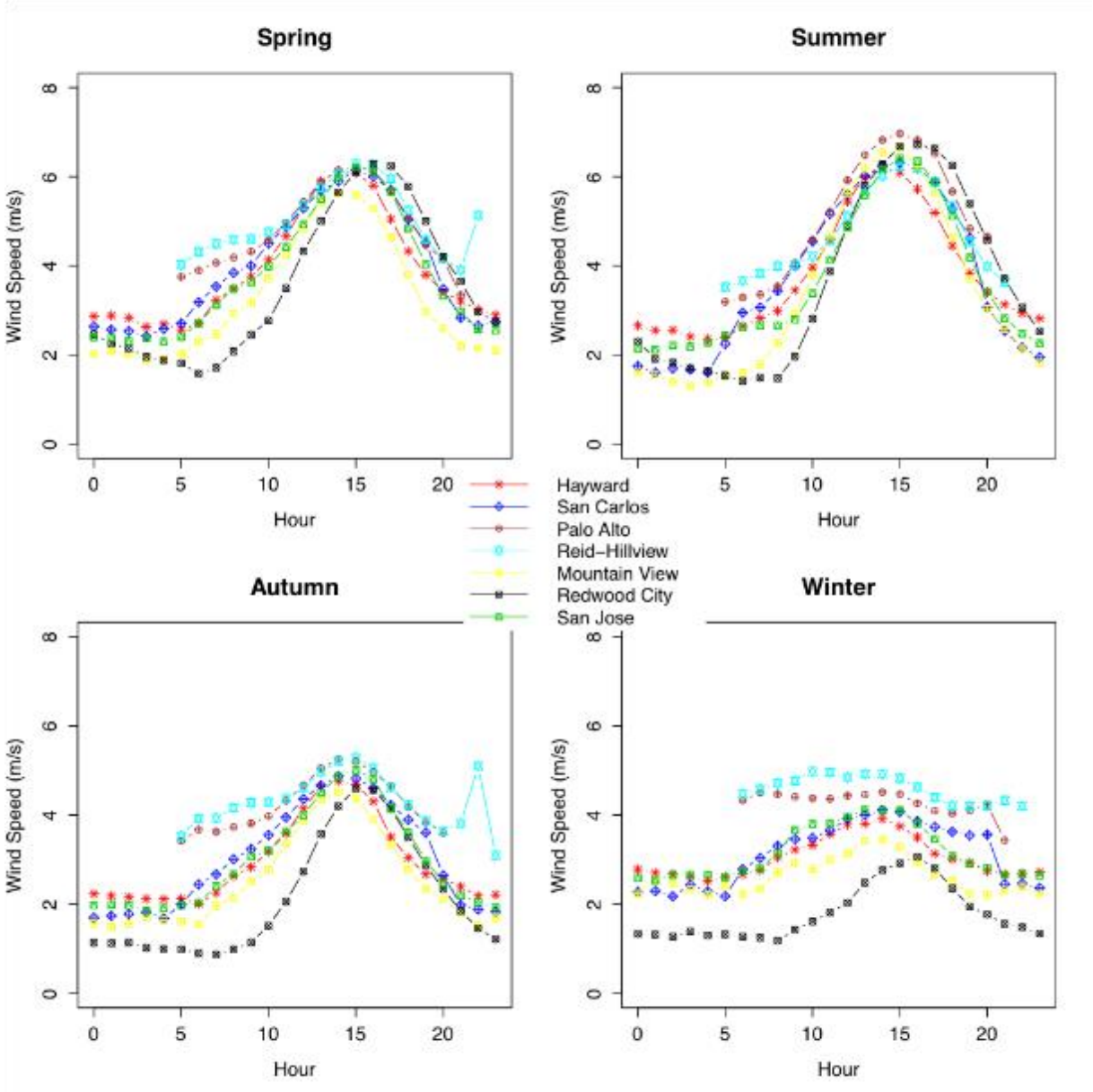

As measured at nearby National Weather Stations.

Source: Lawrence Berkeley National Laboratory

Figure B-5: Wind Roses for Stations Near ZWEDC

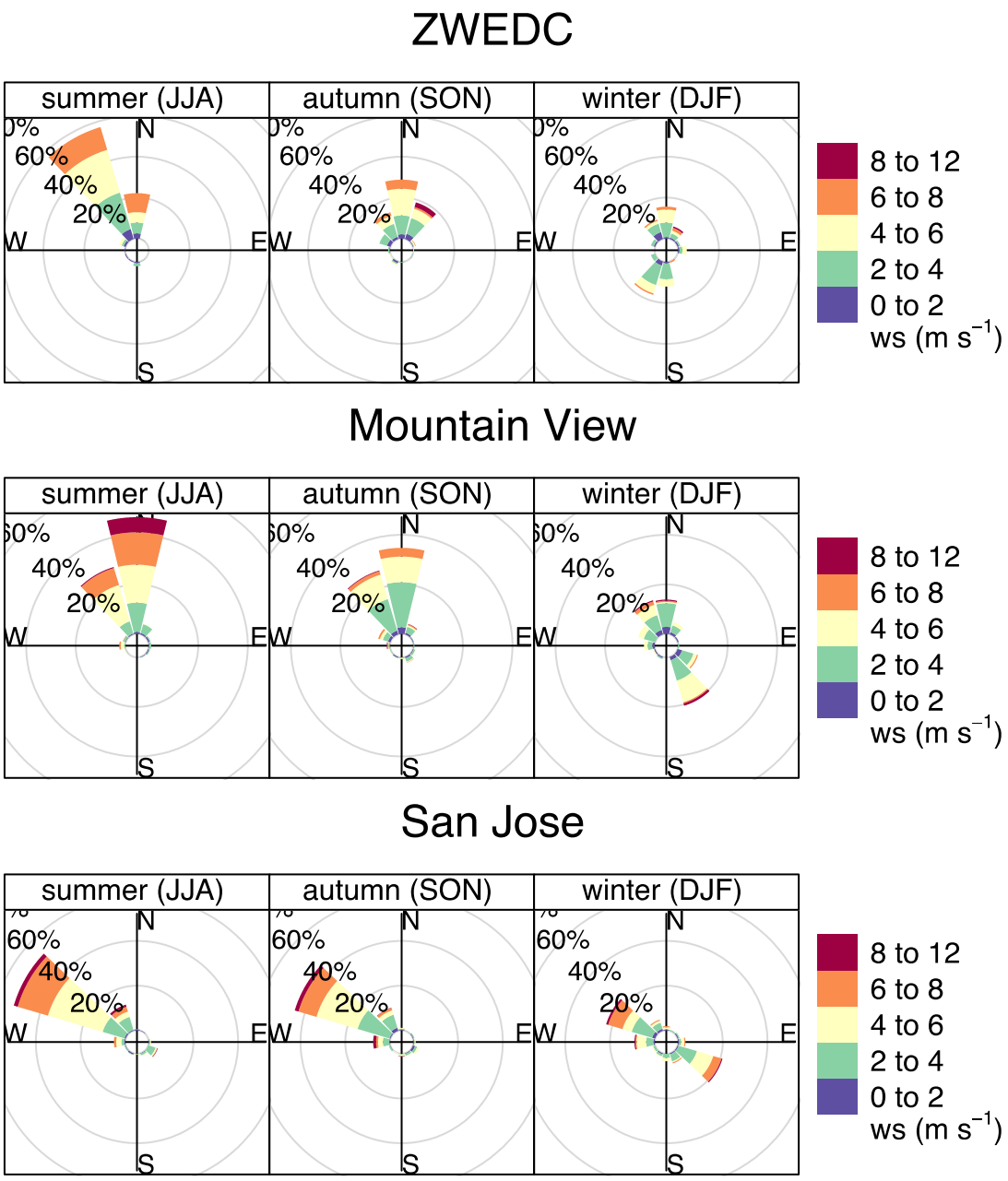

Two closest National Weather Stations to ZWEDC are Mountain View and San José.

Source: Lawrence Berkeley National Laboratory

AERMOD Input Processing and Results

The main model inputs to AERMOD are processed by AERMET and AERMAP. AERMET processes the raw meteorological data and calculates boundary layer parameters to generate the surface and profile meteorological data files that are directly input into

AERMOD. AERMAP generates terrain data and locations of the user-defined receptor networks, where concentration outputs are calculated.

Meteorology Input Preparation

AERMET is split into three stages with each stage having its own input file. Stage 1 extracts and processes the quality assessment (QA) of the NWS hourly surface observations data, the twice-daily upper air sounding data and the site-specific data (if presented).

The AERMOD model cannot simulate dispersion under calm or missing wind conditions. To compensate for the missing values, we utilize AERMINUTE to process the 1-minute winds from the Automated Surface Observing Stations (ASOS) and calculate hourly averaged wind speed and direction to supplement the standard archive of hourly observed winds processed in AERMET.

Three surface characteristics including surface roughness length (Zo), midday albedo (Alb) and daytime Bowen ratio (Bo) (U.S. EPA 2008) are collected for the study site from the US Geological Survey (USGS) National Land Cover Data 1992 archive (NLCD92). The NLCD92 are split into 21 categories for processing PBL parameters. The surface roughness is the height in meters above the surface, where the horizontal wind speed is zero based on a logarithmic scale. It is used to estimate the mechanical turbulence and atmospheric stability. The albedo is the fraction of solar radiation reflected back to space by the Earth's surface. The Bowen ratio is the ratio of sensible heat flux to latent heat flux and indicates the amount of surface moisture that is available. These two characteristics are necessary for estimation of the PBL parameters for sensible heat driven convective conditions.

National Oceanic and Atmospheric Administration (NOAA)'s NCDC provides the Integrated Surface Hourly (ISH), which was renamed around 2004 with Integrated Surface Data (ISD) for thousands of meteorological stations worldwide (NCDC 2016). As discussed in previously, we chose the Mountain View station located at MOFFETT FEDERAL AIRFLD APT (745090-23244) for processing surface meteorological inputs for years 2014-2016.

The upper air soundings data provided by the NOAA's Earth System Research Laboratory (ESRL) Radiosonde Database is also listed by stations and are found by their USAF or WBAN number. The sounding data includes measurements that characterize the vertical distribution of physical properties of an atmospheric column such as pressure, temperature, wind speed, and wind directions. The only nearby upper air soundings station is OAKLAND INT AP (72493-23230) and its data are used for ZWEDC odor studies.

Terrain and Receptor Network Processing

AERMAP is EPA's terrain pre-processor for AERMOD and its output files can be directly input into AERMOD through the RE pathway. AERMAP determines the elevation and hill height scale for each receptor based on the USGS digital terrain data (US EPA 2004b).

We chose to use a Cartesian gridded receptor network that is suited for simulating dispersion of multiple source types (area, line, and point) at the ZWEDC facility. According to SCAQMD modeling guidance for AERMOD, a grid spacing of 100 meters or less must be used to identify the maximum impacted receptors (http://www.aqmd.gov/home/library/air-quality-data-studies/meteorological-data/modeling-guidance). Since the s ZWEDC facility is approximately 3 km northwest from populated areas, the receptor network is prepared for a domain of 6 km by 6 km at a 50 m grid spacing centered on the ZWEDC facility (Figure B-6) consisting of 14,400 receptor locations.

Figure B-6: Illustration of Cartesian Receptor Domain in Relation to Surrounding Communities

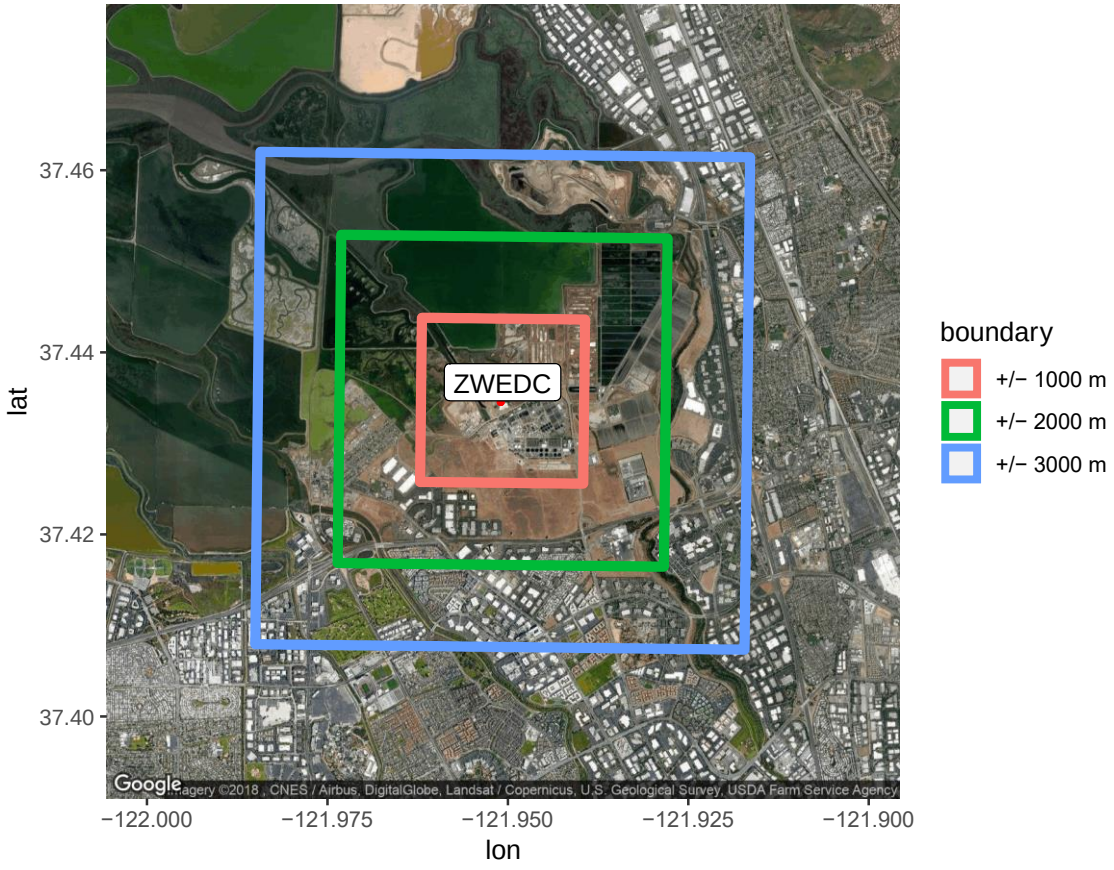

Source: Lawrence Berkeley National Laboratory

Appendix B: In addition to the location coordinates of the receptor grids, the receptor elevation (ELEV) and the hill height scale (HILL) are obtained from the terrain data provided by the National Elevation Dataset (NED). The receptor elevation is the terrain

elevation where the receptor located and the hill height scale represents the terrain that dominates the flow in the vicinity of the receptor. In other words, HILL can be viewed as the height of the terrain surrounding the receptor that will most influence the flow under stable conditions.

Layout Parameters for Emission Sources

There are three main outdoor odor emission sources. Two are area sources, the biofilters and outdoor composting windrows. One is a point sources, the release from the PRV. During delivery, there are on-road trucking activities and the receiving hall is open from the west end for incoming and the east end for outgoing trucks. The trucks and the hall are potential odor sources with emissions that are emitted on an intermittent basis. Receiving and trash storage are located in the west part of the logistic hall, while digestate storage is located in the east end. To account for their fugitive emissions, we include two more area sources to represent the receiving/storage of inbound wastes and the storage of the outbound digestates. The trucking activities are modeled as a line source on the nearby road with a 3 m width. The line source modeled in AERMOD is equivalent to an elongated area source with dimensions of 3 m by 30 m. dimension, using the maximum 10:1 aspect ratio recommended by AERMOD. This is equivalent to 2 large or 3 median sized trucks driving in tandem.

The layout of composting windrows is a function of the geometry of the digestate piles, the residence time, and the digestate mass. If we assume the same pile geometry currently used at Z-Best (300 ft by 20 ft with approximately 700 ton/pile) and a 14-week cycle, we estimate that the digestates produced at current ZWEDC operation scale (4000 to 5000 tons per month) will fill 18 to 22 piles. We chose 20 piles for our modeling case, which cover an area of approximately 100 m by 120 m.

Modeling the point sources requires five building parameters: 1)the building height, the maximum tier height in the face of the flow, 2) the building width, the projected width of the building that is perpendicular to the flow, 3)the building length, the projected length of the building along the flow, 4) the along-flow distance from the stack to the center of the upwind face of the projected building, and 4)the across-flow distance from the stack to the center of the upwind face of the projected building. These parameters are obtained from the BAAQMD to determine the downwash effects around a stack source. Downwash occurs when aerodynamics wakes and eddies produced by nearby buildings affect stack emissions. The flow moves around the building, so the plume from the stack is entrained into the wakes and eddies from the building. Typically, downwash results in elevated concentrations in areas close to the emissions source.

Odor Emission Rates for Sources

Determination of Odor Unit

Odor associated with one or more compounds can be perceived by individuals only when the odorous compounds are present in sufficiently high concentrations to trigger

olfactory responses. The intensity of odor is measured by odor units, which are the number of dilutions required to reduce odor detection to a level that would occur is only 50 percent of the exposed population. Since we do not measure odorous compound concentrations, the odor unit emission rates are obtained from the literature or estimated for some compounds.

For a single odorous compound, the odor units are calculated by dividing its concentration by its odor detection threshold. For a mixture of compounds, the odor units are usually measured in the field. Capelli et al. (2013) present an empirical method to convert from chemical concentration to odor units. The odor activity value (OAV) is calculated by summing over the concentration divided by the odor threshold for all measured species:

Equation 1 $$OAV = \sum_i \frac{C_i}{OT_i}$$

OAV = odor activity value (ou/m^3)

C_i = concentration of compound i (mg/m^3)

OT_i = odor threshold of compound i (mg/ou)

Therefore, the odor emission rate (E_{ou}) derived from multiple species can be approximated as follows:

Equation 2 $$E_{ou} = OAV \times F = \sum_i \frac{C_i \times F}{OT_i} = \sum_i \frac{E_i}{OT_i}$$

Where, E_{ou} is the odor unit emission rate (ou/s), F is the flow rate (m^3/s), E_i is the emission rate of species i. Odor thresholds in Ruth (1984) and the AIHA document are reported in mg/m^3 or ppm and must be converted to mg/ou. Wu et al (2016) states that the conversion is done by normalizing the odor threshold in mg/m^3 by the unity odor threshold concentration, which is 1 ou/m^3. Converting odor thresholds from mg/m^3 to mg/ou is simply a 1:1 conversion.

Table B-2 lists typical offensive odorous species associated with organic waste management together with their odor threshold concentrations (OTC) (Brown et al. 2007; Rosenfeld et al. 2007).

Table B-2: Typical Offensive Odorants Associated with Organics Waste Processing.

Compound	Odor Descriptors	OTC (ug/m3)	OTC (ppb)
Odor wheel character: Sulfur-cabbage-garlic; Class: Sulfur			
Hydrogen sulphide	Rotten eggs	7.00E-01	5.02E-01
Methyl mercaptan	Sulphidy	4.00E-02	2.00E-02
Carbon oxysulphide	Pungent		
Dimethyl sulphide	Decayed cabbage	2.50E+00	9.84E-01
Ethyl mercaptan	Garlic	3.00E-02	1.30E-02
Sulphur dioxide	Irritating	1.18E+03	4.48E+02
Allyl mercaptan	Garlic-like	2.00E-01	6.60E-02
Carbon disulphide	Disagree, sweet	2.43E+01	7.70E+00
Propyl mercaptan	Unpleasant	2.00E-01	6.40E-02
Crotyl mercaptan	Skunk-like	3.70E-01	1.00E-01
Dimethyl disulphide	Rotten cabbage	1.00E-01	2.60E-02
Thiophenol	Putrid, garlic	1.20E+00	2.66E-01
Benzyl mercaptan	Unpleasant	1.32E+01	2.60E+00
Dimethyl trisulphide	Rotten cabbage	6.20E+00	1.20E+00
Odor wheel character: Fishy-ammonia; Class: Nitrogen			
Ammonia	Pungent, irritating	2.66E+01	3.83E+01
Methylamine	Fish, ammonia-like	2.50E+01	2.00E+01
Dimethylamine	Fishy, ammonical	3.78E+01	2.05E+01
Trimethylamine	Fishy, pungent	8.00E-01	3.32E-01
Odor wheel character: Rancid; Class: Acid			
Formic acid	Pungent, penetrating	4.50E+01	2.40E+01
Acetic acid	Sour, vinegar-like	2.50E+03	1.02E+03
Propionic acid	Sour	8.40E+01	2.80E+01
Butyric acid	Sour, perspiration	1.00E+00	2.78E-01
Valeric acid	Unpleasant	2.60E+00	6.24E-01
Caprinic acid	Rancid, sour	1.20E+04	1.70E+03
Odor wheel character: Solventy-hydrocarbon; Class: Substituted Benzene			
Benzene	Sweet, solventy	4.50E+03	1.41E+03
Toluene	Rubbery, mothballs	8.03E+03	2.13E+03

Compound	Odor Descriptors	OTC (ug/m3)	OTC (ppb)
Methyl methacrylate	Arid, fruity, sulphidy	2.05E+02	5.00E+01
Styrene	Solventy, rubbery	2.02E+02	4.74E+01
Cumene (isopropylbenzene)	Sharp, aromatic	3.92E+01	8.00E+00
Naphthalene	Mothball, tar-like	1.50E+03	2.86E+02
1,4-Dichlorobenzene	Mothballs	9.00E+04	1.50E+04
Odor wheel character: Fecal, Putrid; Class: Complex Nitrogen Compounds			
Indole	Strong, moth ball	3.00E-01	6.40E-02
Skatole	Perfume	4.00E-04	7.48E-05
Pyridine	Burnt, sickening	9.00E+00	2.80E+00
Putrescine	Putrid,rotting flesh		
Odor wheel character: Other			
Phenol	Medicinal, sweet	1.79E+02	4.65E+01
Benzothiazole	Penetrating	4.42E+02	8.00E+01

Source: Lawrence Berkeley National Laboratory

Emission rates for PRV venting

Odor emission rate upon venting can be determined as follows:

$$E_{OD} = F_{biogas} \times C_{OD} \qquad \textit{Equation 3}$$

Where E_{OD} is the odor emission rate in odor unit per time (ou/s), F_{biogas} is the volumetric biogas emission rate (m^3/s), and C_{OD} is the odor unit per volume biogas (ou/m^3). Here we use H_2S as the characteristic odor compounds in biogas to determine the odor concentration. Odor concentration is approximated by odor activity value of H_2S using Equation 1.

H_2S concentration in biogas and its odor detection threshold are obtained from the literature. Odor detection threshold is defined as the lowest concentration that can be detected by 50 percent of the human panelists. As odor perception is largely subjective and population dependent, the H_2S odor detection threshold reported in the literature also varies from 0.4 to 14 $\mu g/m^3$ (Nagata 2003; Ruth 1984; Rosenfeld and Suffet 2004; and Wu et al. 2016). To be conservative on the impact assessment, we use 0.6 $\mu g/m^3$ to reflect a low detection threshold.

H_2S in biogas is formed from the Sulfur containing compounds such as proteins in food wastes (Yang et al. 2014) and can vary with feedstock sources and decomposition stages. The literature values also vary greatly. Korres et al. (2013) reported H_2S concentration in biogas generally ranges from 0 to 2000 ppm while other studies reported more narrow ranges. Ong et al. (2017) reported 70 – 650 ppm H_2S in MSW digester gas and Kuo et al. (Kuo and Dow 2017) measured H_2S in biogas produced from

an AD facility co-digesting food waste with sludge and found the concentration was less than 400 ppm. H_2S concentration is essentially a parameter related to facility specific operations and we initially chose 500 ppm following Rapport et al. (2010) to quantify a base case odor emission rate.

Biogas emission rate is measured onsite using the carbon dioxide, temperature, and velocity analyzers as described in earlier sections. The hourly biogas emission rates range between 80 to 240 m^3/hour, with venting duration lasting between around a tenth of an hour to an hour.

Combining the H_2S odor detection threshold (0.6 μg/m3), concentration (500 ppm) and biogas emission rates (80 to 240 m^3/hour), we derive the odor emission rates to range approximately between 20000 to 80000 ou/s. For the base case simulations, we assume 50000 ou/s as the emission rate to understand the temporal and spatial patterns in odor dispersion and impact. The offsite odor impact is evaluated for the full range of H_2S concentration levels from 100 ppm to 2000 ppm in combination with venting frequencies to identify sensitive conditions that require mitigation.

Emission Rates for Trucking Activity and Waste Receiving Hall

Concentration measurements at the truck are not available. We apply the geometric mean of uncontrolled odor emission factors (1.26×10^7 ou/tonnage-inbound) for waste receiving from Sironi et al. (2006) and assume the amount of waste per delivery is 20 percent of the total inbound wastes, which corresponds to 3 large truck loads arriving the same time. As the trucks are covered, we assume 5 percent of the odor is leaked out and derive an emission rate of 566 ou/s for the base case simulation. To understand the uncertainties in truck emissions, we provide a low emitting case with 1 percent leakage rate, and a high emitting case with 10 percent leakage rate.

In the Logistic Hall, the western part ("Receiving_storage1") is used for waste receiving, sorting, and storage, while the eastern part ("Storage2") is used for storing digestate after IVC treatment. Uncontrolled odor emission factors used here are the geometric means from Sironi et al. (2006) for waste receiving (1.26×10^7 ou/tonnage-inbound) and for curing after normalizing to the 1-day storage time in ZWEDC (6.66×10^5 ou/tonnage-inbound). We assume 5 percent leakage rate, equivalent to 95 percent control efficiency by the enclosure of the receiving hall and derive 2830 ou/s and 150 ou/s as the base case emission rates, respectively for waste receiving and storage in the western and eastern part of the Logistic hall. To understand the uncertainties in receiving and storage emissions, we provide a low emitting case with 1 percent leakage rate and a high emitting case with 10 percent leakage rate.

Despite some preliminary VOC measurements that were made at the western part of logistic hall ("Receiving_Storage1"), the majority of compounds with offensive odors were not detected, and only 8 species (acetic acid, propionic acid, toluene, styrene, naphthalene, pyridine, phenol, benzothiazole) in Table B-2, have measured concentrations. Most of the detectable VOC species are less volatile and less odorous

and have higher odor detection thresholds and only make minor contributions to odor. The total contributions from the all species detected are generally less than 140 ou/s (or 1400 ou/s) assuming the leakage rate is 1 percent (or 10 percent) of the exhaust air flow rate through the biofilters. The magnitude of these numbers are comparable to but less than that of the values computed from literature emission factors as described above (Logistic Hall first row in Table 3). For this reason, we do not use measured VOC species for deriving odor concentrations.

Emission Rates for Composting and Biofilters

Using the composting emission rates for H_2S, NH_3 and VOCs that the project team measured at the Z-Best windrow piles, we can approximate the odor emission rates using Equation 2. The mean emission rates per pile are used for the base case simulations. Using the horizontal dimensions of the piles, the base case per area emission rate is computed to be 25.0 ou/s-m^2 and the total emission rate is 3.0×10^5 ou/s for a hypothetical composting area of 100 m by 120 m at ZWEDC (see previous section of Layout Parameters for Emission Sources). Low and high emission cases are also prepared using the minimum and maximum measured emission rates.

Similarly, we use the emission rates measured for H_2S, NH_3 and VOCs to approximate the odor emission rates at the biofilters using Equation 2. The base case biofilter odor emission rate is estimated to be 2.1×10^4 ou/s. Low and high emission cases are prepared using the minimum and maximum measured emission rates.

The contribution of H_2S, NH_3, and VOCs to the total odor emission rates (Figure B-7) indicated that hydrogen sulfide dominates the odors from both compost and biofilters.

Figure B-7: Contribution of Measured Species to Total Odor Emission Rates

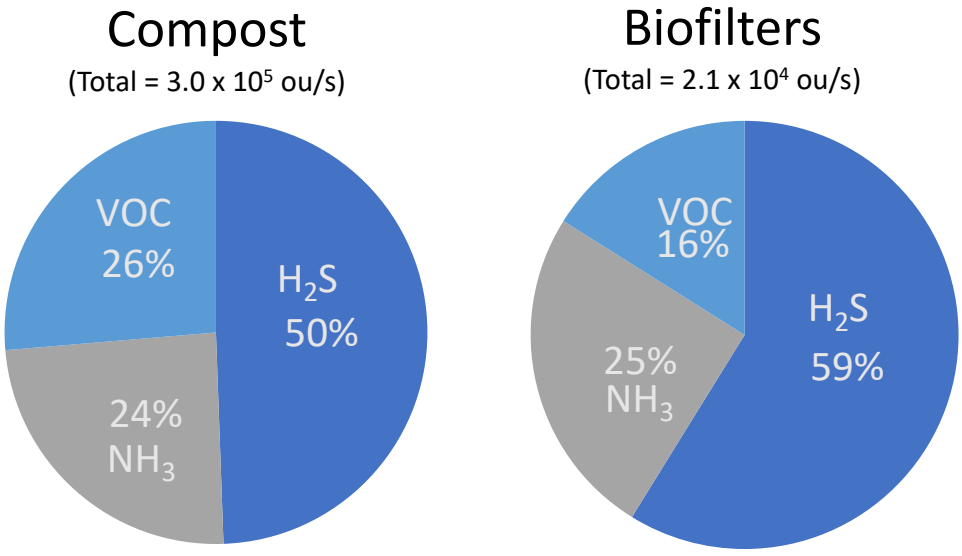

Source: Lawrence Berkeley National Laboratory

In addition to measurement data, we used an alternative method to evaluate the magnitude of the compost odor emission rates. We use literature odor emission factors measured in aerobic biological treatment plants (see Sironi et al. 2006) to approximate the odor emissions from composting digestates. Using emission factors from both composting and curing processes, we can compute the total odor emission rates at the ZWEDC operational scale to be between 1.8×10^5 ou/s and 6.3×10^5 ou/s. These rates are of the same order of magnitude as and bound the values that we computed using H_2S, NH_3 and VOC measurements.

For point source PRV venting, we link the odor impacts to a full range of H_2S concentration levels from 100 ppm to 2000 ppm in combination with venting frequencies to identify sensitive conditions that require mitigation.

Methods for Odor Impact Assessment

Peak-to-Mean Factors to Scale Hourly Model Outputs

Concentrations associated with odor dispersion are random variables with small variances. At a fixed sampling point, as the averaging period is reduced, the plume direction fluctuates, and the variance of the time-weighted average air concentrations become larger. The centerline concentration of an instantaneous or short-time averaged plume is significantly higher than it is for a long time-averaged plume (Schulte et al. 2007). Odor perception and sensation by humans are proportional to the instantaneous peak concentration of the odorant rather than to mean values.

A recent peak-to-mean approach is applied to scale the hourly modeled concentrations to more realistic shorter-time periods that odor is experienced in following Piringer et al.(2016) that account for the influence of atmospheric stability and distance from the source. Ultimately, the separation distances determined at different times of day, seasons, operational conditions with a range of assessment parameters are examined to understand influential and sensitive conditions that require mitigation to limit odor impact.

The maximum peak-to-mean scaling ratio between the long and short-term peak concentrations (Smith n.d.) is defined as:

$$\varphi_0 = \frac{c_p}{c_m} = \left(\frac{t_m}{t_p}\right)^a$$

Where

φ_0 is the maximum peak-to-mean scaling ratio near the odor source;

c_p is the peak concentration over short period of interest t_p;

c_m is the mean concentration over measurement period t_m;

a is an empirical exponent, see below.

The exponent *a* depends on source configuration (e.g. area vs point), atmospheric stability, distance from the source, etc (see most recent review by Brancher et al. 2017). The exponent *a* is smaller for non-point sources than high stack point sources. For area and line sources here, we use 0.14 (Brancher et al. 2017). For point source release, the peak-to-mean approach to determine the short-term peak concentrations used here was developed for an application of the Austrian odor dispersion model (Piringer et al. 2014; 2016). The concept is based on the above traditional power law relationship with improvements achieved by including the the effects of atmospheric stability and the distance from the source.

In our study, we have t_m = 1 hour. The choice of t_p varies from 1-5 seconds to 1-10 minutes to 1 hour in international odor regulations (review by Brancher et al. 2017). Here we choose to investigate three choices for t_p = 5 second, 6 minutes, and 1 hour and examine their influence on the resulting impact assessment. φ_0 derived for the two short-term integration time scales (φ_0_5 sec and φ_0_6 min) are listed in Table B-3 computed using the *a* values from the literature (Beychock n.d.) for point sources and Brancher et al. 2017 for area and line sources).

Table B-3: Empirical Exponents and Maximum Peak-to-Mean Factor

Stability class	*a*	φ_0_5 sec	φ_0_6 min
very unstable	0.68	87.7	4.8
unstable	0.55	37.3	3.5
neutral	0.43	16.9	2.7
slightly stable	0.3	7.2	2.0
stable	0.18	3.3	1.5
very stable	0.18	3.3	1.5
All classes	0.14	2.51	1.38

Peak-to-mean factor (φ_0) shown for scaling concentrations from 1 hour to 5 seconds and 6 minutes, respectively.

Source: Lawrence Berkeley National Laboratory

The maximum scaling ratio decreases with distance as the plume gets increasingly homogeneous due to turbulent mixing. The decay pattern is empirically formulated as

$$\varphi = 1 + (\varphi_0 - 1)\exp(-x/\tau)$$

Where *x* is the distance from the source and τ is the characteristic length of attenuation which can be derived from formulas in Piringer et al. (2014; 2016) to yield the following:

$$\tau = \frac{\left(\frac{\sigma_u}{u}\right)^2+\left(\frac{\sigma_v}{u}\right)^2+\left(\frac{\sigma_w}{u}\right)^2}{1.2489\times\left(\frac{\sigma_w}{u}\right)^3}$$

where u is the mean wind speed, and σ_u, σ_v, and σ_w are the standard deviations of the three wind components and their ratios to u are roughly constant within a given atmospheric stability class. $\frac{\sigma_u}{u}$, $\frac{\sigma_v}{u}$, $\frac{\sigma_w}{u}$ values. Their dependence on atmospheric stability was first proposed by Robins (Robins 1979) and can also be determined using field measurements with a three-axis ultrasonic anemometer. Field measurements showed the Robins values underestimated the attenuation length scale (τ), and this causes a more rapid decay of the peak-to-mean ratio with distance from the source (Piringer, Knauder, Petz, et al. 2014).

Due to lack of three-axis ultrasonic anemometer measurements for our site, we review published values of field measured $\frac{\sigma_u}{u}$, $\frac{\sigma_v}{u}$, $\frac{\sigma_w}{u}$ ratios from Piringer et al. (Piringer et al. 2007; Piringer et al. 2013; Piringer, Knauder, Petz, et al. 2014; Piringer, Knauder and Petz 2014; Piringer et al. 2015; Piringer et al. 2016) to determine the upper and lower bounds of the characteristic attenuation length scale.

The atmospheric stability class for each simulated hour is determined by transforming the Obukhov stability parameter (OSP) at that hour with dependence on the local roughness length. The Obukhov stability parameter is defined as 1/L, where L is the Monin-Obukhov Length. The hourly Monin-Obukhov stability parameter and the local roughness length are obtained from AERMOD surface input data. The transforming scheme follows Golder (Golder 1972) which provide OSP calculation values for stability classes under roughness length conditions between 0.01 and 0.5 m.

Determination of Separation Distance

Separation distance to avoid odor nuisance is a simple metric that links odor generating sources to their impact on downwind communities, and it has been widely used in odor regulations around the world (Brancher et al. 2017). Odor dispersion modeling is the most common method to determine separation distance. This method develops dispersion maps indicating the distance from an odor generating source where an odor is likely to exceed acceptable limits (Piringer et al. 2007).

Odor dispersion models simulate the atmospheric dilution of the odor source flow and predict ambient odor concentrations on an hourly basis. The peak-to-mean factor is applied to scale the hourly concentration to short-time peak concentrations to mimic odor sensation of the human nose. The time series of odor concentrations are evaluated for proximity to individual receptor locations to determine the exceedance probability of the threshold concentration (C_T) and compared to the allowable probability (P_T) of a given odor impact criteria (OIC). The directional dependent separation distances are usually presented on a dispersion map. In this study we report the maximum separation distances among all directions as a conservative metric for evaluating offsite odor impacts.

Separation distances depend on the choices of peak averaging time, C_T and P_T. The combination of C_T and P_T reflects a level of protection. Odor protection choices vary widely in the international framework. A stringent protection level generally combines a low C_T with a low P_T, while moderate protection levels can combine a low C_T with a high P_T or a high C_T with a low P_T (Brancher et al. 2017). The project team investigated different combinations of C_T and P_T that reflect "stringent" and "moderate" protection levels with peak averaging times (5 seconds, 6 minutes, and 1 hour) as illustrated in Figure B-8. Specifically, the combinations to form varying protection levels are:

- Stringent: odor concentration threshold = 5 ou/m^3, exceedance probability = 2 percent
- Moderate 1: odor concentration threshold = 10 ou/m^3, exceedance probability = 2 percent
- Moderate 2: odor concentration threshold = 5 ou/m^3, exceedance probability = 10 percent

Note that the values chosen are not intended to replicate any odor jurisdictions but rather to provide a reasonable range of conditions to understand the odor annoyance potentials from the PRV venting in relationship to uncertainties in the assessment parameters.

Figure B-8: Assessment Parameters Used in This Study Compared to Generic Procedures to Determine Separation Distances

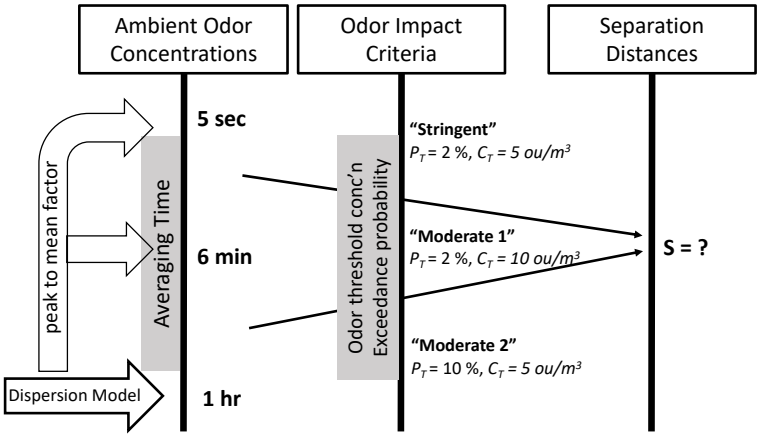

Adapted from Schauberger and Piringer (2012).

Source: Lawrence Berkeley National Laboratory

For continuous emission sources and sources with a known emission schedule, the exceedance probability $P(C > C_T)$ can be directly computed from the concentration time series. As the PRV venting is intermittent with unknown frequency, the exceedance probability at a given receptor location $P(C > C_T)$ over an evaluation period of interests (T) can be expressed as follows:

$$P(C > C_T) = P(venting) \cdot P(C > C_T|venting)$$

Where $P(venting)$ is the PRV venting probability, and $P(C > C_T|venting)$ is the exceedance probability given the occurrence of PRV venting. $P(C > C_T|venting)$ can be determined similarly to the procedures that assume continuous emissions. and Over an evaluation period, the venting probability or frequency $P(venting)$ is the fraction of hours when venting occurs and $P(C > C_T|venting)$ is the fraction of hours when the ambient odor concentration (after applying a peak-to-mean factor) exceeds the threshold concentration C_T.

$P(C > C_T|venting)$ is determined using the base-case inputs (described in Section 2.2), and will be used to first isolate meteorological influences on separation distance patterns. Next, operational conditions such as $P(venting)$ and emission rates (determined by the H_2S levels in the biogas and biogas emission rates) will be combined to determine sensitive operational conditions according to their overall impacts of separation distances.

We compute the separation distances for time of day or aggregated hours within time periods that overlap with human activities in this region from 7 AM to 9 PM (referred to as "active hours") when offsite odor is most likely to interfere with outdoor human activities. The time 7 AM roughly corresponding to the start of commute time, while 9 PM corresponding to the closing hour of local businesses. Seasonal patterns in separation distances are also examined. The procedures commonly derive separation distances over all the hours and our analysis intends to distinguish potential repetitive patterns associated with time of day or season that are important to influence the odor memory and consequent human reactions to odor (Brancher et al. 2017).

Model Simulations and Odor Impact Assessment

PRV Venting

Time and Location Dependent Peak-to-Mean Factors

The peak-to-mean factors depend on atmospheric stability and distance from the source and are time and location dependent. We categorize the atmospheric stability conditions of individual modeling hours into 6 stability classes according to the Golder (Golder 1972) scheme. Hourly maximum peak-to-mean factors are determined at the source location based on their respective stability categories. Spatially, peak-to-mean factors attenuate over distance downwind with characteristic length scale τ. We compute τ (according to Equation 3) from stability dependent wind fluctuation ($\frac{\sigma_u}{u}$, $\frac{\sigma_v}{u}$, $\frac{\sigma_w}{u}$) values including Robins (1973) and observations made by Piringer et al (Piringer et al. 2007; Piringer et al. 2013; Piringer, Knauder, Petz, et al. 2014; Piringer, Knauder and Petz 2014; Piringer et al. 2015; Piringer et al. 2016). Table B-4 presents the resulting attenuation length scales with dependence on atmospheric stabilities. The

upper and lower bounds of the observed characteristic length scale of attenuation are summarized in the last two columns.

Table B-4: Review of the Characteristic Length of Peak-to-Mean Ratio Attenuation by Atmospheric Stability

Atmo-spheric Stability	Robins	Kittsee 2015 τ, m)	Limmersdorf 2014 τ, m)	Linz 2014 τ, m)	Reidling 2016 τ, m)	Weissbach 2014 τ, m)	Observed Max	Observed Min
Very stable	72	189	188	83	58	33	189	33
Stable	72	123	162	59	48	30	162	30
Slightly stable	72	102	125	50	48	29	125	29
Neutral	72	112	86	43	36	32	112	32
Unstable	12	69	81	41	29	34	81	34
Very unstable	5	39	29	26	15	26	39	15

Reported attenuation lengths have units of meters and are reported for the most recently published data at the same site. Shaded area shows observation based characteristic attenuation length (shown by measurement site and published year).

Source: Lawrence Berkeley National Laboratory

The resulting mapping of hourly stability classes as well as stability dependent peak-to-mean factors over distance are illustrated in Figure B-9 Atmospheric stabilities present distinct patterns both diurnally and seasonally at the study site. The early morning and late evening hours are generally under stable or very stable conditions. A couple of hours after sunrise, as the surface is heated, the atmosphere transitions into very unstable and unstable conditions in the morning and into neutral conditions in the afternoon until a couple of hours before sunset. There is a seasonal pattern in the timing and duration of the (very) unstable and neutral conditions corresponding mostly to the variations in the timing of sunrise and sunset over the course of a year.

Peak-to-mean factors are greatest under the very unstable condition at the source, followed by unstable, neutral, and stable conditions. The attenuation length scales are generally greater under stable conditions than unstable conditions. This is expected as more vigorous turbulent mixing under unstable conditions tends homogenize the odor plume and therefore reduces the peak- to-mean factor as a function of increasing distance from the source at a faster rate as shown in Figure B-9.

Figure B-9: Hourly Atmospheric Stability Classes and Attenuation of Peak-to-Mean Factors

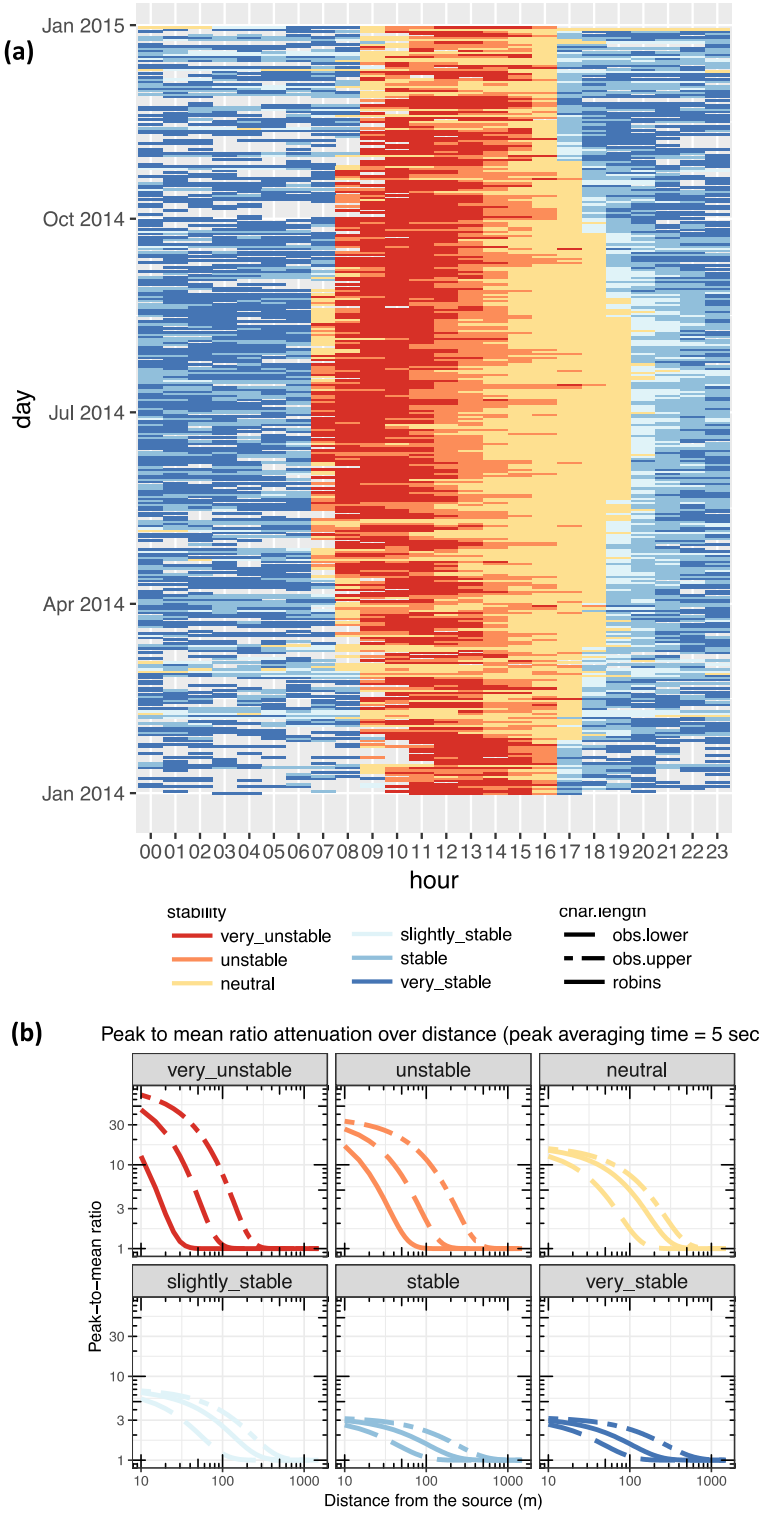

(a) Hourly atmospheric stability classes and (b) attenuation of peak-to-mean factors over a distance for 5-second peaks.

Source: Lawrence Berkeley National Laboratory

The observation based τ values are 2 to 3 times greater than the ones proposed by Robins (1979) for the unstable and very unstable conditions, suggesting potential under estimation of peak-to-mean factors over distance by Robins (1979) (also shown in Figure 69b). Regardless of the stability classes and characteristic lengths considered, the peak-to-mean factors approach 1 at 1000 meters downwind of the source location.

Our study site is located on a rural flat terrain similar to the Kittsee site, which presented greater τ values and therefore larger peak-to-mean factors than other sites. As a conservative choice, we present results in subsequent sections using the upper bound values (the "Observed Max" column) that maximize the peak-to-mean ratios and will discuss the uncertainties around the choice.

Meteorology-Induced Temporal Patterns in Separation Distances

To disentangle the complex relationship between separation distances and the operational conditions associated with PRV venting under various external conditions including meteorology and assessment parameters, the project team examined the spatial and temporal patterns under the fixed base case emission rate to understand the meteorological drivers of separation distances at diurnal and seasonal time scales in relation to assessment parameters. The separation distances derived here are for the worst-case (hypothetical) emission case when venting is constant.

The seasonal spatial patterns in top 2 percent odor concentrations over the "active hours" are shown in Figure B-10. Odor concentrations generally present elongation in the northwest to southeast directions, corresponding to the predominant wind patterns observed in this region. There is also significant seasonal variability. The summer season (June-July-August) has the most narrow spatial extent while fall and winter seasons have more spread-out patterns when winds are weaker and more variable. Using the hourly concentrations without peak to mean scaling and aggregated over all the active hours, the separation distances from the source are generally from 200 meters in the summer to about 500 meters in the winter.

Figure B-10: Seasonal Spatial Patterns for Active Hours in Top 2 Percent of Odor Concentrations

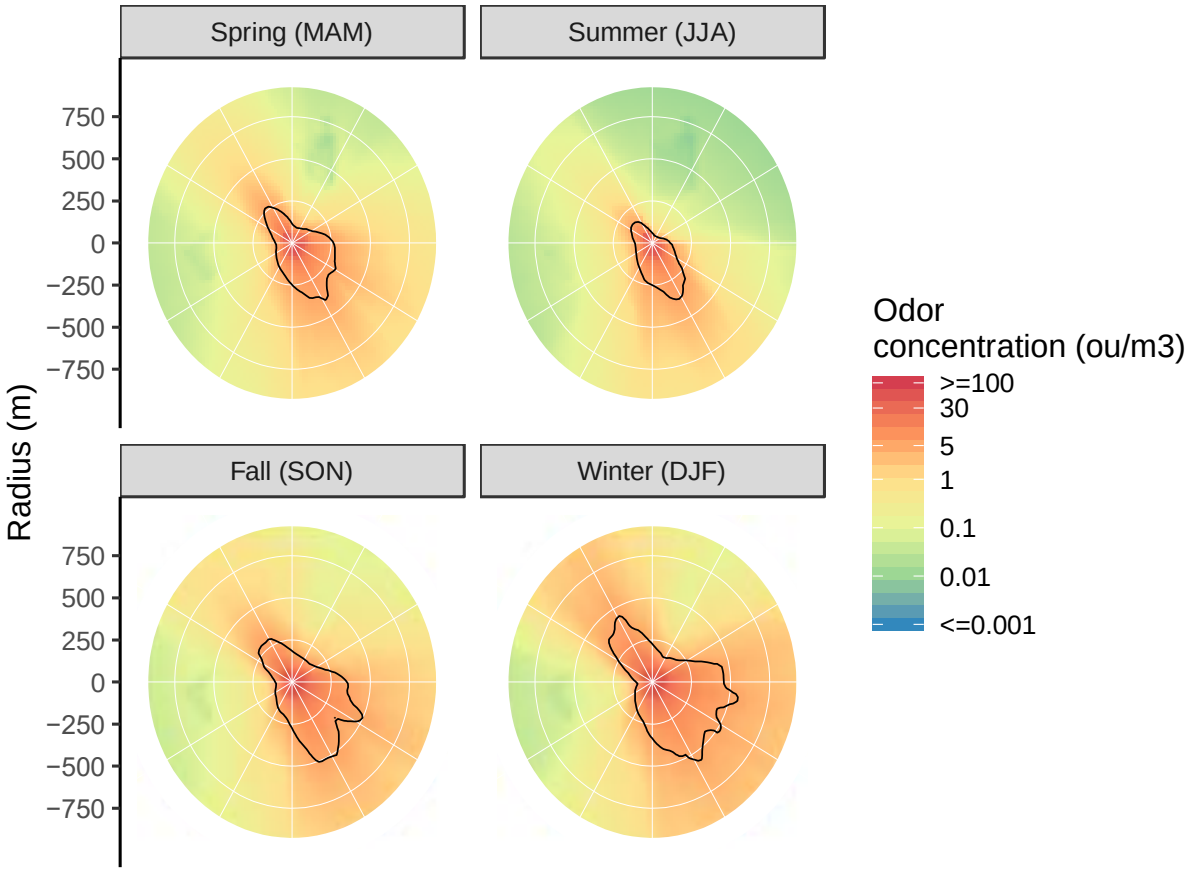

Source: Lawrence Berkeley National Laboratory

In order to examine more closely the time of day dependence and the relationship to parameters used in odor impact criteria, we plotted the maximum separation distances determined for each hour of the day under the three OIC criteria, "stringent", "moderate 1", and "moderate 2". The averaging times now include all three cases, over 5 seconds, 6 minutes, and 1 hour. The time of day patterns are summarized. Distinct patterns emerge from the time of day differences in the separation distances. The separation distances are low (around 200-400 meters range) in the middle of the day and there is a noticeable increase (to > 500 meter range) in separation distance in the early morning and late afternoon regardless of the choice of averaging time or impact criteria (Figure B-11).

Figure B-11: Diurnal Patterns by Season in Separation distances and Distributions of Stability Classes

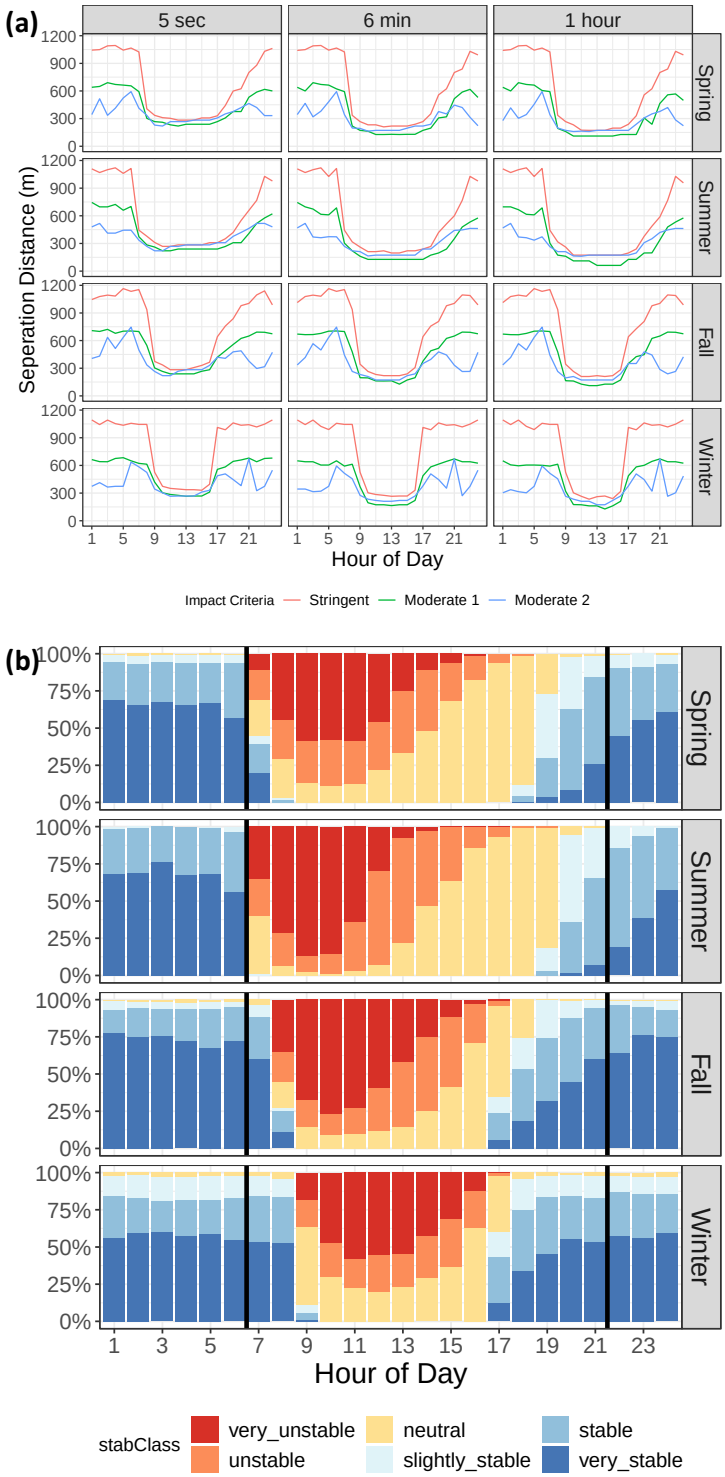

Hour-of-day trends in (a) maximum separation distances and (b) distributions of stability classes.

Source: Lawrence Berkeley National Laboratory

Seasonal differences are most profound in the duration of the low separation distances, which correspond to the distribution patterns of atmospheric stability classes where neutral to very unstable conditions dominate the distribution of active times. An odor plume is quickly diluted during these mixing hours before being transported downwind, resulting in less elevated odor concentrations. In contrast, when stable conditions dominate, atmospheric mixing is much reduced, and a more concentrated odor plume is transported further to downwind areas, resulting in greater separation distances. The effects of varying OIC parameters are most prominent during these low mixing hours, with the greatest separation distance required under the "stringent" criteria, followed by "moderate 1" and "moderate 2."

According to the hour-of-day patterns, we can now stratify the analysis period into "high mixing hours" and "low mixing hours" when the separation distances behave more similarly with respect to each of the categories. The definition of these hours is seasonally dependent as seen in Figure B-11 and is summarized in Table B-5.

Table B-5: Categorization of Active Hours According to Atmospheric Stability (Human Active Hours 7AM–9PM)

Season	High Mixing Hours	Low Mixing Hours
Spring (MAM)	8AM–6 PM	7–AM, 7–9PM
Summer (JJA)	7AM–7PM	8–9PM
Fall (SON)	9AM–4PM	7–8AM, 5–9PM
Winter (DJF)	9AM–4PM	7–8AM, 5–9PM

Source: Lawrence Berkeley National Laboratory

The top 2 percent odor concentrations are plotted in Figure B-12 to examine the directionally dependent separation distances (black contour lines) using all three averaging times. The high mixing hour patterns using hourly data are similar to Figure B-10, while the low mixing hours are vastly different, with their spatial extent much greater than the ones derived from aggregating all the hours between 7 am and 9 pm. Using aggregated hours without distinguishing atmospheric conditions to define separation distances may underestimate the spatial extent of impact because there may be clear repetitive patterns in impacted areas further downwind during the low mixing hours. Using the spatiotemporal dependent peak-to-mean factors computed in this study, we determined that high mixing hours are affected by the choices of peak averaging time more than the low mixing hours. This is indicated by the changes in the spatial extent of odor exceedances. The separation distances derived under low mixing hours are largely indifferent to the choices of concentration averaging times.

Figure B-12: Seasonal Average Top 2 Percent Odor Concentrations with Different Peak Averaging Times

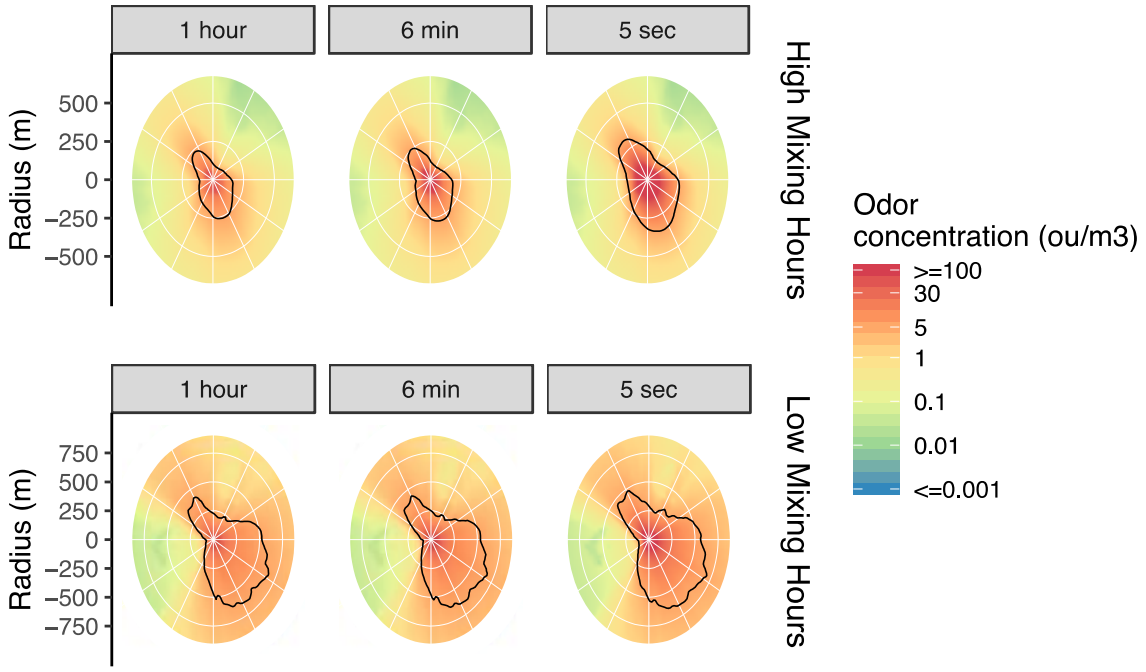

Source: Lawrence Berkeley National Laboratory

Influence of Odor Impact Criteria on Separation Distance

As shown in Figure B-13, the maximum separation distances computed using different averaging times vary most during the high mixing hours. The separation distances evaluated with 5-second averaging times are generally more than 100 meters larger than those with 6-minute averaging times and hourly averaging times. This finding is consistent with past studies that peak-to-mean factors are more important for near field odor impact assessment. During low mixing hours, separation distances largely differ by the impact criteria used, ranging from 300–400 meters under "Moderate 2" criteria, to ~500 meters under "Moderate 1" criteria, and to ~700 meters under the most "Stringent" criteria.

The patterns of dependence on averaging time can be explained by examining the spatial attenuation curves in Figure B-9. Peak-to-mean factors decrease over distance and approach values less than 2 around 500 meters and to 1 around 1000 meters downwind of the source. During low mixing hours, above-threshold odor concentrations can occur at large distances (e.g. 500 to 1000 meters) downwind where small peak-to-mean factors apply and they do not change the concentrations significantly.

Figure B-13: Maximum Separation Distances by Odor Impact Criteria and Averaging Times

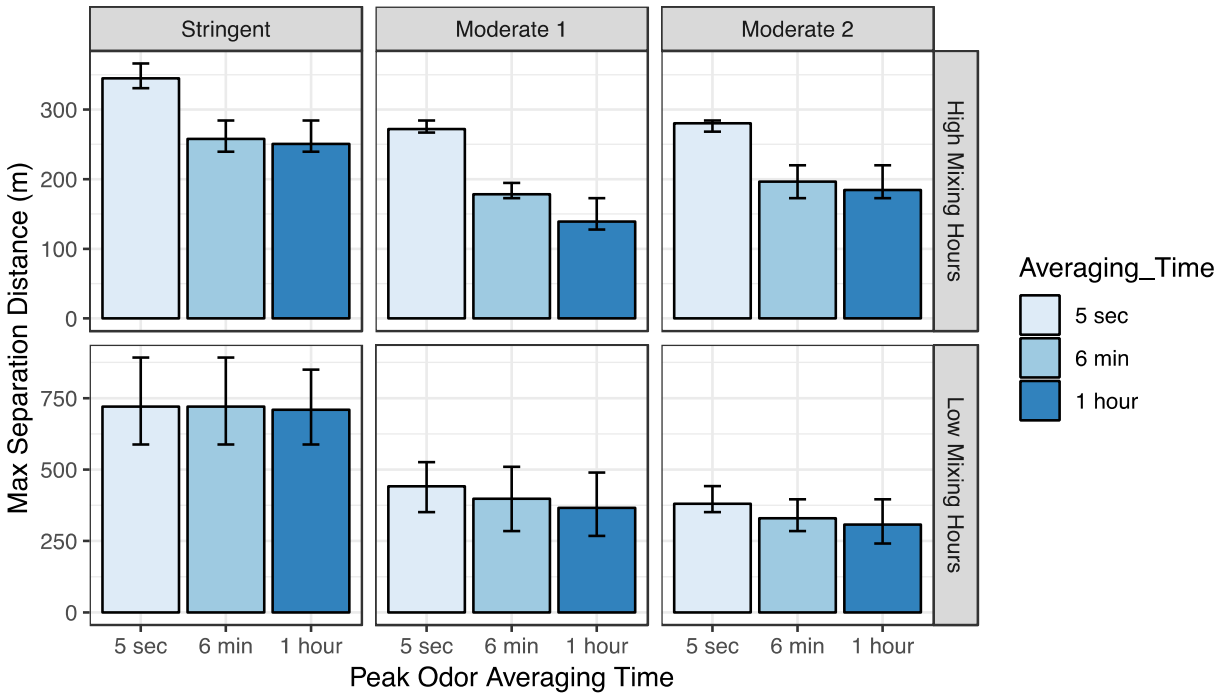

Error bars represent inter-seasonal variations.

Source: Lawrence Berkeley National Laboratory

Influential Operating Conditions

In this section, operational conditions such as $P(venting)$ and emission rate (determined by the H_2S levels in biogas and biogas emission rates) will be combined using the spatial and temporal patterns identified through analysis of the local meteorology to determine sensitive operational conditions of odor annoyances.

The overall exceedance frequency is a function of both venting frequency and the odor emission rate. Odor emission rates depend on the biogas emission rates and the biogas H_2S levels. The measured biogas emission rates are in the range of 76 to 185 m^3/hour with a mean value of 139 m^3/hour and standard deviation of 35 m^3/hour. The biogas emission rates are relatively consistent with a coefficient of variation (standard deviation divided by mean) of 26%. That is, the biogas emission rates generally vary around the mean by 26%. On the contrary, the literature values for biogas H_2S levels vary over a much greater range from 0 to 2000 ppm relative to the 500 ppm value assumed in our base case simulation. Consequently, the variations in odor emission rates are largely governed by the H_2S contamination levels in biogas. In practice, H_2S levels in biogas can be monitored by the facility and therefore understanding at what H_2S level venting should be avoided is important. For above reasons, we focus our evaluation of separation distances on the operation parameters of venting frequency

and H_2S contamination levels, quantified by assuming that the biogas emissions occur at a constant rate (185 m^3/hour as a conservative measure of the impacts).

From the results shown in previous sections, low mixing hours are especially conducive to offsite odor impacts as indicated by their much greater separation distances that occur relative to those associated with high mixing hours. Although these hours are indifferent to the choices of peak averaging times, they are sensitive to impact criteria. The high mixing hours, on the other hand, require greater separation distances when evaluated using peak concentration over 5-seconds than those associated with longer averaging times. As a conservative measure, we base our evaluation of operational conditions on the 5 second concentrations for both high and low mixing hours (Figure B-14).

Figure B-14 shows an array of two-dimensional heat map of separation distances as a function of both H_2S concentrations in biogas and venting frequencies under the stringent criteria. The H_2S concentrations are varied from 100 to 2000 ppm at 100 ppb intervals. The venting frequencies in the model are varied from 5 percent (one twentieth of the hours with venting) to 100 percent (constant venting) at 5 percent intervals.

Figure B-14: Seasonal Separation Distances as a Function of Operating Conditions under Stringent Odor Impact Criteria

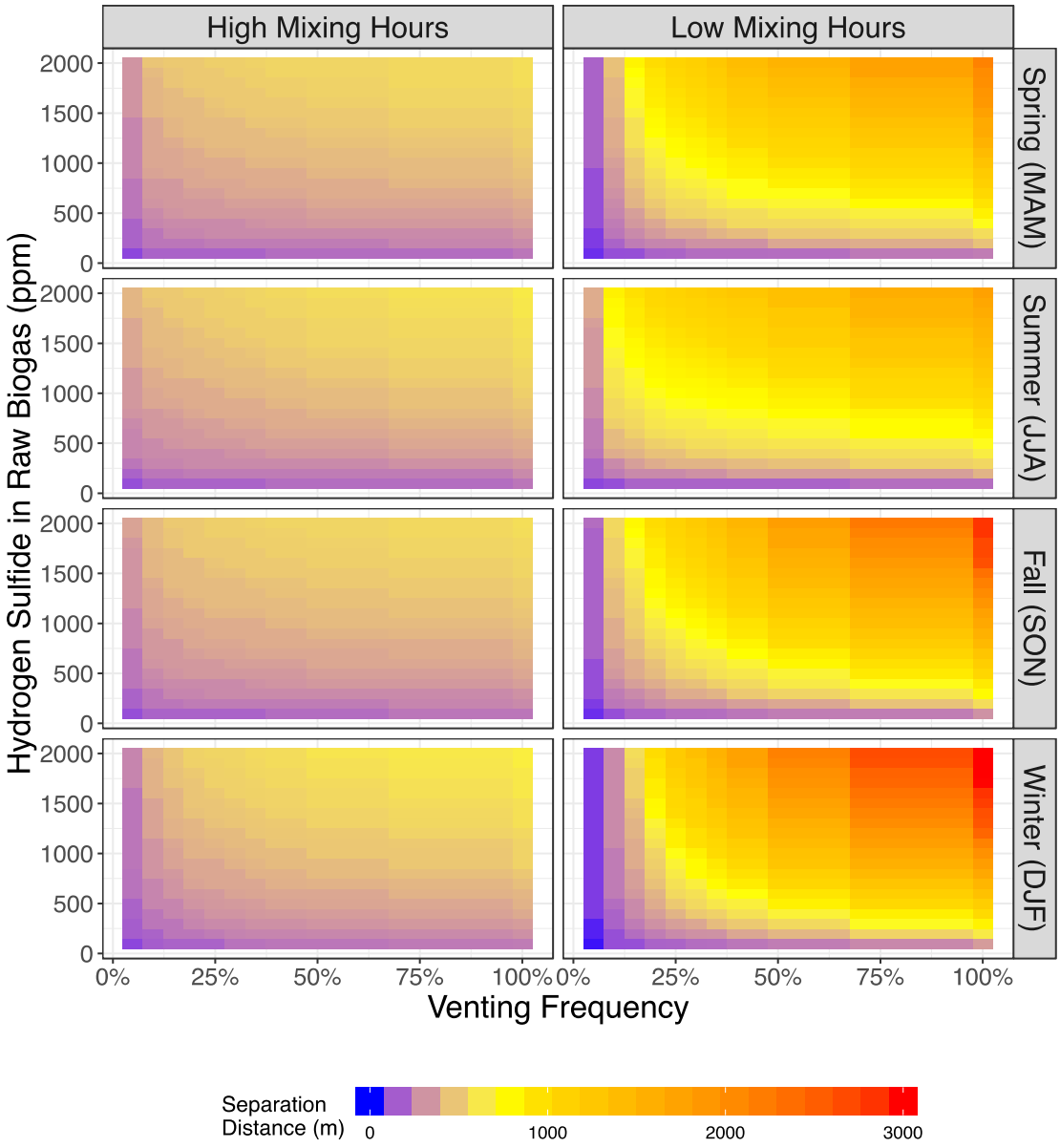

Source: Lawrence Berkeley National Laboratory

Area and Line Sources

Analysis of the temporal variations in odor dispersion and the dependence of separation distances on assessment criteria have revealed much about preventing odor incidents. For area and line source assessments, we aggregate the dispersion patterns based on "High" and "Low" mixing hours identified from previous analyses and report the results based on scaling hourly concentrations to a 6-minute peak to obtain a more realistic assessment. Separation distances based on the most stringent criteria (exceeding 5 odor unit (ou)/m^3 by 2 percent) are presented.

Dispersion Patterns and Separation Distance from Area and Line Sources

The dispersion patterns by individual source types are aggregated over all seasons and all active hours (7 am to 9 pm), both the average and top 2 percent of the odor concentrations are considered. The emission sources in the logistic hall are aggregated into one category labeled as "Receiving".

The offsite impacts are dominated by composting windrow emissions, followed by those from the biofilters. Trucking and receiving hall emissions are insignificant when even evaluated by the most stringent odor impact criteria. The black contour line in the top 2 percent concentration maps effectively delineate the directional dependent separation distance under the most stringent odor criteria (exceeding 5 ou/m^3 at 2 percent probability). The sources are masked in the plots in black (Figure B-15).

Figure B-15: Potential Offsite Odor Exposure by Source

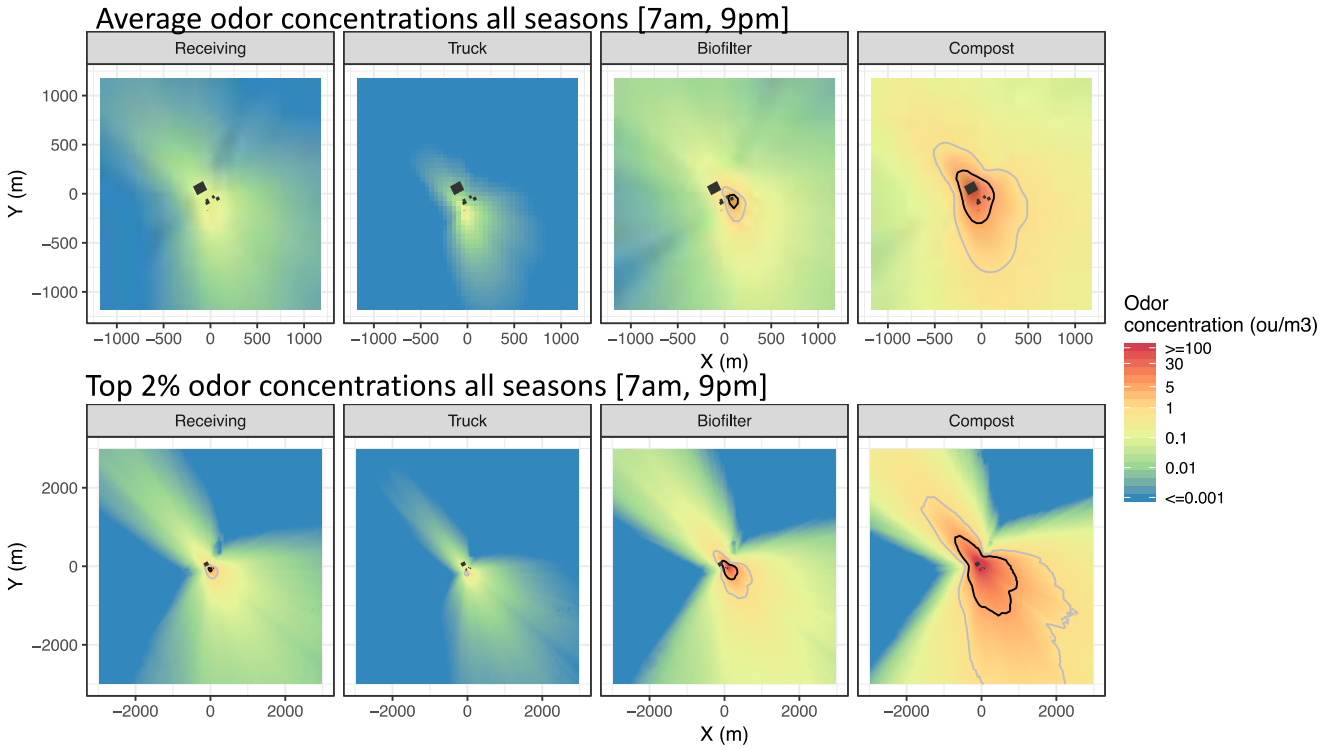

Atmospheric dispersion modeled for ZWEDC location. Onsite compost operation was moved offsite to Z-Best Products in Gilroy in October 2015. The dispersion modeling shown here is based on a hypothetical composting system similar to Z-Best, implemented at ZWEDC. The black line indicates a 5 ou/m3 concentration contour and the grey line 1 ou/m3 contour.

Source: Lawrence Berkeley National Laboratory

All sources except for the compost have insignificant offsite odor impacts <=5 ou/m3) well within 1 km distance away from the source.

We aggregate concentrations by season and by atmospheric stabilities (high vs low mixing) for all sources with and without compost (Figure B-16 and Figure B-17). The

dispersion directions are consistently aligned in the northwest-southeast directions for all seasons, and exhibit similar behavior to that noted for the PRV simulations. Summer time winds blow more consistently from the northwest and accordingly the offsite impacts are dominated in the southeastern direction downwind of ZWEDC. Other seasons, especially the winter time, show more variable dispersion with impacted areas extended to the northwest of ZWEDC. The spatial extend of odor dispersion in the southeastern direction is especially important in the ZWEDC case, because populated regions are located in this direction beginning from ~2000 m with populations increasing at ~3000 m downwind of ZWEDC.

Figure B-16: Potential Offsite Odor Concentrations from Non-Compost Sources

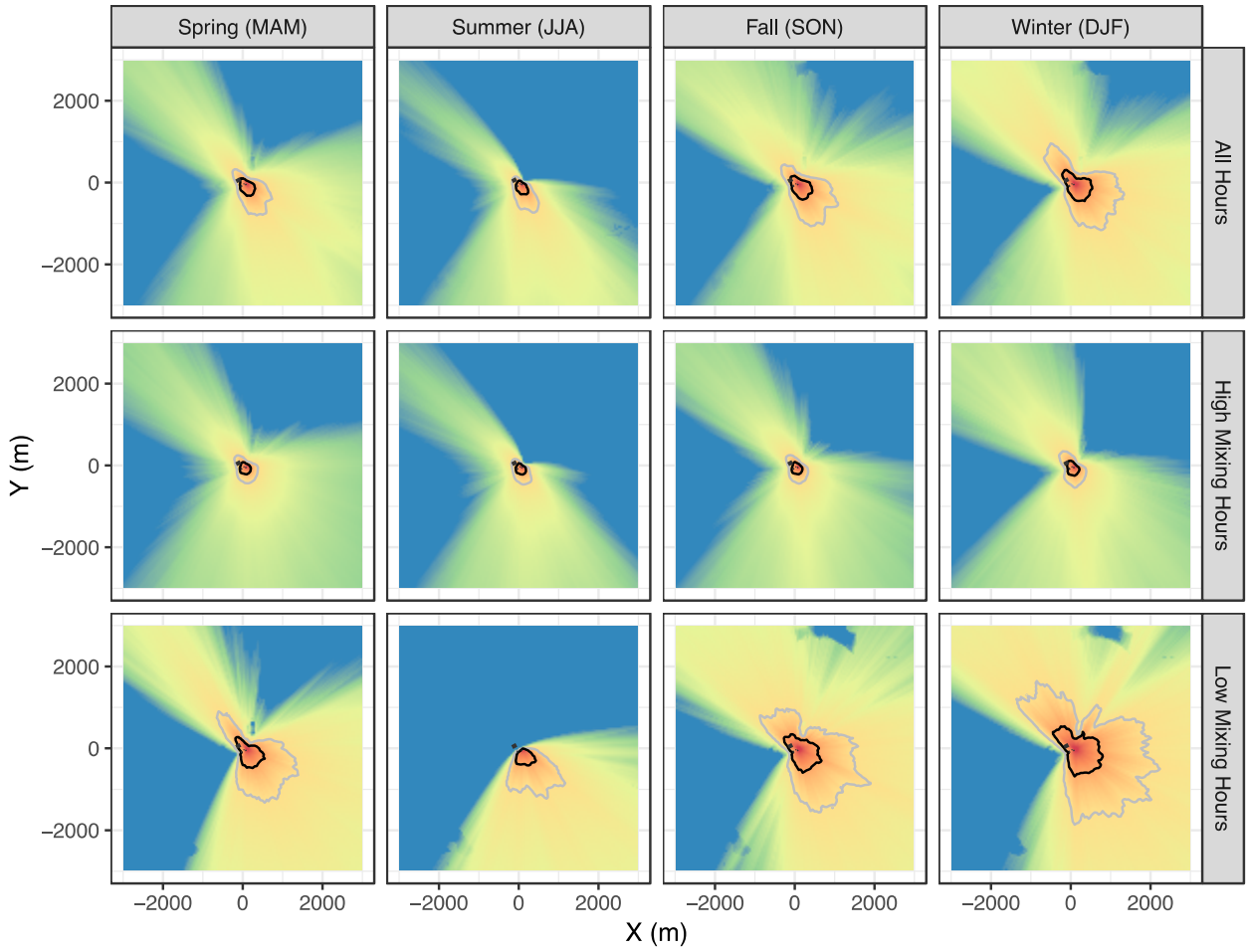

Atmospheric dispersion modeled for ZWEDC location for top 2 percent of odor concentrations. Same annotation and legend as Figure B-15.

Source: Lawrence Berkeley National Laboratory

Similar to the PRV case, the high and low mixing hours exhibit differences in the spatial extent of the offsite impacts evaluated using the 2 percent criteria. All the non-compost sources are currently at ZWEDC, with their significant offsite impacts (>5ou) extend

less than 1000 m downwind from them for all seasons and hours (Figure B-16). If compost windrows are added to the current ZWEDC sources, offsite impacts occur within 1000 m during the high mixing hours for all seasons. For the low mixing hours, the impacts extend beyond 2000 m for all seasons especially, for the fall and winter seasons. The derived maximum separation distances are summarized in Figure B-18 with grey bars indicate individual sources and the blue indicate all sources combined.

Figure B-17: Potential Offsite Odor Concentrations from All Area and Line Sources

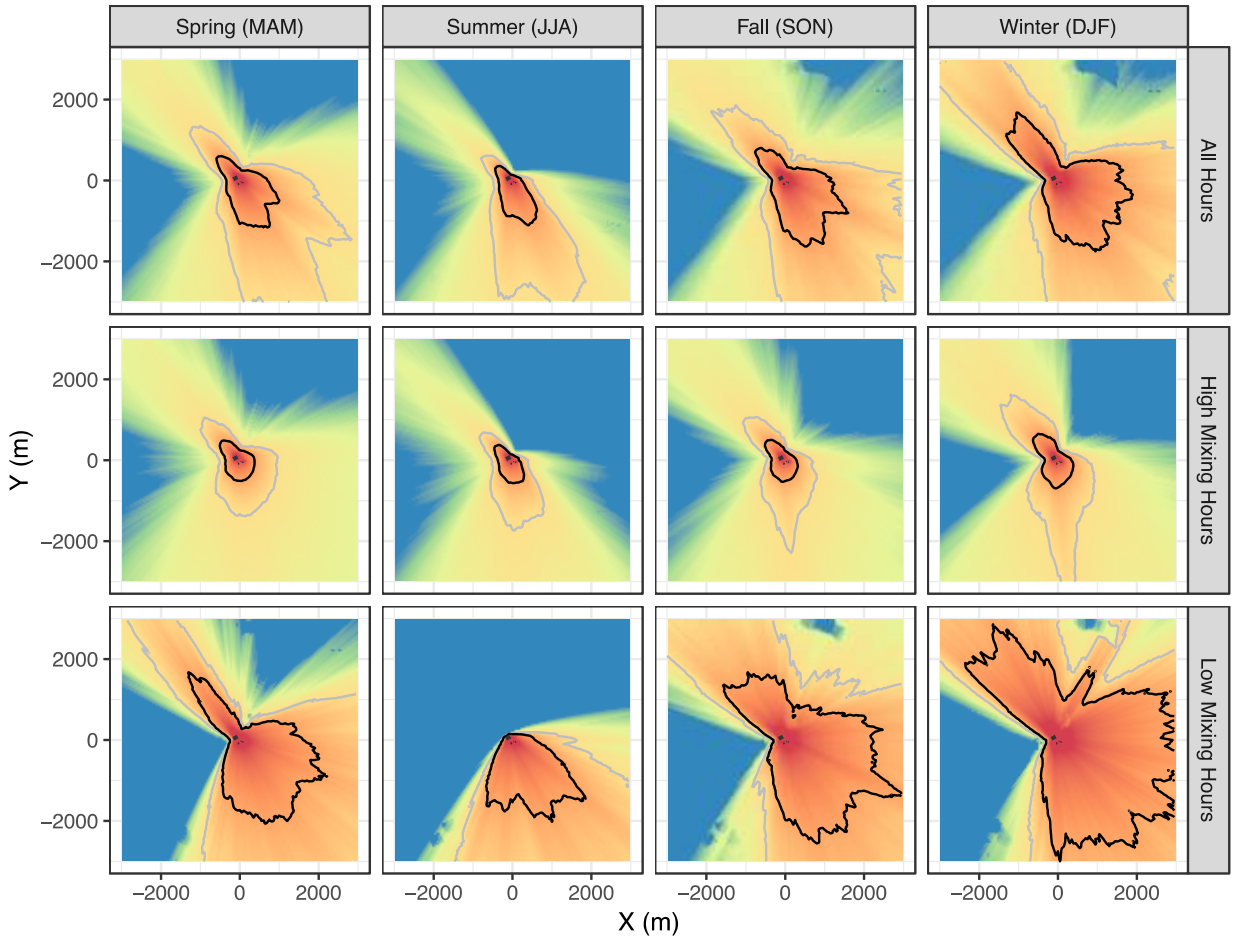

Atmospheric dispersion modeled for ZWEDC location for top 2 percent of odor concentrations. Same annotation and legend as Figure B-15.

Source: Lawrence Berkeley National Laboratory

Figure B-18: Maximum Separation Distances for ZWEDC by Season

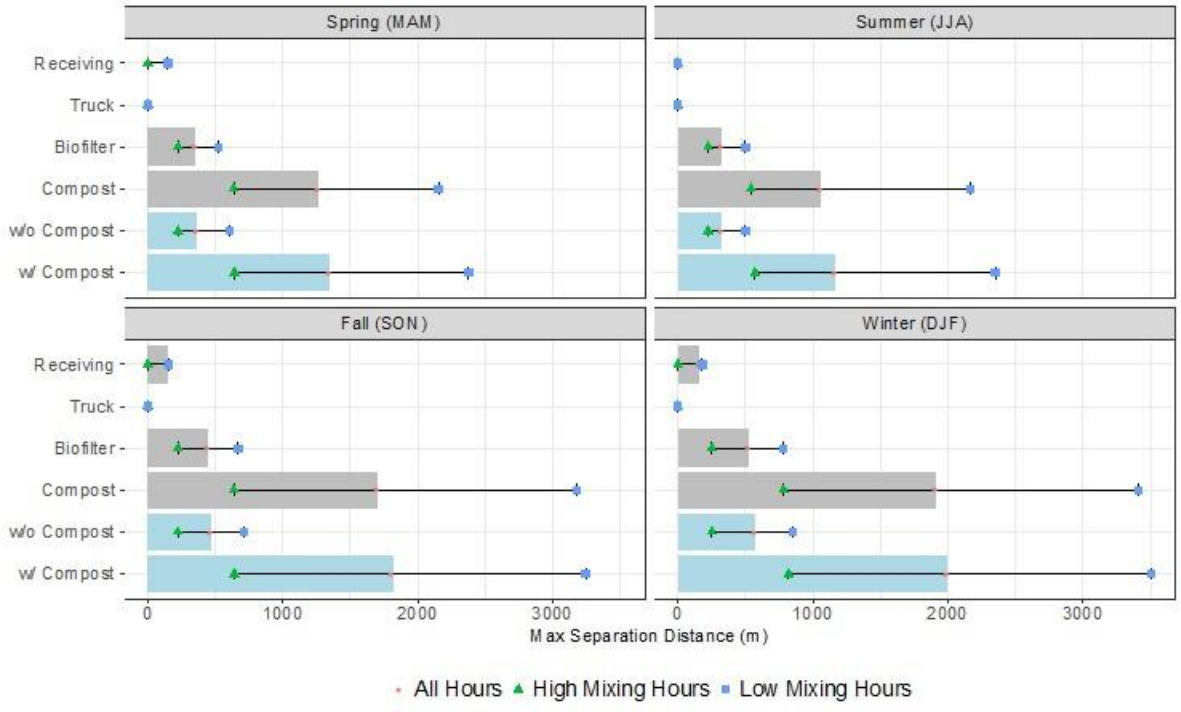

Atmospheric dispersion modeled for ZWEDC location. Odor threshold = 5 ou/m^3 and exceedance probability = 2 percent. Grey bars indicate individual sources and the blue indicate all sources combined.

Source: Lawrence Berkeley National Laboratory

Odor Dispersion at Varying Operational Scales

To extend our analysis results to facilities with a wider range of waste processing capacities and atmospheric mixing conditions similar to the ZWEDC location, we simulated the odor dispersion for operation scales of 0.5, 1, 1.5, and 2 times the full scale ZWEDC capacity (90,000 ton of organic waste per year). The emission rates used are listed in the table below. We consider a single biofilter or a single compost windrow as the fixed unit source, and assume the same per area emission rates and only vary the dimensions of the source layouts by plant scales.

Table B-6: Odor Emission Rates by Sources and Facility Scale

Source	Full Scale (1x)	0.5x Scale	1.5x Scale	2x Scale
RecStor1	3.4E+03	1.7E+03	5.1E+03	6.7E+03
Stor2	1.8E+02	8.9E+01	2.7E+02	3.6E+02
Biofilter	2.2E+04	1.1E+04	3.4E+04	4.5E+04
Compost	2.9E+05	1.5E+05	4.4E+05	5.9E+05
Trucking	6.7E+02	3.4E+02	1.0E+03	1.3E+03

Odor emission rates have units of ou/s.

Source: Lawrence Berkeley National Laboratory

The spatial odor impact patterns (top 2 percent odor concentrations) are presented for cases without composting ("noCompost") and with composting ("AllAreaLine") in Figure B-19. The "noCompost" case represents organic waste dry AD plants without onsite outdoor composting as currently practiced at ZWEDC, the "AllAreaLine" case represents those with digestate composted onsite in an encased system similar to Z-Best.

Considering all seasons and all active hours, we observe that areas beyond 1000 m away from the facility are not significantly (black contours in Figure B-19) affected by the facility's odor sources with no onsite composting. This is true considering all the operational scales from 45,000 tons to 180,000 tons of organic waste processing capacities and across all seasons (Figure B-19).

For the onsite composting case, the offsite impact exceeds 2000 m downwind of the facility even at the lowest capacity level considered here (45,000 tons) during the hours with low atmospheric mixing in fall and winter Figure B-20. Seasonal variations in Figure B-20 and Figure 55 indicate the spatial extents of odor impacts with most of the cases exceeding 3000 meters downwind of the facility during low mixing hours.

There are significant odor challenges for facilities to consider with regard to onsite composting that may occur with similar meteorological patterns, especially for those within 3000 m of populated areas. Much greater separation distances (> 3000 m) need to be considered to limit the offsite odor impact from onsite composting.

Figure B-19: Top 2 Percent Odor Exposure by Organic Waste Processing Scale

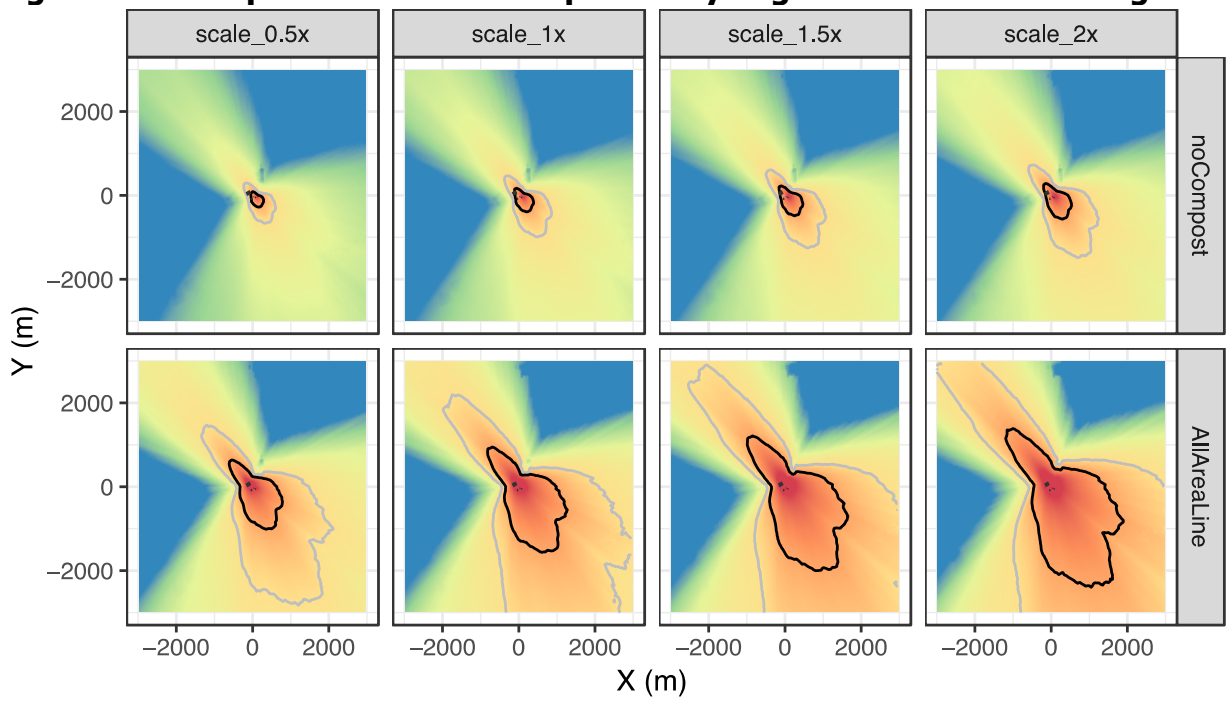

Atmospheric dispersion modeled for ZWEDC location. Same annotation and legend as Figure B-15.

Source: Lawrence Berkeley National Laboratory

Figure B-20: Maximum Separation Distances for Each Source by Season and Facility Scale

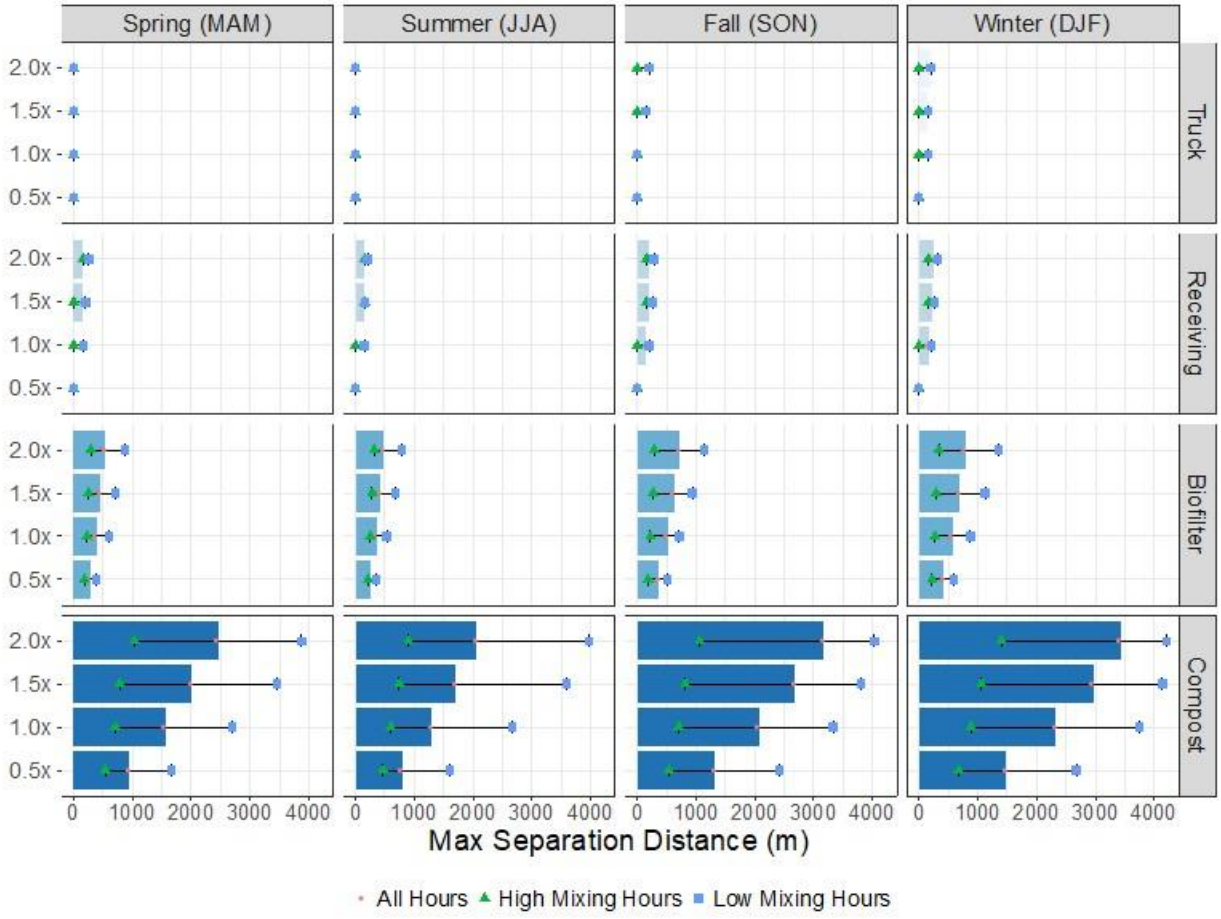

Atmospheric dispersion modeled for ZWEDC location.

Source: Lawrence Berkeley National Laboratory

More generally, we examined the relationship between odor unit emission rates and maximum separation distances for the range of emissions from 100 to 10^6 ou/m^3 (Figure B-21). We fit the relationship using data greater than 500 m separation distance in order to avoid influence of horizontal resolution (50 m) of the receptor domain. There are strong log linear relationships between the two variables which are governed by atmospheric mixing conditions and seasonality. Source geometry has a minor impact on the relationship after 500 m of separation distances. Despite some seasonal variations, we can see at below or around 10^5 ou/s emissions will generally have odor impacts limited within 2000 m away from ZWEDC, which is the case for all sources except composting at ZWEDC. This finding is useful to determine separation distance with existing emission sources or to inform allowable emission limits within specific source-receptor distances.

Figure B-21: Relationship between Separation Distances and Odor Emission Rates

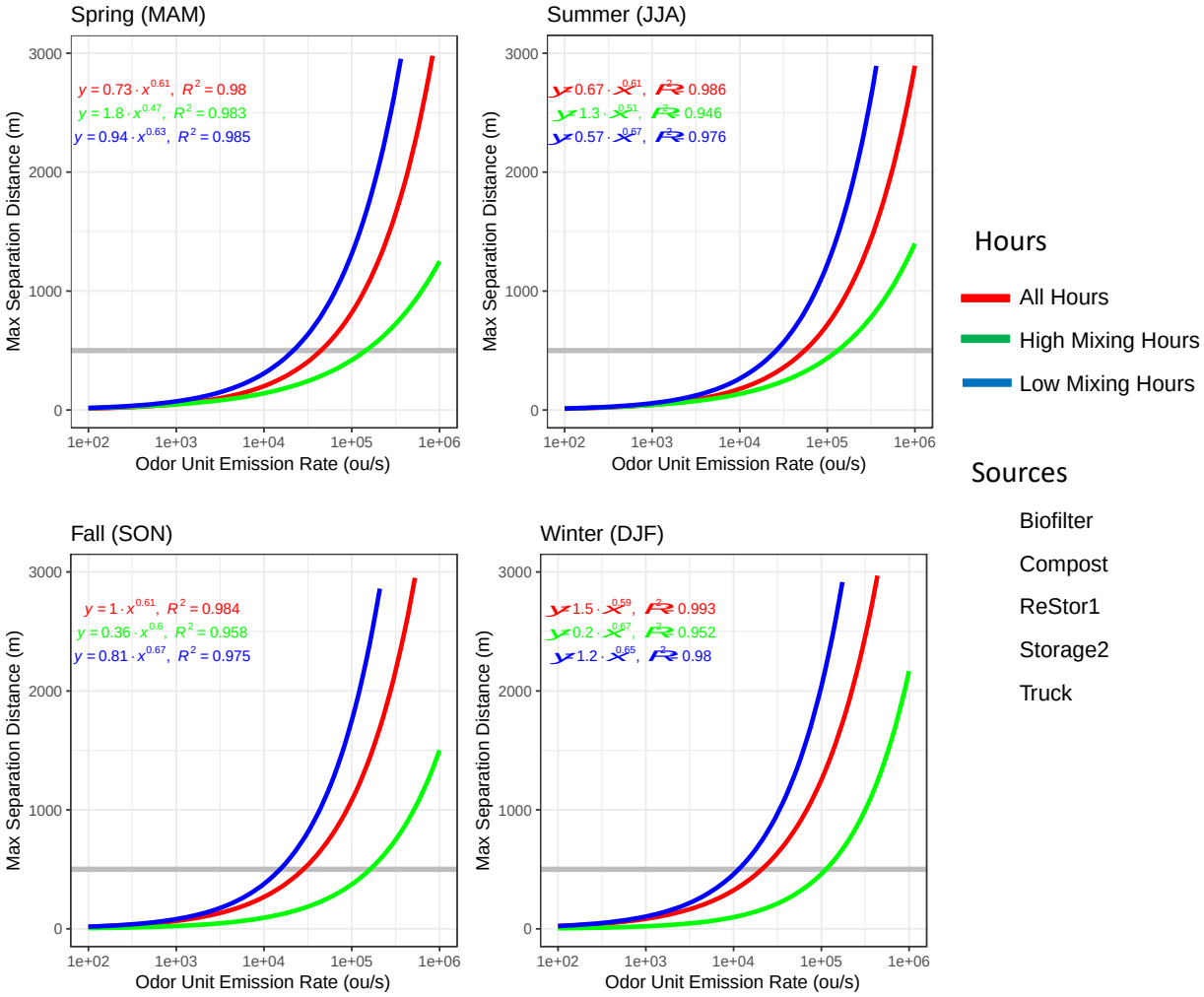

Data points and lines are color coded by the hours for which the separation distances are evaluated. Emission source types are indicated by symbol shapes.

Source: Lawrence Berkeley National Laboratory

APPENDIX C:
Additional Material on Life Cycle Assessment

Table C-1: Emission Factors (kg Per Unit Input).

Parameters	CO_2	CH_4	N_2O	CO	NO_x	$PM_{2.5}$	SO_2	VOC	NH_3	Sources and Assumptions
atrazine.kg	8.6E+00	3.9E-05	3.2E-05	2.0E-03	2.9E-02	7.8E-04	2.3E-04	0.0E+00	0.0E+00	GREET (Wang 2008)
atrazine_brazil.kg	8.6E+00	0.0E+00	0.0E+00	0.0E+00	0.0E+00	0.0E+00	0.0E+00	0.0E+00	0.0E+00	GREET (Wang 2008)
insecticide.kg	1.2E+01	0.0E+00	0.0E+00	0.0E+00	0.0E+00	0.0E+00	0.0E+00	0.0E+00	0.0E+00	GREET (Wang 2008)
insecticide_brazil.kg	1.2E+01	0.0E+00	0.0E+00	0.0E+00	0.0E+00	0.0E+00	0.0E+00	0.0E+00	0.0E+00	GREET (Wang 2008)
cellulase.kg	1.1E-01	0.0E+00	0.0E+00	0.0E+00	0.0E+00	0.0E+00	0.0E+00	0.0E+00	0.0E+00	GREET (Wang 2008)
alpha_amylase.kg	2.5E-01	0.0E+00	0.0E+00	0.0E+00	0.0E+00	0.0E+00	0.0E+00	0.0E+00	0.0E+00	GREET (Wang 2008)
gluco_amylase.kg	6.3E-01	0.0E+00	0.0E+00	0.0E+00	0.0E+00	0.0E+00	0.0E+00	0.0E+00	0.0E+00	GREET (Wang 2008)
lime.kg	9.4E-01	0.0E+00	6.0E-07	6.0E-05	2.3E-03	1.2E-05	5.6E-05	0.0E+00	0.0E+00	Assumed slaked lime at a biorefinery; Process emissions from (EPA 2013); Combustion emissions

Parameters	CO_2	CH_4	N_2O	CO	NO_x	$PM_{2.5}$	SO_2	VOC	NH_3	Sources and Assumptions
										calculated based on 80% heat conversion efficiency, assuming natural gas as a fuel and using energy consumption from (Research Triangle Institute 2000)
caco3.kg	1.6E-01	0.0E+00	1.1E-06	4.3E-05	6.5E-04	1.0E-05	2.9E-07	0.0E+00	0.0E+00	GREET (Wang 2008)
h2so4.kg	0.0E+00	0.0E+00	4.6E-08	1.7E-06	5.0E-06	1.6E-07	2.0E-03	0.0E+00	0.0E+00	Assumed 99.7% conversion of sulfur; GREET (Wang 2008); (EPA 1993)
hcl.kg	5.3E-01	0.0E+00	0.0E+00	0.0E+00	0.0E+00	0.0E+00	0.0E+00	0.0E+00	0.0E+00	Based on natural gas consumption; (ecoinvent 2018)
naoh.kg	2.1E-01	2.0E-05	1.5E-05	0.0E+00	0.0E+00	0.0E+00	0.0E+00	0.0E+00	0.0E+00	(Wicke et al. 2008)
csl.kg	1.1E-01	0.0E+00	0.0E+00	0.0E+00	0.0E+00	0.0E+00	0.0E+00	0.0E+00	0.0E+00	GREET (Wang 2008)
glucose.kg	8.8E-03	0.0E+00	0.0E+00	0.0E+00	0.0E+00	0.0E+00	0.0E+00	0.0E+00	0.0E+00	GREET (Wang 2008)
corn_starch.kg	2.0E-01	0.0E+00	0.0E+00	0.0E+00	0.0E+00	0.0E+00	0.0E+00	0.0E+00	0.0E+00	GREET (Wang 2008)
k2o.kg	3.0E-01	0.0E+00	2.4E-06	9.3E-05	1.2E-03	2.0E-05	6.4E-07	0.0E+00	0.0E+00	GREET (Wang 2008)

Parameters	CO_2	CH_4	N_2O	CO	NO_x	$PM_{2.5}$	SO_2	VOC	NH_3	Sources and Assumptions
ammonia.kg	2.9E+00	0.0E+00	0.0E+00	7.9E-03	0.0E+00	0.0E+00	2.9E-05	0.0E+00	0.0E+00	Process emissions from (EPA 1993); Emission factors from (EPA 2009)
n.kg	2.3E+00	0.0E+00	1.5E-02	1.5E-03	8.1E-03	2.3E-04	1.3E-05	0.0E+00	0.0E+00	GREET (Wang 2008)
urea.kg	2.6E-01	0.0E+00	0.0E+00	0.0E+00	0.0E+00	0.0E+00	0.0E+00	0.0E+00	0.0E+00	GREET (Wang 2008)
p2o5.kg	3.5E-01	0.0E+00	1.3E-06	5.5E-05	1.6E-03	2.3E-05	3.6E-07	0.0E+00	0.0E+00	GREET (Wang 2008)
p.kg	1.2E+00	0.0E+00	0.0E+00	0.0E+00	0.0E+00	0.0E+00	0.0E+00	0.0E+00	0.0E+00	GREET (Wang 2008)
nacl.kg	4.9E-02	0.0E+00	0.0E+00	0.0E+00	0.0E+00	0.0E+00	0.0E+00	0.0E+00	0.0E+00	GREET (Wang 2008)
triethylaluminum.kg	4.8E+00	0.0E+00	0.0E+00	0.0E+00	0.0E+00	0.0E+00	0.0E+00	0.0E+00	0.0E+00	Based on stoichiometry; Assumes aluminum is recycled
coal.MJ	1.9E-04	2.0E-10	5.1E-11	5.2E-06	1.0E-06	2.2E-08	8.1E-09	6.7E-06	0.0E+00	GREET (Wang 2008)
diesel.MJ	5.1E-03	3.6E-06	2.4E-07	2.2E-06	4.1E-06	4.6E-07	1.6E-05	2.9E-06	0.0E+00	GREET (Wang 2008)
rfo.MJ	7.2E-02	0.0E+00	1.4E-08	5.2E-07	2.1E-06	8.3E-08	3.7E-09	0.0E+00	0.0E+00	GREET (Wang 2008)
refgas.MJ	7.1E-02	0.0E+00	0.0E+00	0.0E+00	0.0E+00	0.0E+00	0.0E+00	0.0E+00	0.0E+00	GREET (Wang 2008)

Parameters	CO_2	CH_4	N_2O	CO	NO_x	$PM_{2.5}$	SO_2	VOC	NH_3	Sources and Assumptions
ethylene.MJ	5.5E-02	0.0E+00	0.0E+00	0.0E+00	0.0E+00	0.0E+00	0.0E+00	0.0E+00	0.0E+00	Assumed 10% loss by energy in production (crude) emitted; Used simple energy content-based allocation for ethylene (byproduct of cracking heavy molecules in petroleum refinery)
propene.MJ	7.1E-02	0.0E+00	0.0E+00	0.0E+00	0.0E+00	0.0E+00	0.0E+00	0.0E+00	0.0E+00	Assumed 10% loss by energy in production (crude) emitted; Used simple energy content-based allocation for propene (byproduct of cracking heavy molecules in petroleum refinery)
acetone.kg	1.8E+00	1.7E-02	7.1E-09	1.9E-03	4.6E-03	1.5E-04	6.9E-03	3.5E-03	9.7E-09	Assume production via cumene process; (ecoinvent 2019)
crudeoil.MJ	6.1E-03	0.0E+00	1.4E-08	5.4E-07	1.6E-06	4.9E-08	3.9E-09	0.0E+00	0.0E+00	GREET (Wang 2008)
electricity.US.kWh	4.5E-01	3.6E-05	5.9E-06	0.0E+00	3.3E-04	0.0E+00	3.6E-04	0.0E+00	0.0E+00	(eGRID2016 2018)
electricity.NGCC.kWh	1.8E-01	0.0E+00	0.0E+00	8.3E-05	9.9E-05	1.0E-06	4.0E-06	2.0E-06	0.0E+00	(EIA 1999)
electricity.Coal.kWh	9.8E-01	1.1E-05	1.6E-05	0.0E+00	9.5E-04	0.0E+00	2.9E-03	0.0E+00	0.0E+00	(eGRID2012 2012)

Parameters	CO_2	CH_4	N_2O	CO	NO_x	$PM_{2.5}$	SO_2	VOC	NH_3	Sources and Assumptions
electricity.WECC.kWh	4.3E-01	9.5E-06	5.8E-06	0.0E+00	5.1E-04	0.0E+00	3.5E-04	0.0E+00	0.0E+00	(eGRID2012 2012)
electricity.MRO.kWh	7.2E-01	1.3E-05	1.3E-05	0.0E+00	1.0E-03	0.0E+00	2.0E-03	0.0E+00	0.0E+00	(eGRID2012 2012)
electricity.TRE.kWh	5.2E-01	7.6E-06	5.9E-06	0.0E+00	3.3E-04	0.0E+00	1.0E-03	0.0E+00	0.0E+00	(eGRID2012 2012)
gasoline.MJ	7.5E-02	6.9E-06	1.6E-07	5.6E-06	1.7E-05	1.9E-07	5.7E-05	0.0E+00	0.0E+00	Assumed sufficiently similar to diesel; (Sheehan et al. 1998)
h2.kg	7.2E+00	6.0E-02	4.0E-05	6.0E-03	1.2E-02	2.0E-03	9.5E-03	0.0E+00	0.0E+00	
naturalgas.MJ	1.0E-03	1.2E-04	1.7E-08	6.6E-07	1.9E-06	6.0E-08	4.7E-09	6.1E-06	0.0E+00	(EPA 2013); (EIA 2019); GREET (Wang 2008)
uranium.kg	7.1E+01	0.0E+00	1.2E-03	4.7E-02	1.3E-01	4.2E-03	3.3E-04	2.5E-02	0.0E+00	(Lenzen 2008); GREET (Wang 2008)
steel_chinese.kg	4.0E-01	0.0E+00	5.9E-06	2.3E-04	1.1E-03	2.2E-05	1.3E-05	0.0E+00	0.0E+00	(Scown et al. 2011); GREET (Wang 2008)
flatbedtruck.mt_km	1.2E-01	0.0E+00	0.0E+00	8.6E-06	2.5E-05	2.8E-06	2.8E-06	0.0E+00	0.0E+00	(Cohon et al. 2010)
tankertruck.mt_km	8.5E-02	0.0E+00	0.0E+00	0.0E+00	1.7E-05	1.9E-06	1.9E-06	0.0E+00	0.0E+00	(Cohon et al. 2010)
gaspipeline.mt_km	0.0E+00	1.6E-03	0.0E+00	0.0E+00	0.0E+00	0.0E+00	0.0E+00	0.0E+00	0.0E+00	Assume all natural gas travels 4000 km (Spath and Mann 2001); (EPA 2013)

Parameters	CO_2	CH_4	N_2O	CO	NO_x	$PM_{2.5}$	SO_2	VOC	NH_3	Sources and Assumptions
rail.mt_km	1.9E-02	0.0E+00	0.0E+00	0.0E+00	3.8E-06	4.3E-07	4.3E-07	0.0E+00	0.0E+00	(Cohon et al. 2010)
barge.mt_km	2.2E-02	0.0E+00	0.0E+00	0.0E+00	4.6E-06	5.1E-07	5.1E-07	0.0E+00	0.0E+00	(Cohon et al. 2010)
marinetanker.mt_km	6.9E-03	8.0E-08	0.0E+00	1.4E-06	1.4E-05	9.0E-07	4.5E-07	0.0E+00	0.0E+00	(Cohon et al. 2010)
corn.bushel	6.7E-01	0.0E+00	0.0E+00	0.0E+00	0.0E+00	0.0E+00	0.0E+00	0.0E+00	0.0E+00	GREET (Wang 2008)
landfill_mixedorganics.wet_kg	0.0E+00	2.7E-02	0.0E+00	1.9E-05	1.4E-05	4.4E-06	4.5E-05	1.5E-07	4.7E-05	WARM (USEPA 2018); (Roe et al. 2004)
organics_composting_wet.kg	0.0E+00	1.5E-03	8.7E-05	2.7E-04	0.0E+00	0.0E+00	0.0E+00	5.9E-04	1.6E-03	GHGs (Amlinger et al. 2008); ammonia (Roe et al. 2004); carbon monoxide (Hellebrand and Schade 2008); VOCs (Smet et al. 1999)
compost_application.kg	-1.5E-01	0.0E+00	0.0E+00	0.0E+00	0.0E+00	0.0E+00	0.0E+00	0.0E+00	0.0E+00	(CARB 2017)
biosolids_land_application_dry.kg	0	1.3E-04	2.1E-04	0.0E+00	0.0E+00	0.0E+00	0.0E+00	0.0E+00	5.5E-05	(Holly et al. 2017); Phyllis2 (ECN.TNO n.d.); (Roe et al. 2004)

Parameters	CO_2	CH_4	N_2O	CO	NO_x	$PM_{2.5}$	SO_2	VOC	NH_3	Sources and Assumptions
biogas_flare.m3	0.0E+00	0.0E+00	1.2E-06	2.5E-04	2.1E-04	5.5E-06	7.3E-04	5.0E-06	0.0E+00	Measured, reported in Preble et al (In prep)
biogas_CHP.m3	0.0E+00	5.7E-03	-1.9E-06	5.5E-04	1.1E-04	5.5E-06	1.3E-04	4.6E-05	0.0E+00	Measured, reported in Preble et al (In prep)
biogas_biofilter.m3	7.2E-01	3.3E-02	1.9E-04	2.0E-04	0.0E+00	0.0E+00	1.0E-04	0.0E+00	1.6E-03	Measured, reported in Preble et al (In prep)
outdoor_compost.wet_kg	0.0E+00	4.5E-03	1.4E-05	1.1E-04	0.0E+00	0.0E+00	0.0E+00	2.2E-05	1.2E-03	Measured, reported in Preble et al (In prep)
naturalgas_combust.MJ	5.0E-02	0.0E+00	0.0E+00	0.0E+00	0.0E+00	0.0E+00	0.0E+00	0.0E+00	0.0E+00	Based on stoichiometry of methane combustion; Assumes perfect oxidation
diesel_combust.MJ	7.5E-02	0.0E+00	0.0E+00	2.1E-05	1.5E-05	4.6E-07	8.2E-06	2.9E-06	0.0E+00	GREET (Wang 2008)

Source: Lawrence Berkeley National Laboratory

Table C-2: Upstream Material and Energy Requirements.

primary	Input Output References	value	Source
atrazine_brazil.kg	diesel.MJ	4.9E+01	GREET (Wang 2008)
	rfo.MJ	4.9E+01	GREET (Wang 2008)
	electricity.NGCC.kWh	7.6E+00	GREET (Wang 2008)
	naturalgas.MJ	3.7E+01	GREET (Wang 2008)
insecticide.kg	diesel.MJ	1.4E+02	GREET (Wang 2008)
	electricity.US.kWh	1.2E+01	GREET (Wang 2008)
	naturalgas.MJ	5.3E+01	GREET (Wang 2008)
	tankertruck.mt_km	4.3E-01	GREET (Wang 2008)
	rail.mt_km	1.3E+00	GREET (Wang 2008)
insecticide_brazil.kg	diesel.MJ	1.4E+02	GREET (Wang 2008)
	electricity.NGCC.kWh	1.2E+01	GREET (Wang 2008)
	naturalgas.MJ	5.3E+01	GREET (Wang 2008)
cellulase.kg	csl.kg	1.8E-01	GREET (Wang 2008)
	glucose.kg	1.3E+00	GREET (Wang 2008)
	ammonia.kg	6.0E-02	GREET (Wang 2008)
	glycerin.kg	4.0E-01	GREET (Wang 2008)
	nacl.kg	2.0E-01	GREET (Wang 2008)
	electricity.MRO.kWh	1.1E+00	GREET (Wang 2008)
	naturalgas.MJ	2.2E+00	GREET (Wang 2008)
alpha_amylase.kg	glucose.kg	7.0E-04	GREET (Wang 2008)
	electricity.MRO.kWh	1.9E+00	GREET (Wang 2008)
	naturalgas.MJ	5.0E+00	GREET (Wang 2008)
gluco_amylase.kg	glucose.kg	4.7E-01	GREET (Wang 2008)
	corn_starch.kg	4.7E-01	GREET (Wang 2008)
	electricity.MRO.kWh	8.9E+00	GREET (Wang 2008)
	naturalgas.MJ	1.3E+01	GREET (Wang 2008)

primary	Input Output References	value	Source
lime.kg	caco3.kg	1.4E+00	GREET (Wang 2008)
	coal.MJ	4.0E+00	GREET (Wang 2008)
	diesel.MJ	3.2E-01	GREET (Wang 2008)
	electricity.US.kWh	8.2E-02	GREET (Wang 2008)
	naturalgas.MJ	8.2E-01	GREET (Wang 2008)
	tankertruck.mt_km	1.9E-01	Distance from Gabi (Thinkstep 2018)
caco3.kg	diesel.MJ	1.4E+00	GREET (Wang 2008)
	electricity.US.kWh	6.5E-03	GREET (Wang 2008)
	naturalgas.MJ	1.2E+00	GREET (Wang 2008)
	flatbedtruck.mt_km	8.0E-02	GREET (Wang 2008)
h2so4.kg	electricity.US.kWh	6.6E-02	GREET (Wang 2008)
	tankertruck.mt_km	4.3E-01	GREET (Wang 2008)
	rail.mt_km	1.3E+00	GREET (Wang 2008)
hcl.kg	coal.MJ	9.2E-01	GREET (Wang 2008)
	diesel.MJ	2.7E-02	GREET (Wang 2008)
	rfo.MJ	2.7E-02	GREET (Wang 2008)
	electricity.US.kWh	9.7E-01	GREET (Wang 2008)
	gasoline.MJ	2.3E-03	GREET (Wang 2008)
	naturalgas.MJ	8.8E+00	GREET (Wang 2008)
naoh.kg	coal.MJ	3.8E-01	GREET (Wang 2008)
	rfo.MJ	2.0E-01	GREET (Wang 2008)
	electricity.US.kWh	1.8E+00	GREET (Wang 2008)
	naturalgas.MJ	3.3E+00	GREET (Wang 2008)
	tankertruck.mt_km	4.3E-01	GREET (Wang 2008)
	rail.mt_km	1.3E+00	GREET (Wang 2008)

primary	Input Output References	value	Source
csl.kg	electricity.MRO.kWh	6.5E-03	GREET (Wang 2008)
	naturalgas.MJ	2.2E+00	GREET (Wang 2008)
	corn.bushel	2.2E-01	GREET (Wang 2008)
glucose.kg	naoh.kg	2.8E-06	GREET (Wang 2008)
	corn_starch.kg	9.4E-01	GREET (Wang 2008)
	naturalgas.MJ	1.7E-01	GREET (Wang 2008)
corn_starch.kg	electricity.MRO.kWh	9.0E-02	GREET (Wang 2008)
	naturalgas.MJ	4.0E+00	GREET (Wang 2008)
	corn.bushel	6.9E-02	GREET (Wang 2008)
k2o.kg	diesel.MJ	2.4E+00	GREET (Wang 2008)
	naturalgas.MJ	2.7E+00	GREET (Wang 2008)
	tankertruck.mt_km	4.3E-01	GREET (Wang 2008)
	rail.mt_km	1.3E+00	GREET (Wang 2008)
ammonia.kg	naturalgas.MJ	4.0E+01	GREET (Wang 2008)
	tankertruck.mt_km	4.3E-01	GREET (Wang 2008)
	rail.mt_km	1.3E+00	GREET (Wang 2008)
n.kg	diesel.MJ	1.8E+00	GREET (Wang 2008)
	naturalgas.MJ	4.4E+01	GREET (Wang 2008)
	tankertruck.mt_km	4.3E-01	GREET (Wang 2008)
	rail.mt_km	1.3E+00	GREET (Wang 2008)
urea.kg	electricity.US.kWh	3.2E-01	GREET (Wang 2008)
	naturalgas.MJ	8.1E+00	GREET (Wang 2008)
	tankertruck.mt_km	4.3E-01	GREET (Wang 2008)
	rail.mt_km	1.3E+00	GREET (Wang 2008)

primary	Input Output References	value	Source
p2o5.kg	diesel.MJ	3.9E+00	GREET (Wang 2008)
	naturalgas.MJ	1.5E+00	GREET (Wang 2008)
	tankertruck.mt_km	4.3E-01	GREET (Wang 2008)
	rail.mt_km	1.3E+00	GREET (Wang 2008)
p.kg	electricity.NGCC.kWh	6.4E+00	GREET (Wang 2008)
	naturalgas.MJ	2.3E+01	GREET (Wang 2008)
nacl.kg	rfo.MJ	1.3E-01	GREET (Wang 2008)
	electricity.US.kWh	7.1E-02	GREET (Wang 2008)
	naturalgas.MJ	7.9E-01	GREET (Wang 2008)
triethylaluminum.kg	ethylene.MJ	7.5E+01	Based on stoichiometry
	h2.kg	2.7E-02	Based on stoichiometry
	tankertruck.mt_km	4.3E-01	GREET (Wang 2008)
	rail.mt_km	1.3E+00	GREET (Wang 2008)
coal.MJ	diesel.MJ	2.3E-03	GREET (Wang 2008)
	rfo.MJ	2.5E-04	GREET (Wang 2008)
	electricity.US.kWh	2.1E-03	GREET (Wang 2008)
	gasoline.MJ	1.9E-04	GREET (Wang 2008)
	naturalgas.MJ	5.8E-05	GREET (Wang 2008)
	flatbedtruck.mt_km	2.6E-03	GREET (Wang 2008)
	rail.mt_km	5.3E-02	GREET (Wang 2008)
	barge.mt_km	2.2E-02	GREET (Wang 2008)
diesel.MJ	refgas.MJ	2.4E-02	GREET (Wang 2008)
	crudeoil.MJ	1.0E+00	GREET (Wang 2008)
	electricity.US.kWh	2.6E-03	GREET (Wang 2008)
	naturalgas.MJ	2.4E-02	GREET (Wang 2008)
	tankertruck.mt_km	3.5E-03	(Sheehan et al. 1998)
	liquidpipeline.mt_km	2.1E-02	(Sheehan et al. 1998)

primary	Input Output References	value	Source
rfo.MJ	refgas.MJ	1.6E-02	GREET (Wang 2008)v
	crudeoil.MJ	1.0E+00	-
	electricity.US.kWh	2.6E-03	GREET (Wang 2008)
	naturalgas.MJ	1.6E-02	GREET (Wang 2008)
	tankertruck.mt_km	3.5E-03	GREET (Wang 2008)
	liquidpipeline.mt_km	2.1E-02	GREET (Wang 2008)
refgas.MJ	crudeoil.MJ	1.0E+00	-
ethylene.MJ	diesel.MJ	6.2E-05	GREET (Wang 2008)
	refgas.MJ	2.6E-02	GREET (Wang 2008)
	electricity.TRE.kWh	3.1E-03	GREET (Wang 2008)
	naturalgas.MJ	1.1E+00	GREET (Wang 2008)
	tankertruck.mt_km	5.2E-04	GREET (Wang 2008)
	liquidpipeline.mt_km	1.6E-03	GREET (Wang 2008)
propene.MJ	crudeoil.MJ	1.0E+00	-
acetone.kg	h2so4.kg	4.9E-04	Ecoinvent (Wernet et al. 2016)
	propene.MJ	1.5E+01	Ecoinvent (Wernet et al. 2016)
	electricity.US.kWh	2.7E-01	Ecoinvent (Wernet et al. 2016)
	gasoline.MJ	2.7E+01	Ecoinvent (Wernet et al. 2016)
	naturalgas.MJ	1.9E+00	Ecoinvent (Wernet et al. 2016)
	tankertruck.mt_km	4.3E-01	GREET (Wang 2008)
	rail.mt_km	1.3E+00	GREET (Wang 2008)

primary	Input Output References	value	Source
crudeoil.MJ	crudeoil.MJ	7.5E-02	GREET (Wang 2008)
	electricity.US.kWh	1.5E-03	GREET (Wang 2008)
	naturalgas.MJ	1.6E-02	GREET (Wang 2008)
	tankertruck.mt_km	5.5E-03	GREET (Wang 2008)
	liquidpipeline.mt_km	2.9E-02	GREET (Wang 2008)
	rail.mt_km	2.4E-02	GREET (Wang 2008)
	barge.mt_km	4.4E-03	GREET (Wang 2008)
	marinetanker.mt_km	1.1E-01	GREET (Wang 2008)
electricity.US.kWh	coal.MJ	5.0E+00	(eGRID2016 2018)
	diesel.MJ	6.7E-03	(eGRID2016 2018)
	rfo.MJ	3.0E-02	(eGRID2016 2018)
	electricity.US.kWh	6.5E-02	(eGRID2016 2018)
	naturalgas.MJ	1.9E+00	(eGRID2016 2018)
	uranium.kg	2.8E-07	(eGRID2016 2018)
electricity.NGCC.kWh	electricity.NGCC.kWh	6.5E-02	(eGRID2016 2018)
	naturalgas.MJ	7.2E+00	(eGRID2016 2018)
electricity.Coal.kWh	coal.MJ	1.1E+01	(eGRID2016 2018)
	electricity.Coal.kWh	6.5E-02	(eGRID2016 2018)
electricity.WECC.kWh	coal.MJ	3.3E+00	(eGRID2016 2018)
	diesel.MJ	9.4E-04	(eGRID2016 2018)
	electricity.WECC.kWh	8.2E-02	(eGRID2016 2018)
	naturalgas.MJ	2.6E+00	(eGRID2016 2018)
	uranium.kg	1.3E-07	(eGRID2016 2018)

primary	Input Output References	value	Source
electricity.MRO.kWh	coal.MJ	7.9E+00	(eGRID2016 2018)
	diesel.MJ	3.7E-03	(eGRID2016 2018)
	electricity.MRO.kWh	5.8E-02	(eGRID2016 2018)
	naturalgas.MJ	2.0E-01	(eGRID2016 2018)
	uranium.kg	1.9E-07	(eGRID2016 2018)
electricity.TRE.kWh	coal.MJ	3.7E+00	(eGRID2016 2018)
	diesel.MJ	1.9E-04	(eGRID2016 2018)
	electricity.TRE.kWh	8.0E-02	(eGRID2016 2018)
	naturalgas.MJ	3.9E+00	(eGRID2016 2018)
	uranium.kg	1.7E-07	(eGRID2016 2018)
gasoline.MJ	refgas.MJ	3.7E-02	GREET (Wang 2008)
	crudeoil.MJ	1.0E+00	GREET (Wang 2008)
	electricity.US.kWh	2.5E-03	GREET (Wang 2008)
	naturalgas.MJ	3.7E-02	GREET (Wang 2008)
	tankertruck.mt_km	3.5E-03	GREET (Wang 2008)
	liquidpipeline.mt_km	2.1E-02	GREET (Wang 2008)
h2.kg	electricity.US.kWh	2.7E-01	(Spath and Mann 2001)
	naturalgas.MJ	1.4E+02	(Spath and Mann 2001)
	gaspipeline.mt_km	1.2E+00	GREET (Wang 2008)
naturalgas.MJ	naturalgas.MJ	2.0E-02	GREET (Wang 2008)
	gaspipeline.mt_km	7.7E-02	GREET (Wang 2008)
uranium.kg	electricity.WECC.kWh	1.0E+02	(Scown et al. 2011)
	electricity.MRO.kWh	4.4E+01	(Scown et al. 2011)
	naturalgas.MJ	1.4E+03	(Lenzen 2008)
	flatbedtruck.mt_km	4.5E+00	GREET (Wang 2008)

primary	Input Output References	value	Source
steel_chinese.kg	coal.MJ	6.9E-01	GREET (Wang 2008)
	electricity.Coal.kWh	8.2E-01	GREET (Wang 2008)
	electricity.Renewables.kWh	3.5E-01	GREET (Wang 2008)
	naturalgas.MJ	6.8E+00	GREET (Wang 2008)
	rail.mt_km	8.0E-01	GREET (Wang 2008)
	barge.mt_km	1.0E+01	GREET (Wang 2008)
flatbedtruck.mt_km	diesel.MJ	1.8E+00	Fuel economy from (Strogen et al. 2012)
	flatbedtruck.mt_km	2.5E-01	(Sheehan et al. 1998); assumption of 25% empty miles
tankertruck.mt_km	diesel.MJ	1.2E+00	Fuel economy from (Strogen et al. 2012)
	tankertruck.mt_km	2.5E-01	(Sheehan et al. 1998); assumption of 25% empty miles
rail.mt_km	diesel.MJ	2.7E-01	Fuel economy from (Strogen et al. 2012)
	rail.mt_km	2.5E-01	(Sheehan et al. 1998); assumption of 25% empty miles
barge.mt_km	diesel.MJ	3.2E-01	Fuel economy from (Strogen et al. 2012)
	barge.mt_km	2.5E-01	Assume 25% empty miles
marinetanker.mt_km	rfo.MJ	1.0E-01	Average of crude tanker & product tanker energy intensities (Strogen et al. 2012)
	marinetanker.mt_km	2.5E-01	Assume 25% empty miles

primary	Input Output References	value	Source
corn.bushel	atrazine.kg	3.5E-03	GREET (Wang 2008)
	glyphosate.kg	3.5E-03	GREET (Wang 2008)
	insecticide.kg	6.0E-05	GREET (Wang 2008)
	caco3.kg	1.1E+00	GREET (Wang 2008)
	k2o.kg	1.5E-01	GREET (Wang 2008)
	n.kg	4.2E-01	GREET (Wang 2008)
	p2o5.kg	1.5E-01	GREET (Wang 2008)
	diesel.MJ	9.6E+00	Assumed all energy provided diesel; GREET (Wang 2008)
	flatbedtruck.mt_km	2.0E+00	Assumed 50 miles; GREET (Wang 2008)
compost_application.kg	n.kg	-1.0E-02	(CARB 2017)
outdoor_compost.wet_kg	diesel.MJ	5.8E-02	(CARB 2017)
	electricity.US.kWh	7.9E-03	(CARB 2017)
	flatbedtruck.mt_km	5.0E-02	Assume 50 km
organics_composting_wet.kg	diesel.MJ	5.8E-02	(CARB 2017)
	electricity.US.kWh	7.9E-03	(CARB 2017)

Source: Lawrence Berkeley National Laboratory

Table C-3: Monte Carlo Simulation Inputs.

	Parameter	Model Value	Distribution Type	Distributional Parameters	Source/Assumption
CH_4	landfill_mixedorganics.wet_kg	2.70E-02	triangle	Min = 2.23E-02 Max = 3.00E-02	Distributional parameters calculated by varying landfill gas collection efficiency data from WARM model (USEPA 2018)
	organics_composting_wet.kg	2.09E-03	triangle	Min = 1.42E-04 Max = 7.63E-03	Minimum and maximum (Amlinger et al. 2008)
	biosolids_land_application_dry.kg	1.32E-04	triangle	Min = 1.19E-04 Max = 1.66E-04	Distribution from non-combustion emissions; varied carbon content of dry digestate, Phyllis2 (ECN.TNO n.d.)
CO_2	outdoor_compost.wet_kg	4.46E-03	triangle	Min = 1.27E-03 Max = 1.22E-02	Distributional parameters from measured data
	gasoline.MJ	7.48E-02	triangle	Min = 7.28E-02 Max = 7.92E-02	Combustion emissions distribution (Venkatesh et al. 2011)
	diesel_combust.MJ	7.53E-02	triangle	Min = 7.36E-02 Max = 8.01E-02	(Venkatesh et al. 2011)
N_2O	organics_composting_wet.kg	8.70E-05	triangle	Min = 2.20E-05 Max = 3.00E-04	Minimum and maximum (Amlinger et al. 2008)
CO	electricity.NGCC.kWh	9.00E-05	uniform	+/- 20%	
	landfill_mixedorganics.wet_kg	1.87E-05	triangle	Min = 1.31E-05 Max = 2.75E-05	Minimum and maximum from Ecoinvent (Wernet et al. 2016)
	organics_composting_wet.kg	5.22E-05	triangle	Min = 1.00E-06 Max = 1.11E-04	Minimum from Hellebrand and Schade 2008 and maximum from measured data
	biogas_CHP.m3	5.51E-04	normal	SD = 4.28E-05	Distributional parameters from measured data
	diesel_combust.MJ	2.10E-05	uniform	+/- 20%	

	Parameter	Model Value	Distribution Type	Distributional Parameters	Source/Assumption
NO_X	electricity.NGCC.kWh	1.08E-04	uniform	+/- 20%	
	landfill_mixedorganics.wet_kg	1.37E-05	triangle	Min = 2.39E-06 Max = 2.28E-05	Minimum and maximum from Ecoinvent (Wernet et al. 2016)
	biogas_CHP.m3	1.07E-04	normal	SD = 1.03E-04	Measured, reported in Preble et al (In prep)
	diesel_combust.MJ	1.49E-05	uniform	+/- 20%	
$PM_{2.5}$	electricity.NGCC.kWh	1.00E-06	uniform	+/- 20%	
	landfill_mixedorganics.wet_kg	4.44E-06	triangle	Min = 3.15E-06 Max = 6.70E-06	Minimum and maximum from Ecoinvent (Wernet et al. 2016)
	biogas_flare.m3	5.46E-06	triangle	Min = 5.11E-06 Max = 1.10E-05	Measured, reported in Preble et al (In prep)
	diesel_combust.MJ	4.60E-07	uniform	+/- 20%	
SO_2	electricity.NGCC.kWh	4.00E-06	uniform	+/- 20%	
	naturalgas.MJ	4.74E-09	uniform	+/- 20%	
	landfill_mixedorganics.wet_kg	4.54E-05	triangle	Min = 3.44E-05 Max = 4.96E-05	Minimum and maximum from Ecoinvent (Wernet et al. 2016)
	biogas_CHP.m3	1.32E-04	triangle	Min = 1.50E-06 Max = 5.68E-04	Distributional parameters from measured data
	diesel_combust.MJ	8.19E-06	uniform	+/- 20%	
VOC	electricity.NGCC.kWh	2.00E-06	uniform	+/- 20%	

	Parameter	Model Value	Distribution Type	Distributional Parameters	Source/Assumption
	naturalgas.MJ	6.10E-06	uniform	+/- 20%	
	landfill_mixedorganics.wet_kg	1.51E-07	triangle	Min = 1.51E-07 Max = 3.21E-07	Minimum and maximum from Ecoinvent (Wernet et al. 2016)
	biogas_CHP.m3	4.55E-05	triangle	Min = 5.00E-06 Max = 4.00E-04	Measured, reported in Preble et al (In prep)
NH_3	organics_composting_wet.kg	1.76E-03	triangle	Min = 1.14E-03 Max = 2.36E-03	Minimum and maximum (Roe et al. 2004)
	outdoor_compost.wet_kg	1.16E-03	triangle	Min = 6.70E-04 Max = 1.58E-03	Measured, reported in Preble et al (In prep)

Table C-4: Social Cost Multipliers - Marginal Costs ($/tonne of emission)

IAM	Location	$PM_{2.5}$	SO_2	NO_X	NH_3	VOC
EASIUR (Heo, Peter J. Adams, et al. 2016; Heo, Peter J Adams, et al. 2016)	ZWEDC facility (San Jose, CA 95134)	390250	34475	19743	108800	-
EASIUR (Heo, Peter J. Adams, et al. 2016; Heo, Peter J Adams, et al. 2016)	Z Best (Gilroy, CA 95020)	192500	32725	12823	43900	-
AP3 (Muller and Mendelsohn 2007)	Santa Clara County (FIPS: 06085)	523842.5	238548.2	86300.09	322440.8	23635.8

Table C-5

primary	Input Output References	value	Source
atrazine_brazil.kg	diesel.MJ	4.9E+01	GREET (Wang 2008)
	rfo.MJ	4.9E+01	GREET (Wang 2008)
	electricity.NGCC.kWh	7.6E+00	GREET (Wang 2008)
	naturalgas.MJ	3.7E+01	GREET (Wang 2008)
insecticide.kg	diesel.MJ	1.4E+02	GREET (Wang 2008)
	electricity.US.kWh	1.2E+01	GREET (Wang 2008)
	naturalgas.MJ	5.3E+01	GREET (Wang 2008)
	tankertruck.mt_km	4.3E-01	GREET (Wang 2008)
	rail.mt_km	1.3E+00	GREET (Wang 2008)
insecticide_brazil.kg	diesel.MJ	1.4E+02	GREET (Wang 2008)
	electricity.NGCC.kWh	1.2E+01	GREET (Wang 2008)
	naturalgas.MJ	5.3E+01	GREET (Wang 2008)
cellulase.kg	csl.kg	1.8E-01	GREET (Wang 2008)
	glucose.kg	1.3E+00	GREET (Wang 2008)
	ammonia.kg	6.0E-02	GREET (Wang 2008)
	glycerin.kg	4.0E-01	GREET (Wang 2008)
	nacl.kg	2.0E-01	GREET (Wang 2008)
	electricity.MRO.kWh	1.1E+00	GREET (Wang 2008)
	naturalgas.MJ	2.2E+00	GREET (Wang 2008)
alpha_amylase.kg	glucose.kg	7.0E-04	GREET (Wang 2008)
	electricity.MRO.kWh	1.9E+00	GREET (Wang 2008)
	naturalgas.MJ	5.0E+00	GREET (Wang 2008)

primary	Input Output References	value	Source
gluco_amylase.kg	glucose.kg	4.7E-01	GREET (Wang 2008)
	corn_starch.kg	4.7E-01	GREET (Wang 2008)
	electricity.MRO.kWh	8.9E+00	GREET (Wang 2008)
	naturalgas.MJ	1.3E+01	GREET (Wang 2008)
lime.kg	caco3.kg	1.4E+00	GREET (Wang 2008)
	coal.MJ	4.0E+00	GREET (Wang 2008)
	diesel.MJ	3.2E-01	GREET (Wang 2008)
	electricity.US.kWh	8.2E-02	GREET (Wang 2008)
	naturalgas.MJ	8.2E-01	GREET (Wang 2008)
	tankertruck.mt_km	1.9E-01	Distance from Gabi (Thinkstep 2018)
caco3.kg	diesel.MJ	1.4E+00	GREET (Wang 2008)
	electricity.US.kWh	6.5E-03	GREET (Wang 2008)
	naturalgas.MJ	1.2E+00	GREET (Wang 2008)
	flatbedtruck.mt_km	8.0E-02	GREET (Wang 2008)
h2so4.kg	electricity.US.kWh	6.6E-02	GREET (Wang 2008)
	tankertruck.mt_km	4.3E-01	GREET (Wang 2008)
	rail.mt_km	1.3E+00	GREET (Wang 2008)
hcl.kg	coal.MJ	9.2E-01	GREET (Wang 2008)
	diesel.MJ	2.7E-02	GREET (Wang 2008)
	rfo.MJ	2.7E-02	GREET (Wang 2008)
	electricity.US.kWh	9.7E-01	GREET (Wang 2008)
	gasoline.MJ	2.3E-03	GREET (Wang 2008)
	naturalgas.MJ	8.8E+00	GREET (Wang 2008)

primary	Input Output References	value	Source
naoh.kg	coal.MJ	3.8E-01	GREET (Wang 2008)
	rfo.MJ	2.0E-01	GREET (Wang 2008)
	electricity.US.kWh	1.8E+00	GREET (Wang 2008)
	naturalgas.MJ	3.3E+00	GREET (Wang 2008)
	tankertruck.mt_km	4.3E-01	GREET (Wang 2008)
	rail.mt_km	1.3E+00	GREET (Wang 2008)
csl.kg	electricity.MRO.kWh	6.5E-03	GREET (Wang 2008)
	naturalgas.MJ	2.2E+00	GREET (Wang 2008)
	corn.bushel	2.2E-01	GREET (Wang 2008)
glucose.kg	naoh.kg	2.8E-06	GREET (Wang 2008)
	corn_starch.kg	9.4E-01	GREET (Wang 2008)
	naturalgas.MJ	1.7E-01	GREET (Wang 2008)
corn_starch.kg	electricity.MRO.kWh	9.0E-02	GREET (Wang 2008)
	naturalgas.MJ	4.0E+00	GREET (Wang 2008)
	corn.bushel	6.9E-02	GREET (Wang 2008)
k2o.kg	diesel.MJ	2.4E+00	GREET (Wang 2008)
	naturalgas.MJ	2.7E+00	GREET (Wang 2008)
	tankertruck.mt_km	4.3E-01	GREET (Wang 2008)
	rail.mt_km	1.3E+00	GREET (Wang 2008)
ammonia.kg	naturalgas.MJ	4.0E+01	GREET (Wang 2008)
	tankertruck.mt_km	4.3E-01	GREET (Wang 2008)
	rail.mt_km	1.3E+00	GREET (Wang 2008)
n.kg	diesel.MJ	1.8E+00	GREET (Wang 2008)
	naturalgas.MJ	4.4E+01	GREET (Wang 2008)
	tankertruck.mt_km	4.3E-01	GREET (Wang 2008)
	rail.mt_km	1.3E+00	GREET (Wang 2008)

primary	Input Output References	value	Source
urea.kg	electricity.US.kWh	3.2E-01	GREET (Wang 2008)
	naturalgas.MJ	8.1E+00	GREET (Wang 2008)
	tankertruck.mt_km	4.3E-01	GREET (Wang 2008)
	rail.mt_km	1.3E+00	GREET (Wang 2008)
p2o5.kg	diesel.MJ	3.9E+00	GREET (Wang 2008)
	naturalgas.MJ	1.5E+00	GREET (Wang 2008)
	tankertruck.mt_km	4.3E-01	GREET (Wang 2008)
	rail.mt_km	1.3E+00	GREET (Wang 2008)
p.kg	electricity.NGCC.kWh	6.4E+00	GREET (Wang 2008)
	naturalgas.MJ	2.3E+01	GREET (Wang 2008)
nacl.kg	rfo.MJ	1.3E-01	GREET (Wang 2008)
	electricity.US.kWh	7.1E-02	GREET (Wang 2008)
	naturalgas.MJ	7.9E-01	GREET (Wang 2008)
triethylaluminum.kg	ethylene.MJ	7.5E+01	Based on stoichiometry
	h2.kg	2.7E-02	Based on stoichiometry
	tankertruck.mt_km	4.3E-01	GREET (Wang 2008)
	rail.mt_km	1.3E+00	GREET (Wang 2008)
coal.MJ	diesel.MJ	2.3E-03	GREET (Wang 2008)
	rfo.MJ	2.5E-04	GREET (Wang 2008)
	electricity.US.kWh	2.1E-03	GREET (Wang 2008)
	gasoline.MJ	1.9E-04	GREET (Wang 2008)
	naturalgas.MJ	5.8E-05	GREET (Wang 2008)
	flatbedtruck.mt_km	2.6E-03	GREET (Wang 2008)
	rail.mt_km	5.3E-02	GREET (Wang 2008)
	barge.mt_km	2.2E-02	GREET (Wang 2008)

primary	Input Output References	value	Source
diesel.MJ	refgas.MJ	2.4E-02	GREET (Wang 2008)
	crudeoil.MJ	1.0E+00	GREET (Wang 2008)
	electricity.US.kWh	2.6E-03	GREET (Wang 2008)
	naturalgas.MJ	2.4E-02	GREET (Wang 2008)
	tankertruck.mt_km	3.5E-03	(Sheehan et al. 1998)
	liquidpipeline.mt_km	2.1E-02	(Sheehan et al. 1998)
rfo.MJ	refgas.MJ	1.6E-02	GREET (Wang 2008)v
	crudeoil.MJ	1.0E+00	-
	electricity.US.kWh	2.6E-03	GREET (Wang 2008)
	naturalgas.MJ	1.6E-02	GREET (Wang 2008)
	tankertruck.mt_km	3.5E-03	GREET (Wang 2008)
	liquidpipeline.mt_km	2.1E-02	GREET (Wang 2008)
refgas.MJ	crudeoil.MJ	1.0E+00	-
ethylene.MJ	diesel.MJ	6.2E-05	GREET (Wang 2008)
	refgas.MJ	2.6E-02	GREET (Wang 2008)
	electricity.TRE.kWh	3.1E-03	GREET (Wang 2008)
	naturalgas.MJ	1.1E+00	GREET (Wang 2008)
	tankertruck.mt_km	5.2E-04	GREET (Wang 2008)
	liquidpipeline.mt_km	1.6E-03	GREET (Wang 2008)
propene.MJ	crudeoil.MJ	1.0E+00	-
acetone.kg	h2so4.kg	4.9E-04	Ecoinvent (Wernet et al. 2016)
	propene.MJ	1.5E+01	Ecoinvent (Wernet et al. 2016)
	electricity.US.kWh	2.7E-01	Ecoinvent (Wernet et al. 2016)
	gasoline.MJ	2.7E+01	Ecoinvent (Wernet et al. 2016)
	naturalgas.MJ	1.9E+00	Ecoinvent (Wernet et al. 2016)
	tankertruck.mt_km	4.3E-01	GREET (Wang 2008)

primary	Input Output References	value	Source
acetone.kg (cont'd)	rail.mt_km	1.3E+00	GREET (Wang 2008)
crudeoil.MJ	crudeoil.MJ	7.5E-02	GREET (Wang 2008)
	electricity.US.kWh	1.5E-03	GREET (Wang 2008)
	naturalgas.MJ	1.6E-02	GREET (Wang 2008)
	tankertruck.mt_km	5.5E-03	GREET (Wang 2008)
	liquidpipeline.mt_km	2.9E-02	GREET (Wang 2008)
	rail.mt_km	2.4E-02	GREET (Wang 2008)
	barge.mt_km	4.4E-03	GREET (Wang 2008)
	marinetanker.mt_km	1.1E-01	GREET (Wang 2008)
electricity.US.kWh	coal.MJ	5.0E+00	(eGRID2016 2018)
	diesel.MJ	6.7E-03	(eGRID2016 2018)
	rfo.MJ	3.0E-02	(eGRID2016 2018)
	electricity.US.kWh	6.5E-02	(eGRID2016 2018)
	naturalgas.MJ	1.9E+00	(eGRID2016 2018)
	uranium.kg	2.8E-07	(eGRID2016 2018)
electricity.NGCC.kWh	electricity.NGCC.kWh	6.5E-02	(eGRID2016 2018)
	naturalgas.MJ	7.2E+00	(eGRID2016 2018)
electricity.Coal.kWh	coal.MJ	1.1E+01	(eGRID2016 2018)
	electricity.Coal.kWh	6.5E-02	(eGRID2016 2018)
electricity.WECC.kWh	coal.MJ	3.3E+00	(eGRID2016 2018)
	diesel.MJ	9.4E-04	(eGRID2016 2018)
	electricity.WECC.kWh	8.2E-02	(eGRID2016 2018)
	naturalgas.MJ	2.6E+00	(eGRID2016 2018)
	uranium.kg	1.3E-07	(eGRID2016 2018)
electricity.MRO.kWh	coal.MJ	7.9E+00	(eGRID2016 2018)
	diesel.MJ	3.7E-03	(eGRID2016 2018)

primary	Input Output References	value	Source
electricity.MRO.kWh (cont'd)	electricity.MRO.kWh	5.8E-02	(eGRID2016 2018)
	naturalgas.MJ	2.0E-01	(eGRID2016 2018)
	uranium.kg	1.9E-07	(eGRID2016 2018)
electricity.TRE.kWh	coal.MJ	3.7E+00	(eGRID2016 2018)
	diesel.MJ	1.9E-04	(eGRID2016 2018)
	electricity.TRE.kWh	8.0E-02	(eGRID2016 2018)
	naturalgas.MJ	3.9E+00	(eGRID2016 2018)
	uranium.kg	1.7E-07	(eGRID2016 2018)
gasoline.MJ	refgas.MJ	3.7E-02	GREET (Wang 2008)
	crudeoil.MJ	1.0E+00	GREET (Wang 2008)
	electricity.US.kWh	2.5E-03	GREET (Wang 2008)
	naturalgas.MJ	3.7E-02	GREET (Wang 2008)
	tankertruck.mt_km	3.5E-03	GREET (Wang 2008)
	liquidpipeline.mt_km	2.1E-02	GREET (Wang 2008)
h2.kg	electricity.US.kWh	2.7E-01	(Spath and Mann 2001)
	naturalgas.MJ	1.4E+02	(Spath and Mann 2001)
	gaspipeline.mt_km	1.2E+00	GREET (Wang 2008)
naturalgas.MJ	naturalgas.MJ	2.0E-02	GREET (Wang 2008)
	gaspipeline.mt_km	7.7E-02	GREET (Wang 2008)
uranium.kg	electricity.WECC.kWh	1.0E+02	(Scown et al. 2011)
	electricity.MRO.kWh	4.4E+01	(Scown et al. 2011)
	naturalgas.MJ	1.4E+03	(Lenzen 2008)
	flatbedtruck.mt_km	4.5E+00	GREET (Wang 2008)
steel_chinese.kg	coal.MJ	6.9E-01	GREET (Wang 2008)
	electricity.Coal.kWh	8.2E-01	GREET (Wang 2008)

primary	Input Output References	value	Source
steel_chinese.kg (cont'd)	electricity.Renewables .kWh	3.5E-01	GREET (Wang 2008)
	naturalgas.MJ	6.8E+00	GREET (Wang 2008)
	rail.mt_km	8.0E-01	GREET (Wang 2008)
	barge.mt_km	1.0E+01	GREET (Wang 2008)
flatbedtruck.mt_km	diesel.MJ	1.8E+00	Fuel economy from (Strogen et al. 2012)
	flatbedtruck.mt_km	2.5E-01	(Sheehan et al. 1998); assumption of 25% empty miles
tankertruck.mt_km	diesel.MJ	1.2E+00	Fuel economy from (Strogen et al. 2012)
	tankertruck.mt_km	2.5E-01	(Sheehan et al. 1998); assumption of 25% empty miles
rail.mt_km	diesel.MJ	2.7E-01	Fuel economy from (Strogen et al. 2012)
	rail.mt_km	2.5E-01	(Sheehan et al. 1998); assumption of 25% empty miles
barge.mt_km	diesel.MJ	3.2E-01	Fuel economy from (Strogen et al. 2012)
	barge.mt_km	2.5E-01	Assume 25% empty miles
marinetanker.mt_km	rfo.MJ	1.0E-01	Average of crude tanker & product tanker energy intensities (Strogen et al. 2012)
	marinetanker.mt_km	2.5E-01	Assume 25% empty miles
corn.bushel	atrazine.kg	3.5E-03	GREET (Wang 2008)
	glyphosate.kg	3.5E-03	GREET (Wang 2008)
	insecticide.kg	6.0E-05	GREET (Wang 2008)
	caco3.kg	1.1E+00	GREET (Wang 2008)
	k2o.kg	1.5E-01	GREET (Wang 2008)
	n.kg	4.2E-01	GREET (Wang 2008)
	p2o5.kg	1.5E-01	GREET (Wang 2008)
	diesel.MJ	9.6E+00	Assumed all energy provided diesel; GREET (Wang 2008)
	flatbedtruck.mt_km	2.0E+00	Assumed 50 miles; GREET (Wang 2008)
compost_application.kg	n.kg	-1.0E-02	(CARB 2017)

primary	Input Output References	value	Source
outdoor_compost.wet_kg	diesel.MJ	5.8E-02	(CARB 2017)
	electricity.US.kWh	7.9E-03	(CARB 2017)
	flatbedtruck.mt_km	5.0E-02	Assume 50 km
organics_composting_wet.kg	diesel.MJ	5.8E-02	(CARB 2017)
	electricity.US.kWh	7.9E-03	(CARB 2017)

Source: Lawrence Berkeley National Laboratory

APPENDIX D:
Financial Model Calculations

Description of Data and Assumptions

The model processes multiple incoming waste streams defined by (a) the type of waste—municipal solid waste (MSW), yard, or manure, (b) percent of inorganic waste, referred to as residuals, the waste contains, and (c) the tipping fee received by the facility for taking the waste in. This information, along with the fraction of annual waste coming from each category, is presented in Table D-1. The "OS_" designations are used by the facility's primary hauler for MSW, with tipping fees that scale with increasing level of residuals. The residual caps shown here include a 5 percent addition over the specified thresholds, as the facility estimates this is the typically accepted buffer with the waste residuals always coming in well over the specified cap. Tipping fees and fraction of intake are 2016 values. The model calculates yard waste intake endogenously, as ZWEDC puts a defined (approximate) fraction of yard waste into each digester and sends the remaining yard waste onward to a composting facility at a negligible profit. This pass-through of excess yard waste is excluded from this analysis.

Table D-1: Waste Feedstock Types and Characteristics

Hauler	Waste Type	Residuals Cap	Tipping Fee ($/ton)	Fraction of Intake (percent)
A	OS 1	0.10	75	2.8
A	OS 2	0.15	80	0.5
A	OS 3	0.25	90	0.0
A	OS 4	0.35	105	68.6
B	MSW	0.35	81	16.1
B	Yard	0.0	81	--
C	MSW	0.35	66	11.5
D	Manure	0.0	56	0.5

Source: Lawrence Berkeley National Laboratory

Outbound waste data is used to determine disposal costs in the model. The majority of residuals (inorganic materials) that come into the facility is sent to landfill, but a small portion is separated out for recycling (plastics, metals, glass) or composting (fiber). According to tonnage reports, approximately 1 percent of residuals are recyclables and

1 percent are fibrous materials. Outbound tonnage reports also indicate that approximately 70 percent of incoming organic mass remains after digestion (digestate) and must be sent to composting.

Information about the facility's design and operation was obtained from conversations with facility staff along with "Monthly Operating Statistics" spreadsheets from 2016 and 2017. This data is primarily used to calibrate theoretical results for biogas and electricity production to empirical values, estimate the fraction of biogas that is sent to the CHP units versus being flared, and estimate facility electricity consumption.

The project team used facility financial statements, depreciation schedules, utility bills, and other contract documents to estimate unit costs for each cost category as well as other economic parameters such as payment periods. Table D-2 shows the facility's capital costs and payment lifetimes along with annual operations and maintenance (O&M) costs, while Source: Lawrence Berkeley National Laboratory

Table D-3 shows the current estimated labor breakdown. Capital and labor costs are separated into various categories according to how they will scale up for larger facilities and how they will be included or excluded from various scenarios. Capital costs shown in Table D-2 are up-front "sticker" costs, meaning they do not include financing. The model calculates the total financed cost of capital and amortizes it over the expected life of the facility in order to calculate annual average costs and per-ton processing costs. O&M costs for the facility include operational needs such as fuel, materials, and parts, maintenance and testing, and equipment rentals, along with business expenses such as office supplies, legal and accounting services, taxes, and insurance. Utilities costs are calculated separately and described below. O&M cost for the CHP units is based on an annual maintenance contract the facility has with the CHP manufacturer. Labor cost breakdown is based on conversations with the facility's leadership; the average total cost per full-time equivalent employee is estimated at $90,000/year based on 2016 financial data.

Table D-2: Capital and O&M Costs

Capital	Capital Cost ($M)	Finance Lifetime (years)	O&M Cost ($k/year)	Unit
Facility	43.5	13	3,000	Per 90 kTPY capacity
Site development	15	13	--	Constant
CHP	1.1	10	50	Per 800 kW CHP
Composting	0.04	0.5	--	Per 90 kTPY capacity, only included if composting is done on-site

Source: Lawrence Berkeley National Laboratory

Table D-3: Labor Breakdown

Labor	Full-time equivalents	Unit
Overhead	3	Constant
Facility operations	12	Per 90 kTPY capacity
Waste processing	5	Per 110,000 tons accepted with 35 percent residuals (scales linearly with both waste intake and residual fraction)
Composting	1	Per 90 kTPY capacity, only included if composting is done on-site

Source: Lawrence Berkeley National Laboratory

Electricity used to operate the facility is metered separately from the electricity sold from the CHP units, due to the value of selling electricity on the BioMAT feed-in tariff being higher than the utility's industrial electricity rate. A consumption rate of 8 cents/kWh is assumed, according to current PG&E industrial customer rate schedules. The base selling rate for the BioMAT tariff is 12.77 cents/kWh, which is multiplied by a temporal factor that varies by season and time of day. These temporal factors range from 0.28 during mid-day (10 AM to 5 PM) March-June, when there is an excess of

solar power and energy is very cheap, to 1.479 during peak hours (5-10 PM) July-September. Based on assumptions about ZWEDC's operating schedule, and their inability to control when they produce electricity, we assume average monthly factors of 1.044 for July-September, 1.073 for October-February, and 0.876 from March-June. Additionally, the facility had to pay interconnection costs to begin net metering (or selling) electricity to PG&E. Though these costs were initially quoted upwards of a million dollars, through negotiation and redesign the facility ended up paying approximately $200,000 as an up-front cost.

Other utilities needed on-site are heat, water, and wastewater. All process heat required is supplied from the CHP units' waste heat. No significant water costs or consumption occurs that we are aware of. Wastewater costs can be significant due to the high concentrations of nutrients and solids in the wastewater. After an extruder was added to the front-end of the waste processing operation, the facility incurred extremely high wastewater treatment costs due to the worsened quality of the wastewater stream. The facility then installed a screw press that helped to lower the total solids content of the wastewater stream and therefore lower costs. Based on wastewater bills, and assuming the costs of wastewater scale with the amount of waste coming into the facility, unit wastewater costs are estimated at 15 cents per ton of waste intake, which amounts to approximately $16,000 per year.

Transportation and disposal of various material streams is a significant cost for the facility. Residuals that are sorted out from incoming waste must be trucked to a nearby landfill, though the tipping fees are paid directly from the City of San José to the landfill with no additional cost to ZWEDC. After the organics have been processed through the digestion facility, the solid byproduct (digestate) needs to be composted. Since on-site composting operations ceased in 2015, the facility has paid to send the digestate to a facility in Gilroy, CA. Table D-4 describes the current per-ton costs for the management of material streams.

Table D-4: Trucking and Tipping Costs for Residuals and Byproducts

Material	Cost ($/ton)	Description
Residuals	8	Trucking to landfill
Recyclables	38	Average combined trucking and tipping fee to Greenwaste MRF
Fiber	10	Trucking to Gilroy
	55	Tipping to compost facility
Digestate	10	Trucking to Gilroy
	45	Tipping to compost facility

Source: Lawrence Berkeley National Laboratory

Operational Calculations

Masses

The starting point for each set of calculations in the model is the amount of organic mass that is to be processed in the digesters ($m_{digester}$) in terms of tons per year. For each scenario and sensitivity analysis, we calculate financial metrics for facilities processing 60,000 TPY to 270,000 TPY.

The majority of waste going into the digesters is from the organic fraction of municipal solid waste (OFMSW). A small amount of yard waste is also added to the digesters to improve the structure of the waste pile which enables better digestion. We calculate the amount of OFMSW going into the digester (m_{OFMSW}) according to the total digester mass and an assumed fraction of yard waste ($r_{yard\ to\ OFMSW}$) of 0.05 based on waste tonnage data and conversations with ZWEDC staff. The amount of yard waste that goes into the digesters (m_{yard}) is then simply product of the mass of OFMSW and the ratio of yard to organic waste.

$$m_{OFMSW} = \frac{m_{digester}}{1 + r_{yard\ to\ OFMSW}}$$

$$m_{yard} = m_{OFMSW} * r_{yard\ to\ OFMSW}$$

Incoming MSW contains a significant quantity of inorganic residuals. The facility receives tipping fees based on the total tonnage of incoming waste, not just the organic fraction of it, and therefore it is important to know this tonnage for revenue calculations. Additionally, there are costs associated with separating and disposing of residuals, so the tonnage of those materials must be known as well. The fraction of residuals in each waste stream ($f_{residual,i}$) as well as each waste stream's proportion of total waste coming into the facility (f_i). From these values, we can calculate a weighted

average residual fraction for all incoming waste ($\bar{f}_{residual}$), total municipal waste intake (m_{MSW}), and mass of residuals ($m_{residual}$).

$$m_{MSW} = \frac{m_{OFMSW}}{1 - \bar{f}_{residual}}$$

$$m_{residual} = m_{MSW} * f_{residual}$$

$$m_{total} = m_{MSW} + m_{yard}$$

The anaerobic digestion process causes a reduction in solid waste mass due to the transformation of mass into biogas as well as creation and loss of moisture. The digestate is placed in in-vessel composting (IVC) tunnels before it is sent for further processing, causing an additional loss in moisture. A 30 percent mass reduction is assumed from when the waste goes into the digesters to when the digestate is removed from the IVC ($mass\ reduction_{digestion}$). This value is based on facility tonnage reports. The digestate then goes through an aerobic composting process, when additional mass is lost to moisture evaporation and gaseous emissions. We assume a mass reduction of 10 percent in this process ($mass\ reduction_{compost}$), based on conversations with the facility. With these assumptions, we can calculate the mass of digestate coming out of the facility ($m_{digestate}$) or the mass of compost ($m_{compost}$) for scenarios when compost operations occur on-site.

$$m_{digestate} = m_{digester} * (1 - mass\ reduction_{digestion})$$

$$m_{compost} = m_{digestate} * (1 - mass\ reduction_{compost})$$

Biogas and Methane Production

The theoretical mass of methane generated (m'_{CH4}) is calculated based on moisture (μ_i) and carbon content (ν_i) of each waste stream and the overall carbon conversion rate of the digestion process (ε_{carbon}). We assume yard waste and OFMSW have moisture contents of 60 percent and 70 percent, respectively, and that the non-moisture portion of yard waste and OFMSW has carbon contents of 35 percent and 53 percent. The negligible amount of manure that comes into the facility is grouped in with the MSW for these calculations. The mass of carbon contained in the waste (m_C) is therefore:

$$m_C = m_{yard} * \left(1 - \mu_{yard}\right) * \nu_{yard} + m_{OFMSW} * (1 + \mu_{OFMSW}) * \nu_{OFMSW}$$

We assume the anaerobic digestion process converts approximately 30 percent of carbon in the waste to biogas, and that that biogas as an average composition of 55 percent methane (CH4) (f_{CH4}), 40 percent carbon dioxide (CO2) (f_{CO2}), and 5 percent other, by volume. The theoretical methane generated is then calculated as:

$$m'_{CH4} = m_C * \varepsilon_{carbon} * \left(\frac{f_{CH4}}{f_{CH4} + f_{CO2}}\right) * \left(\frac{MW_{CH4}}{MW_C}\right)$$

Where MW_x represents the molecular weight of compound x.

ZWEDC facility data from January 2016-December 2017 is then analyzed to determine the actual methane generated (m_{CH4}) as compared to this theoretical estimate, in order to calculate a calibration factor. This calibration factor (α_{CH4}) allows us to accurately represent the real-world operations of the facility while maintaining a general understanding of the underlying theoretical process. We exercise some judgment in choosing this factor as opposed to using the raw data directly based on known operational issues and data gaps at the facility during this time. Additionally, the data is only available on a monthly aggregate basis that does not account for the approximately 21-day residence time of the digesters and corresponding offset between waste intake and gas production data. This offset makes it difficult to even pick-and-choose months where no data collection or operational problems occurred and use those values directly. In the end, we use a 0.70 calibration factor for the ZWEDC facility's current operations, meaning that the facility actually generates 30 percent less methane than we would expect. This difference from the theoretical estimate could be due to: lower carbon content of waste, lower carbon conversion, lower CH4:CO2 ratio, fugitive gas losses, and/or data recording issues.

$$m_{CH4} = m'_{CH4} * \alpha_{CH4}$$

Electricity Generation

The theoretical quantity of electricity generated (e') is calculated using the mass (m_{CH4}) and heating value (HV_{CH4}) of methane, the CHP generator efficiency (ε_{CHP}), and assumptions about biogas flaring and venting, expressed as the fraction of biogas that is sent to the CHP units (f_{CHP}).

$$e' = m_{CH4} * f_{CHP} * HV_{CH4} * \varepsilon_{CHP}$$

ZWEDC's CHP units have a 41.6 percent electrical efficiency (not including energy captured as heat) according to the equipment manuals. ZWEDC sent approximately 72 percent of their biogas, by volume, to the CHP units in 2017. This number rises slightly to 75 percent when excluding two months during which major facility disruptions occurred due to large-scale maintenance operations and subsequent equipment issues. Biogas that is not sent to the generators is usually flared due to low methane percentage in the gas or limited biogas storage capacity. A small portion of this gas is vented to the atmosphere when necessary to prevent storage bladder damage.

Once again, we can calibrate this result to ZWEDC's actual performance in 2017 using facility data. Based on the heating value of methane and generator efficiency, we would expect 6 kWh per kg of methane, or 2.2 kWh per m3 of biogas.[3] In 2017, ZWEDC records that they did in fact generate an average 2.2 kWh per m3 of biogas sent to the CHPs. Therefore, at this stage, we use an electricity calibration factor (α_e) of 1.

[3] Assuming methane density of 0.67 kg/m3 at average San José temperatures and biogas 55 percent methane by volume

$$e = e' * \alpha_e$$

Cost Calculations

The model uses the results of the operational calculations to calculate the costs and revenues involved in operating the facility.

Costs are calculated for all categories, then are scaled or zeroed out depending on scenario parameters. For example, a scenario where compost occurs off-site will not include the compost capital and labor costs, while a scenario where composting is done on-site will include these costs but exclude trucking and tipping costs for digestate.

Each of the below calculations is performed for each waste intake level for each scenario.

Notation: c for unit costs, C' for total costs (for capital), C for annual costs.

Capital and Site Costs

Capital costs are based on the size of the facility and generators needed to process the waste and energy estimated for each waste intake level. We assume a baseline facility size (s_{fac}) of 90,000 TPY, as this is the capacity of the existing facility. The majority of the facility is built as two parallel modules, which each have their own biogas storage bladder and exhaust air biofilters. Therefore, we assume the facility can only be scaled up in increments ($s_{fac,increment}$) of 45,000 TPY. The "number" of facilities required (N_{fac}) is therefore a step function of the amount of waste being sent to the digesters.

Similarly, the number of CHP units required (N_{CHP}) is a step function of the amount of electricity being generated by the facility (e). We assume a set CHP size (s_{CHP}) due to current facility design and the fact that identical equipment will have more consistent and simplified maintenance, and more predictable consequences if an outage of any one generator were to occur. The capacity factor (CF) of the CHP units is the ratio of actual energy production to maximum rated production; we assume a maximum desired capacity factor of 0.8 for the facility. This allows energy production to fluctuate throughout the year without going over the generator's capacity.

The model currently assumes waste intake is consistent throughout the year, based on facility data, but if that assumption were to change then the facility and CHP units would need to be sized for the peak season, as long-term storage is not viable for organic waste and is not available at the facility for biogas. The model also assumes biogas flow is constant throughout the day, which is reasonable given that the digesters operate around-the-clock and only one digester (at most) out of sixteen is cleared out and refilled each day. If short-term biogas storage was to be installed at the facility, for example to maximize electricity revenues by selling only at peak times, the CHP units would need to be sized up accordingly.

$$N_{fac} = 1 + \left\lceil \max\left(\frac{m_{digester} - s_{fac}}{s_{fac,increment}}, 0 \right) \right\rceil$$

$$N_{CHP} = 1 + \left\lceil \frac{e}{365 * 24 * CF} * \frac{1}{s_{CHP}} \right\rceil$$

The "sticker" price of the facility ($C'_{fac\ cap}$) is then the number of facilities times the assumed unit price of the facility ($c_{fac\ cap}$), plus site development costs that do not scale with facility size (c_{site}). Site development for the ZWEDC facility included site foundations, which were expensive as the facility is built on landfill, bringing utilities to the site, on-site roads, storm water drainage, etc. Generally, constructing larger facilities could incur economies of scale beyond site development costs. However, due to the modular nature of the ZWEDC facility there is not reason to believe this would be the case.

CHP price ($C'_{CHP\ cap}$) is the CHP unit price ($c_{CHP\ cap}$) multiplied by the number of units, while compost capital ($C'_{compost\ cap}$) is the unit price multiplied by the number of facilities. Compost capital is calculated separately, as this cost may or may not be present depending on whether or not composting is done in-house. Capital equipment needed for composting could include windrow turners, aeration infrastructure, and windrow bags.

$$C'_{fac\ cap} = N_{fac} * c_{fac\ cap} + c_{site}$$

$$C'_{CHP\ cap} = N_{CHP} * c_{CHP\ cap}$$

$$C'_{compost\ cap} = N_{fac} * c_{compost\ cap}$$

Actual capital costs are higher than the above prices due to long payment schedules and associated financing costs. Therefore, a loan payment function is used to calculate the monthly payment amount (PMT) of a loan for a certain principal (P), at fixed capital interest rate (r_c), over a set number of payment periods (p). A "capital lifetime" ($L\ (months)$) based on depreciation schedules gives the number of payment periods, while the calculated capital prices (C') are the principal, and the assumed interest rate is 5 percent. From this monthly payment, average annual costs (C) over the life of the facility ($L_{facility}\ (months)$) are calculated. In general, the capital lifetime is lower than the actual useful life of the equipment, so the total amortized costs will be lower than the payments the facility is currently making. We assume all equipment will last the full facility lifetime of 25 years.

$$PMT(r_c, p, P) = \frac{P * r_c/12}{1 - (1 + r_c/12)^{-p}}$$

$$C_i = PMT(r_c\ , L_i, C'_i) * 12 * \frac{L_i}{L_{facility}}$$

for i $\in$ fac cap, CHP cap, compost cap

The final capital cost is the utility interconnection ($C_{interconnect}$). We assume the unit price ($c_{interconnect}$) is paid lump-sum at the start of the facility building process, and therefore the average annual cost is simply the cost divided by the lifetime of the facility in years.

$$C_{interconnect} = \frac{c_{interconnect}}{L_{facility}/12}$$

Labor Costs

Labor is calculated based on the approximate annual cost of one full-time employee (c_{labor}) and the number of employees required for the facility (N_{FTE}). Labor is divided into four types that scale differently with operational parameters, and the number of employees needed for each labor type is calculated based on a "base" facility. The "base" facility is representative of ZWEDC's operations and is characterized by number of employees (n_{FTE}) for each labor type, waste intake ($m_{MSW,base}$), residual fraction ($f_{residual,base}$), and digestate production ($m_{digestate,base}$). Adjusting from this known scenario allows us to estimate unknown labor needs at various facility scales and operational conditions.

Overhead labor ($N_{FTE,overhead}$) is a constant input that does not change with facility size or operating conditions. This assumption relies on the knowledge that we are only examining facilities up to three times ZWEDC's current operations. For facilities drastically larger or smaller, this assumption may be revisited. Operations labor ($N_{FTE,ops}$) scales linearly with the size of the facility (and therefore stepwise with the amount of waste being processed). Labor required for waste sorting ($N_{FTE,sorting}$) scales linearly with both the amount of waste coming in and the residual level of that waste. Lastly, composting labor ($N_{FTE,compost}$) scales linearly with the mass of digestate being produced, and is included only for scenarios where compost operations happen on-site. Ceiling functions are used to ensure no fractional employees are included.

$$N_{FTE,overhead} = \lceil n_{FTE,overhead} \rceil$$

$$N_{FTE,ops} = \lceil n_{FTE,ops} * N_{fac} \rceil$$

$$N_{FTE,sorting} = \left\lceil n_{FTE,sorting} * \left(\frac{m_{MSW}}{m_{MSW,base}}\right) * \left(\frac{f_{residual}}{f_{residual,base}}\right) \right\rceil$$

$$N_{FTE,compost} = \left\lceil n_{FTE,compost} * \left(\frac{m_{digestate}}{m_{digestate,base}}\right) \right\rceil$$

$$N_{FTE} = N_{FTE,overhead} + N_{FTE,ops} + N_{FTE,sorting} + N_{FTE,compost}$$

$$C_{labor} = N_{FTE} * c_{labor}$$

Operations and Maintenance Costs (Non-Labor)

Operations and maintenance (O&M) costs are estimated at a high level. Annual costs per-facility ($c_{fac\ o\&m}$) and per-CHP unit ($c_{chp\ o\&m}$) are assumed, and these values are simply multiplied by the number of facilities and CHP units for the total cost ($C_{fac\ o\&m}\ and\ C_{chp\ o\&m}$). Facility O&M includes parts, fuel, equipment rentals, and outside maintenance, as well as business expenses such as office supplies, legal, accounting, and consulting. CHP O&M is calculated separately because the number of CHP units does not scale exactly with the number of facilities, and the CHP maintenance cost is known from the facility's contract with the equipment manufacturer.

$$C_{fac\ o\&m} = N_{fac} * c_{fac\ o\&m}$$

$$C_{CHP\ o\&m} = N_{CHP} * c_{CHP\ o\&m}$$

Additional O&M costs include electricity ($C_{electricity}$), for which an annual per-facility cost ($c_{electricity}$) is assumed, and wastewater ($C_{wastewater}$), which has a per-ton unit cost ($c_{wastewater}$) that is multiplied by total intake mass. Although the facility generates more electricity than it consumes, electricity costs are calculated separately from electricity revenues because the rates paid for consumption and production are different. Additionally, this gives the model flexibility to incorporate non-electricity biogas uses in the future. The electricity use scales linearly with the facility size, which scales piecewise with waste intake, due to the assumption that the majority of the facility's equipment will need to operate continuously regardless of how much waste is coming in. Wastewater treatment costs can be significant due to the high amounts of suspended solids and biological and chemical agents in the water that leaves the facility. A large portion of the facility's wastewater is produced at the extruders, which remove excess water from incoming waste and outgoing digestate. Therefore, wastewater costs are assumed to scale with the amount of waste being processed by the facility.

$$C_{electricity} = N_{fac} * c_{electricity}$$

$$C_{wastewater} = m_{total} * c_{wastewater}$$

Byproducts and Waste Materials

AD facilities have a number of materials to manage throughout their operational process. For each material stream, costs are incurred for both transportation of the material ($c_{trucking}$) and tipping fees paid to the accepting facilities ($c_{tipping}$).

As waste comes into the facility inorganic residuals are sorted from the organic material. The vast majority of residuals must be landfilled, while fiber and other recyclables may be discarded at specialized facilities due to their value or because of contractual obligations. The total mass of residual is calculated as previously discussed, then assumed fractions for landfill ($f_{landfill}$), recyclables ($f_{recyclables}$), and fiber (f_{fiber}) are used to calculate their respective masses. Digestate is sent to a compost facility under current operations. The costs of managing these materials are simply the mass of

the material times the sum of per-ton trucking and tipping fees. If composting were to occur on-site, these cost of digestate management would be zero.

$$C_i = m_{residual} * f_i * (c_{trucking,i} + c_{tipping,i})$$

for i $\in$ landfill, recyclable, fiber

$$C_{digestate} = m_{digestate} * (c_{trucking,digestate} + c_{tipping,digestate})$$

Revenues

The primary source of revenue for the facility is incoming tipping fees. These fees are set by contract with the various haulers that send waste to the facility. The waste data input file contains the assumed tip fee for each incoming waste stream along with the fractional breakdown of incoming waste across streams. Therefore, a weighted average per-ton tipping fee (r_{tipfee}) can be calculated for the given waste scenario and multiplied by the total intake mass to calculate tip fee revenue (R_{tipfee}).

$$R_{tipfee} = m_{MSW} * r_{tipfee}$$

The facility also makes money by selling electricity. The structure of electricity revenues may vary widely based on a facility's location, customer, and what the local laws and rate structures look like. Based on ZWEDC's current contract with their local utility, we calculate electricity revenue ($R_{electricity}$) using a baseline rate ($r_{electricity}$) and an average monthly adjustment factor (α_{elec}). The adjustment factor is calculated from a set of multipliers for each season and time of day described in the contract; these multipliers represent when electricity is more or less valuable to the utility. Hypothetically, ZWEDC could optimize operations to generate electricity at times with peak adjustment factors, but this is generally not feasible with current biogas storage capacity and other operational logistics and would likely require the installation of additional CHP units. The baseline rate and adjustment factor is assumed to be constant at all facility scales. However, the BioMAT program is limited to generators less than 3 MW (current facility capacity is 1.6 MW), so the facility would have to switch to selling electricity by net metering or wholesale agreement if it scaled up beyond 3 MW. The effects of this change are explored through the sensitivity analysis.

$$R_{electricity} = e * r_{electricity} * \left(\frac{1}{12} * \sum_{m=1}^{12} \alpha_{elec,m}\right)$$

Lastly, a facility that composts digestate on-site may collect revenues from the sale of the final compost. The total revenue ($R_{compost}$) is simply the mass of compost created multiplied by an assumed per-ton price ($r_{compost}$).

$$R_{compost} = m_{compost} * r_{compost}$$

Economic Calculations

Average Annual Cash Flow

Once the costs for each category are calculated, these costs can be transformed into a number of useful metrics. The most straightforward metric is the average annual cash flow of the facility ($\bar{C}_{net}$) at each modeled waste intake level. Each cost category (e.g. facility capital, labor, wastewater) is multiplied by a category- and scenario-specific scalar (S). This scalar is equal to 1 for any costs that are included as calculated, -1 for any revenues, and 0 for costs that are excluded. Additionally, the scalar could be a fraction. For example, two scenarios could be run with scalars of 0.8 and 1.2 on a particular cost category in order to conduct a sensitivity analysis:

$$\bar{C}_{net} = \sum_{i} C_i * S_i$$

for all cost categories i.

Net Present Value

Net present value (NPV) of the facility can also be calculated, but temporal factors such as inflation and discounting must be considered. NPV is calculated for a 25-year period, the expected lifetime of the facility capital. Net cash flow ($C_{net,y}$) is calculated for each year of the facility lifetime, then discounted to present worth based on an assumed 7 percent annual discount rate (r_d). The results for each year are summed to obtain the NPV of the facility (NPV).

Costs are categorized as constant, inflating, or payment for annual net cost calculations. Constant costs appear as the same amount in each year of the NPV analysis whereas inflating increase annually assuming a 2 percent inflation rate (r_I). In the current model, the only constant cost is the rate received for electricity sales, as the facility is currently in a 10-year contract in which the rates do not increase. All other non-capital costs are inflating, such as labor, trucking, and purchased electricity costs.

Capital costs are handled separately, as these costs are paid off according to a depreciation schedule and with payments that include interest considerations, as discussed previously in the payment function. The monthly payment value (PMT_p) and capital lifetime (L_p) of each type of capital are used to determine the cost for each of the 25 years in the NPV analysis ($C_{p,t}$).

$$NPV = \sum_{t=0}^{L_{facility}} \frac{C_{net,y}}{(1 + r_d)^t}$$

$$C_{net,y} = \sum_{c} (C_c * S_c) + \sum_{i} (C_i * S_i * (1 + r_I)^y) + \sum_{p} \left(PMT_p * 12 * \varphi_{p,y} * S_p\right)$$

for all constant cost categories c, all inflating cost categories i, and all payment cost categories p.

$$\varphi_{p,y} = \max\left(min\left(\frac{L_p}{12} - y, 1\right), 0\right)$$

Processing Cost per Ton

The model calculates the average cost of processing one ton of incoming waste at the facility. This metric is useful to compare to the tipping fee revenues the facility receives from waste haulers, as well as for a decision maker to compare to the cost of other alternatives, such as landfill tipping fees. The per-ton processing cost is simply the net annual cash flow of the facility, minus tipping fee revenues and excess yard waste expenses, divided by the total mass of waste processed each year.

$$\Omega = \frac{\bar{C}_{net} - R_{tipfee} - C_{yardexcess}}{m_{total} - m_{yard,excess}}$$